HINDERED SETTLING

by

YU SEN CHONG

B.Sc., Nanyang University, 1966

A THESIS SUBMITTED IN PARTIAL FULFILMENT
OF THE REQUIREMENTS FOR THE DEGREE OF
MASTER OF APPLIED SCIENCE
in the Department
of
CHEMICAL ENGINEERING

We accept this thesis as conforming to
the required standard

Members of the Department of Chemical
Engineering

THE UNIVERSITY OF BRITISH COLUMBIA

December, 1968

ABSTRACT

Natural and commercially available particles of uniform shape and size were used to study the effect of particle shape on hindered settling in creeping flow ($Re_o <$ 0.1), where fluid flow behaviour is independent of particle Reynolds number and the effect of shape is most prominent. Particles of different shapes used were spherical glass beads, cubic salt (NaCl) crystals and ABS plastic pellets, flaky sugar crystals and angular mineral (silicate) crystals. They were carefully sized by sieving and liquid elutriation to avoid other effects like size segregation. Constant settling data were processed in the form of $u\nu$ rather than u to eliminate the effect of temperature variation on viscosity.

The effect of the wall on hindered settling rate was found to be small in most cases. The method proposed by Beranek and Klumpar for correlating fluidization data on different shaped particles was found to be only moderately successful in correlating the present settling data for different shapes.

Results were plotted as $\log u\nu$ versus $\log \epsilon$, and the index n of the equation $u\nu/(u\nu)_{ext} = \epsilon^n$ was calculated by least squares. It varied from an average value of 4.8 for the smooth spheres to 5.4 for the cubes to 5.8 for the flaky or angular particles. In contrast to the corresponding term proposed by Richardson and Zaki, the term $(u\nu)_{ext}$ was measurably lower than $u\nu$ for free settling of the spherically isotropic particles. More significantly, the index n was graph-

ically found to display a definite trend with the random loose fixed bed porosity, which is shape dependent and easily measured, and may therefore turn out to be a simple and useful parameter for taking account of shape variation.

ACKNOWLEDGEMENTS

I am greatly indebted to Drs. Norman Epstein and David A. Ratkowsky, under whose guidance this study was made, for their invaluable assistance and encouragement during the course of this project. The help of Dr. Epstein in the final writing is deeply appreciated.

I wish to thank the University of British Columbia for financial assistance received in the form of a Graduate Fellowship, and the National Research Council of Canada for additional support.

The cooperation of Mr. Muelchen and the other staff of the Chemical Engineering Workshop in fabricating the apparatus, and the assistance of Mr. Musil of Metallurgy in the use of the photomicrograph facilities, are also appreciated.

TABLE OF CONTENTS

LIST OF TABLES

LIST OF FIGURES

Figure | Page

INTRODUCTION

Single spherical particle settling or free settling of spheres in a quiescent infinite fluid within the creeping flow regime was studied theoretically by Stokes (1), and the well known Stokes' law has been verified by various experimental data (2). Hindered settling, in contrast to free settling of isolated particles, describes a swarm of particles settling simultaneously, as in most practical sedimentations. It is different from free settling because of the interference on the fluid stream surrounding a given particle by the presence of neighbouring particles.

An early investigation of sedimentation made by Coe and Clevenger (3) showed that sedimentation usually began with a constant rate, and that particles were continuously depositing on the bottom of the container to form a bed of sediment. The settling rate in this period is called the contant initial settling rate. From a hydrodynamic point of view, hindered settling of a monosize system is similar to particulate fluidization when there are no boundaries to the particle bed. In fact studies in these two areas are complementary to each other. Because of their wide application in chemical engineering and other fields, a considerable amount of study has been made of such fluid-particle systems.

Most work in the literature deals with spherical particle systems, presumably because a sphere has the most simple configuration, of which the size and shape are easily defined. Investigations on nonspherical particles are mostly restricted to free settling.

LITERATURE SURVEY

1. Single Particle

The earliest study on resistance of a single spherical body moving relative to fluid was made by Stokes (1), whose analytical result is applicable within the creeping or viscous flow region, where fluid inertia is negligible compared to viscous shear. Later, study was extended to somewhat higher Reynolds numbers by Proudman and Pearson (4), Whitehead (5), Oseen (6) and Jenson (7). An analytical solution of creeping flow past an ellipsoid has been developed by Oberbeck (8) and Gans (9), who proved that a body possessing three perpendicular planes of symmetry has no tendency to assume any particular orientation as it settles. Subsequently, theoretical study on free settling of a single particle was extended to settling at higher Reynolds numbers, to cases where the fluid is bounded by solid walls and a bottom, to irregular shaped body settling, and to improved mathematical techniques of analysis. The studies are well described by Happel and Brenner (10).

An experimental study on single non-spherical particles of well-defined shape was made by Pernolet (11), who investigated cubes, disc and prisms over a narrow range of Reynolds number. Pettyjohn and Christiansen (12) specifically studied isometric particles over a large range of Reynolds number, and were able to correlate the Stokes' law shape factors of five isometric bodies in creeping flow region, as well as drag coefficients at higher Reynolds number region, with sphericity. Similar work was done by Chowdhury (13) and a similar conclusion was obtained. Heiss and Coull (14) studied the effect of orientation and shape on the settling velocity of non-isometric particles in the viscous region, and reached the conclusion that sphericity alone was not sufficient to take account of both shape and orientation effects on the free settling of non-isometric orthotropic bodies. Correlation of sphericity to Stokes' law shape factor was possible by including as additional parameters the diameter of a sphere of equal volume and the diameter of a circle of equal projected area to the body in question. Recently Blumberg and Mohr (15) have extended the study of cylindrical particles in viscous flow to orientations intermediate between horizontal and vertical. Other experimental studies on orthotropic bodies were those of McNown and Malaika (16), who investigated discs, cylinders, a prismatic body and a conical body settling parallel to the particle axis, and determined the limit of the viscous flow region for the various shapes; and Jayaweera (17), who studied the free settling of cylinders and cones over a particle Reynolds number range of 0.01 to 1000. At high particle Reynolds number, free settling of single particles was found to depend on the density ratio of solid to liquid, as well as on shape, by both Christiansen (18) and Isaacs (19).

Becker (20) has attempted to correlate shape and Reynolds number with drag coefficient, for various literature data. A review by Torobin and Gauvin (21) covered extensive references on the effect of particle shape and roughness. So far, even for single particle settling, the choice of a suitable shape factor which is applicable to all the experimental data has been found to be extremely difficult because of the complicating effects of orientation, and of rotation of non-isometric orthotropic bodies. The problem is further complicated by the different character of flow at different Reynolds numbers, by the dependence of free roientation on Reynolds number, and by the vast irregularity and diversity of particle shapes to be considered.

2. Multiparticle

Empirical and analytical approaches to the dynamics of hindered settling have often followed two methods:

i. treating the dynamics of a single particle and trying to extend the result to a multiple particle system by appropriate modification of the boundary conditions, which usually turned out to be some function of the concentration of particles in the fluid (22, 23, 24, 25, 26).

ii. modifying the continuum mechanics of a single phase fluid by treating the suspension as a liquid, the properties of which are altered by the presence of particles (10, 27, 28, 29, 30).

Some empirical equations also resulted from adopting the law of flow through packed beds with certain modifications (31, 32, 33).

The problem of the motion of a swarm of solid spherical particles through fluid has been treated theoretically by various investigators by the approach of method ii. The viscosity of dilute suspension was derived by Einstein (34), and was later adopted by Vand and Hawskley (35, 27) in developing their equation for sedimentation in the viscous region. Their equation was confirmed by Hanratty and Bandukwala (28) to be valid over a certain concentration range for spherical particles. Based on the equation of motion, neglecting the fluid inertia, and on Darcy's equation for fluid flow through packed beds, Brinkman (36) also arrived at a solution for concentrated suspensions which was verified experimentally by Verschoor (37). By modification of the boundary conditions on a fluid flowing past a single sphere, various models have been assumed and studied either analytically or numerically, namely the hexagonal configuration of Richardson and Zaki (26), the free surface model of Happel (22) for viscous region settling, and the numerical solution at higher Reynolds number by LeClair and Hamielec (24) following the model of Kuwabara (23).

An experimental study by Robinson (38) suggested a modification of Stokes' law for predicting the settling rates of a suspension of fine, closely sized particles. Steinour (30), using a similar approach, was able to find the correction factor to account for the change in the properties of the pseudo-single phase suspension due to the presence of particles. Loeffler and Ruth (33) considered that the settling condition should agree with Stokes' law as porosity approaches unity and be similar to flow through a packed bed at a porosity of 0.48,the value assigned to loosely packed spherical particles. By comparison to the Kozeny equation they obtained a porosity dependent correction function which could be incorporated into the free settling equation, Richardson (31) and

Harris (32), respectively, calculated the friction factor for fluid flow through an expanded bed at different concentrations. Oliver (39) also obtained a semi-empirical expression by modifying the stream function for a single spherical body and inserting a correction factor for the viscosity change due to the surrounding particles.

Other empirical expressions based on the approaches stated earlier were also found in particulate fluidization (40, 41, 42).

An overall experimental study of hindered settling and particulate fluidization of spherical particles over a wide range of Reynolds number was undertaken by Richardson and Zaki (43), and later hindered settling of spherical particles was carried out by Gasparyan and Ikaryan (25). The results of both studies were comparable and similarly correlated. Without resorting to any sophisticated hydrodynamics, both pairs of investigators plotted the settling velocity, u, against the porosity, ϵ on log-log coordinates. The slope of the resulting straight line was found by Richardson and Zaki (43) to depend on the free settling Reynolds number, Re_o, of the given uniform-size particles, with extrapolation to a porosity of unity giving approximately the free settling velocity, u_∞ :

$$\frac{u}{u_\infty} = \epsilon^n \tag{1}$$

The exponent n depended on wall effect, in addition to Re_o:

$$n = 4.65 + 19.5\frac{D}{D_t} \qquad Re_o < 0.2 \tag{2a}$$

$$n = (4.35 + 17.5\frac{D}{D_t})Re_o^{-0.03} \qquad 0.2 < Re_o < 1 \qquad (2b)$$

$$n = (4.45 + 18\frac{D}{D_t})Re_o^{-0.1} \qquad 1 < Re_o < 200 \qquad (2c)$$

$$n = 4.45\ Re_o^{-0.1} \qquad 200 < Re_o < 500 \qquad (2d)$$

$$n = 2.39 \qquad 500 < Re_o \qquad (2e)$$

This method of correlation had previously been attempted by Hancock (44). The correlation, though simple, was found to be generally valid in ideal hindered settling without flocculation and particulate fluidization. Fluidization data of Wilhelm and Kwauk (42) and of Lewis et al (40) were also found to be well correlated in this way.

Most of the previous investigations have been done on spherical particles, and occasionally on irregular particles, but without particle shape as a specified variable of study.

The effect of particle shape in particulate fluidization at high Reynolds number has been studied by Richardson and Zaki (43) for non-spherical particles of regular geometrical shape, namely cubes, plates, cylinders and hexagonal prisms. It was found that in the high Reynolds number range, the particulate fluidization expansion data of these particles did not differ very much from the corresponding results for spherical particles. When correlated in exponential form the power n could be related to the Heywood volumetric shape factor:

$$K_V = \frac{\pi}{6}\frac{D_V^3}{D_c^3} \qquad (3)$$

Irregular shape particle hindered settling over a large Reynolds number range was studied by Gasparyan and Ikaryan (45). Using the hypothesis that a layer of immobile fluid clings to the surface of an irregular particle, so as to form a smooth pseudo-particle, they were able to extend their hindered settling equation for spherical particles to irregular particles by means of appropriate correction factors. The so-called "form coefficient" and "volume coefficient" were different for different systems of irregular particles, and thus have to be determined experimentally for any specific particle shape.

In sedimentation of non-spherical particles at low Reynolds number, which often prevails in practical problems, the shape correction factors like those of Gasparyan are not known, and a spherical shape is therefore usually assumed for predictive purposes. However, experimental data in the viscous region of Richardson and Meikle (31) on sedimentation of alumina powder, of Jottrand (46) on fluidization of sand, and of Gasparyan and Ikaryan (45) on sedimentation of crushed basalt, crushed barite, and other irregular particles when correlated in the Richardson-Zaki exponential form,show values of the exponent n significantly different from that for spherical particles in the same Reynolds number range. Thus values of 5.6 were obtained for sand, around 6.5 for crushed basalt particles and as high as 10.5 for alumina powder, compared to 4.65 found by Richardson and Zaki for spheres.

Mueller and Schramm (47) suggested that in the low Reynolds number region, expansion of a fluidized bed of nonspherical particles which possess a maximum length dimension less than 1.5 times the maximum width could be predicted from the same graph which applies to spherical particles; and that only at Reynolds numbers beyond the creeping flow region was a different graph for irregular particles required. The graph presented by these authors can also be found in the textbook by Zenz and Othmer (48), who indicate that the graph was prepared by drawing smooth curves through the experimental data of a number of investigators. The graph is a log-log plot of $(Re/C_D)^{1/3}$ against $(Re^2C_D)^{1/3}$ with bed porosity as parameter. Thus the variables velocity and diameter each appear only on the respective coordinate axes, thereby eliminating the usual trial and error procedure when either of these variables is the unknown.

For convenience, Figure 1 was prepared based on the accepted drag coefficient-Reynolds number plot for single sphere settling (49), and on Richardson and Zaki's empirical equations for hindered settling, assuming no wall effect. The graph appears to be in fair agreement with that of Mueller and Schramm. The variable, diameter, on the abscissa, when applied to a nonspherical particle, was taken by Mueller and Schramm to be the diameter of a sphere having the same volume as the given particle. It is noted that in the creeping flow region ($Re_o <$ approx. 0.2) the lines for each porosity are straight and parallel to each other, and have a slope of 2. This result arises from Stokes' law, which can be put in the form

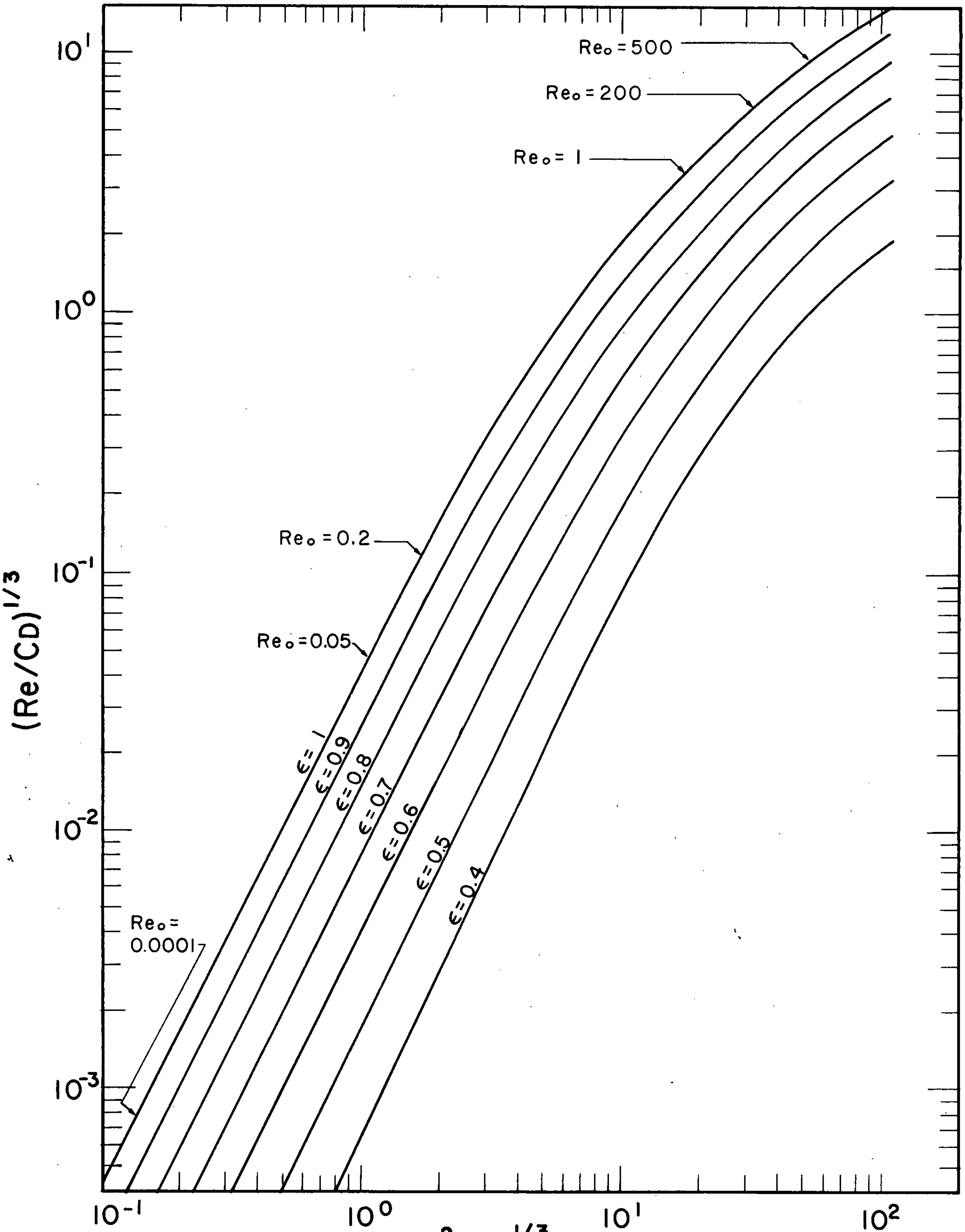

Figure 1. Modified Plot of C_D - Re for Single Particle and Suspension

$$C_D = \frac{24}{Re_o} \tag{4 }$$

or $$\left(\frac{Re_o}{C_D}\right)^{1/3} \propto \left(C_D Re_o^2\right)^{2/3} \tag{4a}$$

The vertical spacing between these lines of different porosity is proportional to the index n of equation 1 and 2, and is constant in the creeping flow region, where n = 4.65. In the light of the few experimental data on nonspherical particles in creeping flow mentioned earlier, the graph obviously does not apply to alumina powder and crushed basalt. Even for nonspherical particles in which the maximum length is equal to the maximum width, for example the data of the present work on cubic salt crystals in creeping flow, the prediction of this graph is poor. It is interesting to note that, on the one hand, Richardson and Zaki's results on artificial nonspherical particles showed a smaller difference between the index n for non-spheres and that for spheres in the high Reynolds number range than in creeping flow, while on the other hand Mueller and Schramm suggested that a separate graph was required for irregular particles only in the region beyond creeping flow.

It can be concluded that no extensive investigation has been done on the effect of shape on the relationship between hindered settling rate and concentration, except possibly in the high Reynolds number range. A study of the particle shape effect, particularly in the creeping flow regions, should therefore be useful and significant.

3. The Work of Beranek and Klumpar

In their paper titled "A New Theory of Fluidization", Beranek and Klumpar (50), in correlating expansion data of fluidized beds, suggested that a plot of $(1-\epsilon)/(1-\epsilon_b)$ against either u/u_∞ or $(u-u_{in})/u_\infty$ was superior to other methods of correlation which did not fit their experimental data. Here ϵ is the porosity of the expanded bed, ϵ_b is the fixed bed porosity corresponding to a random loose packed bed obtained by letting the particles in suspension settle freely until they had reached a constant height, and u_{in} is the incipient fluidization velocity. The term $(1-\epsilon)/(1-\epsilon_b)$ was denoted as "characterizing the geometric similarity". Without using any conventional shape factor, they were able to plot both spherical particle data and irregular particles data, obtained at different free settling Reynolds numbers, on the same curve. However, plotting of data at different free settling Reynolds numbers on a single curve is in principle wrong, since it is well known that dependence of u/u_∞ on porosity for particles of fixed shape (e.g. spherical) varies with free settling Reynolds number. This point becomes more obvious by reference to Figure 2, where the Richardson-Zaki empirical equations for spherical particles are plotted in the manner of Beranek, assumming ϵ_b equal to 0.435.

That Beranek and Klumpar were apparently able to correlate their data on a single curve may be attributed to

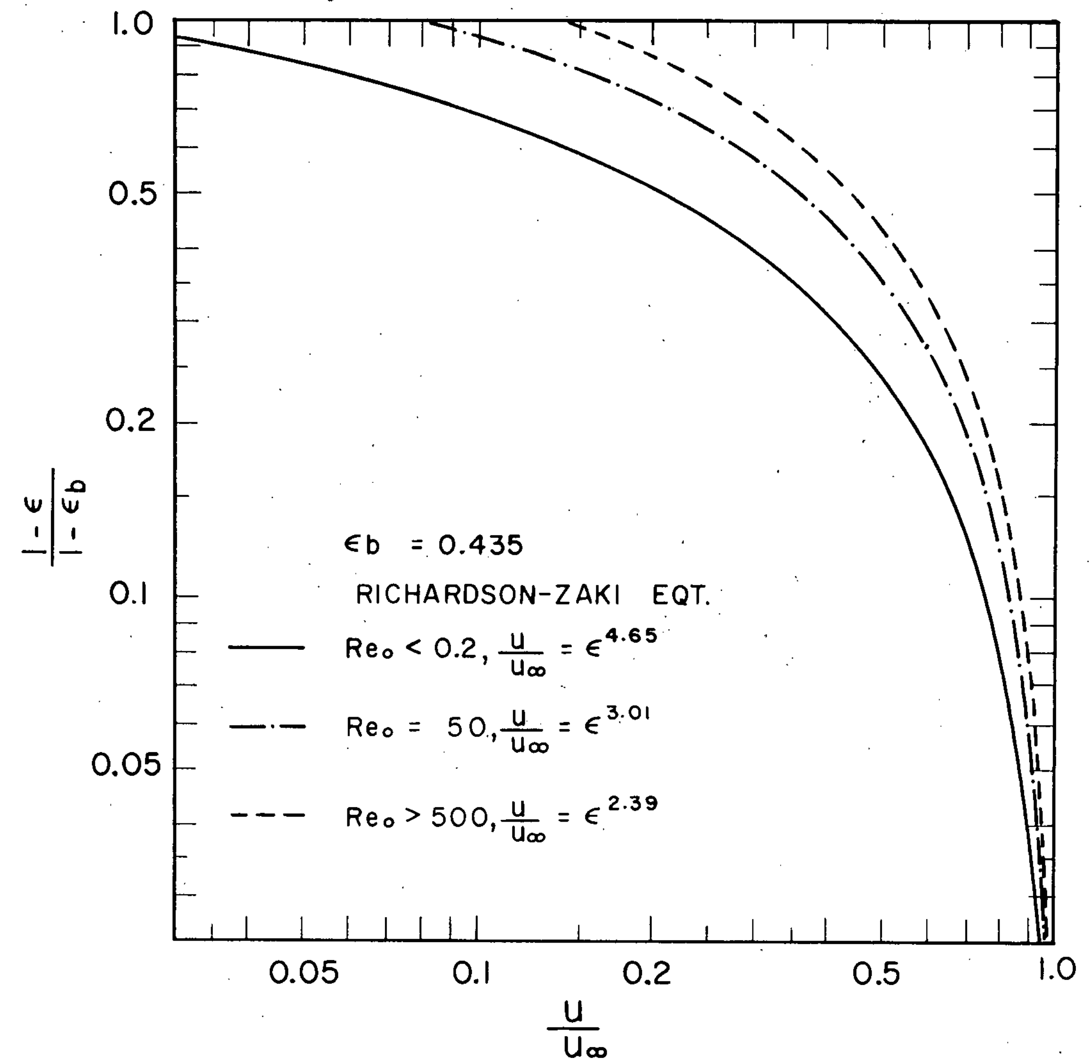

Figure 2. Beranek-Klumpar Plot based on Richardson-Zaki Empirical Equations

the relatively narrow range of free settling Reynolds number covered.

If spherical and nonspherical particle data at similar values of Re_o could really fall on the same curve as suggested by Beranek, it must be ϵ_b which accounts for the shape variation of the particles. Random loose fixed bed porosity has indeed been reported to be related to the sphericity of particles (51). The use of such a fixed bed porosity has the advantage of being much easier to measure than conventional shape factors, and of giving a statistical "shape measurement" without referring to the orientation of particles, which is assumed random in a randomly packed bed.

As the effect of Reynolds number level on the concentration dependence of bed expansion was ignored by Beranek and Klumpar, in fact no conclusion can be drawn as to the validity of their correlation. Furthermore Beranek and Klumpar, in presenting their result, included some data on porous particles, and also the data of Wilhelm and Kwauk(42), whose fixed bed porosity was not for random loose packing. The previously mentioned studies (31, 45, 46) show that hindered settling and particulate fluidization data, plotted in exponential form, give more sensitive variation of index, n, with shape in creeping flow than at higher Reynolds numbers. In the creeping flow region, where the fluid flow behaviour is independent of Reynolds number, comparison of effects due to shape may be simplified. Therefore a study of hindered settling of various shape particles in the creeping flow region, which will be described in this work, should clarify the validity or otherwise of the above stated suggestion by Beranek and Klumpar.

GENERAL THEORETICAL CONSIDERATIONS

1. Free Settling

Consider a single, uniform density particle of size, L settling with a constant terminal velocity u_∞ and constant orientation in an infinite fluid medium of viscosity μ. When the motion is in the creeping flow region, the total drag force on the particle, which consists of both viscous shear forces and pressure forces, is proportional to L, u_∞ and μ, and is independent of the fluid density ρ:

$$F = KL\mu u_\infty \qquad (5)$$

The criterion of flow behaviour is the particle Reynolds number, which is the ratio of fluid inertia to viscous forces and is defined as

$$Re_o = \frac{Lu_\infty}{\nu} \qquad (6)$$

At low Re_o, fluid inertia is relatively unimportant compared to viscous shear, and equation 5 applies at any Re_o within certain limits. The flow is called creeping flow or viscous flow and is characterized by the absence of wakes and of boundary layer separation of fluid behind the particle. Beyond the creeping flow region the fluid inertia can no longer be neglected, and the resistance force on the particle cannot be expressed by equation 5.

A sphere is the simplest shaped particle, the size of which can be described by a single dimension, diameter D, irrespective of its orientation. Equation 5, written for a sphere, becomes

$$F = 3\pi D\mu u_\infty \tag{5a}$$

which can be proved analytically from the equation of motion and has been verified experimentally. The Reynolds number then becomes

$$Re_o = \frac{Du_\infty}{\nu} \tag{6a}$$

In general, for all particle shapes and Reynolds numbers, the drag force is expressed as

$$F = C_D A_p \frac{u_\infty^2 \rho}{2} \tag{7}$$

For a sphere, where A_p is the projected area of the particle normal to the flow axis.

$$C_D = \frac{24}{Re_o} \qquad Re_o < 0.2 \tag{4}$$

$$C_D = f(Re_o) \qquad Re_o > 0.2 \tag{4b}$$

By equating the drag force exerted on a spherical particle to the gravitational force less the buoyancy force on it, the terminal settling velocity of the particle can be calculated as

$$u_\infty = \frac{D^2(\rho_p - \rho)g}{18\mu} \tag{8}$$

which is a familiar special form of Stokes' law applicable to particle motion in a gravitational field.

The more regular particles of interest with shapes other than spherical may be classified into spherically isotropic particles, which have three equal mutually perpendicular axes of symmetry, and orthotropic particles, which possess three mutually perpendicular planes of symmetry and of which spherically isotropic particles are a particular case. Nonspherical particle settling is more complicated than that of spheres because of the unlimited number of orientations which are possible and the variation of translational resistance with orientation. The problem is further complicated by rotation of particles at higher Reynolds numbers, or by shape assymmetry even at low Re_o.

Within the creeping flow region, a spherically isotropic particle settles in its initial orientation and in the direction of the gravitional force. The translational resistance is the same in any orientation and is larger than that on a sphere of equal volume (12). The drag force exerted on a steadily settling particle in creeping flow is then given by

$$F = \frac{3\pi}{K_{ST}} D_V \mu u_\infty \tag{5b}$$

Thus

$$u_\infty = K_{ST} \frac{D_V^2 (\rho_p - \rho) g}{18\mu} \tag{8a}$$

where D_V is the diameter of a sphere of equal volume and K_{ST} is called the Stokes' law shape factor, which was found to be a function of sphericity (12).

An orthotropic particle, if settling in the creeping flow region, will preserve its initial orientation, but will not necessarily fall in the direction of the gravitational force except when its axis is parallel to the gravitational force (14). The translational resistance depends on the orientation for a specified shape particle. A similar Stokes' law shape factor can be derived for some artificial orthotropic particles (14), but since correlation of this factor to sphericity alone is insufficient, such parameters as ratio of axis lengths, and diameters defined in various ways, become necessary to account for the volume and orientation of the particle (14, 15).

Particles without any axis of symmetry and irregular particles, when settling in creeping flow, will rotate and thus rotational resistance arises in addition to translational resistance. Both resistances contribute to the drag force of the fluid exerted on the particle.

Beyond the creeping flow region, settling of a particle may involve spinning, wobbling and other secondary motions, and the particle orientates in such a way that resistance to fluid flow is a maximum, at least for many particles studied (20).

Analytical proofs for creeping flow are available for bodies of revolution like spheres and spheroids. These proofs can be intuitively applied to particles of symmetric shape with plane surfaces, for which analytical solutions are difficult but experimental verifications are possible.

To account for variation in shape, many methods have been suggested for "measuring the shape" of nonspherical particles and their equivalent diameters. The equivalent diameter of a nonsphere has usually been based on a sphere of equal volume, or equal surface area or equal settling velocity, each of which has its own justification on hydrodynamical grounds. Examples are given in Tables 1 and 2.

The Stokes' law shape factor, K_{ST}, has been correlated to the other shape factors, which can be determined by non-hydrodynamic measurements (12). Use of shape factor may be successful for particular shapes, but not generally satisfactory for all shapes, especially when orientation effects are important and other parameters are required.

The measurement of a shape factor such as sphericity is always difficult. As previously mentioned, the fixed bed porosity of uniform size and shape particles has been suggested to be in some way related to sphericity (51). Fixed bed packing, however, does not give an unique porosity for a set of particles. Spheres, for example, give four considerably different porosities corresponding to special geometric arrangements in the bed (53) of which random packing can be considered to be mixtures in varying proportions. Random loose packing however, was found to give roughly a constant porosity.

2. Hindered Settling

In a multiparticle system, the effect of the presence of other particles in the vicinity of the particle must be considered; this effect may be hydrodynamical or mechanical. Richardson and Zaki (43), by means of dimensional analysis and considering the possible effect of the wall on particle motion, arrived at the following grouping of dimensionless quantities

Table 1

Equivalent Diameters

Equivalent diameter	Definition: Diameter of sphere of same
D_V	volume or drag force
D_S	surface area
D_u	settling rate

Table 2

Shape Factors

Shape factor	Variable compared	Fixed variable
$\psi = A_S/A$	surface area	volume or drag force
$\phi = C'/C$	perimeter of projection	projected area
$K_V = \pi D_V^3/6D_c^3$	volume	
$K_{ST} = u_\infty/u_V$	settling rate	volume or drag force

for spherical particles:

$$\frac{u}{u_\infty} = \phi\left(\frac{Du_\infty}{\nu}, \frac{D}{D_t}, \epsilon\right) \tag{9}$$

where ϵ is the porosity of the bed. The empirical equations were presented in the form

$$\frac{u}{u_{ext}} = \epsilon^n \tag{1a}$$

where u_{ext} is the velocity obtained by extrapolating the log-log plot of settling rate versus porosity to a porosity of unity, and was found to be approximately the same as the free settling velocity of a single particle in an infinite medium. Thus, multiparticle settling is related to free settling by a correction term which is a function of porosity. In the creeping flow region, $Re_o < 0.2$, this function does not vary with Re_o, and equation 1a becomes

$$\frac{u}{u_{ext}} = \epsilon^{4.65} \tag{1b}$$

when wall effect is negligible. The function varies with Reynolds number beyond the creeping flow region.

Analytical solutions of creeping flow hindered settling have been proposed (22, 23, 24, 26) based on some idealized models. The agreement with experiment is not entirely satisfactory, the experimental results always showing higher settling rates than predicted. Two particles settling represents a particular case of multiparticle settling. Both analytical and experimental results, in good agreement (10) with each other, have shown that mutual interference of two spherical particles always reduces the drag force on the particles, and consequently the settling rate is faster than the free settling rate. This result is in apparent contradiction to equation 1a, considering porosity as fractional volume of fluid unoccupied by solid. It is therefore suggested that when the number of particles is small, for example at high porosity, the general equation for an "infinite" number of particles should not be applied.

In analysing spherical particle hindered settling it is always assumed that the hindrance effect is essentially hydrodynamical, and also that the spheres do not rotate, though rotation does not affect the drag force appreciably in viscous flow. For nonspherical particles, however, even free settling may involve non-vertical motion and rotation. Thus the hindered settling rate may be further changed by mechanical contact between particles, in addition to pure hydrodynamic interference caused by neighbours. Analysis which includes the possible effects of rotation and orientation of an infinite number of nonspherical particles may be rather complicated. Even in the diverse studies of spherical multiparticle systems, the conclusions are not unique. An investigation of the effect of shape on hindered settling in creeping flow is therefore reasonably restricted to an experimental study on uniform particles of various available, suitable shapes. This study was confined to the constant rate sedimentation period, the universal existence of which for uniform size particles can be justified even on theoretical grounds (see Appendix I).

3. Wall Effect

The wall effect on a single particle arises from the backflow of liquid which is displaced by the settling particle in a vessel with a finite boundary. In the creeping flow region, when a sphere settles axially along a tube, the actual drag force on the sphere (10) is given by

$$F' = \frac{F}{1-k(\frac{D}{D_t}) + o(\frac{D}{D_t})^3} \tag{10}$$

where F is the drag force on a sphere settling in an infinite medium given by equation 5a and k has a numerical value of 2.104. The sphere settles without rotation in this center location. At any other (eccentric) position, however, a torque is exerted on the sphere and it rotates in one direction or another while settling. Consquently k changes in accordance with the radial location of the particle. The value of k decreases very slightly (about 3%) when the location of the sphere changes from the cylinder axis to a distance from the axis equal to 0.4 of the cylinder radius. Further eccentricity causes an abrupt increase in k. Nonspherical particles, besides undergoing rotation, may also drift sideways. The same correction for wall effect as for spheres is applicable to nonspherical particles if D_v is used as the characteristic diameter of the particle (54). The approximate form for equation 10, obtained by performing the division and neglecting higher orders of D/D_t, is

$$F' = F(1+k\frac{D}{D_t}) \tag{11}$$

The corresponding correction for free settling velocity is

$$u_\infty = u_o\left(1 + k\frac{D}{D_t}\right) \tag{12}$$

The latter was found to be valid at low D/D_t (<0.1) in the creeping flow region (55). At higher Reynolds numbers wall effect becomes less significant. The problem, taking into account fluid inertia, has been studied by Faxen and others (10).

Wall effect in multiparticle settling has not been solved theoretically. Richardson and Zaki have attempted to include the wall effect for sedimentation of spheres in the index n of equation 1. The same trend as for free settling was found, with wall effect being important at low Reynolds numbers and absent at high Reynolds numbers.

EXPERIMENTAL

1. Variables Studied

The main object of the experimental work was to investigate the effect of particle shape on hindered settling in creeping flow and testing the correlation of Beranek and Klumpar. Other effects such as segregation, which was found to have an appreciable effect on settling behaviour, were to be avoided as far as possible. The experimental data collected were hindered settling rate, u, and the corresponding bed porosity, ϵ. Fixed bed porosity, ϵ_b, is required for the Beranek-Klumpar plot. Since estimated free settling rate was found to be obviously different from the extrapolated value, u_{ext}, at porosity of unity, data on free settling rate, u_o, were collected for spherically isotropic particles. The possible effect of the boundary on settling was studied by performing tests on the same systems in columns of different sizes, the highest value of D_v/D_t being 0.045.

2. Materials

A. Particle Selection

It was desirable to have particles of uniform shape and size, a requirement which was impossible to fulfill absolutely. The criteria used for selecting particle size may be described as follows. On the one hand, the size had to be large enough so that such electrostatic effects as flocculation were negligible and individual particle shape could be easily observed. On the other hand, a preliminary test showed that with the experimental method adopted, the particle size had to be relatively small in order to get uniform suspension of the particles. To assure that settling was in the creeping flow regime, an extremely viscous liquid was required for the larger particles. Agitation of the suspension then became difficult. Another objection to the use of large particles was that the relatively large wall effect possibly present in creeping flow might overshadow the effect of particle shape. The initial idea was to manufacture a large quantity of artificial particles cut from square and round rods. Because of the lengthy fabrication time required, however, use was instead made of natural or commercially available particles which conformed to the above requisites as far as possible and, in addition, were of homogeneous density, free running, non-hygroscopic and insoluble in an appropriate settling medium and washing liquid.

B. Discussion on Segregation

Perfectly monosize particles are practically impossible to obtain by various methods of sizing. The degree of segregation by size will be different for different size distributions, and will be attenuated at higher particle concentrations. Kaye and Davies (56) reported that segregation by size was observable visually in the settling of a binary mixture of two sets of particles having a mode mean size distribution ratio of about 1.3, when the porosity was higher than 0.6. Binary mixtures from two consecutive fourth root series Tyler Screens have been observed to give size segregation in fluidization (57).

In a preliminary test it was found that a mixture of sized salt particles from two consecutive fourth root series screens, the smaller fraction of which was colored, displayed minor size segregation up to a porosity of 0.87. Visual observation during settling was difficult. However, the final sediment showed the colored smaller size particles concentrated in the top portion of the bed. A quantitative comparison was obtained by simultaneously settling in similar cylinders 35/42 mesh mineral particles and a 90% mixture of the same material with 10% 42/48 mesh particles, the next smaller size in the fourth root screen series. The results, plotted in Figure 3, show that the effect of size distribution was significant, especially at high porosity. This result emphasized the necessity of using closely sized particles.

The effect of particle size distribution was carefully studied by Loeffler and Ruth (33) using spherical particles. They found that fourth root series screen fractions, with a maximum size distribution of less than 20%, settled at the same rate as carefully ground spheres which had a diameter variation of only 5%. Thus fourth root series screens are capable of producing "monosize spheres" as far as hindered settling is concerned.

C. Separation of Particles

Two methods of separating particles were used: conventional sieving on Tyler fourth root series screens and liquid elutriation. Liquid elutriation, which separates particles by differences in hydrodynamic drag, was introduced in addition to sieving, since particles of different shape may not be well separated by sieving.

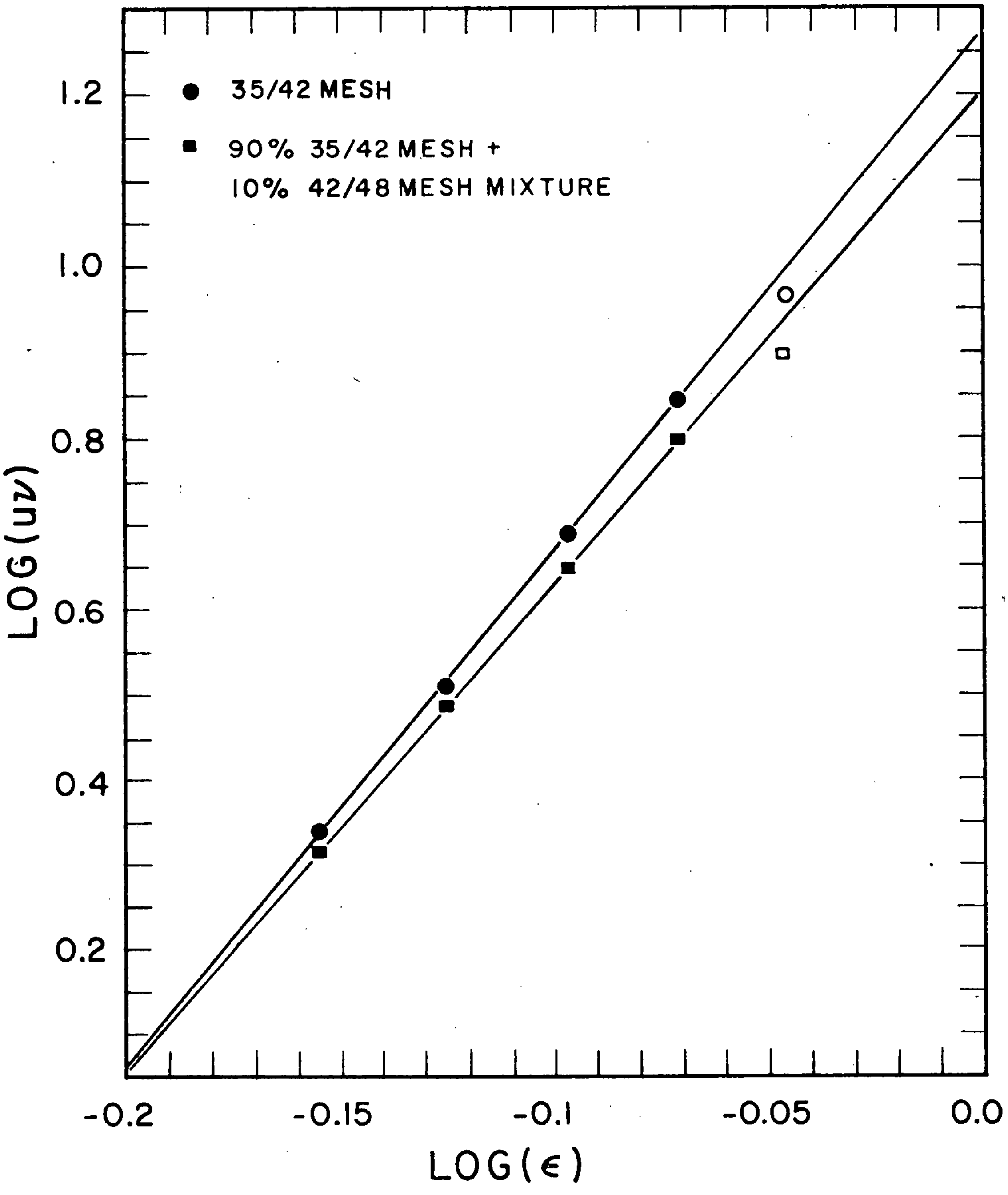

Figure 3. Comparison of Settling Rates of Different Size Distributions of Particles

In sieving, about 400 grams of solid was introduced on to the top screen. After the first sieving, the particle fractions were collected and further screening was performed on these primary fractions, using 100 gram samples obtained by combining like fractions from several primary screenings. Subsequent sieving was carried out for 10-minute intervals, until the change in weight of each particle fraction became negligible. Blind sieves were cleaned after each sieving. Sieving was performed on a Ro-tap shaker.

D. Liquid Elutriation

Liquid elutriation is fundamentally particulate fluidization at high porosity, where segregation by size is prominent. It was carried out in a glass column of 4.6 cm. I.D., equipped with a supporting screen S, and a screen gate G, as shown in Figure 4. Liquid was stored in jar A and was pumped to the column F through an explosion-proof centrifugal pump P. The flow rate of liquid was controlled by a diaphragm valve D. The liquid, after passing through the column, was returned to the storage jar from the overflow H. Pump heat was removed by the water cooling coil C. The fine particles carried over by the liquid were collected on screen B. Detailed description of the elutriation apparatus and its testing is reported in Appendix II. The method was capable of separating spherical particles of different size as effectively as fourth root series Tyler screens.

The particles which underwent elutriation were all sieved as described above. An appropriate quantity of particles

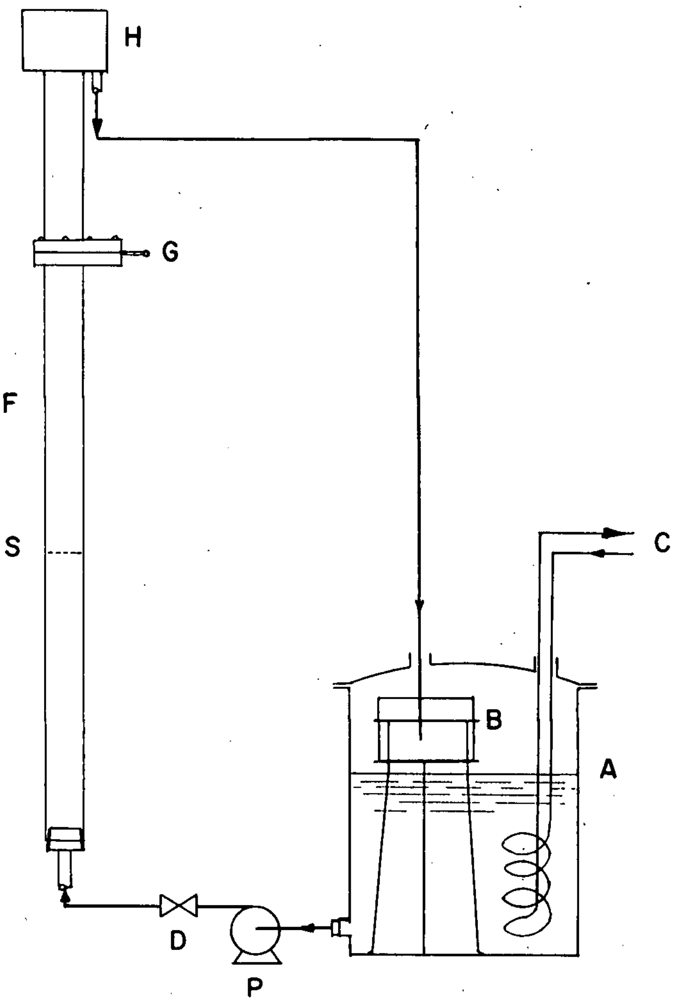

Figure 4. Schematic Drawing of Liquid Elutriation Apparatus

to make a fluidized bed of porosity about 0.95 in the available length was introduced into the column. Cooling water was turned on and elutriating liquid was circulated through the unit, its flow rate being controlled by adjusting the valve.

The quantity of particles to be removed was determined roughly by trial and error on the first batch of a given set of particles. In a trial, the total height of the fluidized bed of a certain quantity of particles was recorded before closing the screen gate to remove the "smaller" size portion. After the screen gate was closed, the column was disassembled and those particles on top of the screen gate were recovered. The remaining particles were tested for segregation by fluidizing in the same column. The topmost part of the bed was again collected by the screen gate, colored, and re-inserted into the column. If visual segregation was observed, further trials were performed which involved fluidizing the total original particles to a larger bed height, which was recorded, and removing a larger quantity of particles than in the previous trial, until no visual segregation could be observed in the remaining particles. Other batches of the particles were separated by fluidizing the same weight of particles to the final recorded bed height and closing the screen gate.

E. Description of the Particles

Five kinds of particles were used. They were: spherical glass beads, cubic salt (NaCl) crystals and cubic ABS copolymer pellets, both of which are isometric and spherically isotropic, flaky sugar crystals, and imperfect octahedron-shaped mineral (silicate) crystals (henceforward referred to as mineral crystals). Their properties are described in Table 3, and their shapes are illustrated in Figure 5.

Table 3

Properties of Particles

Particle shape	Materials	Size, D_v cm	Density g/cm^3	Run No.
Spherical	glass beads	0.0492	2.959	7
		0.114	2.977	1,2
Cubic	salt crystals	0.0282	2.161	5
		0.0341	2.169	3
		0.0391	2.163	4
	ABS pellets	0.288	1.061	6
Flaky	sugar crystals	0.113	1.590	12
		0.135	1.590	11
Angular	mineral crystals	0.0426	2.632	10
		0.0508	2.632	9

The glass beads were practically spherical. Most of the salt crystals were cubic in shape, with rounded off corners. A few twin crystals were present. The ABS pellets, which had been originally chopped from plastic rods and occasionally contained pores within the particles, were used without further treatment. They were not perfect cubes, but they were uniform in shape and size. The sugar crystals did not have any plane of symmetry and

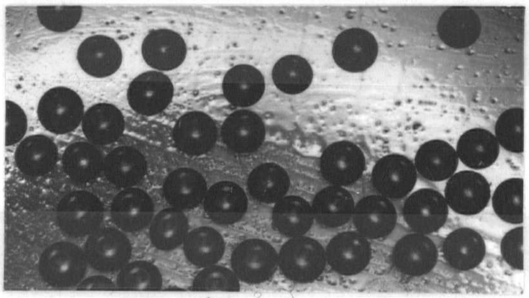

x12

Glass beads, Run 7-3

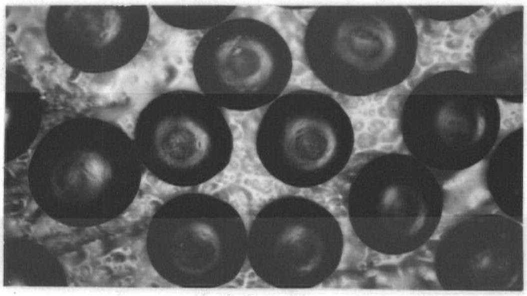

x12

Glass beads, Run 1,2-

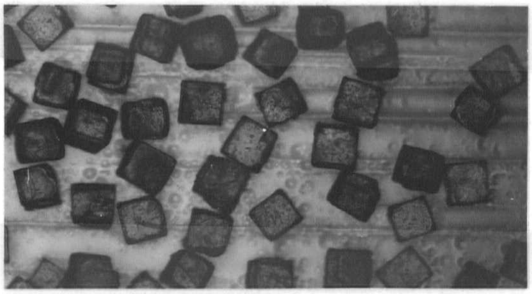

x24

Salt crystals, Run 5-3

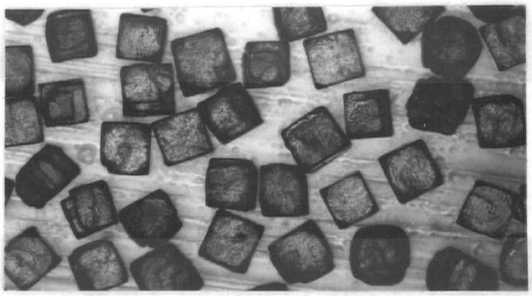

x24

Salt crystals, Run 3-

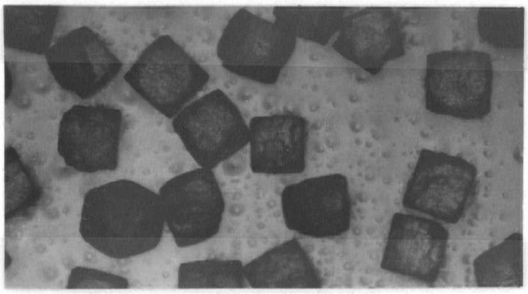

x24

Salt crystals, Run 4-

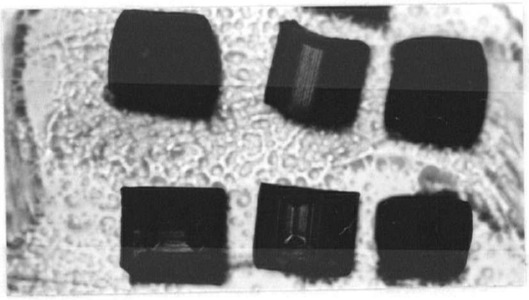

x5

ABS pellets, Run 6-

Figure 5. Photographic Pictures of Particles

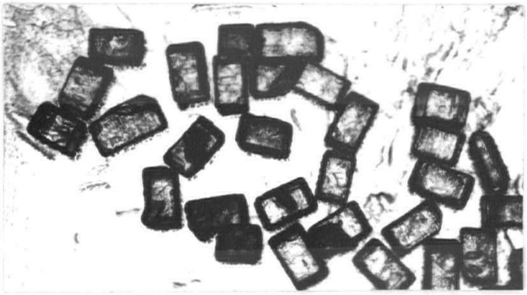

x5

Sugar crystals, Run 12-3

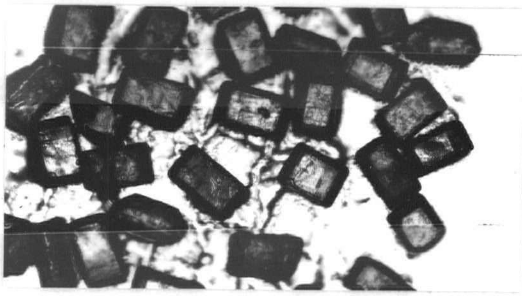

x5

Sugar crystals, Run 11-

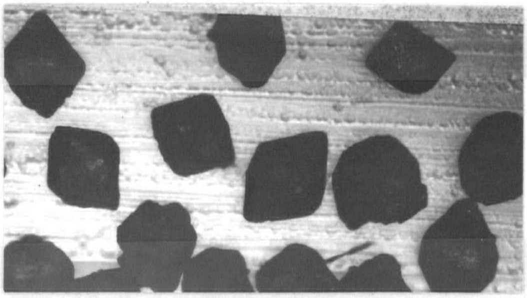

x24

Mineral crystals, Run 10-

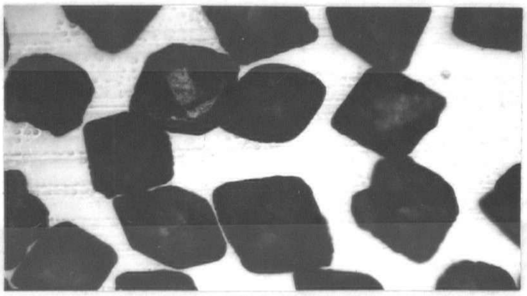

x24

Mineral crystals, Run 9-

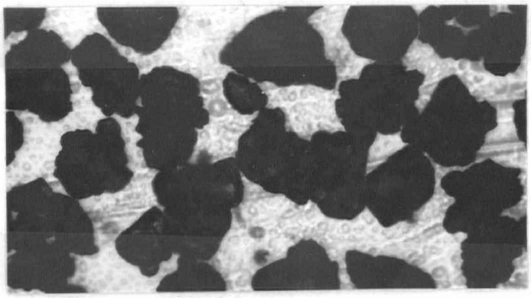

x24

Discarded mineral crystals from liquid elutriation, Run 10-

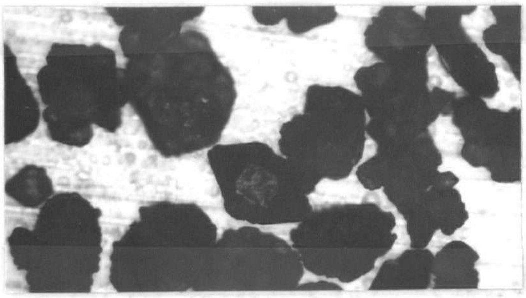

x24

Discarded mineral crystals from liquid elutriation, Run 9-

Figure 5. Photographic Pictures of Particles (continued)

differed markedly from spheres or granules; and the mineral crystals of imperfect octahedron had one axis grown longer than the other two and appeared to be less uniform than the other particles. The particles other than the glass beads and the sugar crystals had microscopically rough surfaces, but the protuberances were small compared to the particle dimensions, and it is therefore likely that the particles were hydrodynamically smooth.

The behaviour of spherical particles was used as a basis for comparison with other work on the same shape and with the behaviour of particles of different shape. Cubic particles were used because cubes are spherically isotropic, and because free settling results for such particles are available in the literature. Thus comparisons will be more significant.

The glass beads and salt crystals were sized by sieving; subsequent elutriation did not show improved separation. Sugar crystals and mineral crystals were sieved before elutriation. The raw particles of sugar contained some broken crystals, besides being contaminated by other brittle needle-shaped material which could not be completely removed by sieving. The mineral crystals contained some irregular particles with rough surfaces, which were still present after sieving. These unwanted particles of odd shape or size were removed by liquid elutriation. Benzene was used as an elutriation liquid. About 10-20% of the particles were removed by elutriation from each set after sieving.

F. Test Liquids

The test liquids had to be Newtonian fluids and to preferably show viscosity stability with respect to time of storage. Test liquids used were water solutions of polyethylene glycol, and blended solutions of different grades of automobile crank case oil for those particles which were soluble in aqueous solution. The advantages of these liquids was that the desired viscosity could be obtained by suitable blending. The oil solutions, which were miscible mixtures of two Newtonian hydrocarbon liquids, were naturally Newtonain liquids. The 45% polyethylene glycol-water solutions were tested and found to behave as Newtonian liquids, at least in the experimental range. Details are given in Appendix III.

3. Apparatus

Settling was carried out in two-foot long, flat-bottomed glass columns with vertical cylindrical walls. The bottom ends of the columns were closed by flat blind flanges. Diameters of the glass columns did not vary significantly in different directions, and the column walls were practically straight. Thus the final bed porosity could be calculated by measuring the final bed height, knowing the weight and density of the particles. The top ends of the column were fitted with threaded flanges, which were accessible to threaded plexiglass plugs. The bottom surfaces of the plugs were slightly conical and the apexes were fitted with venting valves so that trapped air and excess liquid could escape on tightening. Holes of appropriate size were drilled in the top and bottom flanges at accurate positions for mounting. Paper scales graduated to one millimeter were fixed to the column, and several movable hairlines made from cellophone were provided for easy visualization during timing.

Five columns of different internal diameters were available, in order to obtain results at different particle to column size ratios. The mean diameter of each column was determined from direct measurement of diameters in different directions. The volume of each column was calculated from the weight of water which filled the empty column. The diameter and volume of each column is shown in Table 4.

Table 4

Dimensions of Settling Columns

Column No.	Mean inside diameter, cm	Volume cm^3
1	2.54	313
2	3.78	692
3	5.08	1250
4	7.71	2877
5	10.12	4893

The assembly of the apparatus is shown in Figure 6. Each column was mounted on the supporting frame, with space allowable for more than one column to be tested simultaneously, and was carried on an angle iron rack at pivot, 6. The

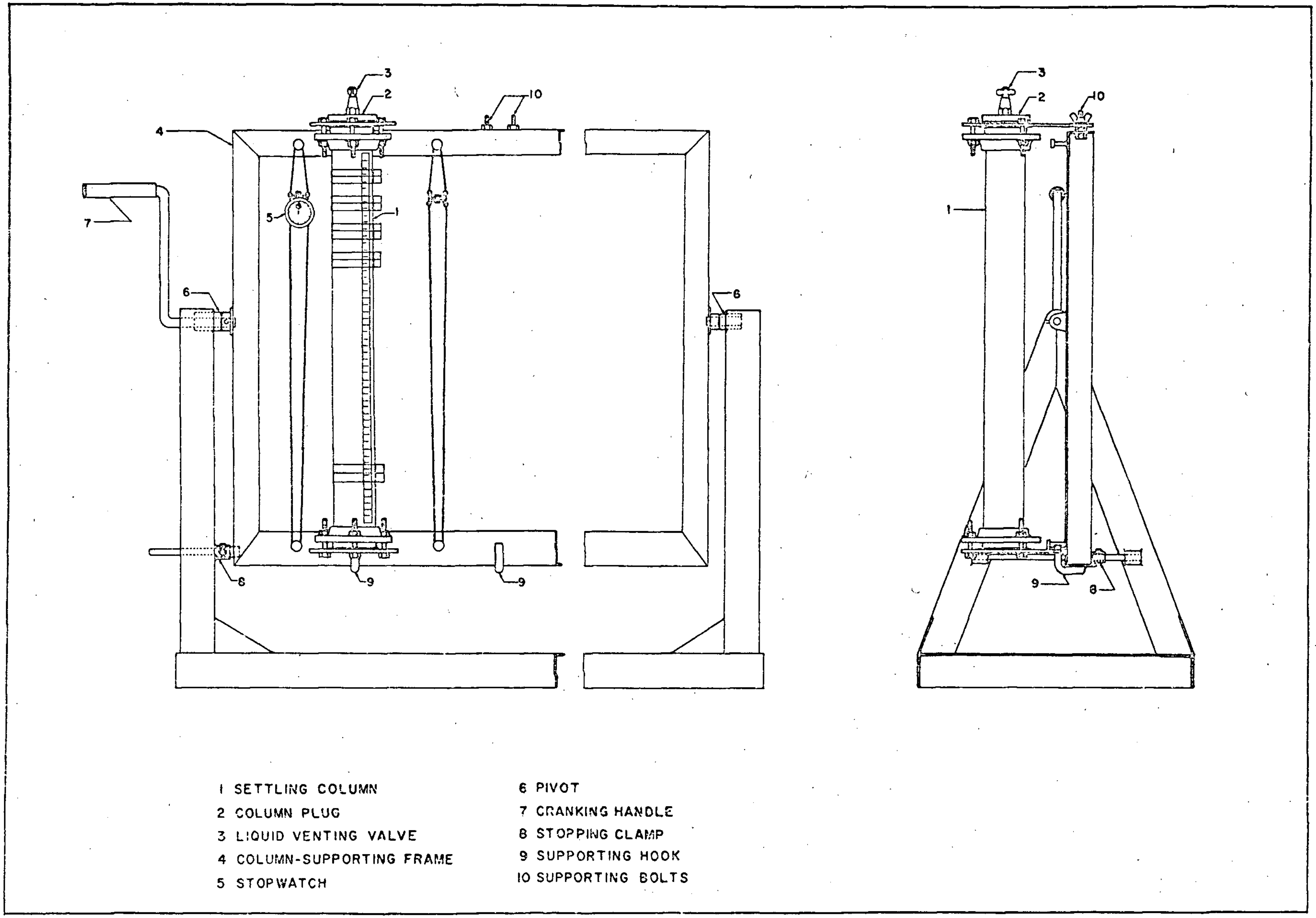

Figure 6. Assembly Drawing of Settling Apparatus

supporting frame could be cranked by handle, 7, and set vertical by the stopping clamp, 8, which was released during cranking. To assure a vertical position of the column during settling, the unit was placed on a horizontal surface adjusted by a level. Hooks, 9, and bolts, 10, were accurately located during fabrication in such a position that any of the columns was in a vertical position when mounted on it. The position of the stopping clamp was adjustable for vertical alignment of the columns.

4. Experimental Procedures

A. Particle Size Measurement

Particle sizes were measured by three different methods. Small samples of appropriate size were obtained by means of a sample splitter.

a. A sample of about 1000 particles was collected, counted and weighed on an analytical balance. From the known density of the particles, the average volume of a single particle was calculated. The average size of the particles could then be easily calculated if a particle shape was defined in the first place.

b. Particles from a sample were settled one at a time in the same liquid as used for the hindered settling runs, at the center position of one of the larger glass columns. The temperature of the liquid was recorded along with the settling rate. From the average value of $u\nu$, a particle size could be calculated.

c. Samples of glass beads and salt crystals were measured on a microscope equipped with a prism to project the enlarged picture of the particles onto a ground glass screen. With a suitable combination of lenses, the size of the enlarged particles pictures, which were of the order of an inch, could be measured by Vernier calipers. The glass beads were measured in an arbitrary but consistent direction. The salt crystals were measured in both directions parallel to their two edges. The measurements were calibrated against a gage of size 1 mm., the image of which was projected onto the screen and measured similarly. This measurement is reported in Appendix X.

B. General Procedure

Experiments were set up to find the hindered settling rate at various bed porosities, as well as the final settled bed porosity, of homogeneous particles of different sizes and shapes. It was essential that the initial particle suspension had uniform concentration corresponding to the overall voidage throughout the column, and that the column was in a vertical position during settling. The viscosity and density of liquids were respectively measured by Cannon-Fenske viscometers and Westphal balance. The particle density was determined by conventional specific gravity bottles. These measurements are described in Appendix IV. The routine procedures used were as follows:

a. Samples were taken from the specified set of particles in order to measure particle size.

b. Density of the particles was also measured. The quantity of particles required for a column to attain the highest desired porosity, and the subsequent increments required for specified lower porosities, were weighed on a scale having a sensitivity of at least $\pm$ 0.05 grams. The possible accumulated error in weight was checked by weighing the particles remaining.

c. Based on the measured physical properties of the solid and the approximate density of the test liquid, the required viscosity of the liquid for creeping flow was estimated; and from a pre-composed empirical chart of viscosity vs. concentration of liquid solution, a suitable quantity of test liquid was prepared with the required concentration. The liquid density at room temperature was measured, as was the viscosity at intervals of $1^{o}F$. over the maximum conceivable range of room temperature to be encountered in the experiments.

d. The particles required for the highest porosity were soaked in the test liquid. The suspension was agitated on the supporting frame by cranking to get the particles completely wetted. A short period of standing was allowed for entrained tiny air bubbles to be released from the liquid. The column was then filled with excess liquid, which was vented through the venting valve when the plug was tightened to exclude air from the system. Agitation was started again until particles and liquid came to thermal equilibrium with the room temperature. The temperature of the liquid was then measured by the same thermometer which had been used in the viscosity measurements.

e. The column was cranked carefully with an appropriate speed and constant observation until uniform suspension throughout the column was believed to have been attained. It was then set vertically. Timing began after the supernatant-suspension interface had fallen several centimeters. Two stopwatches, one of which hung on the string beside the column, were started. Height of interface and corresponding time were recorded constantly. After a certain height, estimated to be within the constant settling rate range from a first trial, the non-hanging watch was stopped, while the one on the string was still used for recording height and time. Observation of particle motion circulation was reported. Those trials which had obvious circulation were discarded.

f. The timing was usually repeated at least once if the result was satisfactory by the criteria of no obvious circulation and constant rate settling. Otherwise more trials were performed.

g. The temperature of the liquid was measured after every two trials. Air was excluded from the liquid after each opening and retightening of the plug for temperature measurement. Final bed height and approximate duration of settling were recorded after the suspension had settled for a long period.

For experiments on lower porosities, increments of particles were added and the procedure from step d. was repeated.

C. Experimental Technique and Settling Data Selection

After the column was set vertical from its rotary cranking motion, circulation of the suspension was often observed, the direction being always opposite to the direction of cranking. An unreproducibly high settling velocity would then result. The circulation phenomenon, illustrated in Figure 7, may be explained as follows.

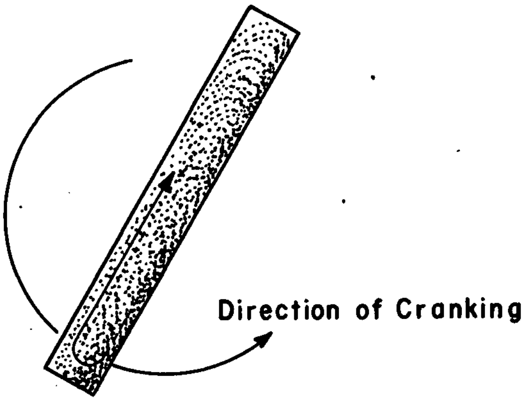

Figure 7. Illustration of Suspension Circulation

Before the column is set vertical, it is in an inclined position, during which particles start settling onto the lower side of the column wall. Because of the obstruction offered by the wall, the particles can only move by "sliding down" along the wall to the bottom of the tube, the liquid displaced being forced upward along the upper wall and thereby creating circulation in the opposite direction to the cranking. By the time the column has been set vertical, this motion still persists until its force is fully damped.

Circulation in the dilute suspension was more vigorous than that in the concentrated suspension, but both cases could result in a faster initial settling velocity than without circulation and invalidated the assumption of uniform initial concentration. Circulation diluted the upper portion of the bed and undoubtedly also introduced unpredictable forces on the particles.

The circulation trouble caused by the cranking motion was minimized by cranking with a suitable speed and watching the tendency for circulation. The column was set vertical with a gentle action, but when the suspension tended to circulate, the column was swung slowly in the opposite direction to a slight inclination in such a way as to produce an opposing circulation, after which it was again gently set vertical. This technique was successful in damping the circulation tendency. For fine particles, the motion and concentration distribution of which were difficult to visualize by eye, some of the particles were colored.

Any inclination of the column during settling also caused circulation to develop, even if the above method did avoid circulation at the beginning. This phenomenon had been noted by Pearce (58). The vertical positioning of the column was therefore checked by a level.

The experimental method adopted was successful in excluding air from the column. In the viscous liquid, a large air bubble always introduces a diffuse interface during the early stage of settling, while tiny air bubbles which rise slowly during settling can interfere with the downward moving particles. The speed of cranking was important to get a uniform suspension throughout the column. When it was too fast, a centrifugal action was introduced and concentration of the suspension at both ends was observed visually, while if it was too slow, the particles would either concentrate at one end or keep on circulating about the middle part of the column. Acceptance of data which conformed to the requirement of uniform concentration was by indirect judgement, based on the sedimentation theory discussed in Appendix I. Irrespective of the mode of the settling flux-concentration curve, any initially uniform suspension should have an initial period of constant settling rate, which corresponds to the specified concentration. The height versus time plot should therefore have a straight line section at the beginning, for the duration of the constant rate period. In the present experiments, height versus time was plotted for each trial. An example of such a plot is included in Appendix XII. Those tests with initial settling curves concave upward (implying more concentrated suspension at the lower end of the bed) or concave downward (implying the opposite) were discarded. The settling rate of a test was then calculated from corresponding height and time intervals within the initial constant rate settling period. It was found that the reproducibility by this selection method was acceptable, standard deviation being rarely higher than 5% and usually within 3%.

D. Data Processing

Because the temperature was not controlled, viscosity of the liquid varied among the tests on a given porosity, besides varying from one porosity to another. In order that viscosity not become an additional parameter in the correlation of settling rate with porosity, the product $u\nu$ instead of u alone was treated as a variable independent of temperature, as shown in Appendix VI. For those tests in which temperature variation was noted, the arithmetic mean of the temperature before and after a test was used to calculate the viscosity. The viscosity at any temperature was obtained by linear interpolation from a series of temperature-viscosity data which bracketed the experimental temperature. Temperature had much effect on viscosity of the test liquids, a change of about 3 per cent per ^{o}F. being typical. In the final correlation the average value of $u\nu$ at one porosity was used.

Similarly, in calculating the size of particles from several measurements of free settling velocity, $u\nu$ was averaged as a product instead of u and ν individually.

RESULTS AND DISCUSSION

1. General

Experimental results for $u\nu$ at different porosities for various runs on different shapes and different particle-to-column diameter ratios are reported in Appendix VII. For each run, average values of $u\nu$ at each porosity were plotted as log $u\nu$ against $\log\epsilon$. It was found that a straight line could be drawn through the data if one or a few points in the dilute region were left out in the curve-fitting. The best straight lines were drawn through the data by the least squares method, using $\log\epsilon$ as the independent variable. Those data in the dilute region which had to be left out in the straight line fitting were obvious from the plot. They invariably turned out to be more than 6% lower than the values from the accepted best fit equation. For the runs like Run 11- and Run 12-, where the data were intrinsically more scattered, data in the dilute region which deviated slightly more from the estimated best fit values were still accepted.

Results were presented in the above form because of its simplicity. Data on sedimentation and particulate fluidization collected from the literature (29, 30, 33, 42) showed that, by discarding a few data in the very dilute and very concentrated regions, straight line fitting was acceptable even at higher Reynolds numbers. By correlating in this manner, particle shape and particle-to-column diameter ratio were expected to show their effect in the index n.

The processed data are presented in Appendix VIII. The slopes of the fitted straight lines in the log $u\nu$ -$\log\epsilon$ plots, and their respective 95% confidence limits, were calculated. The possible effect of the wall was studied by comparing the results obtained for different particle-to-column diameter ratios.

The value of $(u\nu)_{ext}$, obtained by extrapolating the least squares lines to a porosity of unity, and their respective 95% confidence limits, were calculated and compared to the experimental free settling results (Appendix IX) for the glass beads, salt crystals and ABS pellets, the shape factors of which were all known. The corresponding Stokes particle sizes were compared with microscopic size measurements (Appendix X) and results from weighing particle samples.

The method suggested by Beranek and Klumpar (50), that of using fixed bed porosity in order to account for shape variation in correlating settling data on particles of different shapes, was tested.

According to equation 2a, using D_v as particle diameter, a linear relationship exists between log u and D_v/D_t at a fixed porosity. Thus, for the present linear extrapolation of log $u\nu$ versus D_v/D_t to zero D_v/D_t, at constant ϵ, should eliminate any wall effect present. However this method is not appropriate to the present data because of the variation of $u\nu$ within a test, and because of the limited number of values of D_v/D_t available, which may give rather uncertain extrapolation.

The variation of $u\nu$ in the original data might be due to experimental error, including the difficulty of getting absolutely uniform suspensions. From the respective average values of $u\nu$, a wall effect appears to manifest itself, but not prominently.

The results for the five kinds of particles are presented below. In all log $u\nu$-logϵ plots, solid points were not used in the curve-fitting calculation.

2. Index n for Hindered Settling

A. Spherical Glass Beads

The settling data are plotted in Figures 8a-8g, and a summary of results from Appendix VIII is given in Table 5, which shows the least squares values of the index n, with their respective 95% confidence limits.

The measured values of n for the glass beads were all lower than those suggested by Richardson and Zaki (43) with wall correction (equation 2a), but slightly higher than the Richardson-Zaki value of 4.65 without wall correction. For all but Run 7-3, the calculated Richardson-Zaki indices, assuming wall effect, lay outside the 95% confidence limits of the experimental values.

In Figure 9, average values of $u\nu$ for the same set of particles settling in columns of different sizes are compared for wall effect. The qualitative trends seem to be reasonable except in the case of Runs 1-2 and 1-3, the positions of which appear reversed.

Values of n for different particle-to-column diameter ratios are plotted in Figure 10, with the line recommended by Richardson and Zaki (43) included for comparison. The reason why the values of n in the present experiments are different from those of Richardson and Zaki is probably the rigorous criterion for accepting or rejecting settling data used here, as opposed to the methods of either simply timing an initial sett-

Table 5

Summary of Results for Spherical Glass Beads

Run No.	D_V, cm	D_V/D_t	n with 95% Confidence limits	Eqt. 2a, n = 4.65 + 19.5 D/D_t
1-1	0.114	0.045	4.97 ± 0.35	5.53
1-2		0.030	4.83 ± 0.11	5.24
1-3		0.022	4.82 ± 0.09	5.08
2-1		0.045	4.68 ± 0.32	5.53
2-2		0.030	4.74 ± 0.37	5.24
2-3		0.022	4.67 ± 0.16	5.08
7-3	0.0492	0.0097	4.69 ± 0.16	4.84

Table 6

Summary of Results for Cubic Particles

Particles	Run No.	D_V cm	D_V/D_t	n with 95% Confidence limits
Salt	5-3	0.0282	0.0056	5.45 ± 0.08
	3-1A	0.0341	0.0134	5.54 ± 0.12
	3-2		0.0090	5.50 ± 0.09
	3-3		0.0067	5.38 ± 0.07
	3-4		0.0044	5.24 ± 0.06
	4-2	0.0391	0.0103	5.55 ± 0.07
	4-3		0.0077	5.49 ± 0.05
ABS	6-4	0.288	0.0374	5.44 ± 0.13
	6-5		0.0285	5.45 ± 0.22

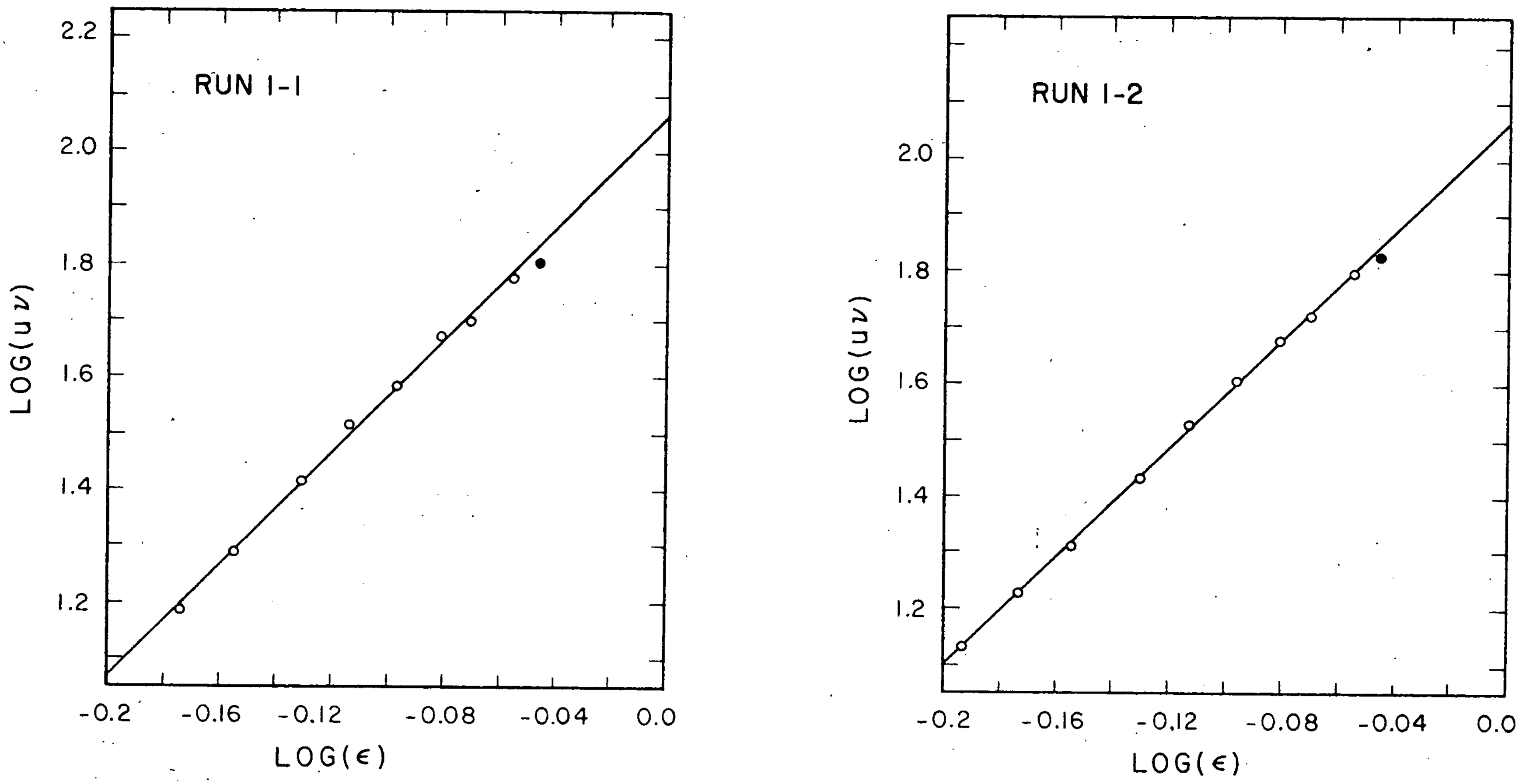

a. D_v = 0.114 cm, D_v/D_t = 0.045

b. D_v = 0.114 cm, D_v/D_t = 0.030

Figure 8. Log$u\nu$-logϵ Plot of Glass Beads in 40 % PEG

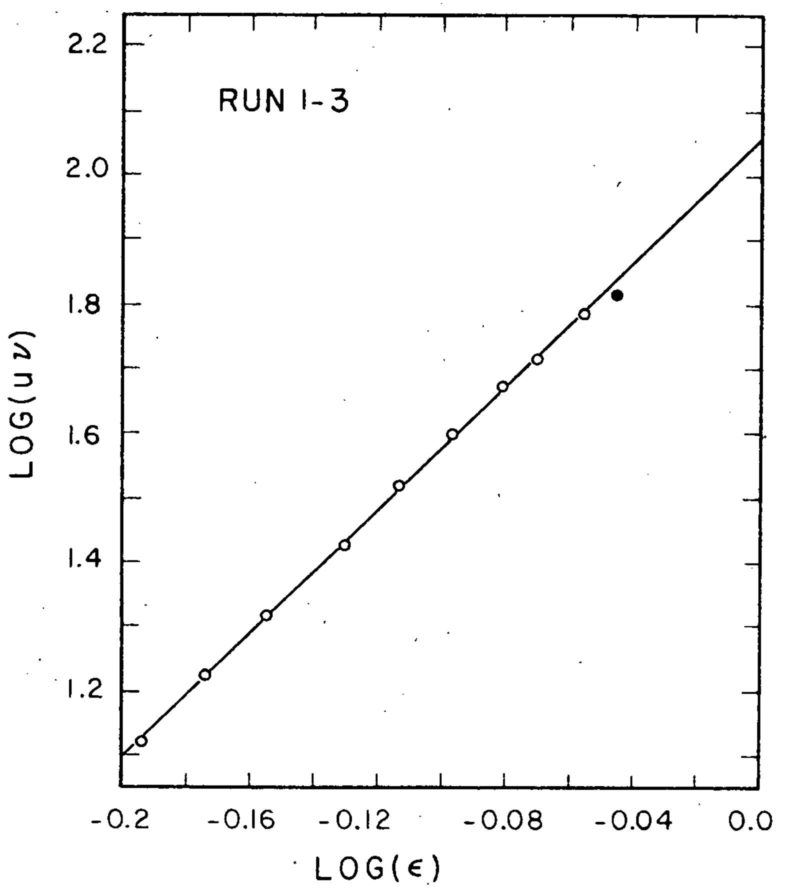

$D_v = 0.114$ cm, $D_v/D_t = 0.022$

Figure 8c. Log$u\nu$-logϵ Plot of Glass Beads in 40% PEG

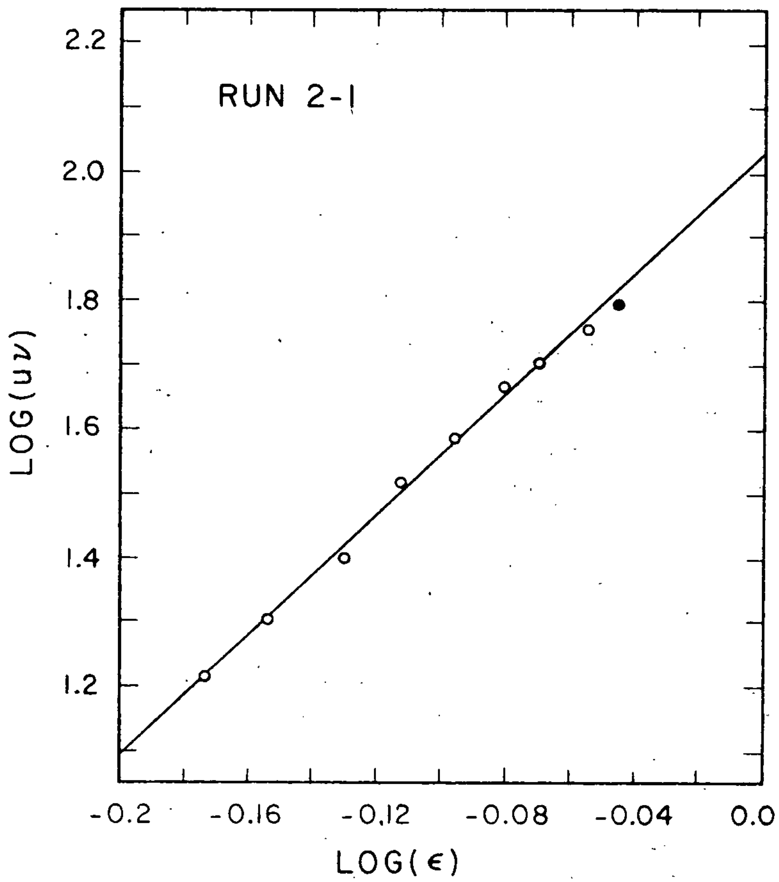

$D_v = 0.114$ cm, $D_v/D_t = 0.045$

Figure 8d. Log$u\nu$-logϵ Plot of Glass Beads in 45% PEG

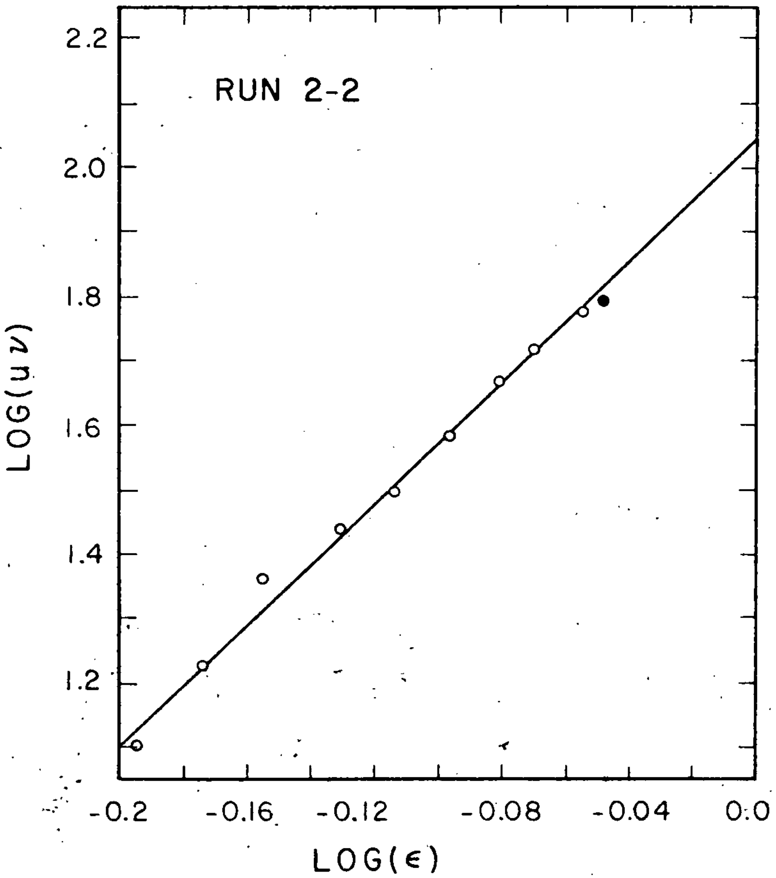

D_v = 0.114 cm, D_v/D_t = 0.030

Figure 8e. Log$u\nu$-log ϵ Plot of Glass beads in 45% PEG

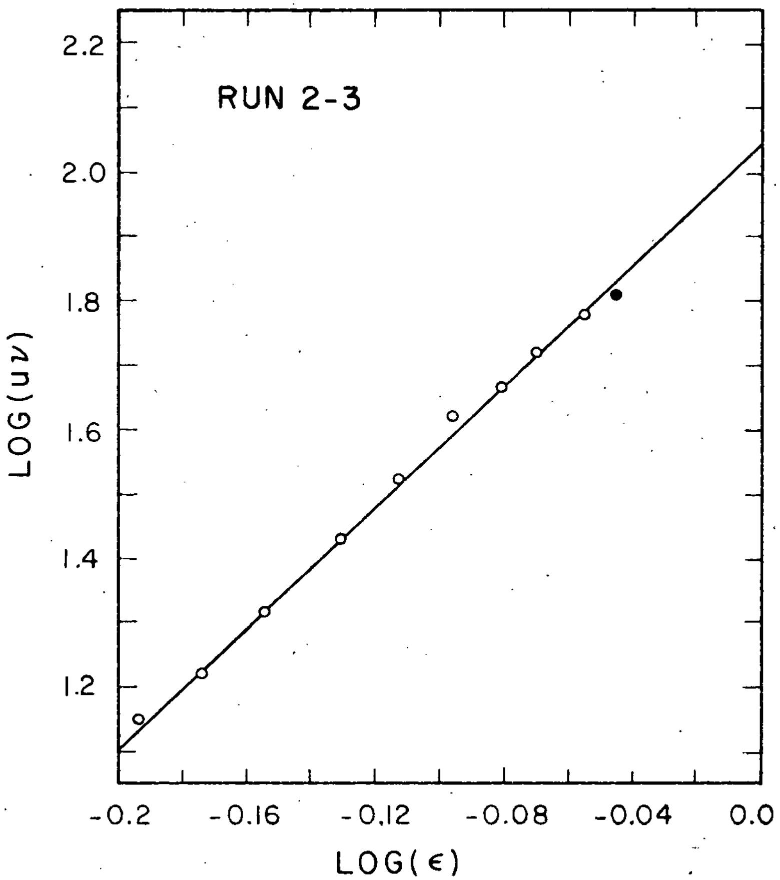

D_v = 0.114 cm, D_v/D_t = 0.022

Figure 8f. Log$u\nu$-logϵ Plot of Glass Beads in 45% PEG

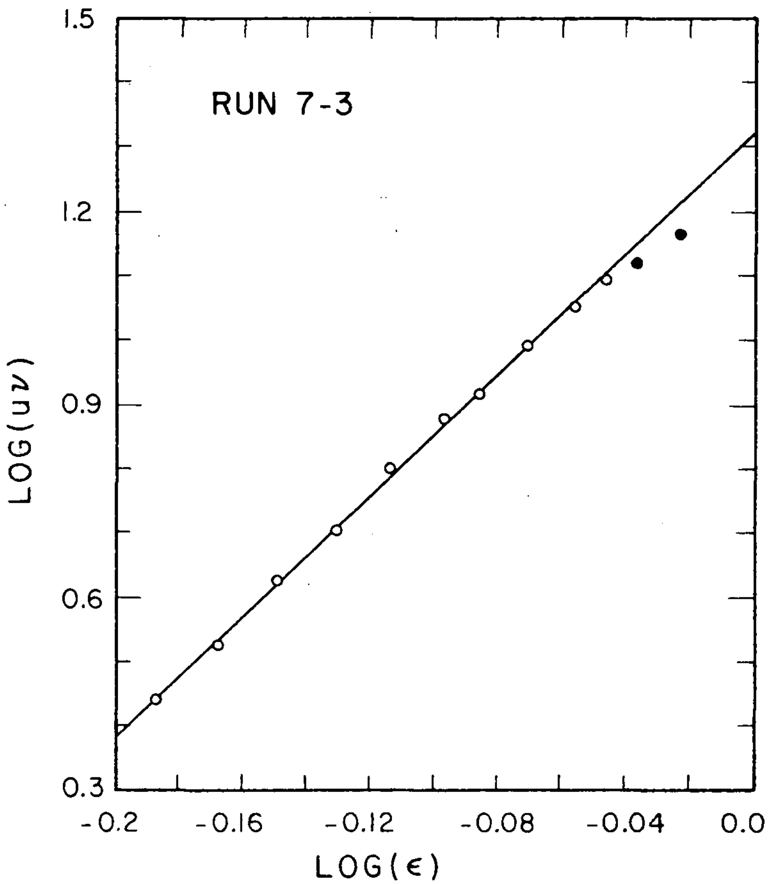

$D_v = 0.0492$ cm, $D_v/D_t = 0.0097$

Figure 8g. Loguν-logϵ Plot of Glass Beads in 35.4% PEG

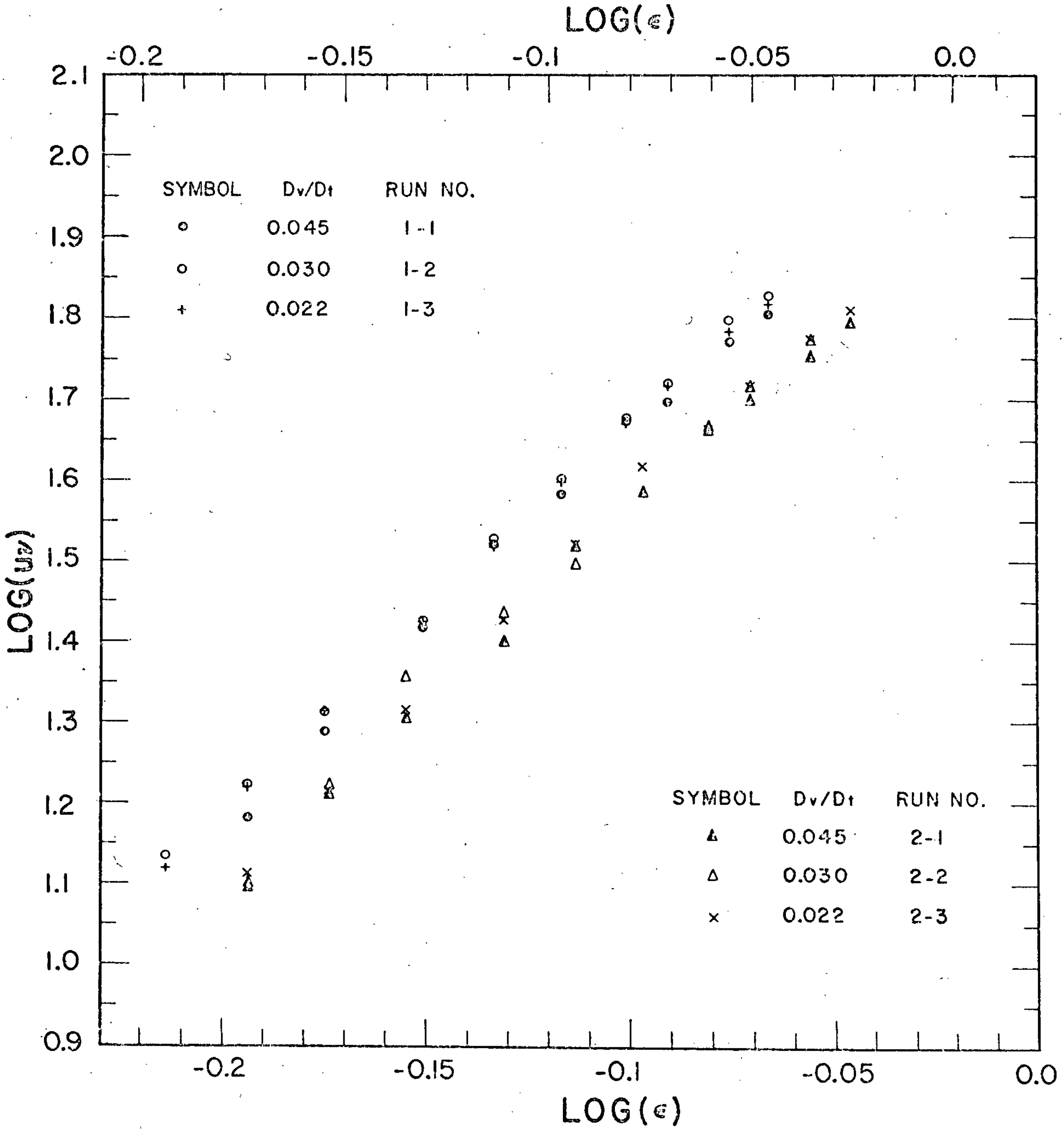

Figure 9. Wall Effect on Glass Bead Settling

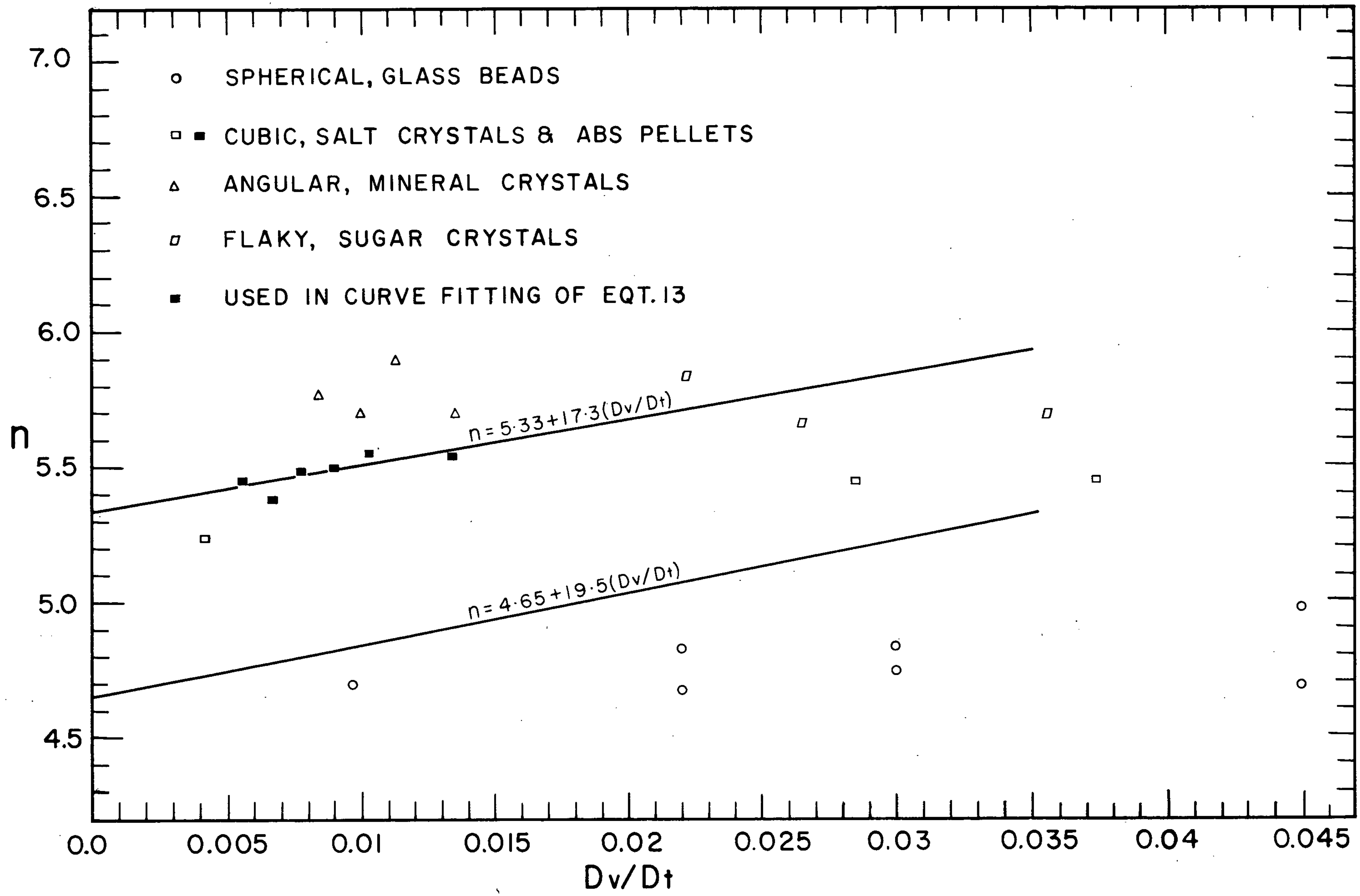

Figure 10. Results of n Plotted against D_v/D_t

ling period, or drawing a tangent to any initial settling curve and computing the constant settling rate from this tangent. The former method was apparently used by Richardson and Zaki. Either method would have given a variation as large as 10% in the present experiments.

B. Cubic Salt Crystals and ABS Pellets

Results for cubic shape particles are plotted in Figures 11a-11i and summarized in Table 6, the detail of which are in Appendix VIII.

The slopes of the best straight lines, given by the index n, were consistently higher than those for the glass beads, as shown in Figure 10. Figure 12 is a plot of the averaged data for particles of the same size settling in columns of different diameters. In this range of D_v/D_t, the effect of the wall was again not prominent, particularly at high porosity where the points overlapped. Differences in values of the index n mainly arose from the differences in settling rate at low porosity. No definite trend could be observed in the graphs. However, by ignoring Run 3-4 on the salt crystals and the two runs on the ABS pellets, and plotting n for each run against D_v/D_t, as in Figure 10, the best straight line fit to the points was given by

$$n = 5.33 + 17.3 \frac{D_v}{D_t} \qquad (13)$$

This form of equation was suggested by Richardson and Zaki who obtained

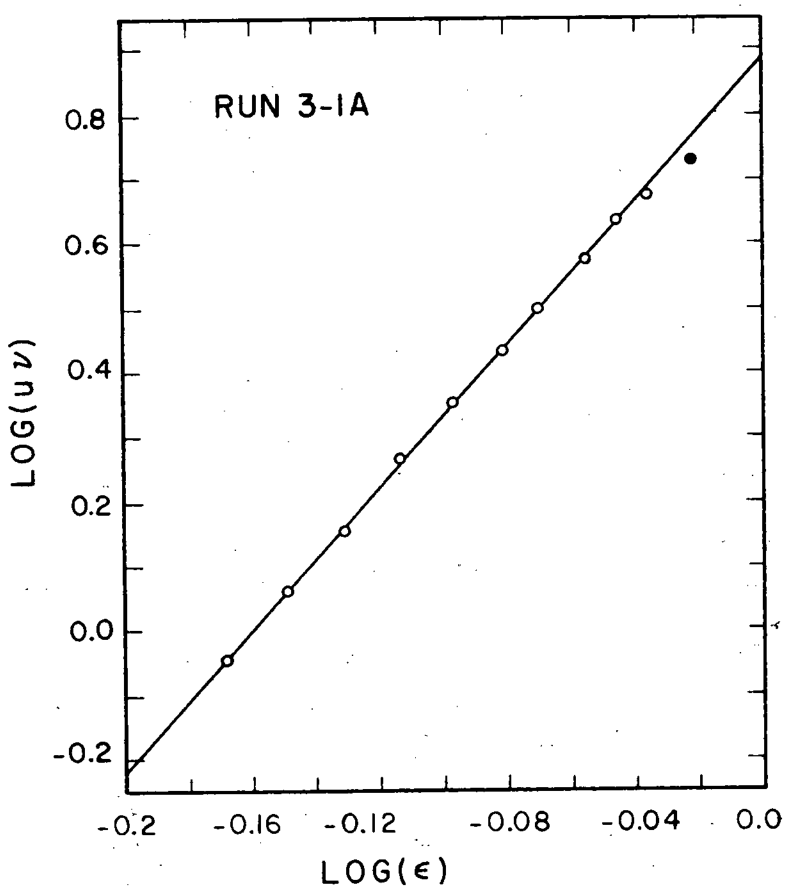

$D_v = 0.0341$ cm, $D_v/D_t = 0.0134$

Figure 11a. Log$u\nu$-logϵ Plot of Salt Crystals in Oil

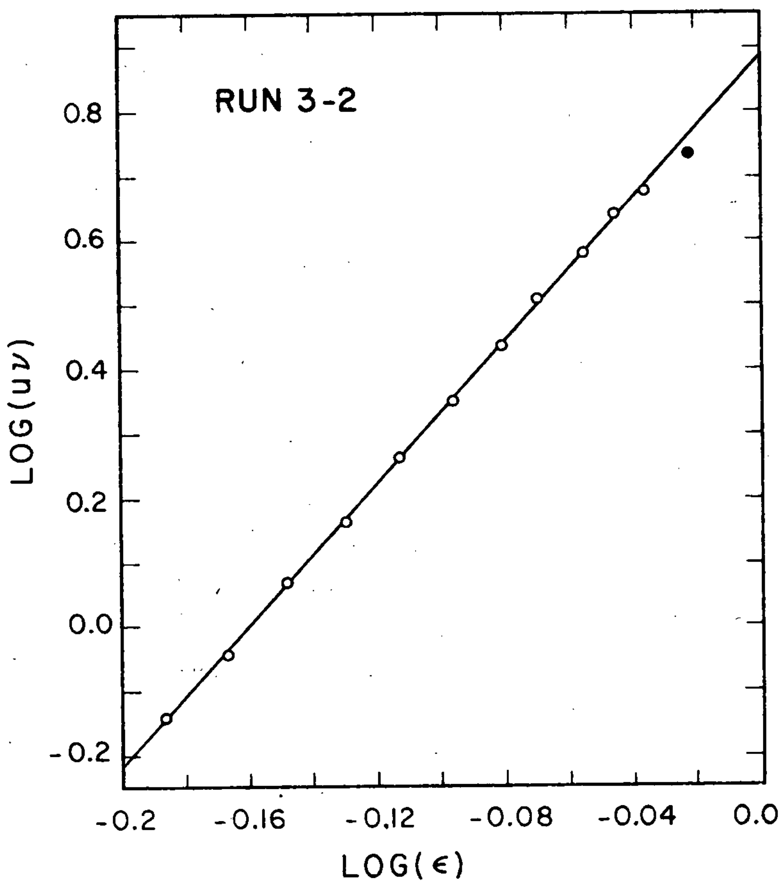

$D_v = 0.0341$ cm, $D_v/D_t = 0.009$

Figure 11b. Log$u\nu$-logϵ Plot of Salt Crystals in Oil

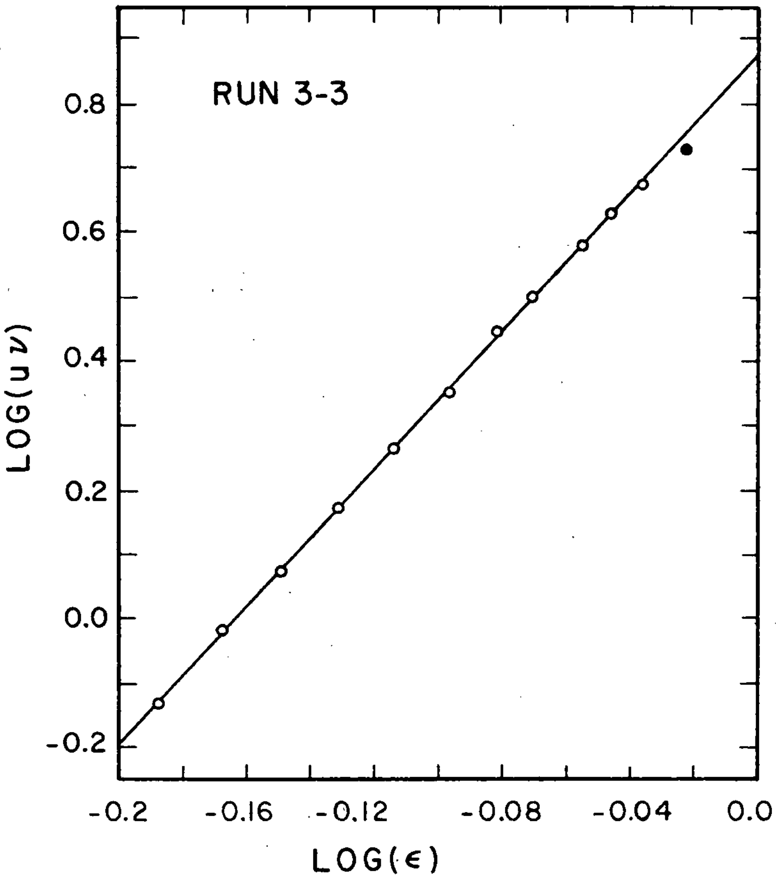

D_v = 0.0341 cm, D_v/D_t = 0.0067

Figure 11c. Log$u\nu$-logϵ Plot of Salt Crystals in Oil

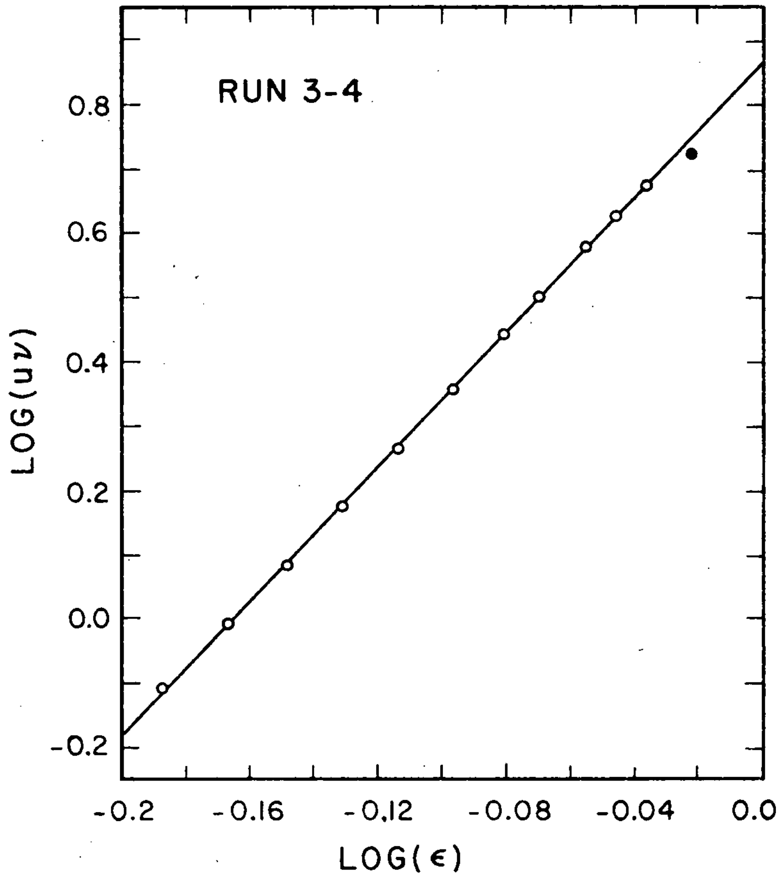

D_v = 0.0341 cm, D_v/D_t = 0.0044

Figure 11d. Log$u\nu$-logϵ Plot of Salt Crystals in Oil

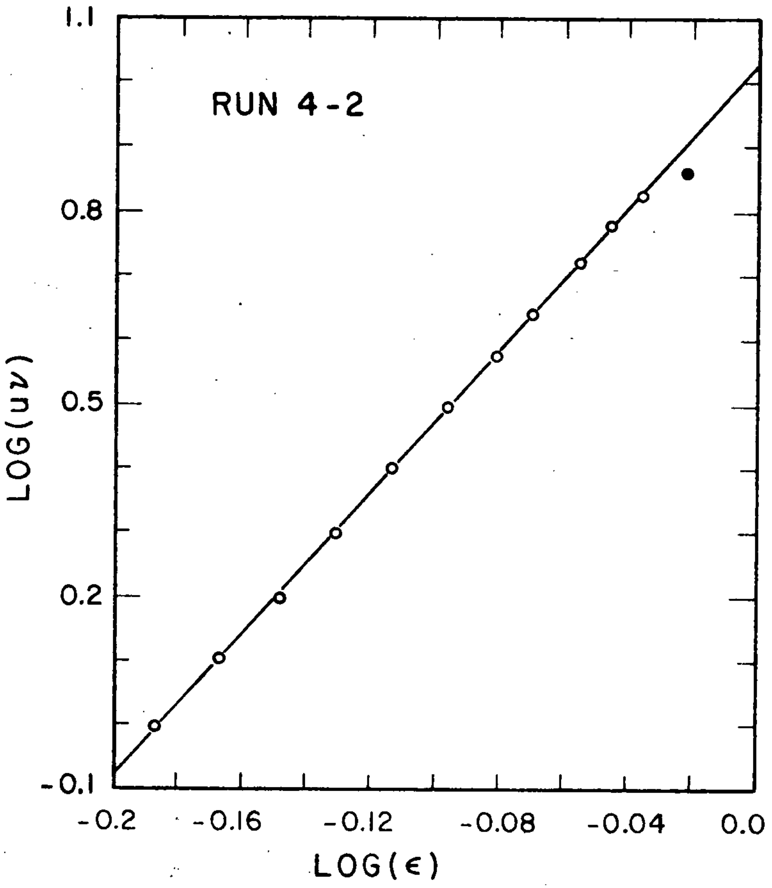

D_v = 0.0391 cm, D_v/D_t = 0.0103

Figure 11e. Log$u\nu$-logϵ Plot of Salt Crystals in Oil

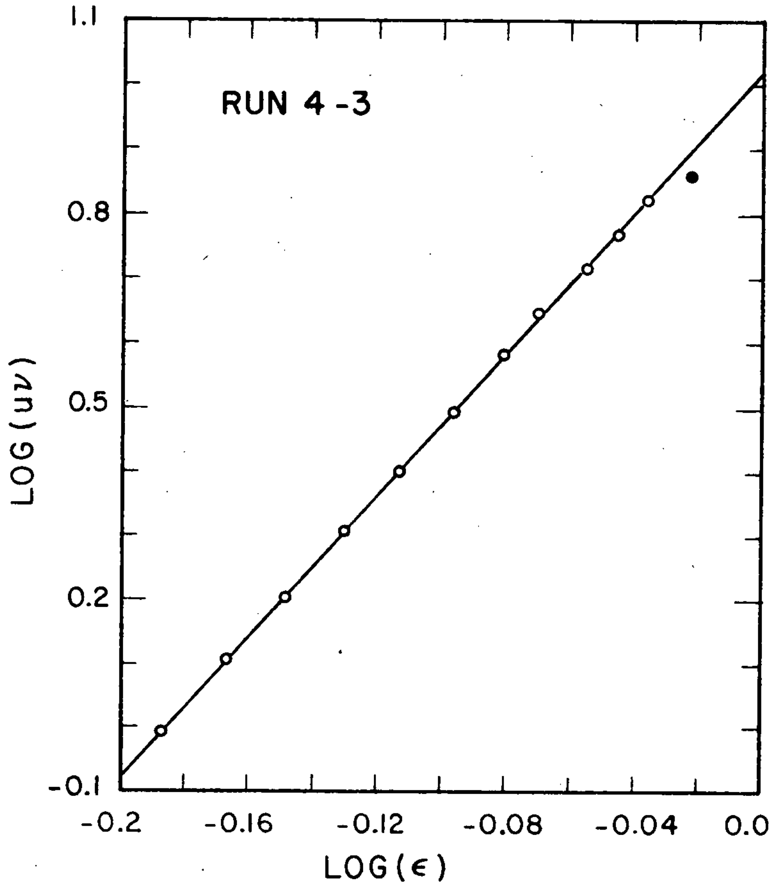

D_v = 0.0391 cm, D_v/D_t = 0.0077

Figure 11f. Log$u\nu$-logϵ Plot of Salt Crystals in oil

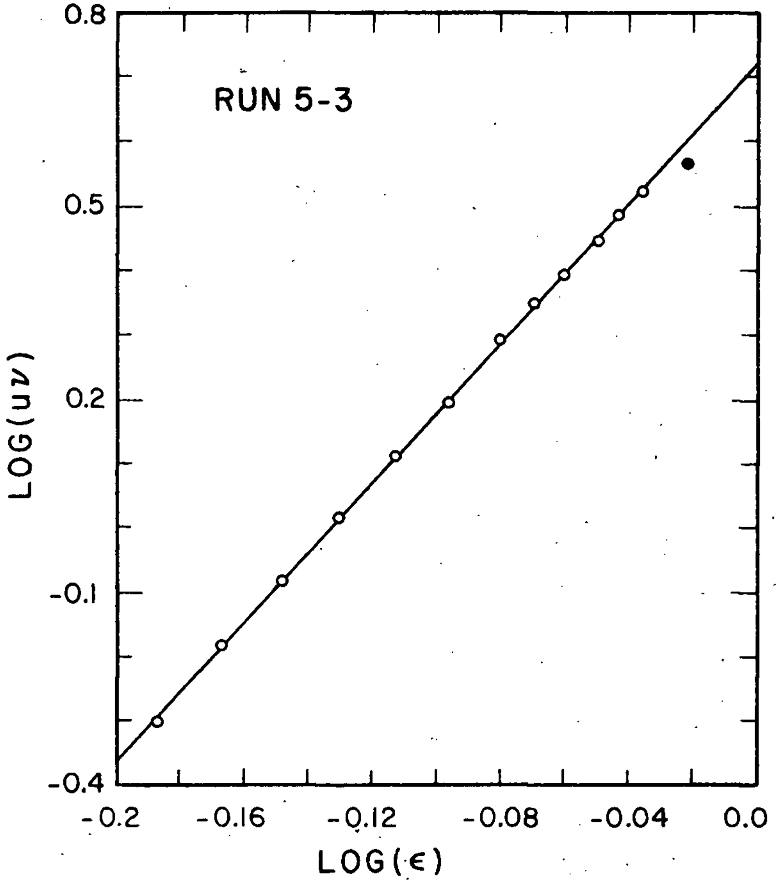

$D_v = 0.0282$ cm, $D_v/D_t = 0.0056$

Figure 11g. Log$u\nu$-logϵ Plot of Salt Crystal in oil.

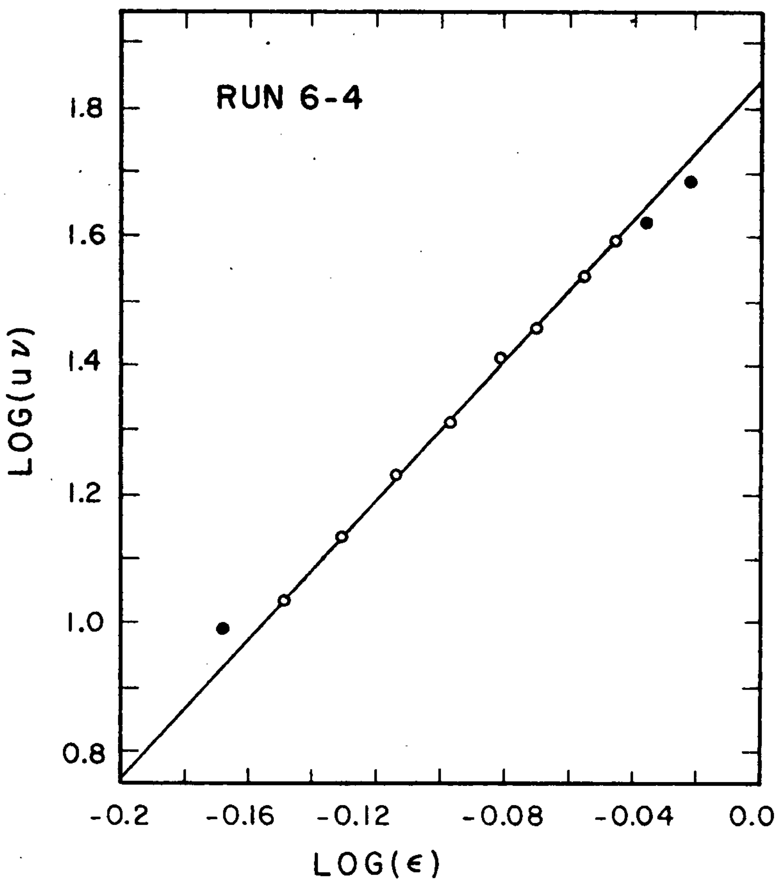

D_v = 0.288 cm, D_v/D_t = 0.0374

Figure 11h. Log$u\nu$-logϵ Plot of ABS Pellets in Oil

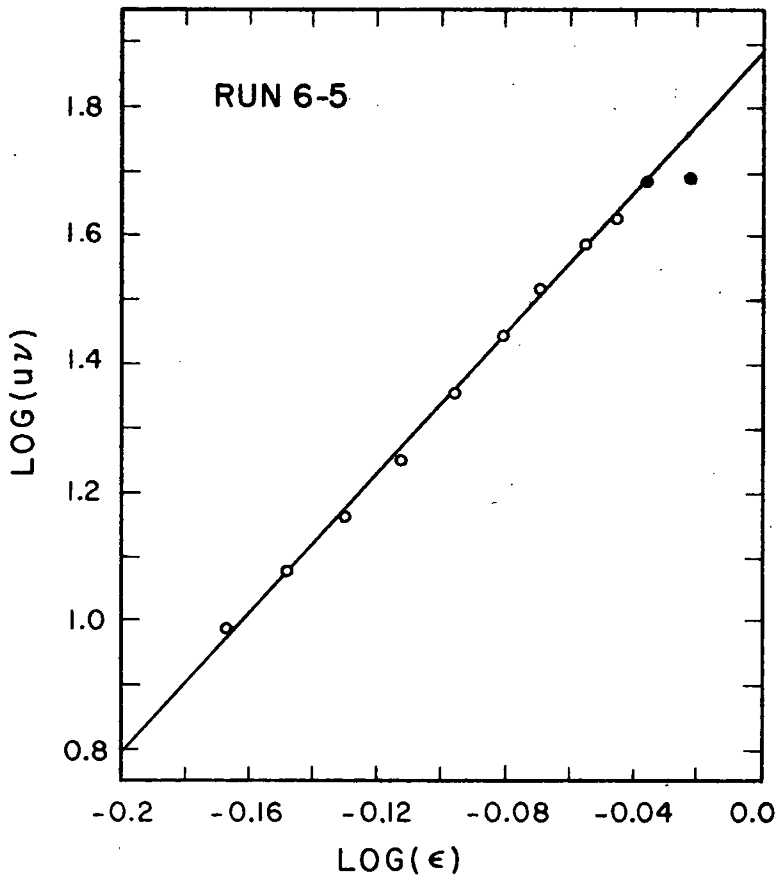

D_v = 0.288 cm, D_v/D_t = 0.0285

Figure 11i. Log$u\nu$-logϵ Plot of ABS Pellets in Oil

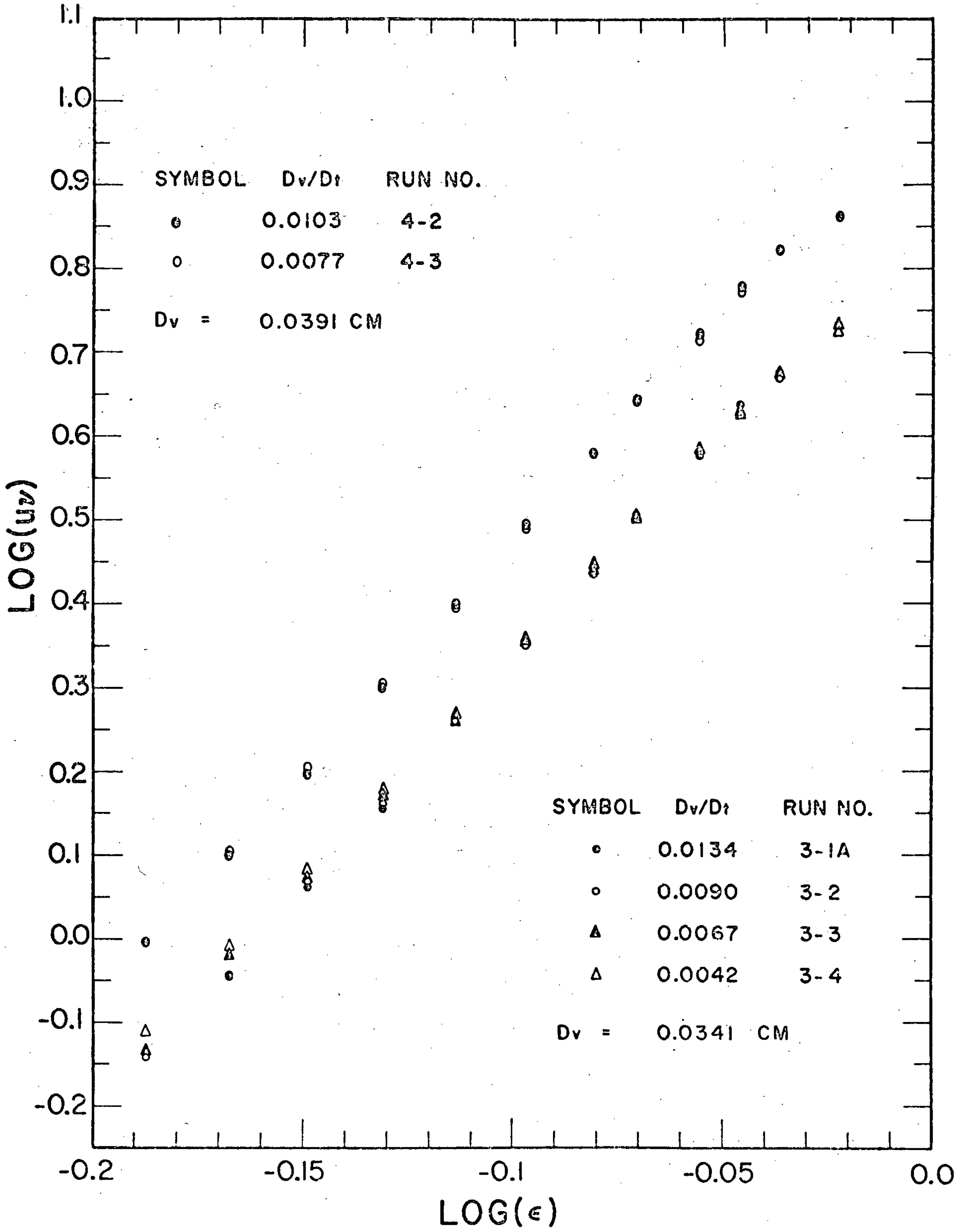

Figure 12. Wall Effect on Salt Particle Settling

$$n = 4.65 + 19.5\frac{D}{D_t} \qquad (2a)$$

for spheres. The line corresponding to equation 13 could not be extended to the ABS pellets, which lie almost in the same region of n as the salt crystals but have higher values of D_v/D_t. The linear relationship may not be applicable to those higher values of D_v/D_t, where n appears to level off, at least temporarily. Richardson and Zaki obtained similar unexplained results for spheres at higher Re_o and higher D/D_t (0.04).

C. Flaky Sugar Crystals and Angular Mineral Crystals

The results are summarized in Talbe 7 and shown in Figures 13a - 14d. The least squares values of the index n for the sugar crystals and the mineral crystals were much higher than those for the glass beads, and somewhat higher than those for the salt crystals and the ABS pellets, in the same range of D_v/D_t (Figure 10). This was consistent, since flaky and angular shapes have a lower sphericity than cubes, which in turn are of course lower in sphericity than spheres.

The settling rate of similar particles in columns of different diameters (Runs 9-, 10-, 11- in Appendix VIII)did not show any consistent wall effect.

The index n thus appears to be more sensitive to particle shape than to wall effect, at least for the present data. Comparison of shape effect is, nevertheless, best made at similar particle-to-column diameter ratios.

It has been reported that n for nonspherical particles of specified shape varied with absolute particle size (59). However, from the present results for different sets of salt

Table 7

Summary of Results for Sugar Crystals

and Mineral Crystals

Particles	Run No.	D_v, cm	D_v/D_t	n with 95% Confidence limits
Sugar	12-3	0.113	0.0222	5.83 ± 0.34
	11-2	0.135	0.0356	5.69 ± 0.33
	11-3	0.135	0.0265	5.66 ± 0.45
Mineral	10-2	0.0426	0.0113	5.89 ± 0.19
	10-3	0.0426	0.0084	5.76 ± 0.08
	9-2	0.0508	0.0135	5.69 ± 0.07
	9-3	0.0508	0.010	5.69 ± 0.10

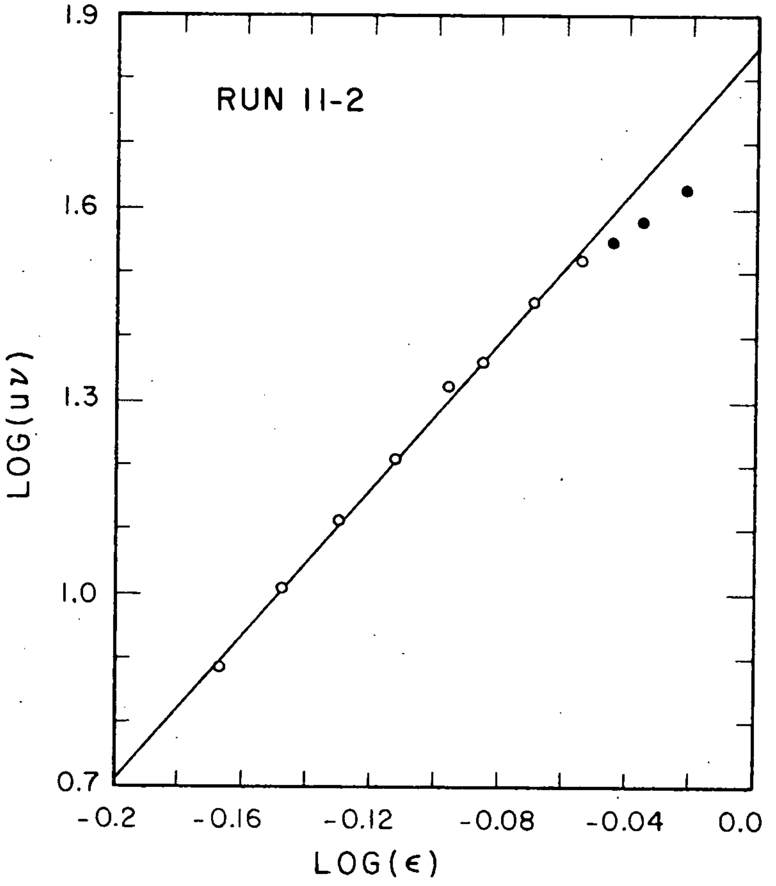

D_v = 0.1346 cm, D_v/D_t = 0.0356

Figure 13a. Loguν-logϵ Plot of Sugar Crystals in Oil

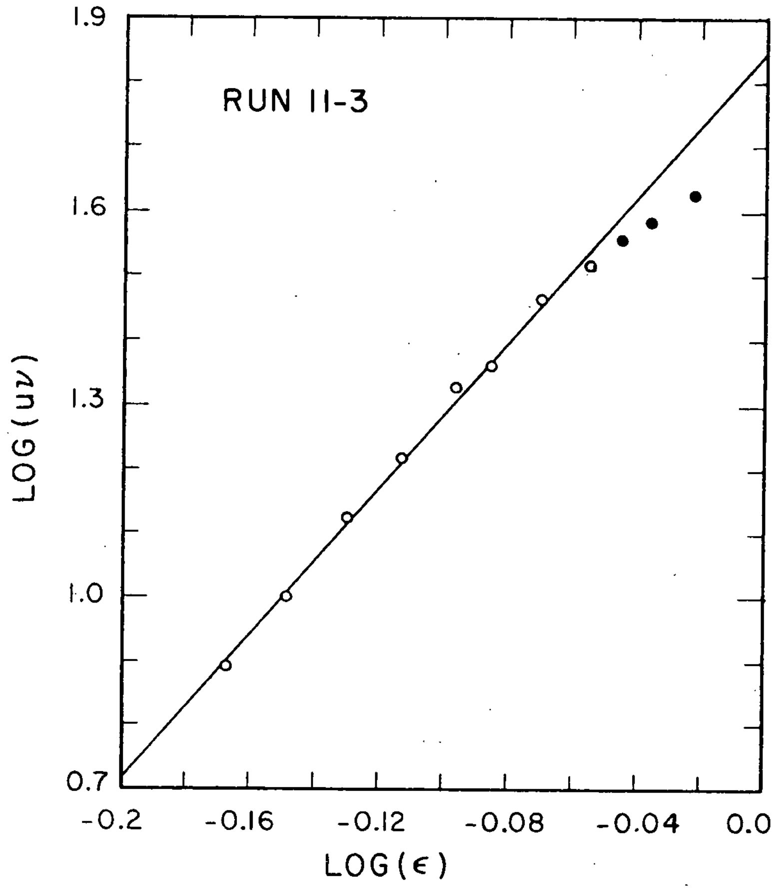

D_v = 0.1346 cm, D_v/D_t = 0.0265

Figure 13b. Loguν-logϵ Plot of Sugar Crystals in Oil

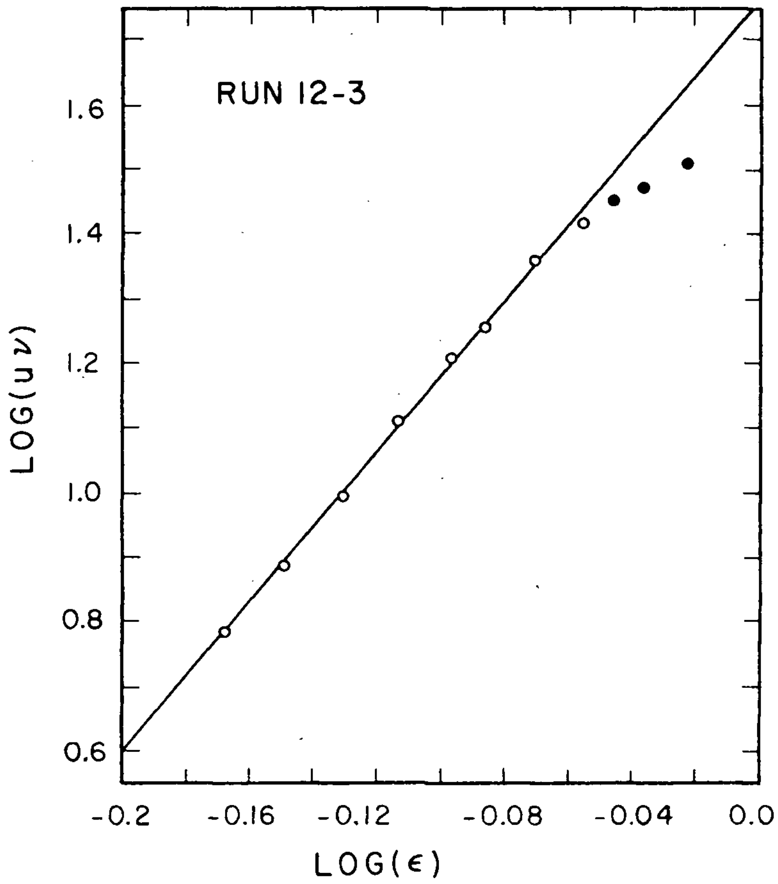

$D_V = 0.1133$ cm, $D_V/D_t = 0.0223$

Figure 13c. Log$u\nu$-logϵ Plot of Sugar Crystals in Oil

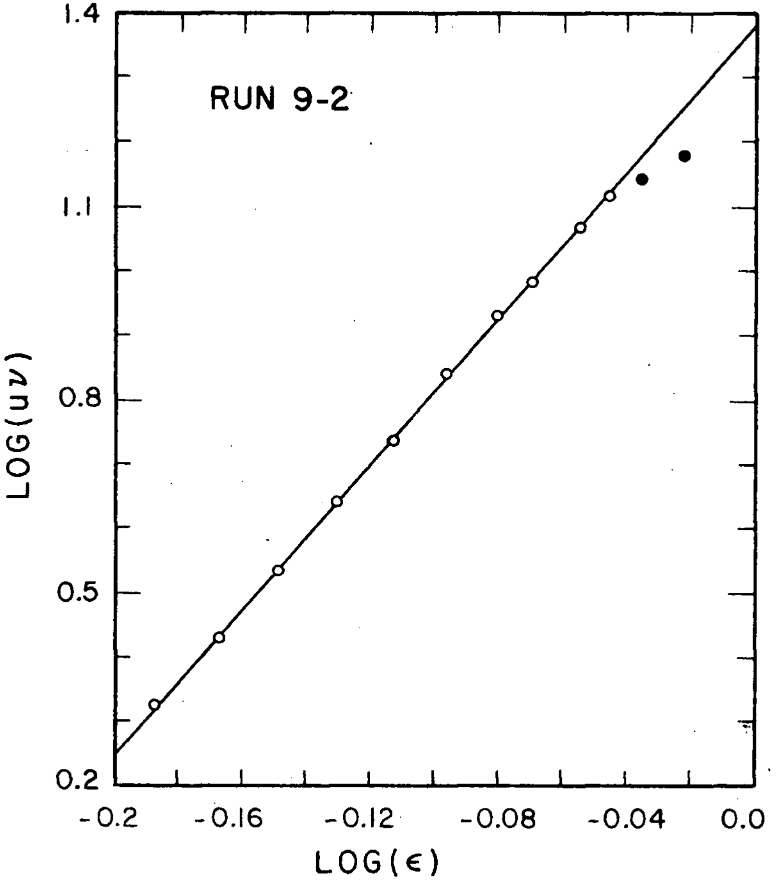

D_v = 0.0508 cm, D_v/D_t = 0.0134

Figure 14a. Log$u\nu$-logϵ Plot of Mineral Crystals in Oil

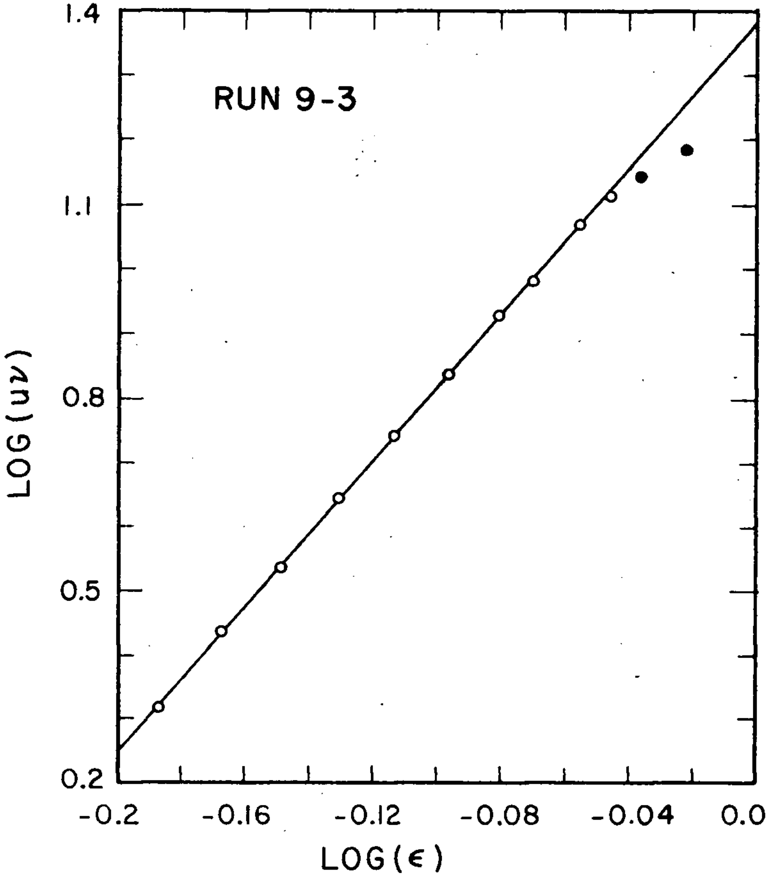

D_v = 0.0508 cm, D_v/D_t = 0.010

Figure 14b. Log$u\nu$-logϵ Plot of Mineral Crystals in Oil

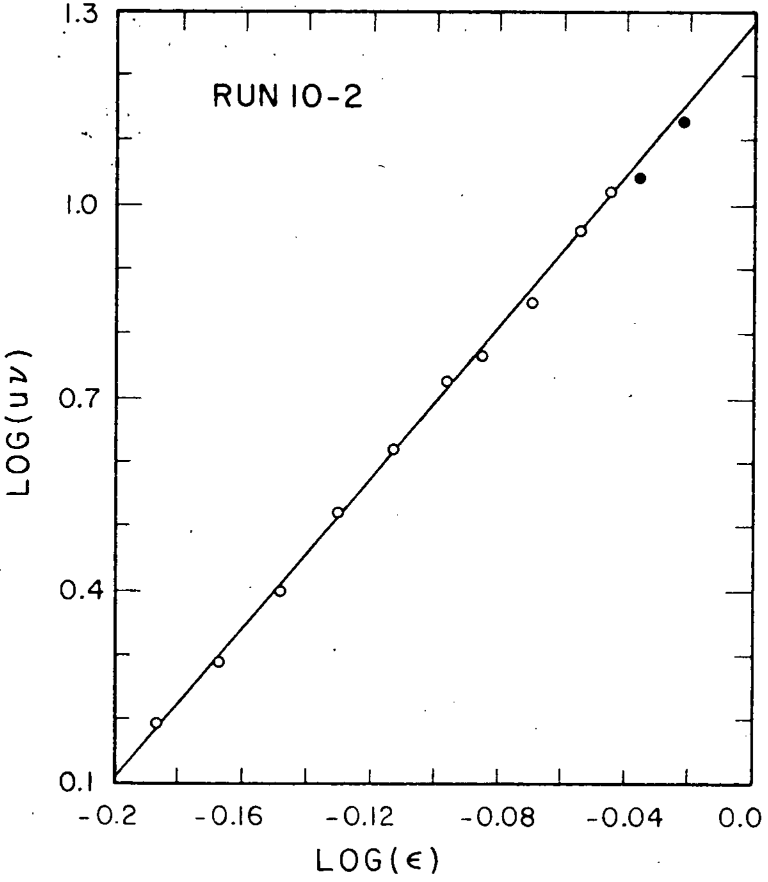

$D_v = 0.0426$ cm, $D_v/D_t = 0.0113$

Figure 14c. Log$u\nu$-logϵ Plot of Mineral Crystals in Oil

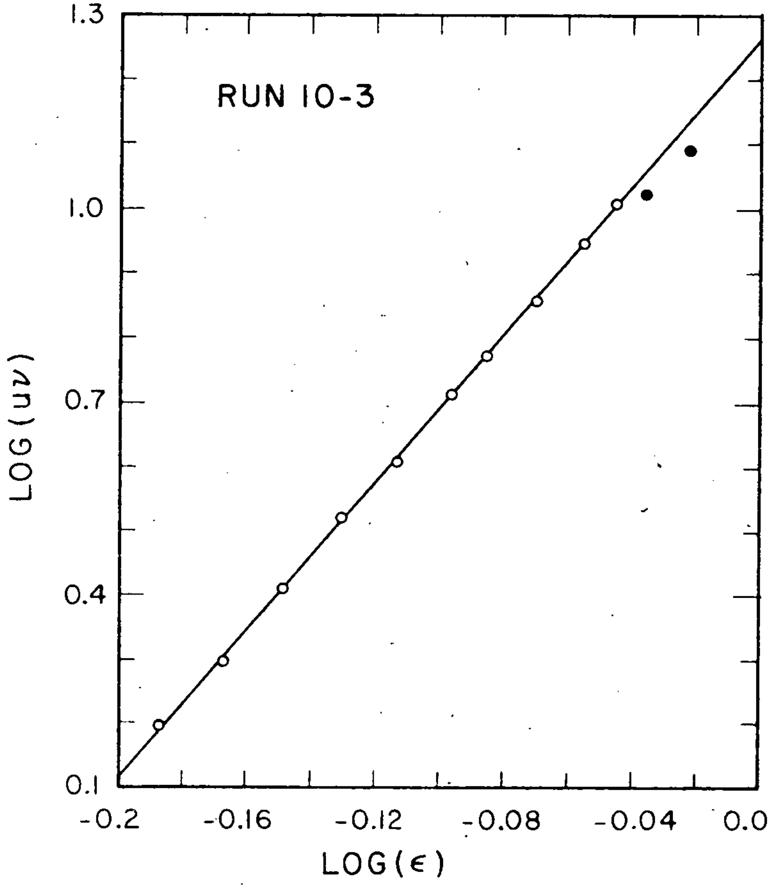

$D_v = 0.0426$ cm, $D_v/D_t = 0.0084$

Figure 14d. Log$u\nu$-logϵ Plot of Mineral Crystals in Oil crystals having average sizes which differed by a factors of 1.5 and similar narrow size distributions (Appendix X), the index n for the same shape did not depend on the particle size.

The deviation of the data at high porosity ($\epsilon \sim 0.90-0.95$) from the best straight line cannot be regarded as an intrinsic behaviour of ideal suspensions. This can be judged from the $\log u\nu - \log \epsilon$ plots, which show that the straight lines for the finer particle suspensions apply to higher porosities than those for the coarser particle suspensions. Despite the greater difficulty in obtaining a narrow cut of the finer particles, the coarser particles were subject to a slightly greater uncertainty in the location of the supernatant-suspension interface, and were also more subject to the possible distorting effect of circulation and the wall.

3. Comparison with Single Particle Results

In Tables 8 and 9, values of $u\nu$ obtained by extrapolating the $\log u\nu - \log \epsilon$ plot to a porosity of unity are compared to the average values of the same product obtained by free settling. Both have also been corrected for wall effect by equation 12. Values of $(u\nu)_{ext}$ and $(u\nu)'_{ext}$ are consistently several percent lower than $(u\nu)_o$ and $(u\nu)_\infty$ respectively, which is different from what Richardson and Zaki (43) suggested.

To check the validity of the small samples used in the free settling experiments, sphere diameter and cube length were calculated from $(u\nu)'_{ext}$ and $(u\nu)_\infty$ by equation 8a:

$$D_v = \left[\frac{18 u \nu \rho}{K_{ST}(\rho_p - \rho) g}\right]^{\frac{1}{2}} \tag{8a}$$

Table 8

Comparison of $u\nu$ for Glass Beads

Run No.	$\ddot{u}\nu$ $(0.01\ cm^3 sec^{-2})$					$\frac{(u\nu)_\infty}{(u\nu)'_{ext}}$	$\frac{u_v\nu}{(u\nu)'_{ext}}$
	$(u\nu)_{ext}$	$(u\nu)'_{ext}$	$(u\nu)_o$	$(u\nu)_\infty$	$u_v\nu$		
1-1	115.4	126.2	125.7	129.6	125.9	1.027	0.998
1-2	116.5	123.8				1.047	1.017
1-3	114.3	119.6				1.083	1.052
2-1	106.8	116.8	123.7	127.6	123.9	1.092	1.061
2-2	111.2	118.2				1.080	1.048
2-3	110.0	115.2				1.107	1.076
7-3	20.85	21.27	23.8	24.3	23.5	1.142	1.105

Table 9

Comparison of $u\nu$ for Cubic Particles

Particle	Run No.	$u\nu$ ($0.01\ cm^3 sec^{-2}$)					$\frac{(u\nu)_\infty}{(u\nu)'_{ext}}$	$\frac{u_v\nu}{(u\nu)'_{ext}}$
		$(u\nu)_{ext}$	$(u\nu)'_{ext}$	$(u\nu)_o$	$(u\nu)_\infty$	$u_v\nu$		
Salt	5-3	5.30	5.36	6.50	6.57	6.54	1.23	1.22
	3-1A	7.68	7.90	8.79	8.91	9.67	1.13	1.22
	3-2	7.63	7.77				1.15	1.24
	3-3	7.51	7.62				1.17	1.27
	3-4	7.33	7.39				1.20	1.31
	4-2	10.72	10.9	11.78	11.97	12.6	1.10	1.16
	4-3	10.53	10.67				1.12	1.18
ABS	6-4	70.2	75.7	87.4	94.3	94.8	1.25	1.25
	6-5	76.5	81.1				1.16	1.17

For a cube

$$K_{ST} = 0.93 \quad (12)$$

and $$L^3 = D_v^3\left(\frac{\pi}{6}\right)$$

The calculated diameters and cube lengths are recorded in Tables 10 and 11. Agreement between diameters and cube lengths calculated from the free settling experiments and those by both microscopic measurements and sample weighing was satisfactory, thus confirming that the small samples used in the free settling experiments were representative, and that the log $u\nu$ - logϵ plots therefore do really extrapolate at a porosity of unity to values of $u\nu$ lower than those obtained by free settling.

Gasparyan and Ikaryan (25) obtained a similar result in the creeping flow region, and found that the difference between the extrapolated u and the u calculated for free settling was greater than 20% at higher Reynolds numbers.

The agreement between the calculated average lengths of the salt crystals and those from both microscopic measurements and sample weighing indicates that the chosen salt crystals behaved as cubes even though they had rounded-off corners.

4. Settled Bed Porosity

The settled bed porosity was found to approach a constant value a short time after the observable settling process had subsided. These values were reproducible, and are plotted against sediment bed height in Figures 15a-c for different shapes of particles. Those data at low bed height were rendered less reliable than the others because of the boundary effect at the

Table 10

Comparison of Diameters of Glass Beads

Run No.	Sieve openings cm	Sphere diameter, cm, from					
		Sample weighing D_v	$(u\nu)_{ext}$	$(u\nu)'_{ext}$	$(u\nu)_o$	$(u\nu)_\infty$	microscope
1-1	0.0991/0.117	0.114	0.109	0.114	0.114	0.116	0.112
1-2	ave. 0.108		0.110	0.113			
1-3			0.109	0.111			
2-1			0.106	0.111			
2-2			0.108	0.111			
2-3			0.107	0.110			
7-3	ave. 0.0456 0.0417/0.0495	0.0492	0.0463	0.0468	0.0494	0.050	0.492

Table 11

Comparison of Cube Lengths of Cubic Particles

Particles	Run No.	Sieve openings cm	D_v cm	Length of Cube, cm., from					
				$(u\nu)_{ext}$,	$(u\nu)'_{ext}$	$(u\nu)_0$	$(u\nu)_\infty$	microscope	Sample weighing
Salt	5-3	0.0208/0.0250	0.0282	0.0212	0.0214	0.0234	0.0236	0.0229	0.0234
		ave. 0.0229						0.0232	
	3-1A	0.0250/0.0295	0.0341	0.0254	0.0258	0.0272	0.0274	0.0273	0.0272
	3-2	ave. 0.0273		0.0253	0.0256			0.0274	
	3-3			0.0252	0.0254				
	3-4			0.0248	0.0249				
	4-2	0.0295/0.0351	0.0391	0.0302	0.0305	0.0316	0.0318	0.0316	0.0316
	4-3	ave. 0.323		0.0295	0.0302			0.0319	
ABS	6-4		0.288	0.207	0.214	0.230	0.239		0.232
	6-5			0.216	0.221				

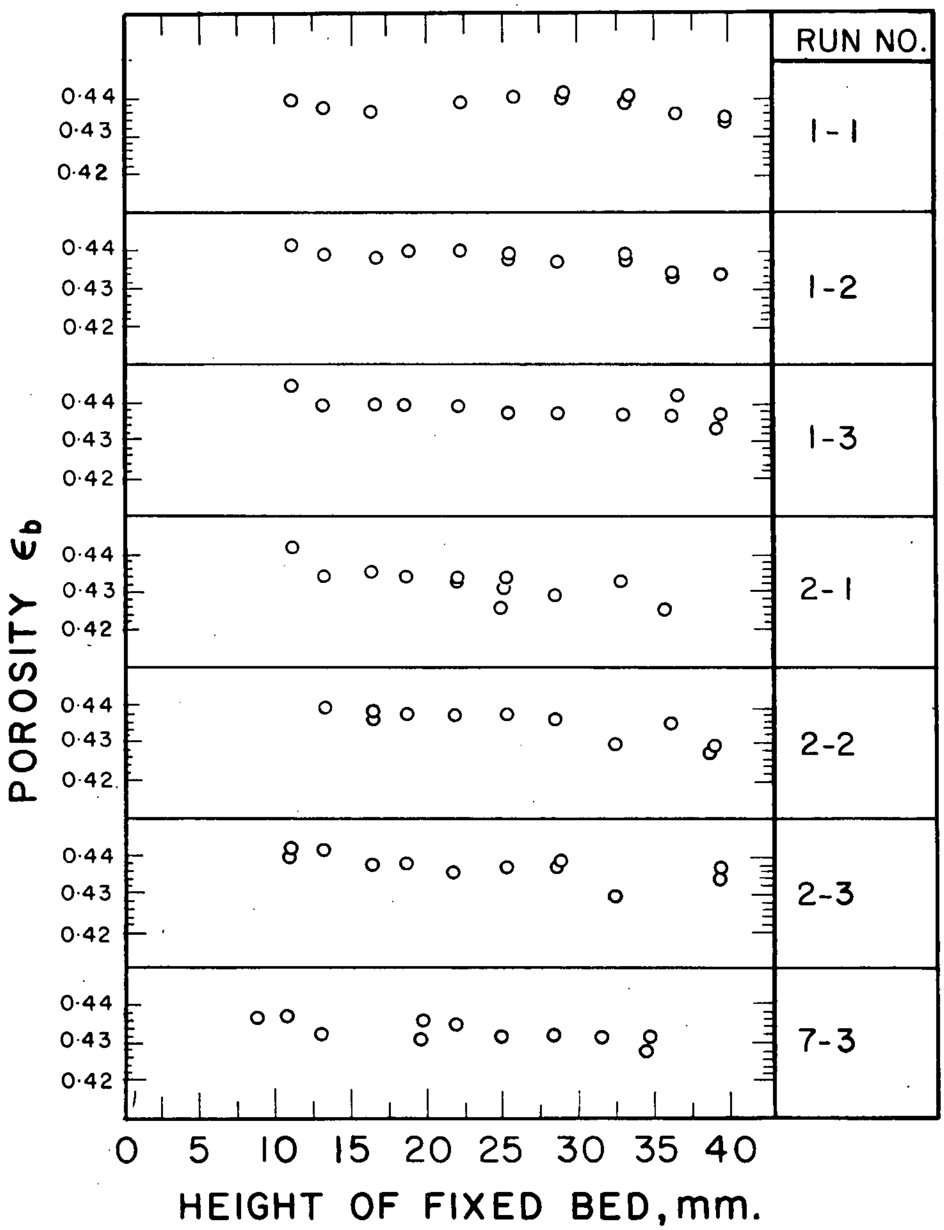

Figure 15a. Settled Bed Porosity of Glass Beads

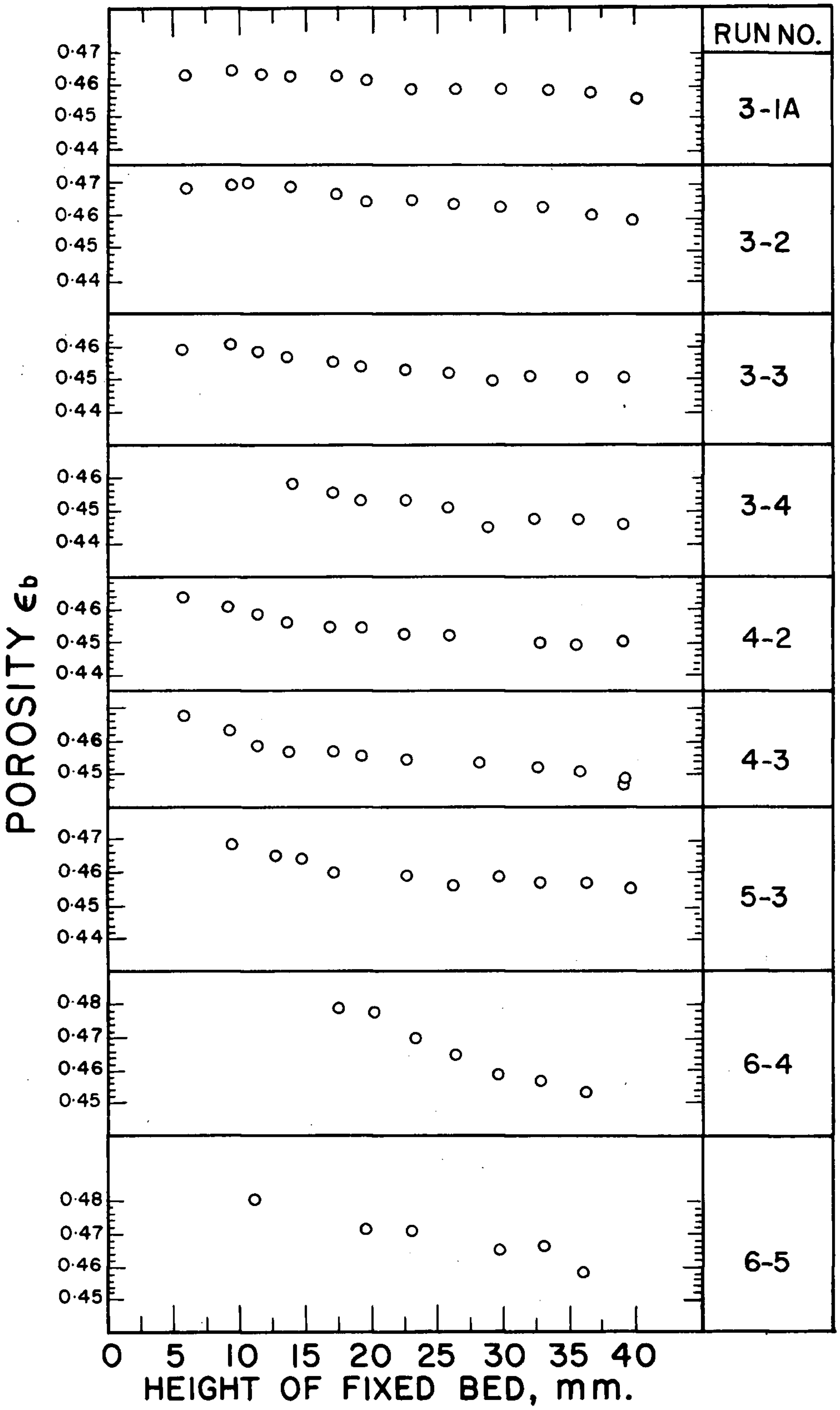

Figure 15b. Settled Bed Porosity of Cubic Particles

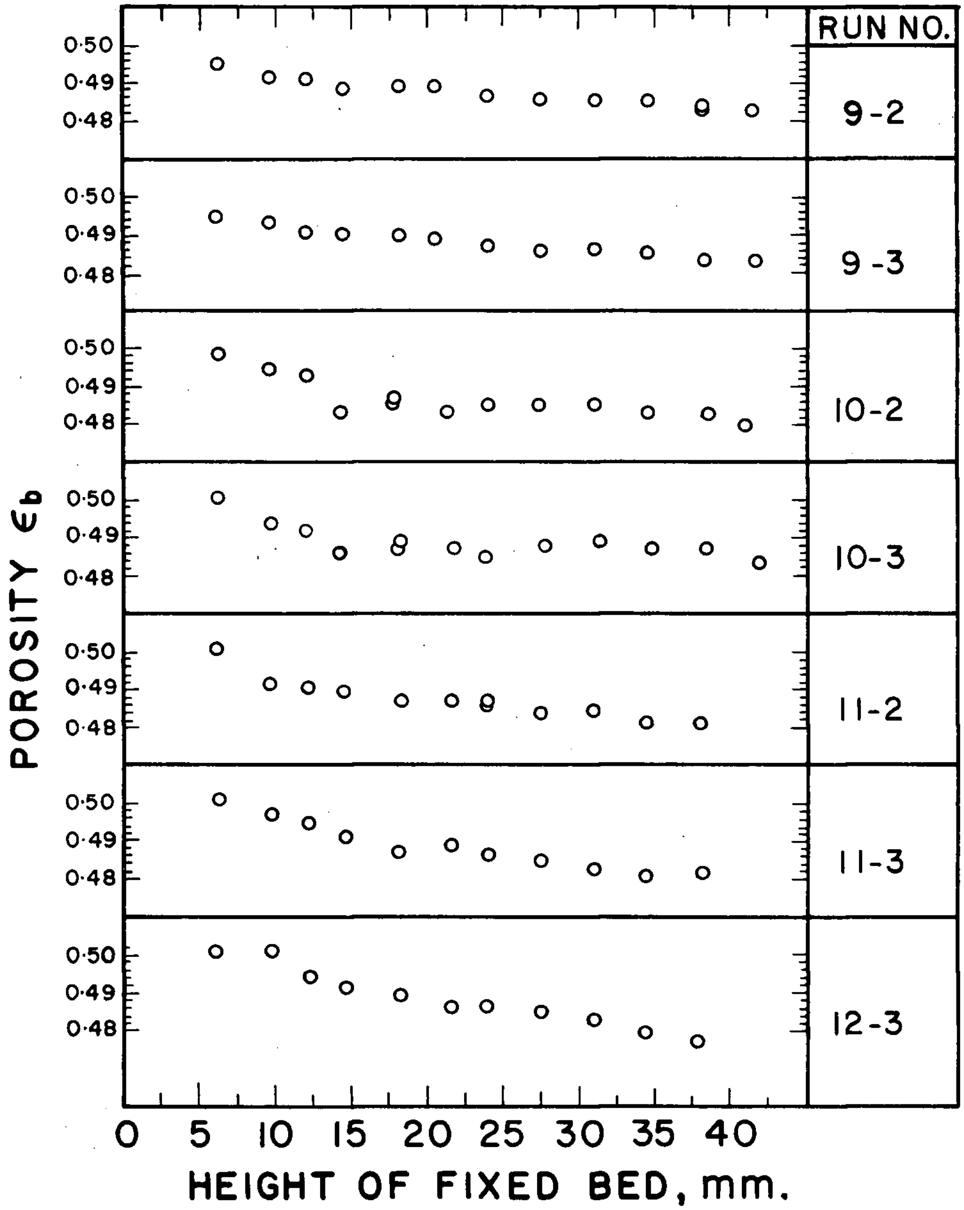

Figure 15c. Settled Bed Porosity of Mineral and Sugar Crystals

bottom, complicated possibly by uneveness of the walls at the bottom of the columns.

Fixed or settled bed porosity decreased slightly with bed height. The probable explanation for this trend is that, the greater the bed height, the greater the applied pressure on the lower portion of the bed, and hence the greater the degree of compaction of the bed.

It was found that those particles with shapes appreciably different from spheres showed a greater sensitivity of ϵ_b to bed height than the spheres. Stacked beds of non-spherical bodies or rough bodies have been observed to form beds of less stable porosity with respect to pressure then smooth spheres (60). This effect, however, was only a minor one for the random loose packed beds of the present experiments.

The mean values of ϵ_b for each run were estimated by drawing a horizontal line through the data, ignoring the points at low bed height. The mean values of ϵ_b obtained were 0.435 (variation 0.432-0.438) for the spherical glass beads, 0.455 (variation 0.450-0.461) for the cubic salt crystals, 0.486 (variation 0.485-0.487) for the mineral crystals and 0.485 for the sugar crystals. The ABS pellets showed an appreciable change of ϵ_b with bed height, due presumably to their low density which requires a greater bed height to produce packing stability. Comparing with the packed bed porosity results of Brownell et. al. (51), the value of ϵ_b obtained for the glass beads agrees very closely to their value of random loose porosity for uniform smooth spheres, while ϵ_b of the salt crystals corresponds to their random loose packed bed of particles having a sphericity of 0.84.

The latter figure is a little higher than the sphericity of a perfect cube, 0.806, and might be attributed to the rounded-off corners of the salt crystals which increased their sphericity.

5. Beranek-Klumpar Plot

Figures 16a-16d, respectively, are tests of four variations of the Beranek-Klumpar method, using the experimental data of the present study. Where u_∞ rather than u_{ext} is used in the abscissa, only the data for spherically isotropic particles are plotted, since u_∞ for the other particles is a function of orientation. The data for ABS pellets were not included because of the large bed height effect on ϵ_b. The term u_{in} was obtained from

$$u_{in} = u_{ext}\epsilon_b^{\,n} \qquad (14)$$

using the experimentally determined values of n for the given run and of ϵ_b for the given particles shape. The best of the four variations is Figure 16a, which does result in some correlation of the data for different shapes, but can hardly be considered a perfect correlation, the maximum horizontal spread between the points averaging about 15%. A distinct difference between the curves for different shapes still persists even when the comparison is restricted to similar particle-to-column diameter ratios.

6. n - ϵ_b Plot

Ignoring the wall effect, the index n was plotted against the settled bed porosity in Figure 17. An obvious trend was found for n to increase with ϵ_b. The latter is related to particle shape in general and sphericity in particuler (51). We thus have

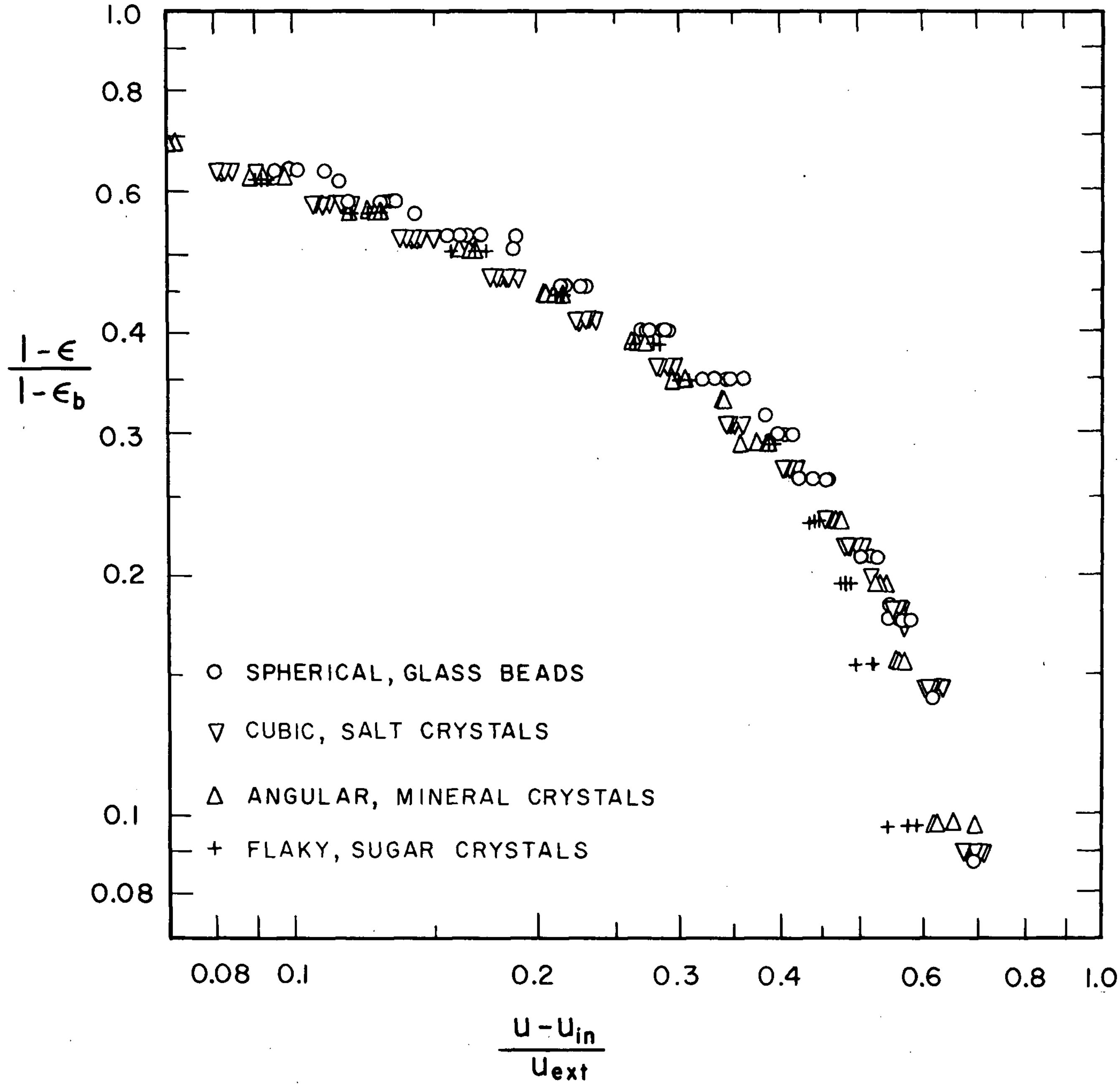

Figure 16a. Beranek-Klumpar Plot using $(u-u_{in})/u_{ext}$

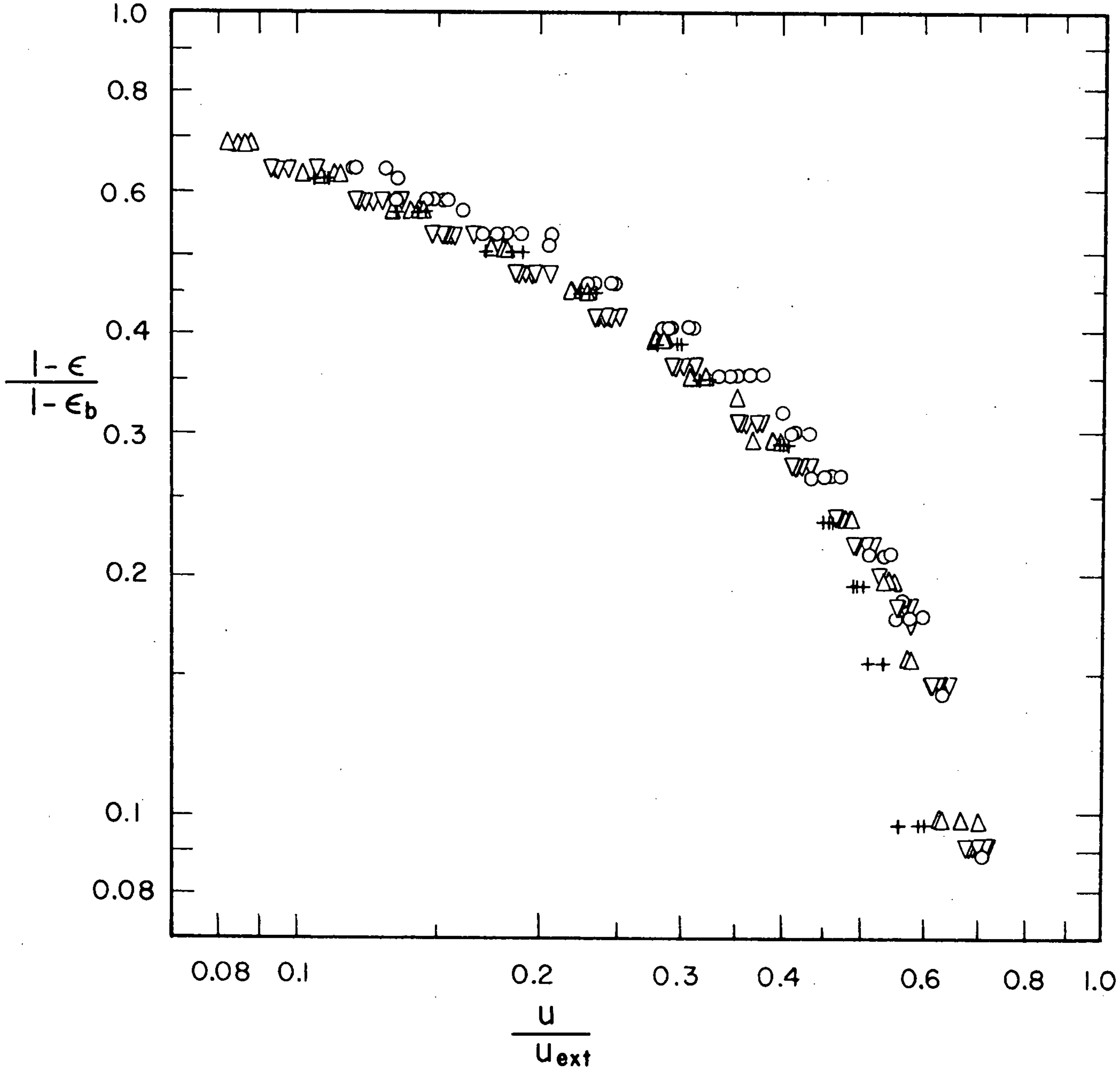

Figure 16b. Beranek-Klumpar Plot using u/u_{ext}

(Symbol - see Figure 16a.)

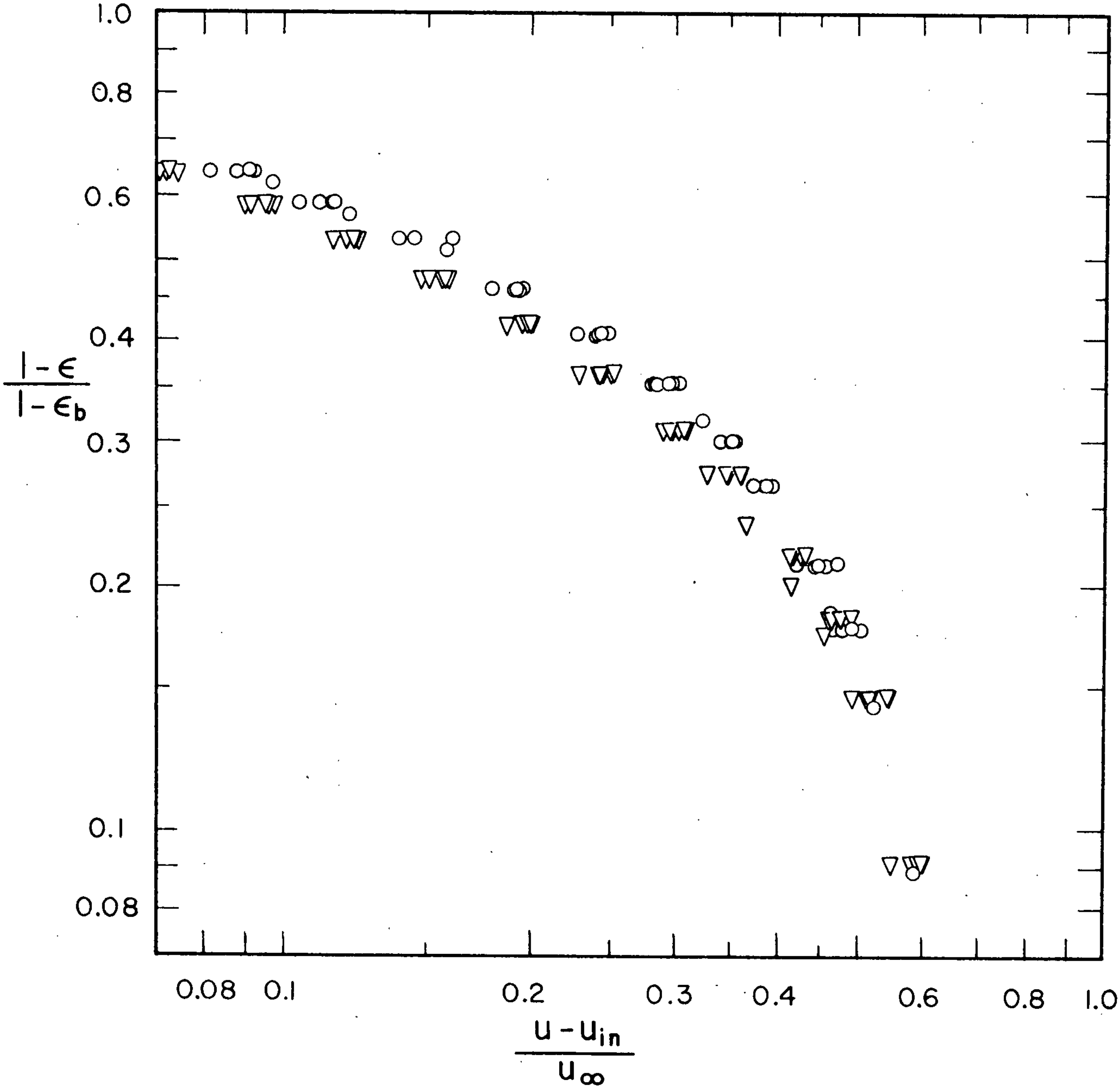

Figure 16c. Beranek-Klumpar Plot using $(u-u_{in})/u_\infty$

(Symbol - see Figure 16a.)

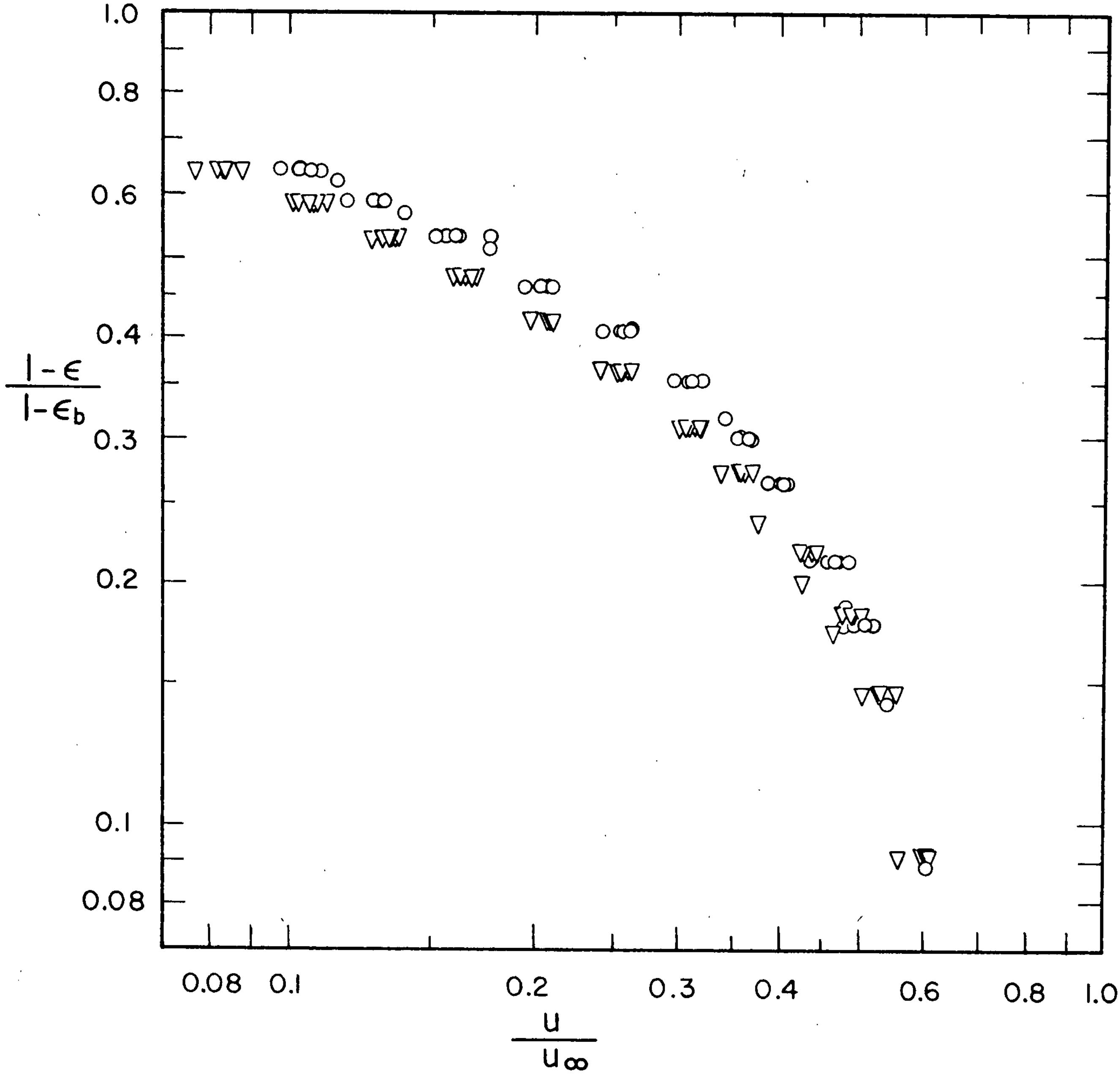

Figure 16d. Beranek-Klumpar Plot using u/u_∞
(Symbol - see Figure 16a.)

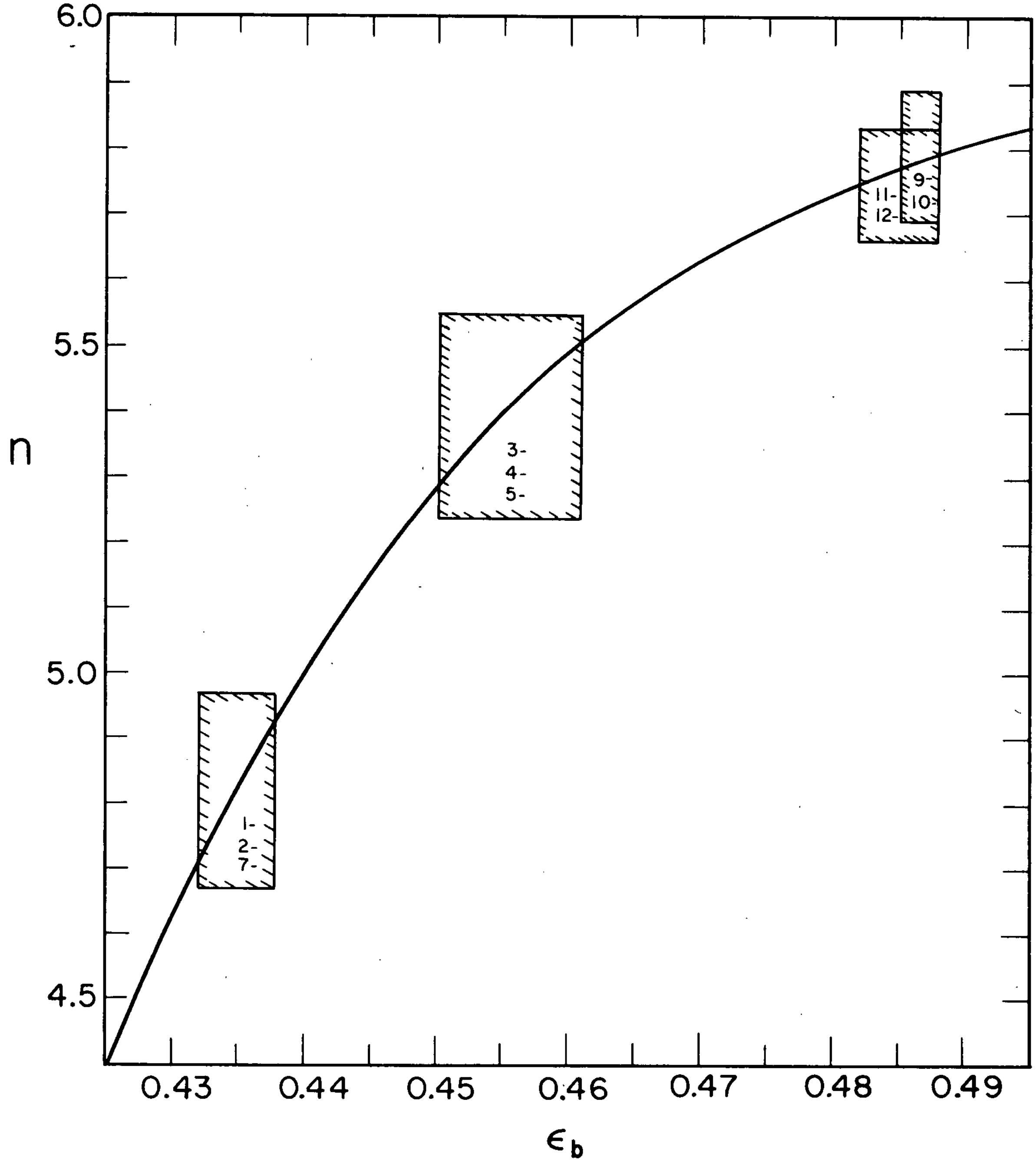

Figure 17. n vs. ϵ_b Plot

(The numbers in the graph indicate Run Nos.)

a potentially useful method of predicting n for different particle shapes. Any uncertainty in the prediction of n by this method is probably smaller than the error (up to 20%) incurred by the Richardson-Zaki method of using u_∞ instead of u_{ext} in

$$\frac{u}{u_{ext}} = \epsilon^n \tag{1a}$$

7. Observations

For spherical glass beads, the top layer of a settling suspension, the thickness of which was of the order of a few particle diameters, consisted of particles arranged randomly in space. Relative motion of the particles within this layer rarely occurred, except that occasionally a particle might move upward through the bed and then fall on its arrival at the interface. Below this calm layer, particles travelled relative to each other in apparently random directions. Clusters of particles were moving downward, while some nearby clusters of particles were rising. A given cluster might rise at one moment and fall at another moment, or might break up during its movement. By "cluster" is meant a group of particles which moved together and rotated as a whole, but not in the same sense as agglomorated particles which occur in flocculation; there was no distinct difference in interparticle distance within and outside a cluster. Lateral motion of particles was observed in the lower portion of a suspension. The motion was not systematically in the radial direction. The occurrence of interparticle contact between spherical particles was uncertain.

The same general type of behaviour was found in the settling beds of nonspherical particles. Orientation of the individual particles was apparently random and changing during settling. There was observable interparticle contact between some particles. A particle would change its orientation when it was diverted by a neighbour either by direct obstruction or by hydrodynamic interference.

It is likely that the net motion of the particles was affected by particle orientation. The overall orientation of a settling bed may not be the one which gives the least resistance to fluid flow and, in addition, mechanical contact between particles causes further energy dissipation. This might be one reason why nonspherical particles with flaky or angular shapes have hindered settling rates more affected by concentration than do spheres.

Experimental settling rates in creeping flow reported here and many in the literature (33, 43, 62) were found to be considerably higher than those for a mechanically extended bed with spheres in cubic array (61), and also considerably higher than those predicted theoretically by both the "free surface" model of Happel (22) and the hexagonal configuration model of Richardson and Zaki (26) (see Figure 18). On the other hand, multiparticle motion in small clusters was reported (10) to have reduced drag, which could explain the faster settling rates of the experimental results compared to those of the idealized models.

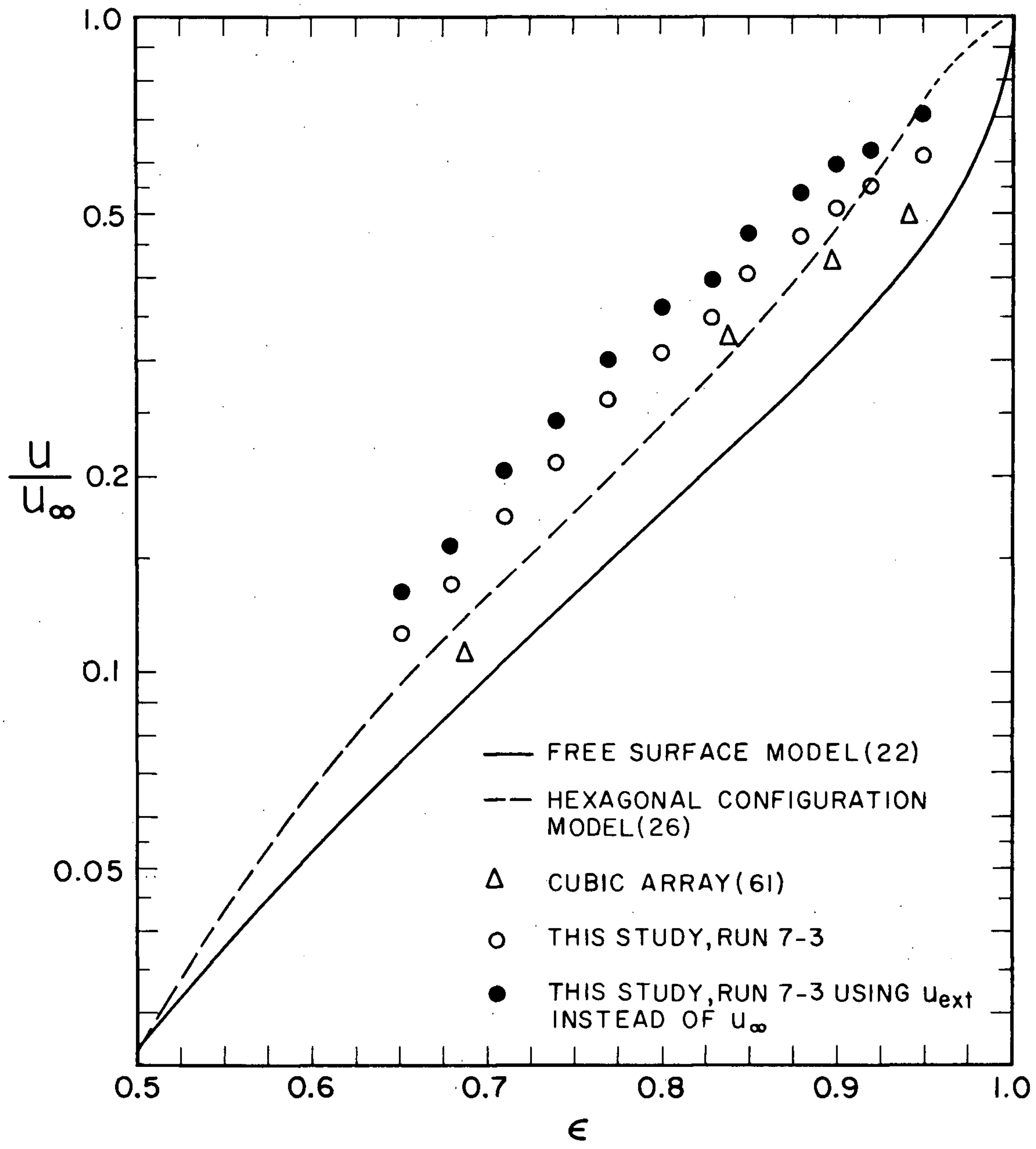

Figure 18. Comparison of the Present Results for Spheres to Models in the Literature

CONCLUSIONS

1. Hindered settling without flocculation of spherical and nonspherical narrowly sized particles of uniform shape in creeping flow can be well represented by a simple straight line fitted to the data on log $u\nu$- logϵ coordinates, if a few data in the dilute region (ϵ~0.90-0.95) are excluded. The non-linearity of this region was believed to arise from the uncertainty in the low concentrations. The slope n of the fitted line depends on particle shape, ranging from an average value of 4.8 for smooth spheres to 5.4 for cubes to 5.8 for angular crystals.

2. The index n for spheres was close to that found in the literature (25, 43), but the results for different particle-to-column diameter ratios ($D_v/D_t < 0.045$) did not show nearly the same effect of the wall as that reported by Richardson and Zaki (43). On the other hand, for cubic salt crystals, n could be represented statistically up to $D_v/D_t = 0.015$ by

$$n = 5.33 + 17.3\ D_v/D_t$$

the wall correction constant of which is close to that of Richardson and Zaki. However, this constant fails completely at values of D_v/D_t above 0.015.

3. The method recommended by Beranek and Klumpar for correlating both spherical and nonspherical particle fluidization data was only moderately successful in correlating the present settling data for different shapes. The fluidization data plotted by Beranek and Klumpar included some on porous particles

and were thus probably misleading; and even those data showed considerable scatter.

4. The settling rates obtained by linear extrapolation on log-log coordinates to a porosity of unity were found to be lower than the corresponding free settling rates obtained by experiment or computed by size measurement. This finding is supported by some careful experimental data in the literature (33).

5. The index n obtained for non-isotropic particles was consistently higher than that for spherically isotropic particles. This greater concentration dependence of the non-isotropic particle settling rates could be caused by the random orientation and consequent greater mutual hindrance of the non-isotropic particles, observed visually.

6. The index n showed a definite increase with the settled or random loose fixed bed porosity of the particles. The latter decreased slightly with bed height for low bed heights.

RECOMMENDATIONS

Prediction of index n by measuring ϵ_b should be useful. It is suggested that more data at low D_v/D_t for various particle shapes, including elongated needle shapes, be collected in the creeping flow region to confirm the method. A procedure for obtaining a more consistent value of ϵ_b should be used. It is also desirable to study the prediction of u_{ext} and its relationship to u_∞ , which has a unique value independent of orientation only for spherically isotropic bodies. For non-isotropic bodies, the free settling velocity u_v of an equivalent volume spheres, which does have a unique value for a given particle, could be applied instead of u_∞ .

Since the present experimental method could not be used for mixing a fast settling suspension, and the method of processing data in the $u\nu$ form is inapplicable beyond creeping flow, further work at high Reynolds numbers should be done by using fluidization as both the mixing and fluid-solid contacting method, with liquid temperature well controlled. This would involve careful design of the fluidization column and examination of the effect of entrance design and supporting screen.

Artificial particles with regular shapes would give more information than irregular shapes since their behaviour in free settling is better understood. In addition, current work (63) on artificially expanded packed beds of spheres could be profitably extended to non-spherical particles.

The wall effect on hindered settling of spherical particles found by Richardson and Zaki did not agree with the present work, which was not aimed specifically to study wall effect. The wall effect on spheres in the high Reynolds number region was studied by Nenzil and Hrdina (64), who used ϵ as a parameter and correlated u with D/D_t. More work is required on wall effect for hindered settling of spheres in creeping flow and the influence of non-sphericity on this effect. This information would be particularly useful for further work in this field involving the use of relatively large particles in small containers.

NOMENCLATURE

A_s	surface area of sphere of equal volume	cm^2
A_p	projected area of particle	cm^2
A	surface area of particle	cm^2
C	perimeter of the particle projected onto a surface	cm^2
C'	circumference of a circle of area equal to the projected area of the particle	cm^2
C_D	drag coefficient	
C_v	calibration constant of viscometer	cs/sec
c	volumetric concentration of suspension, $(1-\epsilon)$	
D	diameter of sphere	cm
D_c	diameter of a circle of same area as the projected area of the particle lying in its most stable position	cm
D_s	diameter of sphere of equal surface area	cm
D_t	column diameter	cm
D_u	diameter of sphere of equal settling rate	cm
D_v	diameter of sphere of equal volume	cm
F	drag force on particle settling in infinite medium	$g.cm.sec^{-2}$
F'	drag force	$g.cm.sec^{-2}$
f	function of	
g	acceleration of gravity	980 $cm.sec^{-2}$
K,k	proportionality constant	
K_{ST}	Stokes' law shape factor	
K_v	Heywood volumetric shape factor defined as $\pi D_v^3/6D_c^3$	
L	dimension of length	cm
n	Richardson-Zaki index	

Re	particle Reynolds number defined as $\frac{Du}{\nu}$ or $\frac{D_V u}{\nu}$	
Re_o	free settling particle Reynolds number defined as $\frac{Du_\infty}{\nu}$, $\frac{D_V u_\infty}{\nu}$, or $\frac{Lu_\infty}{\nu}$	
t_{cr}	duration of constant rate settling	sec
t_e	efflux time of liquid in viscometer	sec
u	hindered settling rate or superficial velocity of liquid in fluidization	cm sec^{-1}
u_{ext}	extrapolated free settling rate	cm sec^{-1}
u_{in}	incipient fluidization velocity	cm sec^{-1}
u_o	single particle free settling rate in bounded medium	cm sec^{-1}
u_∞	single particle free settling rate in infinite medium	cm sec^{-1}
u_V	free settling rate of sphere of equal volume in infinite medium	cm sec^{-1}
$(u\nu)_{ext}$	corresponding to $u_{ext} \times \nu$	$(0.01 cm^3 sec^{-2})$
$(u\nu)'_{ext}$	$(u\nu)_{ext}$ corrected for wall by eqt. 12	$(0.01 cm^3 sec^{-2})$
$(u\nu)_o$	corresponding to $u_o \times \nu$	$(0.01 cm^3 sec^{-2})$
$(u\nu)_\infty$	corresponding to $u_\infty \times \nu$	$(0.01 cm^3 sec^{-2})$
U	upward travelling rate of concentration discontinuity plane in hindered settling	cm sec^{-1}
V	volume	cm^3
W	upward travelling rate of a constant concentration element in hindered settling	cm sec^{-1}
z_i	initial suspension bed height	cm

Greek Letters

ϵ	porosity of suspension or fluidized bed	
ϵ_b	fixed bed porosity	
ρ	density of liquid	$g \cdot cm^{-3}$

ρ_p	density of particle	$g.cm^{-3}$
ϕ	function of	
ψ	sphericity defined as A_s/A	
μ	viscoosity of liquid	cp or $(0.01 g cm^{-1} sec^{-1})$
ν	kinematic viscosity of liquid	cs or $(0.01 cm^2 sec^{-1})$

Abbreviations

DIST	distance
Eqt.	equation
HTB	height of settled bed
PEG	polyethylene glycol
TEMP	temperature
WT.	weight of solid
STD.DEV.	standard deviation

LITERATURE CITED

1. Stokes, G.G., Trans. Cambridge Phil. Soc., 9, II, 51 (1851)
2. Perry, J.H., Chemical Engineers' Handbook, 3rd, McGraw-Hill, New York (1950)
3. Coe, H.S., Clevenger, G.H., Trans. Am. Inst. Mining Engrs., 55, 356 (1916)
4. Proudman, I., Pearson, J.R.A., J. Fluid Mech., 2, 237 (1957)
5. Whitehead, A.N., Quart. J. Math., 23, 143 (1889)
6. Oseen, C.W., Neuere Methoden und Ergebnisse in der Hydrodynamik, Leipzig, Akademishe Verlag (1927)
7. Jenson, V.G., Proc. Roy. Soc., A249, 346 (1959)
8. Oberbeck, H.A., Crelles J., 81, 79 (1876)
9. Gans, R., Sitzber Math-physik klasse Akad. Wissen, Munich, 41, 198 (1911)
10. Happel, J., Brenner, H., Low Reynolds Number Hydrodynamics, Prentice-Hall (1965)
11. Pernolet, V., Ann. Mines, 4me. Series, 20, 379 and 535 (1851)
12. Pettyjohn, E.S., Christiansen, E.B., Chem. Eng. Prog., 44, 157 (1948)
13. Chowdhury, K.C.R., Fritz, W., Chem. Eng. Sci., 11, 92 (1959)
14. Heiss, J.F., Coull, J., Chem. Eng. Prog., 48, 133 (1952)
15. Blumberg, P.N., Mohr, C.M., A.I. Ch.E. Journal, 14, 331 (1968)
16. McNown, J.S., Malaika, J., Trans. Am. Geophys. Union 31, 74 (1950)
17. Jayaweera, K.O.L.F., Mason, B.J., J. Fluid Mech., 22, 709 (1965)
18. Christiansen, E.B., Barker, D.H., A.I. Ch.E. Journal, 11, 145 (1965)
19. Isaacs, J.L. Thodos, G., Can. Jour. Chem. Eng., 45, 150 (1967)
20. Becker, H.A., Can. Jour. Chem. Eng., 37, 85 (1959)

21. Torobin, L.B., Gauvin, W.H., Can. Jour. Chem. Eng., 38, 142 (1960)

22. Happel, J., A.I. Ch.E. Journal, 4, 197 (1958)

23. Kuwabara, S., J. Physics Soc., Japan, 14, 527 (1959)

24. Leclair, B.P., Hamielec, A.E., Viscous Flow through Particles Assemblages at intermediate Reynolds Number. McMaster Univ. (1967)

25. Gasparyan, A.M., Ikaryan, N.S., Izv. Akad. Nauk. Arm. SSR. Ser. Tekhn. Nauk., 15, No. 2, 49 (1962)

26. Richardson, J.F., Zaki, W.N., Chem. Eng. Sci., 3, 65, 1954

27. Hawskley, P.G.W., Some Aspect of Fluid Flow, (1950)

28. Hanratty, T.J., Bandukwala, A., A.I. Ch.E. Journal 3, 293 (1957)

29. Whitmore, R.L., Brit. Jour. Appl. Phy., 6, 239 (1955)

30. Steinour, H.H., Ind. Eng. Chem. 36, 618 (1944)

31. Richardson, J.F., Meikle, R.A., Trans. Instn. Chem. Engrs., 39, 348 (1961)

32. Harris, C., Nature, 183, 530 (1959)

33. Loeffler Jr., A.L., Ruth, B.F., A.I. Ch.E. Journal, 5, 310 (1959)

34. Einstein, A., Ann. Phys. Lpz., 19, 286 (1906)
34, 591 (1911)

35. Vand, V, J. Phys. and Colloid Chem., 52, 277 (1948)

36. Brinkman, H.C., Appl. Sci. Res., A1, 27 (1947)

37. Verschoor, H., Appl. Sci. Res., A2, 155 (1950)

38. Robinson, C.S., Ind. Eng. Chem., 18, 869 (1926)

39. Oliver, D.R., Chem. Eng. Sci., 15, 230 (1961)

40. Lewis, E.W., Bowerman, E.W., Chem. Eng. Prog., 48, 604 (1952)

41. Lewis, W.K, et.al., Ind. Eng. Chem., 41, 1104 (1949)

42. Wilhelm, R.H., Kwauk, M., Chem. Eng. Prog., 44, 201 (1948)

43. Richardson, J.F., Zaki, W.N., Trans. Instn. Chem. Engrs., 32, 35 (1954)

44. Hancock, R.T., Trans. Instn. Min. Engrs., 94, 114 (1938)

45. Gasparyan, A.M., Ikaryan, N.S., Izv. Akad. Nauk. Arm. SSR. Ser. Tekln. Nauk., 15, No. 4, 53 (1962)

46. Jottrand, R., J. Appl. Chem., 2, Sup 1, S17 (1952)

47. Mueller, F., Schramm, W., Mitteilungen, 5, 361 (1966)

48. Zenz, F.A., Othmer, D.F., Fluidization and Fluid-Particle Systems, Reinhold (1960)

49. McCabe, W.L., Smith, J.C., Unit Operations of Chemical Engineering, McGraw-Hill (1956)

50. Beranek, J., Klumpar, I., Chem. Lusty., 50, 1540 and 1673 (1956)

51. Brownell, L.E., Dowbrowski, H.S., Dickey, C.A., Chem. Eng. Prog., 46, 415 (1950)

52. Waddal, H., Physics, 5, 281 (1934)

53. Martin, J.J., McCabe, W.L., Monrad, C.C., Chem. Eng. Prog., 47, 91 (1951)

54. Brenner, H., J. Fluid Mech., 12, 35 (1962)

55. McNown, J.S., et.al., Proc. 7th. Intern. Cong. Appl. Mech., London (1948)

56. Kaye, B.H., Davies, R., Proceeding of the Symposium on the Interaction between fluid and Particles, London, June (1962)

57. Pruden, B., M.A.Sc. Thesis, Dept. of Chem. Eng., UBC (1964)

58. Pearce, K.W., Proceeding of the Symposium on the Interaction between Fluid and Particles, London, June (1962)

59. Whitmore, R.L., Jour. Inst. Fuel, 30, 238 (1957)

60. Coulson, J.M., Trans. Instn. Chem.,Eng. 27, 237 (1949)

61. Happel, J., Epstein, N., Ind. Eng. Chem., 46, 1187 (1954)

62. Shannon, P., Stroupe, E., Tory, E., Ind. Eng. Chem., 2, 203 (1963)

63. Gunn, D.J., Malik, A.A., Trans. Instn. Chem. Engrs., 44, 371 (1966)

64. Neuzil, L., Hrdina, M., Collection Czechoslov. Chem. Commun., 30, 753 (1965)

65. Kynch, G.J., Trans. Faraday Soc., 48, 166 (1952)

66. Shannon, P., et.al., Ind. Eng. Chem., 3, 250 (1964)

67. Buchanan, J.E., Ind. Eng. Chem., 4, 367 (1965)

68. A.S.T.M. Standards on Petroleum Products and Lubricants, D445-53T, Baltimore (1958)

69. Bird, R.B., Stewart, W.E., Lightfoot, E.N., Transport Phenomena, Wiley (1960)

70. De Verteuil, G.F., M.A.Sc. Thesis, UBC (1958)

71. Hodgeman, C.D., Handbook of Chemistry and Physics, The Chemical Rubber Pub. Co., (1962-63)

APPENDIX I THEORY OF SEDIMENTATION

A theory of sedimentation without detailed consideration of the hydrodynamics of particles was suggested by Kynch (65) and verified experimentally by Shannon et. al. (66). The analysis is restricted by the assumption of an ideal suspension, namely, uniform particle shape and density, absence of wall effect, and settling velocities dependent only on the local particle concentration. Consider such a suspension in a cylindrical container. By material balance it can be shown that if there is any concentration gradient present in the settling suspension, an elemental plane of constant concentration will propagate upward through the bed with velocity

$$W = - \frac{\partial (uc)}{\partial c} \qquad \text{(I-1)}$$

where c is the local particle concentration at the elemental plane under consideration. The term uc is the volumetric solid flux. If discontinuity of concentration is present in the bed, the discontinuity plane will move upward through the dispersion at a velocity of

$$U = - \frac{\Delta (uc)}{\Delta c} = - \frac{(uc)_2 - (uc)_1}{c_2 - c_1} \qquad \text{(I-2)}$$

where Δ signifies a finite change of concentration at the discontinuity. With these relationships and the relationship between settling flux, uc, and concentration, c, as shown in Figure I-1, it is possible to predict quantitatively the complete settling curve for a suspension of given concentration, and at least qualitatively, the curve for any dispersion having a certain variation of concentration with height. The shape of the settling flux graph has a profound effect on the settling curve derived from it. The settling flux graph of a microglass bead suspension which was an unflocculated ideal suspension was found to be of the form shown in Figure I-2 (62), though argument arose as to the actual shape of the curve at high concentration (67). In spite of this point, it can still be shown that an initially uniform suspension should have a period of constant initial settling rate, with a solid flux corresponding to the overall concentration. For a suspension of initial concentration c_i which settles discontinuously to an ultimate sediment of concentration c_∞, the initial settling rate is u_i while the upward velocity of discontinuity between c_i and c_∞, according to equation I-2, should be

$$U = \frac{u_i c_i - 0}{c_\infty - c_i} \qquad \text{(I-2a)}$$

All settling is then at constant rate for a period

$$t_{cr} = \frac{z_i}{u_i + U} \qquad \text{(I-3)}$$

where z_i is the initial height of the suspension.

If the flux graph is of the double concave type as suggested by Shannon (66) and shown in Figure I-2, and if the initial concentration c_i happens to be in a concentration region where a discontinuous step change to c_∞ is unstable, the suspension will settle in such a way that the upper portion still corresponds to the initial concentration c_i and the lower part varies abruptly from c_∞ at the bottom to c_3, and thence continuously to c_2, where c_3 and c_2 are inflexion points on the curve. The elemental plane of constant concentration c_2 will propagate upward with velocity corresponding to equation I-1

$$W = - \left[\frac{\partial(uc)}{\partial c} \right]_{\text{at } c_2} \tag{I-1a}$$

and the downward moving rate of supernatant-suspension interface is u_i. The first period of duration

$$t_{cr} = \frac{z_i}{u_i + W} \tag{I-4}$$

is of constant rate. After time t_{cr}, the downward moving supernatant-suspension interface will settle with a decreasing rate as it hits the upward moving element planes of increasing concentration.

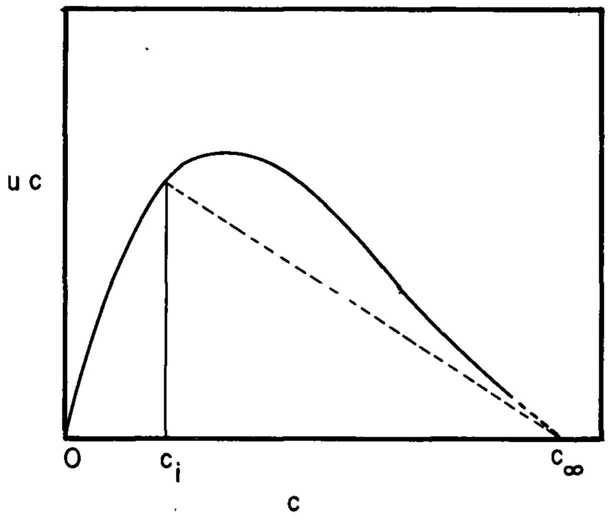

Figure I-1. Sedimentation Flux Plot, Single Concave

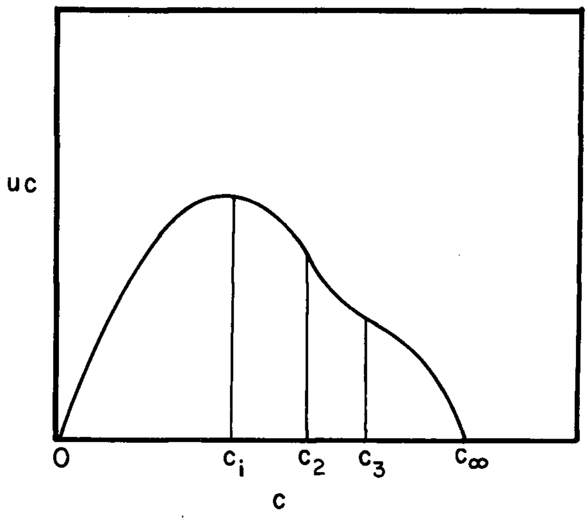

Figure I-2. Sedimentation Flux Plot, Double Concave

APPENDIX II DESCRIPTION AND TESTING OF LIQUID ELUTRIATION APPARATUS

The column consisted of two parts, with a supporting screen midway in the lower part, so that a considerable length of column acted as an entrance calming section (see Figure 4). The two parts of the column were inserted into matching polyethylene blocks with openings equal to the column diameter. The connections between the column and the polyethylene blocks were sealed with O-rings to facilitate easy disassembly of the column. A gate with a screen at the center was installed in the gap between the two blocks. It could be pulled out of the opening so that free flow through the opening was permitted, or pushed into the opening so that only liquid could pass through the screen. Details of the screen gate unit are shown in Figure II-1. The column was clamped to an iron support and set in vertical position by means of a plummet.

The column was tested with spherical glass beads which had been closely sized by sieving. Mixtures of glass beads from two consecutive fourth root series Tyler screens were prepared in the proportion 90% of the larger size fraction and 10% of the smaller, the latter colored black by marking ink. The volume of column available for a fluidized bed was calculated, and the amount of mixture which would produce a fluidized bed of porosity 0.95 was introduced. Visual segregation by size was obvious in the fluidization even at lower porosity. Clear cut separation was naturally impossible. Nevertheless the column was able to separate spherical particles of different sizes as effectively as the fourth root series Tyler screens. A further test was done by fluidizing closely sized glass beads from fourth root series screens in the column and collecting a small portion of the particles at the topmost part of the bed by shutting the screen gate. The recovered "apparently smaller" particles were colored as before and re-inserted in the column. In this case no visual segregation could be observed.

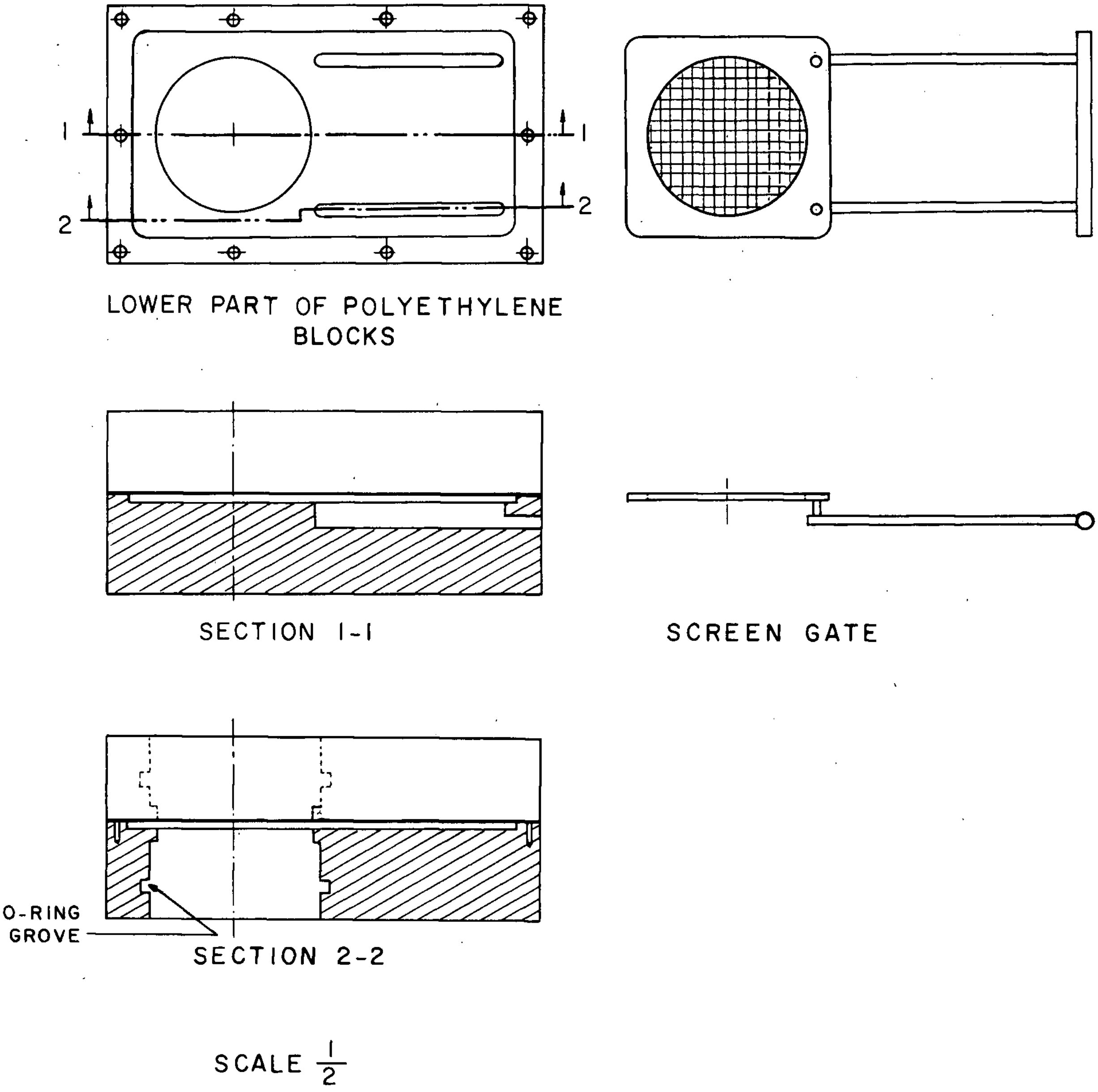

Figure II-1. Detailed Drawing of Screen Gate

APPENDIX III NEWTONIAN BEHAVIOUR OF POLYETHYLENE GLYCOL SOLUTION

The 45% polyethylene water solution was tested for Newtonian behaviour in capillary viscometers (Cannon-Fenske) of different sizes. Table III-1 shows that the calculated viscosity did not change with capillary diameter. This indicated that the liquid behaved like a Newtonian fluid at least below the shear stress experienced by the liquid in the test, the highest of which was in the largest capillary. It can be shown that the capillary viscometers of different sizes calibrated with Newtonian liquids do not give constant apparent viscosity for a

Table III-1

Calculated Viscosity of PEG from

Different Size Viscometers

Temperature: 77.05°F

Viscometer	Approx. I.D. of Capillary* cm	Efflux Time Sec.	Calculated Viscosity cs
C3(size 200)	0.102	2383.6	259.8
D91(size 300)	0.126	1130.7	259.9
C965(size 400)	0.188	222.1	260.0

* from A.S.T.M. D445-53T (68)

non-Newtonian liquid. The maximum shear stress of the test, which occured at the wall of the capillary, and the largest capillary was estimated by the laminar pipe flow equation for a Newtonian fluid (69).

$$\tau_{rz|R} = \frac{\Delta PR}{2L} \qquad \text{(III-1a)}$$

where $\tau_{rz|R}$ is the axial direction shear stress at the wall of the capillary the radius of which is R and ΔP is the pressure difference over the capillary length L. In the viscometer, ΔP can be taken as $L\rho g$ (In fact ΔP is larger than $L\rho g$ since the driving head in the viscometer is larger than the capillary length, which causes the main friction to fluid flow). Neglecting the unsteady state flow, equation III-1a becomes

$$\tau_{rz|R} = \frac{\rho Rg}{2} \qquad \text{(III-1b)}$$

Approximate shear stress for viscometer C965 was estimated as

$$\tau_{rz|R} = \frac{1.082 \times 0.094 \times 980}{2} = 49.8 \text{ dynes/cm}^2$$

The possible maximum shear stress experienced by the liquid in glass bead settling was estimated from the equation for a single sphere settling in an infinite medium (69)

$$\tau_{r\theta|R} = \frac{3}{2}\frac{\mu u_\infty}{R} \sin\theta \qquad \text{(III-2)}$$

where $\tau_{r\theta|R}$ is the shear stress in the angular direction at the sphere surface which is larger than that beyond the surface, u_∞ is the free settling velocity and R is the radius of the sphere. Maximum shear stress occurs at $\theta = \pi/2$. From free settling data on 0.1135 mm glass beads, taking R = 0.058 cm,

$$\tau_{relR} = \frac{3}{2}\,\frac{140.5}{0.058} = 36.3 \text{ dynes/cm}^2$$

which is within the shear stress of the test. Thus 45% polyethylene glycol water solution conformed to Newtonian behavior in the present experimental condition.

APPENDIX IV MEASUREMENT OF DENSITY AND VISCOSITY

A. Measurement of Liquid Density

Liquid density was measured with a Westphal balance which had been calibrated with distilled water at room temperature, from which the appropriate correction factor was applied to all subsequent measurements. The sensitivity of the balance depended on the viscosity of the liquid and was estimated to be better than 0.001 gram/cu.cm.

B. Measurement of Particle Density

Conventional specific gravity bottles were used to measure the density of the particles. The density was based on the known density of water (71), in which the particles were immersed. For those particles which were soluble in water, a second immersing medium, benzene, was used. The bottles which contained liquid and particles were boiled to drive out the air bubbles trapped between the particles. All weighings were made at the same temperature by letting the bottles stand in a constant temperature bath slightly above room temperature, and immediately tightening the cap on removing the bottle from the bath in order to avoid losing liquid by evaporation.

C. Measurement of Liquid Viscosity

The kinematic viscosity of various test liquids was determined by Cannon-Fenske viscometers of appropriate size, essentially conforming to the specifications and procedures described in ASTM manual (68). The viscometers were immersed in a constant temperature bath with temperature controlled to within $\pm$ 0.05^{o}F. The efflux time of the test liquid was measured by a stopwatch graduated in divisions of 0.2 seconds. The stopwatches used were all tested against N.B.S. time signals broadcasted on Station WWV over 12-hour periods, and were found to be accurate to within 0.02%. Calibration of a series of viscometers ranging from size 100 to size 400 is reported in Appendix V.

APPENDIX V CALIBRATION OF VISCOMETERS

The Cannon-Fenske viscometers ranging from size 100 to size 450 were calibrated by comparing the efflux time of a liquid in two viscometers of consecutive size number in the same bath at 77°F. Viscometer No. B78 was the standard on which all the other larger viscometers were based. It was calibrated by Cannon Laboratories. This step-up procedure of calibration, which was originally suggested in A.S.T.M. D445-53T (68) for basic calibration of master viscometer, was found to be satisfactory for the routine viscometers. The calibration constant of each of the viscometers used are listed in Table V-1. The correction for kinetic energy is negligible for the larger size viscometers at liquid efflux time higher than 200 seconds. Thus viscosity was calculated as

$$\nu = C_v t_e$$

where t_e is the efflux time of the liquid in the viscometer of calibration constant, C_v. The calibration constant of the viscometer of the highest size number was checked by the standard oil supplied by Cannon Laboratories. The difference was less than 0.5%. Procedures for filling, cleaning and measuring efflux time are described in the A.S.T.M. manual (68).

The excellent agreement in Table V-1 between C_v (2.590) for the largest viscometer as determined by the standard oil (S-600) and that obtained by the step-up procedure using the blended solutions of automobile crank case oils (2.583) is a strong indication that the later oils were Newtonian.

Table V-1

Summary of Viscometer Calibration

Calibrated viscometer No.	Calibrated viscometer Size No.	Reference viscometer No.	Standard liquid	Efflux time sec	Efflux time ratio	Ave. Efflux time ratio	Calibration constant at 77°F C_v cs/sec
B78	100	*	-	-	-	-	0.01246
H69	150	B78	Oil A	208.7	2.581	2.582	0.03218
			Oil B	324.4	2.584		
C3	200	H69	Oil C	334.7	3.390	3.388	0.1090
			Oil D	338.7	3.387		
C8	200	**	-	-	-	-	0.1086
D91	300	C3	Oil E	222.4	2.109	2.108	0.2299
			Oil F	336.7	2.107		
J781	300	D91	PEG sol'n	619.7	1.081	1.081	0.2485
C965	400	D91	Oil G	225.5	5.095	5.096	1.171
			Oil H	249.0	5.096		
E60	400	D91	Oil H	254.0	4.985	4.985	1.149
V389	450	C965	Oil I	160.4	2.205	2.206	2.583
			PEG sol'n	337.9	2.206		
V389	450	***	Oil S-600	562.5	-	-	2.590

* Calibrated by Cannon Laboratories, Penn. State College.

** Calibrated by De Verteuil (70).

*** Standard oil supplied by Cannon Laboratories, kinematic viscosity = 1457 cs. at 77°F

APPENDIX VI JUSTIFICATION OF USING $u\nu$

In the viscous flow region the free settling rate of a particle in a given orientation is

$$u_\infty = k \frac{L^2(\rho_p-\rho)g}{18\rho\nu_\infty}$$

or

$$u_\infty\nu_\infty = k \frac{L^2(\rho_p-\rho)g}{18\rho} \tag{8b}$$

The general expression for multiparticle settling system is

$$\frac{u}{u_\infty} = \phi(\epsilon, \mathrm{Re}_o, \frac{D_v}{D_t}) \tag{9}$$

and under viscous flow conditions in a given container

$$\frac{u}{u_\infty} = \phi'(\epsilon) \tag{VI-1}$$

where u and u_∞ are measured under the same physical conditions. Temperature change has much effect on the viscosity but not on the other physical properties in equation. Thus

$$u_\infty\nu_\infty = \text{constant} \tag{VI-2}$$

if u of equation VI-1 is measured at a temperature for which the liquid viscosity is ν, which is different from the value ν_∞ at which u_∞ is measured, u_∞ can be corrected to

$$u_\infty' = \frac{u_\infty\nu_\infty}{\nu}$$

which is then the free settling velocity at viscosity ν. Equation VI-1 then becomes

$$\frac{u\nu}{u_\infty \nu_\infty} = \phi'(\epsilon) \qquad \text{(VI-1a)}$$

Thus when temperature is not constant, $u\nu/u_\infty\nu_\infty$ has the same functional relationship as u/u_∞ provided that the right hand side of equation 8b is independent of temperature.

Variation of the right hand side of equation 8b with temperature was checked by the data from Run 2-, Glass beads in Polyethylene Glycol solution. The particle dimension, L, and particle density, ρ_p , should not contribute significant change since solid expansion coefficient is very small (0.274×10^{-4} in volume, (2)). Variation of liquid density over 8 Fahrenheit deg. of 45% PEG solution was from

$1.085\ g/cm^3$ at 67.2^oF

to $1.0825\ g/cm^3$ at 75.2^oF

The corresponding variation of $(\rho_p - \rho)/\rho$ was calculated based on $\rho = 2.977\ g/cm^3$ as

1.744 at 67.2^oF

and 1.750 at 75.2^oF

Percentage change is 0.35%. Temperature effect on the other liquid was expected to be of the same order. Actual temperature variation in the experiment was much smaller than 8 Fahrenheit degrees, as shown in the original data in Appendix VII.

APPENDIX VII ORIGINAL DATA ON HINDERED SETTLING

The first number in Run No. signifies a combination of particles and liquid. Except in Run 8-P and 8-M, where P and M stand for "pure" and "mixture" respectively, the second number represents and the size of the column used in the settling. The column diameters of 2.54 cm, 3.78 cm, 5.08 cm, 7.71 cm and 10.12 cm are denoted respectively by the numbers 1 to 5.

Nomenclature in all computer print out is explained in Appendix XIII.

APPENDIX VII INDEX

SETTLING DATA

* D_V is used to indicate particle size

APPENDIX VII INDEX (continued)

SETTLING DATA

APPENDIX INDEX (continued)

SETTLING DATA

RUN 1-1
PARTICLES= GLASS BEADS DENSITY= 2.977 GM/CM^3
LIQUID= P.E.G.SOLN 40/100 DENSITY= 1.071 GM/CM^3
PARTICLE SIZE D_V= 0.1135 CM, D_t = 2.54 CM, D_V/D_t = 0.0447
SIEVE OPENINGS 0.991/1.168 MM, NO ELUTRIATION

TEMP °F	DIST CM	SETTLING TIME SEC	U CM/SEC	U*NU $0.01CM^3/SEC^2$	EPS
74.23	20.0	51.8	0.386	63.0	0.90
74.23	20.0	51.5	0.388	63.4	0.90
75.42	20.0	49.2	0.407	64.8	0.90
74.55	30.0	81.8	0.367	59.5	0.88
75.00	30.0	82.3	0.365	58.6	0.88
78.10	15.0	45.4	0.330	49.9	0.85
78.10	15.0	45.9	0.327	49.3	0.85
78.10	15.0	45.5	0.330	49.7	0.85
77.30	15.0	45.6	0.329	50.4	0.85
75.26	15.0	52.0	0.288	46.1	0.83
74.20	15.0	52.7	0.285	46.5	0.83
74.20	15.0	52.8	0.284	46.4	0.83
74.20	15.0	51.4	0.292	47.6	0.83
74.20	15.0	49.8	0.301	49.2	0.83
73.38	15.0	65.7	0.228	37.9	0.80
73.28	15.0	64.4	0.233	38.7	0.80
69.30	10.0	56.8	0.176	31.8	0.77
69.30	10.0	52.4	0.191	34.5	0.77
69.70	10.0	67.5	0.148	26.5	0.74
69.70	10.0	69.2	0.145	25.9	0.74
69.80	10.0	91.4	0.109	19.6	0.70
69.80	10.0	92.4	0.108	19.4	0.70
71.80	6.0	69.9	0.086	14.7	0.67
71.80	6.0	65.9	0.091	15.6	0.67
72.90	6.0	66.5	0.090	15.1	0.67

RUN 1-2
PARTICLES= GLASS BEADS DENSITY= 2.977 GM/CM^3
LIQUID= P.E.G.SOLN 40/100 DENSITY= 1.071 GM/CM^3
PARTICLE SIZE D_V= 0.1135 CM, D_t = 3.78 CM, D_V/D_t = 0.0300
SIEVE OPENINGS 0.991/1.168 MM, NO ELUTRIATION

TEMP °F	DIST CM	SETTLING TIME SEC	U CM/SEC	U*NU $0.01CM^3/SEC^2$	EPS
75.03	30.0	72.2	0.416	66.8	0.90
75.03	30.0	73.0	0.411	66.0	0.90
75.00	30.0	72.2	0.416	66.8	0.90
75.00	30.0	72.4	0.414	66.6	0.90
74.00	20.0	48.2	0.415	68.0	0.90
74.00	20.0	48.0	0.417	68.3	0.90
73.40	20.0	52.8	0.379	62.8	0.88
73.40	20.0	51.5	0.388	64.4	0.88
74.00	30.0	79.9	0.375	61.5	0.88
74.63	30.0	78.7	0.381	61.7	0.88
75.57	15.0	43.6	0.344	54.7	0.85
75.00	15.0	47.0	0.319	51.3	0.85
74.83	15.0	46.8	0.321	51.7	0.85
77.13	15.0	48.8	0.307	47.3	0.83
77.13	15.0	48.6	0.309	47.5	0.83
76.60	15.0	48.9	0.307	47.7	0.83
76.10	15.0	49.4	0.304	47.7	0.83
73.60	15.0	62.6	0.240	39.6	0.80
73.60	15.0	60.8	0.247	40.8	0.80
73.60	15.0	61.7	0.243	40.2	0.80
73.80	15.0	61.8	0.243	39.9	0.80
73.88	15.0	73.4	0.204	33.6	0.77
73.40	10.0	50.8	0.197	32.7	0.77
73.40	10.0	48.2	0.207	34.4	0.77
73.40	10.0	48.2	0.207	34.4	0.77
70.50	10.0	69.1	0.145	25.5	0.74
70.50	10.0	64.1	0.156	27.5	0.74
70.50	10.0	65.0	0.154	27.1	0.74
70.50	10.0	65.7	0.152	26.8	0.74
70.12	10.0	86.6	0.115	20.5	0.70
69.20	6.0	64.4	0.093	16.9	0.67
70.50	6.0	62.0	0.097	17.1	0.67
71.00	6.0	64.1	0.094	16.3	0.67
72.10	6.0	75.0	0.080	13.6	0.64
71.00	6.0	76.8	0.078	13.6	0.64

RUN 1-3
PARTICLES= GLASS BEADS DENSITY= 2.977 GM/CM^3
LIQUID= P.E.G.SOLN 40/100 DENSITY= 1.071 GM/CM^3
PARTICLE SIZE D_V= 0.1135 CM, D_t = 5.08 CM, D_V/D_t = 0.0223
SIEVE OPENINGS 0.991/1.168 MM, NO ELUTRIATION

TEMP °C	DIST CM	SETTLING TIME SEC	U CM/SEC	U*NU $0.01CM^3/SEC^2$	EPS
22.15	20.0	52.4	0.382	65.1	0.90
22.15	20.0	51.0	0.392	66.9	0.90
22.15	20.0	53.4	0.375	63.9	0.90
22.15	20.0	51.6	0.388	66.2	0.90
22.05	20.0	52.8	0.379	64.9	0.90
22.05	20.0	51.8	0.386	66.1	0.90
21.95	20.0	55.8	0.358	61.6	0.88
21.95	20.0	56.6	0.353	60.8	0.88
22.15	20.0	56.6	0.353	60.3	0.88
22.15	20.0	56.8	0.352	60.1	0.88
22.40	20.0	55.9	0.358	60.5	0.88
21.65	20.0	66.8	0.299	52.1	0.85
21.85	20.0	67.4	0.297	51.2	0.85
22.10	20.0	65.3	0.306	52.4	0.85
22.10	20.0	65.8	0.304	52.0	0.85
22.10	20.0	65.4	0.306	52.3	0.85
22.80	20.0	72.1	0.277	46.2	0.83
22.80	20.0	69.8	0.287	47.7	0.83
22.75	20.0	71.5	0.280	46.7	0.83
22.75	15.0	53.1	0.282	47.1	0.83
22.65	20.0	72.0	0.278	46.5	0.83
21.58	15.0	65.4	0.229	40.0	0.80
22.00	15.0	62.5	0.240	41.2	0.80
22.50	15.0	66.0	0.227	38.3	0.80
22.40	12.0	51.4	0.233	39.5	0.80
22.40	12.0	50.6	0.237	40.1	0.80
22.35	12.0	51.6	0.233	39.4	0.80
22.25	12.0	60.6	0.198	33.7	0.77
22.25	12.0	63.2	0.190	32.3	0.77
22.20	12.0	63.4	0.189	32.2	0.77
22.20	12.0	61.0	0.197	33.5	0.77
22.20	12.0	62.5	0.192	32.7	0.77
22.15	9.0	58.4	0.154	26.3	0.74
22.15	9.0	58.8	0.153	26.1	0.74
22.20	9.0	57.3	0.157	26.8	0.74
22.20	9.0	56.8	0.158	27.0	0.74
21.65	9.0	78.9	0.114	19.9	0.70
21.80	6.0	51.8	0.116	20.0	0.70
21.85	6.0	51.0	0.118	20.3	0.70
21.85	6.0	47.4	0.127	21.9	0.70
21.85	6.0	49.7	0.121	20.8	0.70
21.80	6.0	61.6	0.097	16.9	0.67
21.80	6.0	62.0	0.097	16.7	0.67
21.90	6.0	62.8	0.096	16.5	0.67

21.90	6.0	62.4	0.096	16.6	0.67
21.70	6.0	81.0	0.074	12.9	0.64
21.70	6.0	78.3	0.077	13.3	0.64
21.70	6.0	77.4	0.078	13.5	0.64
21.70	6.0	79.6	0.075	13.1	0.64

RUN 2-1
PARTICLES= GLASS BEADS DENSITY= 2.977 GM/CM^3
LIQUID= P.E.G.SOLN 45/100 DENSITY= 1.082 GM/CM^3
PARTICLE SIZE D_V= 0.1135 CM, D_t = 2.54 CM, D_V/D_t = 0.0447
SIEVE OPENINGS 0.991/1.168 MM, NO ELUTRIATION

TEMP °F	DIST CM	SETTLING TIME SEC	U CM/SEC	U*NU $0.01CM^3/SEC^2$	EPS
71.00	37.0	186.0	0.1989	63.4	0.90
71.05	37.0	196.0	0.1888	60.1	0.90
71.05	37.0	186.0	0.1989	63.3	0.90
71.10	37.0	191.5	0.1932	61.4	0.90
71.20	37.0	208.0	0.1779	56.4	0.88
71.20	37.0	208.0	0.1779	56.4	0.88
72.20	20.0	126.8	0.1577	48.9	0.85
72.20	20.0	122.8	0.1629	50.5	0.85
72.20	20.0	123.4	0.1621	50.2	0.85
72.20	20.0	122.3	0.1635	50.7	0.85
72.00	20.0	137.5	0.1455	45.3	0.83
72.00	20.0	134.2	0.1490	46.4	0.83
72.00	20.0	135.8	0.1473	45.8	0.83
73.40	16.0	127.6	0.1254	37.7	0.80
73.40	16.0	123.7	0.1293	38.9	0.80
73.40	12.0	94.3	0.1273	38.3	0.80
72.20	16.0	128.8	0.1242	38.5	0.80
74.40	38.0	344.5	0.1103	32.4	0.77
75.30	38.0	330.0	0.1152	33.2	0.77
75.40	38.0	332.0	0.1145	32.9	0.77
72.10	16.0	198.1	0.0808	25.1	0.74
73.20	28.0	421.0	0.0665	20.1	0.70
75.30	20.0	354.0	0.0565	16.3	0.67

RUN 2-2
PARTICLES= GLASS BEADS DENSITY= 2.977 GM/CM^3
LIQUID= P.E.G.SOLN 45/100 DENSITY= 1.082 GM/CM^3
PARTICLE SIZE D_v= 0.1135 CM, D_t = 3.78 CM, D_v/D_t = 0.0300
SIEVE OPENINGS 0.991/1.168 MM, NO ELUTRIATION

TEMP °F	DIST CM	SETTLING TIME SEC	U CM/SEC	U*NU $0.01CM^3/SEC^2$	EPS
70.70	38.0	196.5	0.1934	62.1	0.895
71.50	38.0	202.5	0.1877	59.1	0.880
71.40	38.0	234.5	0.1620	51.2	0.850
71.40	38.0	227.0	0.1674	52.9	0.850
71.40	38.0	234.5	0.1620	51.2	0.850
72.87	21.0	137.6	0.1526	46.5	0.830
72.87	20.0	134.0	0.1493	45.5	0.830
72.87	20.0	132.6	0.1508	46.0	0.830
72.87	20.0	129.2	0.1548	47.2	0.830
71.50	20.0	164.2	0.1218	38.4	0.800
72.50	16.0	157.2	0.1018	31.3	0.770
72.50	16.0	157.2	0.1018	31.3	0.770
72.40	18.0	203.4	0.0885	27.3	0.740
72.20	16.0	182.6	0.0876	27.1	0.740
74.50	30.0	397.0	0.0756	22.2	0.700
75.50	30.0	370.0	0.0811	23.3	0.700
72.60	22.0	424.0	0.0519	15.9	0.670
72.60	22.0	388.5	0.0566	17.4	0.670
74.10	20.0	480.0	0.0417	12.3	0.640
74.60	20.0	460.0	0.0435	12.7	0.640

RUN 2-3
PARTICLES= GLASS BEADS DENSITY= 2.977 GM/CM^3
LIQUID= P.E.G.SOLN 45/100 DENSITY= 1.082 GM/CM^3
PARTICLE SIZE D_V= 0.1135 CM, D_t = 5.08 CM, D_V/D_t = 0.0223
SIEVE OPENINGS 0.991/1.168 MM, NO ELUTRIATION

TEMP °F	DIST CM	SETTLING TIME SEC	U CM/SEC	U*NU $0.01CM^3/SEC^2$	EPS
71.80	20.0	96.4	0.2075	64.9	0.90
71.80	20.0	96.2	0.2079	65.0	0.90
72.00	20.0	96.2	0.2079	64.7	0.90
69.90	20.0	100.8	0.1984	64.9	0.90
69.90	20.0	103.7	0.1929	63.1	0.90
70.20	20.0	108.8	0.1838	59.7	0.88
70.20	20.0	109.5	0.1826	59.3	0.88
70.10	20.0	109.1	0.1833	59.7	0.88
69.58	20.0	128.3	0.1559	51.3	0.85
69.58	20.0	123.6	0.1618	53.3	0.85
69.58	20.0	129.8	0.1541	50.8	0.85
69.80	20.0	123.0	0.1626	53.3	0.85
69.80	20.0	125.6	0.1592	52.2	0.85
69.80	20.0	127.0	0.1575	51.6	0.85
69.95	20.0	141.3	0.1415	46.2	0.83
70.00	20.0	142.0	0.1408	45.9	0.83
70.10	20.0	141.7	0.1411	45.9	0.83
70.10	20.0	137.2	0.1458	47.4	0.83
71.90	10.0	75.2	0.1330	41.5	0.80
71.90	10.0	75.8	0.1319	41.2	0.80
71.90	10.0	76.8	0.1302	40.6	0.80
71.90	10.0	74.4	0.1344	41.9	0.80
72.30	8.0	73.1	0.1094	33.8	0.77
72.30	8.0	74.5	0.1074	33.2	0.77
72.70	8.0	74.0	0.1081	33.1	0.77
72.30	15.1	139.0	0.1086	33.6	0.77
72.70	15.6	149.0	0.1047	32.0	0.77
72.80	20.8	234.0	0.0891	27.2	0.74
72.80	21.0	244.0	0.0863	26.3	0.74
73.00	6.0	68.2	0.0880	26.7	0.74
73.15	20.9	305.5	0.0684	20.7	0.70
73.15	21.3	311.0	0.0686	20.8	0.70
75.50	20.9	278.0	0.0752	21.6	0.70
75.50	20.9	305.0	0.0685	19.7	0.70
70.60	21.2	423.0	0.0500	16.1	0.67
72.05	21.1	398.0	0.0530	16.5	0.67
72.05	20.2	371.0	0.0544	16.9	0.67
72.15	20.1	429.0	0.0469	14.5	0.64
72.15	21.0	481.5	0.0436	13.5	0.64

RUN 7-3
PARTICLES= GLASS BEADS DENSITY= 2.959 GM/CM^3
LIQUID= P.E.G.SOLN 35.4 % DENSITY= 1.062 GM/CM^3
PARTICLE SIZE D_V= 0.0492 CM, D_t = 5.08 CM, D_V/D_t = 0.0097
SIEVE OPENINGS 0.417/0.495 MM, NO ELUTRIATION

TEMP °F	DIST CM	SETTLING TIME SEC	U CM/SEC	U*NU $0.01CM^3/SEC^2$	EPS
73.20	9.0	66.4	0.1355	14.75	0.95
73.20	9.0	66.8	0.1347	14.67	0.95
73.75	12.0	97.2	0.1235	13.30	0.92
73.75	12.0	98.8	0.1215	13.08	0.92
73.75	12.0	99.4	0.1207	13.00	0.92
71.60	12.0	113.4	0.1058	11.90	0.90
71.60	12.0	107.4	0.1117	12.57	0.90
71.60	12.0	107.3	0.1118	12.58	0.90
71.60	12.0	109.0	0.1101	12.38	0.90
72.70	12.0	117.8	0.1019	11.20	0.88
72.70	12.0	119.8	0.1002	11.02	0.88
72.70	12.0	111.6	0.1075	11.83	0.88
72.70	12.0	118.5	0.1013	11.14	0.88
73.70	12.0	132.0	0.0909	9.80	0.85
73.70	12.0	132.2	0.0908	9.79	0.85
74.05	12.0	156.4	0.0767	8.22	0.82
74.90	12.0	152.0	0.0789	8.32	0.82
70.70	12.0	167.6	0.0716	8.19	0.82
70.70	12.0	163.9	0.0732	8.38	0.82
72.25	12.0	176.2	0.0681	7.56	0.80
72.55	12.0	176.2	0.0681	7.51	0.80
72.90	9.0	156.0	0.0577	6.32	0.77
73.65	9.0	194.2	0.0463	5.00	0.74
73.65	9.0	190.0	0.0474	5.11	0.74
73.65	9.0	191.2	0.0471	5.08	0.74
71.60	10.0	268.6	0.0372	4.19	0.71
71.60	10.0	262.0	0.0382	4.29	0.71
73.20	10.0	330.0	0.0303	3.30	0.68
74.20	10.0	320.0	0.0313	3.34	0.68
75.20	10.0	381.0	0.0262	2.75	0.65

RUN 3-1A
PARTICLES= SALT CRYSTALS DENSITY= 2.169 GM/CM^3
LIQUID= SAE 10W 84.9%+ KEROSENE, DENSITY= 0.858 GM/CM^3
PARTICLE SIZE D_V= 0.0341 CM, D_t = 2.54 CM, D_V/D_t = 0.0134
SIEVE OPENINGS 0.250/0.298 MM, NO ELUTRIATION

TEMP °F	DIST CM	SETTLING TIME SEC	U CM/SEC	U*NU $0.01CM^3/SEC^2$	EPS
71.10	5.0	29.8	0.1678	5.395	0.95
71.10	5.0	31.0	0.1613	5.186	0.95
71.10	5.0	28.6	0.1748	5.622	0.95
71.80	10.0	65.4	0.1529	4.827	0.92
71.80	10.0	67.1	0.1490	4.704	0.92
71.80	10.0	69.6	0.1437	4.535	0.92
71.95	10.0	65.5	0.1527	4.800	0.92
72.40	10.0	70.2	0.1425	4.429	0.90
72.40	10.0	72.8	0.1374	4.271	0.90
71.80	10.0	84.6	0.1182	3.731	0.88
72.00	10.0	82.3	0.1215	3.815	0.88
72.00	10.0	103.2	0.0969	3.042	0.85
72.00	10.0	95.0	0.1053	3.305	0.85
73.30	10.0	96.0	0.1042	3.168	0.85
71.70	10.0	114.6	0.0873	2.762	0.83
72.50	10.0	116.0	0.0862	2.674	0.83
73.30	10.0	136.4	0.0733	2.229	0.80
73.50	10.0	132.7	0.0754	2.281	0.80
73.40	10.0	163.2	0.0613	1.859	0.77
73.40	10.0	165.7	0.0604	1.831	0.77
73.85	10.0	210.3	0.0476	1.427	0.74
73.85	10.0	210.4	0.0475	1.426	0.74
74.65	10.0	205.0	0.0488	1.435	0.74
70.80	10.0	279.0	0.0358	1.161	0.71
70.80	10.0	294.5	0.0340	1.100	0.71
71.10	10.0	270.6	0.0370	1.188	0.71
70.40	8.0	296.6	0.0270	0.883	0.68
70.20	8.0	285.6	0.0280	0.921	0.68

RUN 3-2
PARTICLES= SALT CRYSTALS DENSITY= 2.169 GM/CM^3
LIQUID= SAE 10W 84.9%+ KEROSENE, DENSITY= 0.858 GM/CM^3
PARTICLE SIZE D_V= 0.0341 CM, D_t = 3.78 CM, D_V/D_t = 0.0090
SIEVE OPENINGS 0.250/0.298 MM, NO ELUTRIATION

TEMP °F	DIST CM	SETTLING TIME SEC	U CM/SEC	U*NU $0.01CM^3/SEC^2$	EPS
71.20	10.0	59.1	0.1692	5.427	0.95
71.20	10.0	60.5	0.1653	5.301	0.95
71.20	10.0	59.5	0.1681	5.390	0.95
71.80	10.0	66.8	0.1497	4.726	0.92
71.80	10.0	67.4	0.1484	4.683	0.92
71.80	10.0	68.7	0.1456	4.595	0.92
71.85	10.0	67.1	0.1490	4.698	0.92
72.40	10.0	71.7	0.1395	4.336	0.90
72.40	10.0	70.7	0.1414	4.398	0.90
72.40	10.0	72.3	0.1383	4.300	0.90
71.90	10.0	84.6	0.1182	3.721	0.88
71.90	10.0	83.0	0.1205	3.793	0.88
72.00	10.0	82.0	0.1220	3.829	0.88
71.80	10.0	96.7	0.1034	3.264	0.85
71.80	10.0	99.8	0.1002	3.163	0.85
71.80	10.0	99.0	0.1010	3.189	0.85
72.90	9.9	95.8	0.1028	3.157	0.85
71.50	10.0	116.0	0.0862	2.743	0.83
72.40	10.0	115.0	0.0870	2.704	0.83
73.45	10.0	136.2	0.0734	2.225	0.80
73.60	10.0	135.3	0.0739	2.231	0.80
73.45	10.0	165.2	0.0605	1.834	0.77
73.45	10.0	167.0	0.0599	1.814	0.77
73.80	10.0	210.7	0.0475	1.426	0.74
73.80	10.0	205.8	0.0486	1.460	0.74
74.30	10.0	205.0	0.0488	1.448	0.74
70.90	8.0	222.8	0.0359	1.161	0.71
70.90	8.0	226.4	0.0353	1.142	0.71
71.20	8.0	215.5	0.0371	1.191	0.71
70.30	8.0	287.6	0.0278	0.912	0.68
70.30	8.0	294.1	0.0272	0.892	0.68
70.30	6.0	273.2	0.0220	0.720	0.65
70.30	6.0	274.8	0.0218	0.716	0.65

RUN 3-3
PARTICLES= SALT CRYSTALS DENSITY= 2.169 GM/CM^3
LIQUID= SAE 10W 84.9%+ KEROSENE, DENSITY= 0.858 GM/CM^3
PARTICLE SIZE D_V= 0.0341 CM, D_t = 5.08 CM, D_V/D_t = 0.0067
SIEVE OPENINGS 0.250/0.298 MM, NO ELUTRIATION

TEMP °F	DIST CM	SETTLING TIME SEC	U CM/SEC	U*NU $0.01CM^3/SEC^2$	EPS
72.70	16.0	92.1	0.1737	5.361	0.95
72.70	16.0	91.1	0.1756	5.420	0.95
72.70	12.0	68.8	0.1744	5.383	0.95
72.70	12.0	68.8	0.1744	5.383	0.95
72.00	13.0	86.3	0.1506	4.730	0.92
72.00	13.0	87.0	0.1494	4.692	0.92
72.00	12.0	79.9	0.1502	4.716	0.92
72.00	12.0	79.9	0.1502	4.716	0.92
72.20	16.0	117.0	0.1368	4.273	0.90
72.20	16.0	120.0	0.1333	4.166	0.90
72.20	16.0	116.2	0.1377	4.302	0.90
71.75	16.0	132.6	0.1207	3.814	0.88
71.75	16.0	133.3	0.1200	3.794	0.88
71.75	16.0	134.5	0.1190	3.760	0.88
71.75	16.0	130.2	0.1229	3.884	0.88
72.30	16.0	161.2	0.0993	3.094	0.85
72.30	16.0	154.5	0.1036	3.228	0.85
72.30	16.0	158.5	0.1009	3.146	0.85
72.30	12.0	118.0	0.1017	3.170	0.85
73.70	16.0	173.0	0.0925	2.785	0.83
73.70	16.0	173.7	0.0921	2.774	0.83
73.70	16.0	171.2	0.0935	2.815	0.83
74.10	16.0	209.5	0.0764	2.278	0.80
74.10	16.0	213.0	0.0751	2.240	0.80
74.70	14.0	182.3	0.0768	2.257	0.80
74.70	20.0	314.5	0.0636	1.869	0.77
74.70	20.0	322.0	0.0621	1.825	0.77
75.10	20.0	322.5	0.0620	1.804	0.77
75.30	16.0	322.5	0.0496	1.436	0.74
75.30	16.0	312.0	0.0513	1.484	0.74
75.30	16.0	311.0	0.0514	1.489	0.74
75.30	16.0	307.0	0.0521	1.508	0.74
73.80	8.0	204.0	0.0392	1.178	0.71
74.20	8.0	200.0	0.0400	1.190	0.71
75.00	8.0	200.8	0.0398	1.162	0.71
75.30	8.0	245.5	0.0326	0.943	0.68
75.30	8.0	239.3	0.0334	0.968	0.68
75.50	8.0	309.4	0.0259	0.745	0.65
75.50	8.0	320.0	0.0250	0.720	0.65

RUN 3-4
PARTICLES= SALT CRYSTALS DENSITY= 2.169 GM/CM^3
LIQUID= SAE 10W 84.9%+ KEROSENE, DENSITY= 0.858 GM/CM^3
PARTICLE SIZE D_V= 0.0341 CM, D_t = 7.71 CM, D_V/D_t = 0.0044
SIEVE OPENINGS 0.250/0.298 MM, NO ELUTRIATION

TEMP °F	DIST CM	SETTLING TIME SEC	U CM/SEC	U*NU $0.01CM^3/SEC^2$	EPS
70.50	14.0	85.8	0.1632	5.318	0.95
70.50	8.0	48.6	0.1646	5.365	0.95
70.50	8.0	49.6	0.1613	5.256	0.95
70.62	8.0	54.5	0.1468	4.770	0.92
70.62	8.0	55.7	0.1436	4.667	0.92
71.83	10.0	75.0	0.1333	4.203	0.90
71.83	10.0	75.0	0.1333	4.203	0.90
70.05	10.0	77.7	0.1287	4.241	0.90
70.39	10.0	85.7	0.1167	3.813	0.88
70.39	10.0	86.7	0.1153	3.769	0.88
70.53	10.0	102.2	0.0978	3.186	0.85
70.53	10.0	103.6	0.0965	3.143	0.85
71.07	10.0	117.3	0.0853	2.739	0.83
71.07	10.0	116.5	0.0858	2.758	0.83
71.20	12.0	140.2	0.0856	2.742	0.83
71.11	10.0	141.0	0.0709	2.277	0.80
71.11	10.0	141.3	0.0708	2.272	0.80
71.52	10.0	173.7	0.0576	1.829	0.77
71.55	10.0	172.2	0.0581	1.844	0.77
71.05	10.0	214.6	0.0466	1.498	0.74
71.05	10.0	213.4	0.0469	1.507	0.74
71.45	8.0	209.6	0.0382	1.215	0.71
71.20	8.0	214.7	0.0373	1.193	0.71
71.45	8.0	259.7	0.0308	0.981	0.68
71.50	6.0	246.8	0.0243	0.773	0.65
71.80	6.0	245.5	0.0244	0.771	0.65

RUN 4-2
PARTICLES= SALT CRYSTALS DENSITY= 2.163 GM/CM^3
LIQUID= SAE 10W 88.1%+ KEROSENE, DENSITY= 0.861 GM/CM^3
PARTICLE SIZE D_V= 0.0391 CM, D_t = 3.78 CM, D_V/D_t = 0.0103
SIEVE OPENINGS 0.295/0.351 MM, NO ELUTRIATION

TEMP °F	DIST CM	SETTLING TIME SEC	U CM/SEC	U*NU $0.01CM^3/SEC^2$	EPS
71.20	10.0	53.0	0.1887	7.30	0.950
71.20	10.0	52.3	0.1912	7.39	0.950
71.20	10.0	54.5	0.1835	7.09	0.950
71.20	10.0	51.7	0.1934	7.48	0.950
72.40	10.0	55.1	0.1815	6.80	0.920
72.40	10.0	56.0	0.1786	6.69	0.920
72.40	10.0	57.5	0.1739	6.52	0.920
70.70	10.0	59.7	0.1675	6.56	0.920
70.70	10.0	59.1	0.1692	6.63	0.920
71.40	10.0	65.0	0.1538	5.92	0.900
71.40	10.0	63.2	0.1582	6.09	0.900
71.40	11.0	70.0	0.1571	6.04	0.900
72.46	10.0	71.9	0.1391	5.20	0.880
72.46	11.0	74.5	0.1477	5.52	0.880
72.46	11.0	79.8	0.1378	5.16	0.880
72.46	11.0	78.0	0.1410	5.28	0.880
71.00	11.0	98.8	0.1113	4.33	0.850
71.00	11.0	98.9	0.1112	4.32	0.850
71.00	11.0	94.7	0.1162	4.51	0.850
71.00	11.0	94.7	0.1162	4.51	0.850
72.73	15.0	148.3	0.1011	3.76	0.830
72.73	11.0	108.3	0.1016	3.77	0.830
72.73	11.0	106.1	0.1037	3.85	0.830
69.25	14.0	180.8	0.0774	3.15	0.800
69.25	11.0	141.9	0.0775	3.15	0.800
69.25	11.0	144.1	0.0763	3.10	0.800
70.50	10.0	156.0	0.0641	2.52	0.770
70.50	10.0	157.1	0.0637	2.51	0.770
70.52	10.0	157.0	0.0637	2.51	0.770
72.00	10.0	191.2	0.0523	1.98	0.740
72.00	10.0	193.2	0.0518	1.96	0.740
72.00	10.0	181.3	0.0552	2.09	0.740
72.40	10.0	191.0	0.0524	1.96	0.740
71.25	10.0	244.4	0.0409	1.58	0.710
71.75	10.0	242.3	0.0413	1.57	0.710
71.75	10.0	242.3	0.0413	1.57	0.710
72.00	8.0	236.1	0.0339	1.28	0.680
72.00	8.0	242.1	0.0330	1.25	0.680
72.15	10.0	303.4	0.0330	1.24	0.680
73.20	8.0	295.5	0.0271	0.99	0.650
73.20	8.0	296.6	0.0270	0.99	0.650

RUN 4-3
PARTICLES= SALT CRYSTALS DENSITY= 2.163 GM/CM^3
LIQUID= SAE 10W 88.1 %+ KEROSENE, DENSITY= 0.861 GM/CM^3
PARTICLE SIZE D_V= 0.0391 CM, D_t = 5.08 CM, D_V/D_t = 0.0077
SIEVE OPENINGS 0.295/0.351 MM, NO ELUTRIATION

TEMP °F	DIST CM	SETTLING TIME SEC	U CM/SEC	U*NU $0.01CM^3/SEC^2$	EPS
71.15	10.0	54.0	0.1852	7.17	0.950
71.15	10.0	53.8	0.1859	7.20	0.950
71.15	10.0	53.4	0.1873	7.25	0.950
71.15	10.0	52.0	0.1923	7.45	0.950
72.15	10.0	56.5	0.1770	6.67	0.920
72.15	10.0	56.4	0.1773	6.69	0.920
72.15	10.0	58.2	0.1718	6.48	0.920
71.40	10.0	66.3	0.1508	5.80	0.900
71.40	10.0	64.7	0.1546	5.94	0.900
71.40	10.0	64.7	0.1546	5.94	0.900
72.55	10.0	72.3	0.1383	5.16	0.880
72.55	10.0	71.2	0.1404	5.24	0.880
72.55	10.0	72.2	0.1385	5.17	0.880
72.55	10.0	72.2	0.1385	5.17	0.880
70.90	11.0	98.0	0.1122	4.37	0.850
70.90	11.0	99.5	0.1106	4.31	0.850
70.90	11.0	95.1	0.1157	4.51	0.850
72.60	15.0	148.8	0.1008	3.76	0.830
72.60	11.0	107.6	0.1022	3.81	0.830
72.60	11.0	106.5	0.1033	3.85	0.830
69.20	14.0	184.3	0.0760	3.09	0.800
69.20	11.0	144.0	0.0764	3.11	0.800
69.20	11.0	145.4	0.0757	3.08	0.800
70.48	10.9	173.3	0.0629	2.48	0.770
70.48	10.9	172.8	0.0631	2.48	0.770
70.48	10.0	156.0	0.0641	2.53	0.770
72.05	10.0	189.5	0.0528	1.99	0.740
72.05	10.0	191.7	0.0522	1.97	0.740
72.05	10.0	180.5	0.0554	2.09	0.740
72.40	10.0	185.7	0.0539	2.02	0.740
70.95	10.0	245.7	0.0407	1.58	0.710
71.65	10.0	236.9	0.0422	1.61	0.710
71.65	10.0	237.7	0.0421	1.61	0.710
71.65	10.0	238.5	0.0419	1.60	0.710
71.90	8.0	234.4	0.0341	1.30	0.680
71.90	8.0	240.0	0.0333	1.27	0.680
72.03	8.0	241.3	0.0332	1.25	0.680
73.05	8.0	299.1	0.0267	0.99	0.650
73.05	8.0	298.0	0.0268	0.99	0.650

RUN 5-3
PARTICLES= SLAT CRYSTALS DENSITY= 2.161 GM/CM^3
LIQUID= SAE 10W 88.1% + KEROSENE, DENSITY= 0.861 GM/CM^3
PARTICLE SIZE D_V= 0.0282 CM, D_t = 5.08 CM, D_V/D_t = 0.0056
SIEVE OPENINGS 0.208/0.250 MM, NO ELUTRIATION

TEMP °F	DIST CM	SETTLING TIME SEC	U CM/SEC	U*NU 0.01CM^3/SEC^2	EPS
70.65	8.0	85.4	0.0937	3.681	0.950
70.65	8.0	85.4	0.0937	3.681	0.950
70.65	8.0	84.7	0.0945	3.712	0.950
70.70	8.0	94.5	0.0847	3.322	0.920
70.70	8.0	95.0	0.0842	3.305	0.920
71.92	10.0	123.9	0.0807	3.068	0.905
71.92	10.0	126.6	0.0790	3.002	0.905
69.92	10.0	128.6	0.0778	3.114	0.905
70.37	10.0	140.7	0.0711	2.813	0.890
70.37	10.0	142.6	0.0701	2.776	0.890
70.55	10.0	159.4	0.0627	2.472	0.870
70.55	10.0	160.4	0.0623	2.456	0.870
71.20	10.0	173.2	0.0577	2.237	0.850
71.40	10.0	174.8	0.0572	2.205	0.850
71.21	10.0	199.4	0.0502	1.942	0.830
71.21	10.0	195.4	0.0512	1.982	0.830
71.35	10.0	244.9	0.0408	1.576	0.800
71.50	10.0	247.2	0.0405	1.555	0.800
70.90	10.0	307.4	0.0325	1.270	0.770
70.90	10.0	298.9	0.0335	1.306	0.770
71.30	8.0	297.4	0.0269	1.039	0.740
71.10	8.0	302.7	0.0264	1.026	0.740
71.41	8.0	375.6	0.0213	0.821	0.710
71.65	8.0	464.0	0.0172	0.660	0.680
71.99	6.0	351.2	0.0171	0.648	0.680
72.90	6.0	453.2	0.0132	0.490	0.650
72.69	7.0	518.4	0.0135	0.503	0.650

RUN 6-4
PARTICLES= ABS CUBIC PELLETS DENSITY= 1.061 GM/CM^3
LIQUID= SAE 30 66%+ KEROSENE DENSITY= 0.876 GM/CM^3
PARTICLE SIZE D_V= 0.2880 CM, D_t = 7.71 CM, D_V/D_t = 0.0374
NOMINAL LENGTH 1/10 INCH, NO SIEVING

TEMP °F	DIST CM	SETTLING TIME SEC	U CM/SEC	U*NU $0.01CM^3/SEC^2$	EPS
70.90	10.0	43.4	0.2304	48.30	0.95
70.90	10.0	42.4	0.2358	49.44	0.95
71.15	10.0	48.8	0.2049	42.57	0.92
71.15	10.0	49.4	0.2024	42.05	0.92
71.15	10.0	49.4	0.2024	42.05	0.92
71.15	10.0	52.6	0.1901	39.49	0.90
70.50	10.0	62.1	0.1610	34.22	0.88
70.50	10.0	60.2	0.1661	35.30	0.88
71.42	10.0	70.0	0.1429	29.36	0.85
71.42	10.0	71.0	0.1408	28.94	0.85
71.42	10.0	72.2	0.1385	28.46	0.85
72.38	10.0	75.3	0.1328	26.31	0.83
72.38	10.0	78.2	0.1279	25.33	0.83
72.38	10.0	74.4	0.1344	26.62	0.83
72.38	11.0	85.8	0.1282	25.39	0.83
71.85	9.0	88.8	0.1014	20.46	0.80
70.05	9.0	114.0	0.0789	17.04	0.77
70.05	9.0	113.8	0.0791	17.07	0.77
70.78	9.0	140.7	0.0640	13.46	0.74
70.78	9.0	138.0	0.0652	13.73	0.74
71.95	6.0	109.6	0.0547	11.01	0.71
72.12	6.0	112.0	0.0536	10.71	0.71
69.67	6.0	136.0	0.0441	9.64	0.68
69.67	9.0	199.4	0.0451	9.86	0.68

RUN 6-5
PARTICLES= ABS CUBIC PELLETS DENSITY= 1.061 GM/CM^3
LIQUID= SAE 30 66 %+ KEROSENE DENSITY= 0.876 GM/CM^3
PARTICLE SIZE D_V= 0.2880 CM, D_t = 10.12 CM, D_V/D_t = 0.0285
NOMINAL LENGTH 1/10 INCH, NO SIEVING

TEMP °F	DIST CM	SETTLING TIME SEC	U CM/SEC	U*NU $0.01CM^3/SEC^2$	EPS
72.80	12.0	45.0	0.2667	52.06	0.95
72.95	12.0	49.0	0.2449	47.56	0.95
72.95	6.0	24.7	0.2429	47.18	0.95
73.30	12.0	48.0	0.2500	47.95	0.92
73.30	12.0	48.0	0.2500	47.95	0.90
74.30	12.0	56.4	0.2128	39.42	0.90
74.30	12.0	54.4	0.2206	40.87	0.90
74.30	12.0	53.8	0.2230	41.33	0.90
75.60	12.0	54.5	0.2202	39.05	0.88
75.70	12.0	55.4	0.2166	38.28	0.88
76.90	12.0	61.8	0.1942	32.85	0.85
77.10	12.0	61.2	0.1961	32.93	0.85
77.10	12.0	62.8	0.1911	32.09	0.85
72.40	12.0	84.2	0.1425	28.21	0.83
72.50	12.0	88.5	0.1356	26.75	0.83
72.50	12.0	84.0	0.1429	28.18	0.83
72.90	12.0	103.2	0.1163	22.62	0.80
73.00	12.0	105.5	0.1137	22.05	0.80
73.00	12.0	101.0	0.1188	23.03	0.80
73.10	9.0	98.2	0.0916	17.70	0.77
71.10	9.0	131.8	0.0683	14.21	0.74
71.10	9.0	129.5	0.0695	14.47	0.74
71.10	9.0	127.2	0.0708	14.73	0.74
71.90	9.0	150.0	0.0600	12.09	0.71
72.15	6.0	100.8	0.0595	11.88	0.71
72.15	6.0	103.2	0.0581	11.61	0.71
73.40	6.0	115.0	0.0522	9.97	0.68
73.40	9.0	185.3	0.0486	9.28	0.68

RUN 8-P
PARTICLES= MINERAL CRYSTALS DENSITY= 2.623 GM/CM^3
LIQUID= SAE 10W 88.1%+ KEROSENE, DENSITY= 0.861 GM/CM^3
PARTICLE SIZE D_V= 0.0384 CM, D_t = 3.50 CM, D_V/D_t = 0.0110
FROM SIEVING 35/42 MESH, SEGGREGATION TEST

TEMP °F	DIST CM	SETTLING TIME SEC	U CM/SEC	U*NU $0.01CM^3/SEC^2$	EPS
74.85	10.0	37.0	0.2703	9.54	0.90
74.85	4.0	15.5	0.2581	9.11	0.90
74.85	4.0	15.4	0.2597	9.16	0.90
74.85	4.0	15.4	0.2597	9.16	0.90
72.30	5.0	26.8	0.1866	7.03	0.85
72.30	5.0	27.0	0.1852	6.98	0.85
73.35	5.0	37.4	0.1337	4.90	0.80
73.35	5.0	37.4	0.1337	4.90	0.80
73.00	5.0	57.2	0.0874	3.23	0.75
73.00	5.0	54.0	0.0926	3.42	0.75
73.50	5.0	59.0	0.0847	3.09	0.75
73.50	5.0	54.7	0.0914	3.34	0.75
73.50	5.0	57.6	0.0868	3.17	0.75
73.50	5.0	55.4	0.0903	3.29	0.75
73.50	5.0	57.4	0.0871	3.18	0.75
74.10	3.0	45.2	0.0664	2.39	0.70
74.10	3.0	52.0	0.0577	2.07	0.70
74.10	3.0	50.8	0.0591	2.12	0.70
74.10	3.0	50.2	0.0598	2.15	0.70

RUN 8-M
PARTICLES= MINERAL CRYSTALS DENSITY= 2.623 GM/CM^3
LIQUID= SAE 10W 88.1%+ KEROSENE, DENSITY= 0.861 GM/CM^3
PARTICLE SIZE D_v= 0.0378 CM, D_t = 3.50 CM, D_v/D_t = 0.0108
MIXTURE 90% 35/42 MESH + 10% 42/48 MESH, SEGGREGATION TEST

TEMP °F	DIST CM	SETTLING TIME SEC	U CM/SEC	U*NU 0.01CM /SEC	EPS
74.75	10.0	42.8	0.2336	8.26	0.90
74.75	4.0	17.8	0.2247	7.95	0.90
74.75	4.0	18.1	0.2210	7.82	0.90
74.75	4.0	18.5	0.2162	7.65	0.90
72.30	5.0	30.0	0.1667	6.28	0.85
72.30	5.0	30.0	0.1667	6.28	0.85
73.40	5.0	41.0	0.1220	4.46	0.80
73.40	5.0	40.7	0.1229	4.50	0.80
73.40	5.0	40.9	0.1222	4.47	0.80
72.95	5.0	60.4	0.0828	3.06	0.75
72.96	5.0	58.4	0.0856	3.17	0.75
73.40	5.0	62.0	0.0806	2.95	0.75
73.40	5.0	57.4	0.0871	3.19	0.75
73.40	5.0	60.1	0.0832	3.04	0.75
73.40	5.0	59.4	0.0842	3.08	0.75
73.40	5.0	60.4	0.0828	3.03	0.75
74.00	3.0	48.2	0.0622	2.24	0.70
74.00	3.0	54.5	0.0550	1.98	0.70
74.00	3.0	53.2	0.0564	2.03	0.70
74.00	3.0	53.3	0.0563	2.03	0.70

RUN 9-2
PARTICLES= MINERAL CRYSTALS DENSITY= 2.632 GM/CM^3
LIQUID= SAE 10W 95%+ KEROSENE DENSITY= 0.862 GM/CM^3
PARTICLE SIZE D_V= 0.0508 CM, D_t = 3.78 CM, D_V/D_t = 0.0134
SIEVE OPENINGS 0.417/0.495 MM, SIEVING + ELUTRIATION

TEMP °C	DIST CM	SETTLING TIME SEC	U CM/SEC	U*NU 0.01CM^3/SEC^2	EPS
26.65	6.0	18.0	0.3333	15.68	0.95
26.65	6.0	18.9	0.3175	14.93	0.95
26.65	6.0	19.2	0.3125	14.70	0.95
26.65	6.0	18.1	0.3315	15.59	0.95
27.37	6.0	20.0	0.3000	13.61	0.92
27.37	6.0	19.2	0.3125	14.18	0.92
27.37	6.0	19.6	0.3061	13.89	0.92
27.55	6.0	19.6	0.3061	13.77	0.92
27.55	6.0	19.7	0.3046	13.70	0.92
27.64	12.0	42.2	0.2844	12.74	0.90
27.64	12.0	40.7	0.2948	13.21	0.90
27.64	12.0	41.7	0.2878	12.89	0.90
27.75	12.0	40.0	0.3000	13.36	0.90
25.97	12.0	49.4	0.2429	11.80	0.88
25.97	15.0	62.8	0.2389	11.60	0.88
25.97	15.0	63.8	0.2351	11.42	0.88
26.20	15.0	60.4	0.2483	11.94	0.88
26.55	15.0	72.8	0.2060	9.74	0.85
26.55	15.0	73.3	0.2046	9.67	0.85
26.55	15.0	75.2	0.1995	9.43	0.85
26.63	15.0	83.4	0.1799	8.47	0.83
26.70	15.0	83.0	0.1807	8.48	0.83
26.85	12.0	80.8	0.1485	6.91	0.80
26.85	12.0	80.8	0.1485	6.91	0.80
26.90	9.0	61.0	0.1475	6.85	0.80
26.90	9.0	77.8	0.1157	5.37	0.77
26.90	9.0	76.4	0.1178	5.47	0.77
23.63	9.0	116.6	0.0772	4.22	0.74
23.63	9.0	111.8	0.0805	4.40	0.74
23.80	9.0	111.0	0.0811	4.40	0.74
24.40	9.0	141.4	0.0636	3.35	0.71
24.40	9.0	136.4	0.0660	3.47	0.71
24.50	9.0	137.8	0.0653	3.42	0.71
24.82	6.0	116.0	0.0517	2.66	0.68
25.67	6.0	111.6	0.0538	2.65	0.68
25.67	6.0	109.6	0.0547	2.70	0.68
25.80	6.0	139.9	0.0429	2.10	0.65

RUN 9-3
PARTICLES= MINERAL CRYSTALS DENSITY= 2.632 GM/CM^3
LIQUID= SAE 10W 95%+ KEROSENE DENSITY= 0.862 GM/CM^3
PARTICLE SIZE D_V= 0.0508 CM, D_t = 5.08 CM, D_V/D_t = 0.0100
SIEVE OPENINGS 0.417/0.495 MM, SIEVING + ELUTRIATION

TEMP °C	DIST CM	SETTLING TIME SEC	U CM/SEC	U*NU 0.01CM^3/SEC^2	EPS
26.50	6.0	18.3	0.3279	15.54	0.95
26.50	6.0	18.3	0.3279	15.54	0.95
26.50	6.0	19.0	0.3158	14.97	0.95
26.50	6.0	18.6	0.3226	15.29	0.95
27.34	6.0	19.5	0.3077	13.98	0.92
27.34	6.0	19.0	0.3158	14.35	0.92
27.34	6.0	19.7	0.3046	13.84	0.92
27.55	6.0	19.6	0.3061	13.77	0.92
27.65	12.0	42.3	0.2837	12.70	0.90
27.65	12.0	41.0	0.2927	13.10	0.90
27.65	12.0	41.7	0.2878	12.88	0.90
27.75	12.0	41.4	0.2899	12.91	0.90
25.90	12.0	47.8	0.2510	12.24	0.88
25.90	15.0	63.3	0.2370	11.55	0.88
25.90	15.0	63.3	0.2370	11.55	0.88
26.10	15.0	61.8	0.2427	11.72	0.88
26.50	15.0	73.3	0.2046	9.70	0.85
26.50	15.0	74.1	0.2024	9.60	0.85
26.50	15.0	74.4	0.2016	9.56	0.85
26.60	15.0	83.0	0.1807	8.52	0.83
26.60	15.0	82.7	0.1814	8.55	0.83
26.65	15.0	83.6	0.1794	8.44	0.83
26.85	12.0	81.0	0.1481	6.89	0.80
26.85	12.0	81.8	0.1467	6.83	0.80
26.90	9.0	60.5	0.1488	6.90	0.80
26.90	9.0	76.6	0.1175	5.45	0.77
26.90	9.0	75.7	0.1189	5.52	0.77
26.90	9.0	75.2	0.1197	5.55	0.77
23.55	9.0	113.2	0.0795	4.37	0.74
23.55	9.0	112.2	0.0802	4.41	0.74
23.70	9.0	112.0	0.0804	4.38	0.74
24.32	9.0	139.2	0.0647	3.41	0.71
24.32	9.0	138.5	0.0650	3.43	0.71
24.45	9.0	135.1	0.0666	3.49	0.71
24.80	7.0	134.7	0.0520	2.68	0.68
25.62	6.0	109.5	0.0548	2.71	0.68
25.62	6.0	107.6	0.0558	2.76	0.68
25.85	6.0	142.5	0.0421	2.06	0.65

RUN 10-2
PARTICLES= MINERAL CRYSTALS DENSITY= 2.632 GM/CM^3
LIQUID= SAE 10W 88.1 %+ KEROSENE, DENSITY= 0.858 GM/CM^3
PARTICLE SIZE D_V= 0.0426 CM, D_t = 3.78 CM, D_V/D_t = 0.0113
SIEVE OPENINGS 0.351/0.417 MM, SIEVING + ELUTRIATION

TEMP °F	DIST CM	SETTLING TIME SEC	U CM/SEC	U*NU $0.01CM^3/SEC^2$	EPS
74.75	9.0	24.5	0.3673	13.00	0.95
74.75	9.0	23.0	0.3913	13.84	0.95
75.60	9.0	29.0	0.3103	10.74	0.92
75.60	9.0	28.4	0.3169	10.97	0.92
75.70	12.0	36.2	0.3315	11.45	0.92
75.70	12.0	38.3	0.3133	10.82	0.92
76.30	9.0	28.6	0.3147	10.70	0.90
76.30	9.0	30.0	0.3000	10.20	0.90
76.30	9.0	29.0	0.3103	10.55	0.90
76.10	12.0	46.0	0.2609	8.92	0.88
76.10	12.0	44.0	0.2727	9.32	0.88
75.95	12.0	58.3	0.2058	7.06	0.85
75.95	12.0	59.2	0.2027	6.96	0.85
73.85	12.0	72.6	0.1653	5.99	0.82
73.85	12.0	76.8	0.1562	5.66	0.82
73.85	9.0	55.6	0.1619	5.86	0.82
74.80	12.0	81.6	0.1471	5.20	0.80
74.80	12.0	77.2	0.1554	5.49	0.80
74.80	12.0	82.2	0.1460	5.16	0.80
71.90	12.0	110.8	0.1083	4.13	0.77
71.90	9.0	81.2	0.1108	4.23	0.77
71.90	9.0	83.6	0.1077	4.10	0.77
73.65	9.0	100.1	0.0899	3.27	0.74
73.65	9.0	98.2	0.0916	3.34	0.74
74.25	9.0	127.6	0.0705	2.53	0.71
74.40	6.0	86.6	0.0693	2.47	0.71
74.40	6.0	86.8	0.0691	2.47	0.71
73.50	6.0	114.2	0.0525	1.92	0.68
73.50	6.0	112.7	0.0532	1.95	0.68
73.20	6.0	143.4	0.0418	1.54	0.65
73.20	6.0	141.0	0.0426	1.57	0.65

RUN 10-3
PARTICLES= MINERAL CRYSTALS DENSITY= 2.632 GM/CM^3
LIQUID= SAE 10W 88.1% + KEROSENE, DENSITY= 0.858 GM/CM^3
PARTICLE SIZE D_V= 0.0426 CM, D_t = 5.08 CM, D_V/D_t = 0.0084
SIEVE OPENINGS 0.351/0.417 MM, SIEVING + ELUTRIATION

TEMP °F	DIST CM	SETTLING TIME SEC	U CM/SEC	U*NU $0.01CM^3/SEC^2$	EPS
74.50	9.0	26.2	0.3435	12.23	0.95
74.50	9.0	25.6	0.3516	12.52	0.95
75.40	12.0	39.5	0.3038	10.57	0.92
75.40	9.0	29.7	0.3030	10.54	0.92
75.40	9.0	29.5	0.3051	10.61	0.92
76.30	9.0	29.6	0.3041	10.34	0.90
76.30	9.0	31.6	0.2848	9.69	0.90
76.30	11.0	36.4	0.3022	10.28	0.90
76.10	11.0	44.3	0.2483	8.49	0.88
76.10	12.0	44.8	0.2679	9.16	0.88
76.00	14.0	66.1	0.2118	7.26	0.85
76.00	12.0	55.6	0.2158	7.40	0.85
76.00	12.0	59.6	0.2013	6.90	0.85
76.00	12.0	56.8	0.2113	7.24	0.85
73.80	12.0	72.0	0.1667	6.04	0.82
73.80	12.0	73.7	0.1628	5.90	0.82
73.80	12.0	74.5	0.1611	5.84	0.82
74.60	12.0	83.3	0.1441	5.12	0.80
74.60	12.0	83.2	0.1442	5.12	0.80
71.80	12.0	114.2	0.1051	4.02	0.77
71.80	9.0	85.1	0.1058	4.04	0.77
71.80	9.0	84.5	0.1065	4.07	0.77
73.60	9.0	99.2	0.0907	3.31	0.74
73.60	9.0	98.0	0.0918	3.35	0.74
74.20	9.0	125.1	0.0719	2.58	0.71
74.20	6.0	85.6	0.0701	2.52	0.71
74.40	6.0	83.0	0.0723	2.58	0.71
73.50	6.0	110.8	0.0542	1.98	0.68
73.50	6.0	112.0	0.0536	1.96	0.68
73.20	6.0	139.0	0.0432	1.59	0.65
73.20	6.0	144.4	0.0416	1.53	0.65
73.20	6.0	142.2	0.0422	1.55	0.65

RUN 11-2
PARTICLES= SUGAR CRYSTALS DENSITY= 1.590 GM/CM^3
LIQUID= SAE 30 66% + SAE 10W DENSITY= 0.876 GM/CM^3
PARTICLE SIZE D_V= 0.1346 CM, D_t = 3.78 CM, D_V/D_t = 0.0356
SIEVE OPENINGS 0.991/1.168 MM, SIEVING + ELUTRIATION

TEMP °F	DIST CM	SETTLING TIME SEC	U CM/SEC	U*NU $0.01CM^3/SEC^2$	EPS
71.90	9.0	39.4	0.2284	43.35	0.95
71.90	9.0	39.4	0.2284	43.35	0.95
71.90	9.0	41.0	0.2195	41.66	0.95
72.70	9.0	44.6	0.2018	37.21	0.92
72.70	9.0	43.4	0.2074	38.24	0.92
72.70	9.0	43.2	0.2083	38.42	0.92
73.40	12.0	60.8	0.1974	35.48	0.90
73.40	12.0	61.7	0.1945	34.96	0.90
73.80	12.0	64.5	0.1860	32.95	0.88
73.80	12.0	64.0	0.1875	33.21	0.88
73.80	12.0	66.4	0.1807	32.01	0.88
73.20	12.0	77.4	0.1550	28.07	0.85
73.20	12.0	78.8	0.1523	27.58	0.85
73.20	12.0	75.0	0.1600	28.97	0.85
73.20	12.0	75.5	0.1589	28.78	0.85
73.70	12.0	96.3	0.1246	22.15	0.82
73.70	12.0	90.6	0.1325	23.55	0.82
73.70	12.0	91.8	0.1307	23.24	0.82
71.50	9.0	85.0	0.1059	20.38	0.80
71.50	9.0	83.0	0.1084	20.87	0.80
71.50	9.0	81.2	0.1108	21.34	0.80
73.70	9.0	103.1	0.0873	15.52	0.77
73.70	9.0	95.4	0.0943	16.77	0.77
74.00	9.0	96.2	0.0936	16.45	0.77
73.60	6.0	78.0	0.0769	13.73	0.74
74.20	6.0	85.5	0.0702	12.25	0.74
72.50	6.0	112.2	0.0535	9.93	0.71
72.50	6.0	107.4	0.0559	10.38	0.71
74.20	5.8	133.0	0.0436	7.62	0.68

RUN 11-3
PARTICLES= SUGAR CRYSTALS DENSITY= 1.590 GM/CM^3
LIQUID= SAE 30 66% + SAE 10W DENSITY= 0.876 GM/CM^3
PARTICLE SIZE D_V= 0.1346 CM, D_t = 5.08 CM, D_V/D_t = 0.0265
SIEVE OPENINGS 0.991/1.168 MM, SIEVING + ELUTRIATION

TEMP °F	DIST CM	SETTLING TIME SEC	U CM/SEC	U*NU $0.01CM^3/SEC^2$	EPS
71.65	9.0	41.0	0.2195	42.03	0.95
71.65	9.0	41.0	0.2195	42.03	0.95
72.70	9.0	44.4	0.2027	37.38	0.92
72.70	9.0	43.0	0.2093	38.60	0.92
72.70	9.0	43.2	0.2083	38.42	0.92
73.40	12.0	60.4	0.1987	35.71	0.90
73.40	12.0	59.4	0.2020	36.32	0.90
73.40	12.0	61.0	0.1967	35.36	0.90
73.85	12.0	65.2	0.1840	32.54	0.88
73.85	12.0	66.0	0.1818	32.14	0.88
73.85	12.0	65.8	0.1824	32.24	0.88
73.20	12.0	75.2	0.1596	28.90	0.85
73.20	12.0	75.3	0.1594	28.86	0.85
73.30	12.0	94.4	0.1271	22.93	0.82
74.05	12.0	92.0	0.1304	22.89	0.82
71.30	9.0	82.8	0.1087	21.07	0.80
71.30	9.0	81.0	0.1111	21.54	0.80
72.00	9.0	81.0	0.1111	21.01	0.80
73.65	9.0	97.0	0.0928	16.53	0.77
73.65	9.0	97.2	0.0926	16.49	0.77
73.90	9.0	97.0	0.0928	16.37	0.77
73.00	6.0	83.4	0.0719	13.12	0.74
73.20	6.0	79.7	0.0753	13.63	0.74
73.20	6.0	80.2	0.0748	13.55	0.74
74.30	6.0	78.3	0.0766	13.34	0.74
73.30	6.0	109.6	0.0547	9.88	0.71
73.30	6.0	108.2	0.0555	10.00	0.71
72.70	6.0	143.0	0.0420	7.74	0.68
73.50	6.0	138.8	0.0432	7.74	0.68

RUN 12-3
PARTICLES= SUGAR CRYSTALS DENSITY= 1.590 GM/CM^3
LIQUID= SAE 30 24% + SAE 10W DENSITY= 0.870 GM/CM^3
PARTICLE SIZE D_V= 0.1133 CM, D_t = 5.08 CM, D_V/D_t = 0.0223
SIEVE OPENINGS 0.883/0.991 MM, SIEVING + ELUTRIATION

TEMP °F	DIST CM	SETTLING TIME SEC	U CM/SEC	U*NU $0.01CM^3/SEC^2$	EPS
74.90	9.0	32.4	0.2778	31.43	0.95
74.90	9.0	31.8	0.2830	32.02	0.95
74.90	9.0	30.4	0.2961	33.50	0.95
76.50	9.0	32.5	0.2769	29.73	0.92
76.50	9.0	33.0	0.2727	29.28	0.92
76.50	9.0	32.4	0.2778	29.82	0.92
78.20	9.0	32.4	0.2778	28.24	0.90
78.20	9.0	31.7	0.2839	28.87	0.90
78.20	9.0	33.0	0.2727	27.73	0.90
78.20	9.0	31.6	0.2848	28.96	0.90
78.20	9.0	33.4	0.2695	27.40	0.90
77.25	12.0	47.5	0.2526	26.49	0.88
77.25	12.0	49.8	0.2410	25.27	0.88
77.25	9.0	36.2	0.2486	26.07	0.88
79.40	12.0	49.4	0.2429	23.78	0.85
79.40	12.0	51.4	0.2335	22.86	0.85
79.40	12.0	52.0	0.2308	22.59	0.85
75.20	12.0	74.6	0.1609	18.02	0.82
75.20	11.9	73.2	0.1626	18.21	0.82
76.80	9.0	59.3	0.1518	16.14	0.80
79.45	9.0	68.2	0.1320	12.90	0.77
79.45	9.0	67.2	0.1339	13.09	0.77
79.50	6.0	59.4	0.1010	9.86	0.74
80.10	6.0	75.0	0.0800	7.65	0.71
80.80	6.0	92.6	0.0648	6.04	0.68

VISCOSITY DATA

Run 1-1,2

Temperature	°F	68.00	69.00	70.00	71.03	71.96	73.01	74.01	75.00	75.97
Viscosity	cs	185.90	181.90	178.06	174.26	170.98	167.21	163.80	160.79	157.55
Temperature	°F	77.02	77.99	78.99						
Viscosity	cs	154.14	151.23	148.26						

Run 1-3

Temperature	°C	18.80	20.10	20.48	21.16	22.02	23.05	24.16	25.00
Viscosity	cs	194.79	184.86	182.26	177.80	171.50	165.02	158.45	153.39

Run 2-1,2

Temperature	°F	68.02	69.00	70.03	71.02	72.00	73.02	74.45	75.10	76.25
Viscosity	cs	341.11	333.74	326.00	318.51	311.31	303.52	293.50	289.47	283.00
Temperature	°F	77.13								
Viscosity	cs	278.46								

Run 2-3

Temperature	°F	68.02	69.00	70.03	71.02	72.00	73.02	75.10	77.13
Viscosity	cs	341.11	333.74	326.00	318.51	311.31	303.52	289.47	278.46

Run 3-1A,2,3

Temperature	°F	67.00	68.00	69.03	70.00	71.00	72.01	73.00	75.02	76.00
Viscosity	cs	35.66	34.86	33.86	33.04	32.24	31.39	30.63	29.15	28.43
Temperature	°F	77.20								
Viscosity	cs	27.64								

VISCOSITY DATA (continued)

Run 3-4

Temperature	°F	68.00	69.01	70.00	71.00	71.95	73.01	74.00	
Viscosity	cs	34.72	33.86	32.99	32.19	31.43	30.62	29.88	

Run 4-2,3

Temperature	°F	68.00	69.00	70.00	71.00	72.00	73.00	74.00	75.00
Viscosity	cs	42.04	40.94	39.88	38.87	37.85	36.90	35.90	34.94

Run 5-3

Temperature	°F	68.00	69.01	70.00	71.00	71.95	73.01	74.00	
Viscosity	cs	42.17	41.05	39.96	38.94	37.98	36.94	36.02	

Run 6-4

Temperature	°F	68.05	69.20	69.98	71.10	72.00	73.00	74.00	
Viscosity	cs	231.6	221.9	216.3	208.2	200.7	193.9	186.9	

Run 6-5

Temperature	°F	68.05	69.20	69.98	71.10	72.00	73.06	74.00	74.90
Viscosity	cs	231.64	221.86	216.3	208.16	200.66	193.87	186.96	181.97
Temperature	°F	76.20	77.20						
Viscosity	cs	173.43	167.34						

Run 7-3

Temperature	°F	70.00	71.00	72.00	73.00	74.00	75.00	76.00	
Viscosity	cs	116.07	113.73	111.64	109.27	107.20	105.18	103.06	

VISCOSITY DATA (continued)

Run 8-P,M

Temperature	°F	72.00	73.05	73.98	74.90
Viscosity	cs	38.01	36.92	36.06	35.24

Run 9-2,3

Temperature	°C	23.00	23.50	24.00	24.50	25.00	25.50	26.00	26.50	27.00
Viscosity	cs	56.56	55.06	53.67	52.32	51.04	49.70	48.51	47.40	46.16
Temperature	°C	27.50	28.00							
Viscosity	cs	45.10	44.00							

Run 10-2,3

Temperature	°C	71.00	71.85	73.00	74.10	75.05	76.10	77.10
Viscosity	cs	39.04	38.18	37.02	35.98	35.10	34.18	33.32

Run 11-2,3

Temperature	°F	70.00	71.00	72.00	73.00	74.00	75.00
Viscosity	cs	203.00	195.90	189.10	182.40	175.80	169.90

Run 12-3

Temperature	°F	74.00	75.00	76.00	77.00	78.00	79.00	80.00	81.20
Viscosity	cs	116.30	112.80	109.00	105.70	102.30	99.15	96.02	91.90

APPENDIX VIII CALCULATED RESULTS FOR HINDERED SETTLING

** Data not used in curve fitting of eqt. 1a

RUN 1-1
PARTICLES= GLASS BEADS — DENSITY= 2.977 GM/CM^3
LIQUID= P.E.G.SOLN 40/100 — DENSITY= 1.071 GM/CM^3
PARTICLE SIZE D_v= 0.1135 CM, D_t = 2.54 CM, D_v/D_t = 0.0447
SIEVE OPENINGS 0.991/1.168 MM, NO ELUTRIATION

EPS	U*NU(AVE) 0.01CM^3/SEC^2	LG(EPS)	LG(U*NU)	STD.DEV.	NO.OF TESTS
0.90	63.7	-0.0458	1.804	0.95	3 **
0.88	59.0	-0.0555	1.771	0.61	2
0.85	49.8	-0.0706	1.698	0.46	4
0.83	47.2	-0.0809	1.673	1.27	5
0.80	38.3	-0.0969	1.583	0.60	2
0.77	33.2	-0.1135	1.521	1.89	2
0.74	26.2	-0.1308	1.419	0.46	2
0.70	19.5	-0.1549	1.289	0.15	2
0.67	15.2	-0.1739	1.181	0.45	3

RE(O) 0.039- 0.055

LEAST SQUARES ESTIMATES
LOG(U*NU)= 2.0622 + 4.97*LOG(EPS)
U*NU = 115.397*EPS** 4.97
CONFIDENCE INTERVAL
N= 4.97 ± 0.35
LOG(U*NU)O 2.0622 ± 0.0403
(U*NU)EXT 105.176- 126.612

DIA. OF SPHERE CORRESPONDING TO
(U*NU)EXT= 115.397 — 0.1091 CM
CORRECTED FOR WALL — 0.1141 CM
(U*NU)EXT OF 105.176- 126.612, — 0.1042- 0.1143CM
CORRECTED FOR WALL — 0.1090- 0.1196CM

RUN 1-2
PARTICLES= GLASS BEADS — DENSITY= 2.977 GM/CM^3
LIQUID= P.E.G.SOLN 40/100 — DENSITY= 1.071 GM/CM^3
PARTICLE SIZE D_v= 0.1135 CM, D_t = 3.78 CM, D_v/D_t = 0.0300
SIEVE OPENINGS 0.991/1.168 MM, NO ELUTRIATION

EPS	U*NU(AVE) 0.01CM^3/SEC^2	LG(EPS)	LG(U*NU)	STD.DEV.	NO.OF TESTS
0.90	67.1	-0.0458	1.827	0.86	6 **
0.88	62.6	-0.0555	1.797	1.33	4
0.85	52.6	-0.0706	1.721	1.83	3
0.83	47.5	-0.0809	1.677	0.21	4
0.80	40.1	-0.0969	1.603	0.49	4
0.77	33.0	-0.1135	1.528	0.84	4
0.74	26.7	-0.1308	1.427	0.86	4
0.70	20.5	-0.1549	1.312		1
0.67	16.8	-0.1739	1.224	0.38	3
0.64	13.6	-0.1938	1.135	0.01	2

RE(O) 0.039- 0.054

LEAST SQUARES ESTIMATES
LOG(U*NU)= 2.0663 + 4.83*LOG(EPS)
U*NU = 116.490*EPS** 4.83
CONFIDENCE INTERVAL
N= 4.83 ± 0.11
LOG(U*NU)O 2.0663 ± 0.0137
(U*NU)EXT 112.880- 120.214

DIA. OF SPHERE CORRESPONDING TO
(U*NU)EXT= 116.490 — 0.1096 CM
CORRECTED FOR WALL — 0.1131 CM
(U*NU)EXT OF 112.880- 120.214, — 0.1079- 0.1114CM
CORRECTED FOR WALL — 0.1113- 0.1149CM

RUN 1-3
PARTICLES= GLASS BEADS — DENSITY= 2.977 GM/CM^3
LIQUID= P.E.G.SOLN 40/100 — DENSITY= 1.071 GM/CM^3
PARTICLE SIZE D_v= 0.1135 CM, D_t = 5.08 CM, D_v/D_t = 0.0223
SIEVE OPENINGS 0.991/1.168 MM, NO ELUTRIATION

EPS	U*NU(AVE) 0.01CM^3/SEC^2	LG(EPS)	LG(U*NU)	STD.DEV.	NO.OF TESTS
0.90	65.5	-0.0458	1.816	1.08	6 **
0.88	60.7	-0.0555	1.783	0.60	5
0.85	52.0	-0.0706	1.716	0.45	5
0.83	46.9	-0.0809	1.671	0.59	5
0.80	39.7	-0.0969	1.599	0.96	6
0.77	32.9	-0.1135	1.517	0.67	5
0.74	26.5	-0.1308	1.424	0.40	4
0.70	20.6	-0.1549	1.313	0.81	5
0.67	16.7	-0.1739	1.222	0.17	4
0.64	13.2	-0.1938	1.120	0.26	4

RE(O) 0.041- 0.045

LEAST SQUARES ESTIMATES
LOG(U*NU)= 2.0579 + 4.82*LOG(EPS)
U*NU = 114.274*EPS** 4.82
CONFIDENCE INTERVAL
N= 4.82 ± 0.09
LOG(U*NU)O 2.0579 ± 0.0119
(U*NU)EXT 111.174- 117.460

DIA. OF SPHERE CORRESPONDING TO
(U*NU)EXT= 114.274 — 0.1086 CM
CORRECTED FOR WALL — 0.1111 CM
(U*NU)EXT OF 111.174- 117.460, — 0.1071- 0.1101CM
CORRECTED FOR WALL — 0.1096- 0.1127CM

RUN 2-1
PARTICLES= GLASS BEADS — DENSITY= 2.977 GM/CM^3
LIQUID= P.E.G.SOLN 45/100 — DENSITY= 1.082 GM/CM^3
PARTICLE SIZE D_v= 0.1135 CM, D_t = 2.54 CM, D_v/D_t = 0.0447
SIEVE OPENINGS 0.991/1.168 MM, NO ELUTRIATION

EPS	U*NU(AVE) 0.01CM^3/SEC^2	LG(EPS)	LG(U*NU)	STD.DEV.	NO.OF TESTS
0.90	62.1	-0.0458	1.793	1.60	4 **
0.88	56.4	-0.0555	1.751	-0.00	2
0.85	50.0	-0.0706	1.699	0.01	4
0.83	45.8	-0.0809	1.661	0.56	3
0.80	38.4	-0.0969	1.584	0.49	4
0.77	32.9	-0.1135	1.517	0.40	3
0.74	25.1	-0.1308	1.399		1
0.70	20.1	-0.1549	1.303		1
0.67	16.3	-0.1739	1.212		1

RE(O) 0.011- 0.014

LEAST SQUARES ESTIMATES
LOG(U*NU)= 2.0287 + 4.68*LOG(EPS)
U*NU = 106.844*EPS** 4.68
CONFIDENCE INTERVAL
N= 4.68 ± 0.32
LOG(U*NU)O 2.0287 ± 0.0369
(U*NU)EXT 98.148- 116.310

DIA. OF SPHERE CORRESPONDING TO
(U*NU)EXT= 106.844 — 0.1059 CM
CORRECTED FOR WALL — 0.1107 CM
(U*NU)EXT OF 98.148- 116.310, — 0.1015- 0.1104CM
CORRECTED FOR WALL — 0.1061- 0.1155CM

RUN 2-2
PARTICLES= GLASS BEADS — DENSITY= 2.977 GM/CM^3
LIQUID= P.E.G.SOLN 45/100 — DENSITY= 1.082 GM/CM^3
PARTICLE SIZE D_v= 0.1135 CM, D_t = 3.78 CM, D_v/D_t = 0.0300
SIEVE OPENINGS 0.991/1.168 MM, NO ELUTRIATION

EPS	U*NU(AVE) 0.01CM^3/SEC^2	LG(EPS)	LG(U*NU)	STD.DEV.	NO.OF TESTS
0.90	62.1	-0.0461	1.793		1 **
0.88	59.1	-0.0555	1.772		1
0.85	51.7	-0.0706	1.714	0.98	3
0.83	46.3	-0.0809	1.665	0.73	4
0.80	38.4	-0.0969	1.584		1
0.77	31.3	-0.1135	1.496	-0.00	2
0.74	27.2	-0.1308	1.435	0.10	2
0.70	22.7	-0.1549	1.356	0.80	2
0.67	16.6	-0.1739	1.221	1.03	2
0.64	12.5	-0.1938	1.098	0.28	2

RE(O) 0.012- 0.015

LEAST SQUARES ESTIMATES
LOG(U*NU)= 2.0459 + 4.74*LOG(EPS)
U*NU = 111.157*EPS** 4.74
CONFIDENCE INTERVAL
N= 4.74 ± 0.37
LOG(U*NU)O 2.0459 ± 0.0474
(U*NU)EXT 99.674- 123.963

DIA. OF SPHERE CORRESPONDING TO
(U*NU)EXT= 111.157 — 0.1080 CM
CORRECTED FOR WALL — 0.1113 CM
(U*NU)EXT OF 99.674- 123.963, — 0.1022- 0.1140CM
CORRECTED FOR WALL — 0.1054- 0.1176CM

RUN 2-3
PARTICLES= GLASS BEADS — DENSITY= 2.977 GM/CM^3
LIQUID= P.E.G.SOLN 45/100 — DENSITY= 1.082 GM/CM^3
PARTICLE SIZE D_v= 0.1135 CM, D_t = 5.08 CM, D_v/D_t = 0.0223
SIEVE OPENINGS 0.991/1.168 MM, NO ELUTRIATION

EPS	U*NU(AVE) 0.01CM^3/SEC^2	LG(EPS)	LG(U*NU)	STD.DEV.	NO.OF TESTS
0.90	64.5	-0.0458	1.810	0.82	5 **
0.88	59.6	-0.0555	1.775	0.21	3
0.85	52.1	-0.0706	1.717	1.05	6
0.83	46.4	-0.0809	1.666	0.72	4
0.80	41.3	-0.0969	1.616	0.55	4 **
0.77	33.1	-0.1135	1.520	0.58	5
0.74	26.7	-0.1308	1.427	0.43	3
0.70	20.7	-0.1549	1.316	0.78	4
0.67	16.5	-0.1739	1.217	0.42	3
0.64	14.0	-0.1938	1.147	0.71	2

RE(O) 0.011- 0.014

LEAST SQUARES ESTIMATES
LOG(U*NU)= 2.0412 + 4.67*LOG(EPS)
U*NU = 109.951*EPS** 4.67
CONFIDENCE INTERVAL
N= 4.67 ± 0.16
LOG(U*NU)O 2.0412 ± 0.0205
(U*NU)EXT 104.873- 115.274

DIA. OF SPHERE CORRESPONDING TO
(U*NU)EXT= 109.951 — 0.1074 CM
CORRECTED FOR WALL — 0.1099 CM
(U*NU)EXT OF 104.873- 115.274, — 0.1049- 0.1100CM
CORRECTED FOR WALL — 0.1073- 0.1125CM

RUN 7-3
PARTICLES= GLASS BEADS DENSITY= 2.959 GM/CM^3
LIQUID= P.E.G.SOLN 35.4% DENSITY= 1.062 GM/CM^3
PARTICLE SIZE D_V= 0.0492 CM, D_t = 5.08 CM, D_V/D_t = 0.0097
SIEVE OPENINGS 0.417/0.495 MM, NO ELUTRIATION

EPS	U*NU(AVE) 0.01CM^3/SEC^2	LG(EPS)	LG(U*NU)	STD.DEV.	NO.OF TESTS
0.95	14.71	-0.0223	1.168	0.06	2 **
0.92	13.13	-0.0362	1.118	0.15	3 **
0.90	12.36	-0.0458	1.092	0.32	4
0.88	11.30	-0.0555	1.053	0.36	4
0.85	9.79	-0.0706	0.991	0.01	2
0.82	8.28	-0.0862	0.918	0.09	4
0.80	7.54	-0.0969	0.877	0.03	2
0.77	6.32	-0.1135	0.801		1
0.74	5.06	-0.1308	0.705	0.06	3
0.71	4.24	-0.1467	0.627	0.07	2
0.68	3.32	-0.1675	0.521	0.03	2
0.65	2.75	-0.1871	0.439		1

RE(0) 0.007- 0.009

LEAST SQUARES ESTIMATES
LOG(U*NU)= 1.3191 + 4.69*LOG(EPS)
U*NU = 20.852*EPS** 4.69
CONFIDENCE INTERVAL
N= 4.69 ± 0.16
LOG(U*NU)0 1.3191 ± 0.0186
(U*NU)EXT 19.980- 21.762

DIA. OF SPHERE CORRESPONDING TO
(U*NU)EXT= 20.852 0.0463 CM
CORRECTED FOR WALL 0.0468 CM
(U*NU)EXT OF 19.980- 21.762, 0.0453- 0.0473CM
CORRECTED FOR WALL 0.0458- 0.0478CM

RUN 3-1A
PARTICLES= SALT CRYSTALS DENSITY= 2.169 GM/CM^3
LIQUID= SAE 10W 84.9%+ KEROSENE, DENSITY= 0.858 GM/CM^3
PARTICLE SIZE D_V= 0.0341 CM, D_t = 2.54 CM, D_V/D_t = 0.0134
SIEVE OPENINGS 0.250/0.298 MM, NO ELUTRIATION

EPS	U*NU(AVE) 0.01CM^3/SEC^2	LG(EPS)	LG(U*NU)	STD.DEV.	NO.OF TESTS
0.95	5.401	-0.0223	0.732	0.218	3 **
0.92	4.717	-0.0362	0.674	0.132	4
0.90	4.350	-0.0458	0.638	0.112	2
0.88	3.773	-0.0555	0.577	0.059	2
0.85	3.172	-0.0706	0.501	0.131	3
0.83	2.718	-0.0809	0.434	0.062	2
0.80	2.255	-0.0969	0.353	0.036	2
0.77	1.845	-0.1135	0.266	0.020	2
0.74	1.429	-0.1308	0.155	0.065	3
0.71	1.150	-0.1487	0.061	0.045	3
0.68	0.902	-0.1675	-0.045	0.027	2

RE(0) 0.022- 0.027

LEAST SQUARES ESTIMATES
LOG(U*NU)= 0.8856 + 5.54*LOG(EPS)
U*NU = 7.685*EPS** 5.54
CONFIDENCE INTERVAL
N= 5.54 ± 0.12
LOG(U*NU)0 0.8856 ± 0.0120
(U*NU)EXT 7.476- 7.900

DIA. OF SPHERE CORRESPONDING TO
(U*NU)EXT= 7.685 0.0304 CM
CORRECTED FOR WALL 0.0308 CM
(U*NU)EXT OF 7.476- 7.900, 0.0300- 0.0308CM
CORRECTED FOR WALL 0.0304- 0.0312CM

RUN 3-2
PARTICLES= SALT CRYSTALS DENSITY= 2.169 GM/CM^3
LIQUID= SAE 10W 84.9%+ KEROSENE, DENSITY= 0.858 GM/CM^3
PARTICLE SIZE D_V= 0.0341 CM, D_t = 3.78 CM, D_V/D_t = 0.0090
SIEVE OPENINGS 0.250/0.298 MM, NO ELUTRIATION

EPS	U*NU(AVE) 0.01CM^3/SEC^2	LG(EPS)	LG(U*NU)	STD.DEV.	NO.OF TESTS
0.95	5.373	-0.0223	0.730	0.065	3 **
0.92	4.676	-0.0362	0.670	0.057	4
0.90	4.345	-0.0458	0.638	0.049	3
0.88	3.781	-0.0555	0.578	0.055	3
0.85	3.193	-0.0706	0.504	0.049	4
0.83	2.723	-0.0809	0.435	0.028	2
0.80	2.228	-0.0969	0.348	0.005	2
0.77	1.824	-0.1135	0.261	0.014	2
0.74	1.444	-0.1308	0.160	0.017	3
0.71	1.164	-0.1487	0.066	0.025	3
0.68	0.902	-0.1675	-0.045	0.014	2
0.65	0.718	-0.1871	-0.144	0.063	2

RE(0) 0.021- 0.026

LEAST SQUARES ESTIMATES
LOG(U*NU)= 0.8823 + 5.50*LOG(EPS)
U*NU = 7.626*EPS** 5.50
CONFIDENCE INTERVAL
N= 5.50 ± 0.09
LOG(U*NU)0 0.8823 ± 0.0108
(U*NU)EXT 7.439- 7.817

DIA. OF SPHERE CORRESPONDING TO
(U*NU)EXT= 7.626 0.0303 CM
CORRECTED FOR WALL 0.0306 CM
(U*NU)EXT OF 7.439- 7.817, 0.0299- 0.0307CM
CORRECTED FOR WALL 0.0302- 0.0309CM

RUN 3-3
PARTICLES= SALT CRYSTALS DENSITY= 2.169 GM/CM^3
LIQUID= SAE 10W 84.9%+ KEROSENE, DENSITY= 0.858 GM/CM^3
PARTICLE SIZE D_V= 0.0341 CM, D_t = 5.08 CM, D_V/D_t = 0.0067
SIEVE OPENINGS 0.250/0.298 MM, NO ELUTRIATION

EPS	U*NU(AVE) 0.01CM^3/SEC^2	LG(EPS)	LG(U*NU)	STD.DEV.	NO.OF TESTS
0.95	5.387	-0.0223	0.731	0.024	4 **
0.92	4.713	-0.0362	0.673	0.016	4
0.90	4.247	-0.0458	0.628	0.072	3
0.88	3.813	-0.0555	0.581	0.052	4
0.85	3.159	-0.0706	0.500	0.056	4
0.83	2.791	-0.0809	0.446	0.021	3
0.80	2.258	-0.0969	0.354	0.019	3
0.77	1.833	-0.1135	0.263	0.033	3
0.74	1.479	-0.1308	0.170	0.031	4
0.71	1.177	-0.1487	0.071	0.014	3
0.68	0.955	-0.1675	-0.020	0.017	2
0.65	0.732	-0.1871	-0.135	0.017	2

RE(0) 0.023- 0.027

LEAST SQUARES ESTIMATES
LOG(U*NU)= 0.8759 + 5.38*LOG(EPS)
U*NU = 7.514*EPS** 5.38
CONFIDENCE INTERVAL
N= 5.38 ± 0.07
LOG(U*NU)0 0.8759 ± 0.0076
(U*NU)EXT 7.383- 7.647

DIA. OF SPHERE CORRESPONDING TO
(U*NU)EXT= 7.514 0.0301 CM
CORRECTED FOR WALL 0.0303 CM
(U*NU)EXT OF 7.383- 7.647, 0.0298- 0.0303CM
CORRECTED FOR WALL 0.0300- 0.0305CM

RUN 3-4
PARTICLES= SALT CRYSTALS DENSITY= 2.169 GM/CM^3
LIQUID= SAE 10W 84.9% + KEROSENE, DENSITY= 0.858 GM/CM^3
PARTICLE SIZE D_V= 0.0341 CM, D_t = 7.71 CM, D_V/D_t = 0.0044
SIEVE OPENINGS 0.250/0.298 MM, NO ELUTRIATION

EPS	U*NU(AVE) 0.01CM^3/SEC^2	LG(EPS)	LG(U*NU)	STD.DEV.	NO.OF TESTS
0.95	5.313	-0.0223	0.725	0.054	3 **
0.92	4.718	-0.0362	0.674	0.073	2
0.90	4.216	-0.0458	0.625	0.021	3
0.88	3.791	-0.0555	0.579	0.031	2
0.85	3.165	-0.0706	0.500	0.030	2
0.83	2.746	-0.0809	0.439	0.010	3
0.80	2.274	-0.0969	0.357	0.003	2
0.77	1.837	-0.1135	0.264	0.010	2
0.74	1.502	-0.1308	0.177	0.006	2
0.71	1.204	-0.1487	0.081	0.015	2
0.68	0.981	-0.1675	-0.009		1
0.65	0.772	-0.1871	-0.112	0.001	2

RE(0) 0.020- 0.022

LEAST SQUARES ESTIMATES
LOG(U*NU)= 0.8653 + 5.24*LOG(EPS)
U*NU = 7.333*EPS** 5.24
CONFIDENCE INTERVAL
N= 5.24 ± 0.06
LOG(U*NU)0 0.8653 ± 0.0065
(U*NU)EXT 7.224- 7.444

DIA. OF SPHERE CORRESPONDING TO
(U*NU)EXT= 7.333 0.0297 CM
CORRECTED FOR WALL 0.0298 CM
(U*NU)EXT OF 7.224- 7.444, 0.0295- 0.0299CM
CORRECTED FOR WALL 0.0296- 0.0301CM

RUN 4-2
PARTICLES= SALT CRYSTALS DENSITY= 2.163 GM/CM^3
LIQUID= SAE 10W 88.1%+ KEROSENE, DENSITY= 0.861 GM/CM^3
PARTICLE SIZE D_V= 0.0391 CM, D_t = 3.78 CM, D_V/D_t = 0.0103
SIEVE OPENINGS 0.295/0.351 MM, NO ELUTRIATION

EPS	U*NU(AVE) 0.01CM^3/SEC^2	LG(EPS)	LG(U*NU)	STD.DEV.	NO.OF TESTS
0.95	7.32	-0.0223	0.864	0.16	4 **
0.92	6.64	-0.0362	0.822	0.11	5
0.90	6.02	-0.0458	0.779	0.09	3
0.88	5.29	-0.0555	0.723	0.16	4
0.85	4.42	-0.0706	0.645	0.11	4
0.83	3.79	-0.0809	0.579	0.05	3
0.80	3.14	-0.0969	0.496	0.03	3
0.77	2.51	-0.1135	0.400	0.01	3
0.74	2.00	-0.1308	0.300	0.06	4
0.71	1.58	-0.1487	0.197	0.00	3
0.68	1.26	-0.1675	0.100	0.02	3
0.65	0.99	-0.1871	-0.004	0.00	2

RE(0) 0.023- 0.029

LEAST SQUARES ESTIMATES
LOG(U*NU)= 1.0301 + 5.55*LOG(EPS)
U*NU = 10.718*EPS** 5.55
CONFIDENCE INTERVAL
N= 5.55 ± 0.07
LOG(U*NU)0 1.0301 ± 0.0080
(U*NU)EXT 10.523- 10.917

DIA. OF SPHERE CORRESPONDING TO
(U*NU)EXT= 10.718 0.0361 CM
CORRECTED FOR WALL 0.0365 CM
(U*NU)EXT OF 10.523- 10.917, 0.0358- 0.0364CM
CORRECTED FOR WALL 0.0361- 0.0368CM

RUN 4-3
PARTICLES= SALT CRYSTALS DENSITY= 2.163 GM/CM^3
LIQUID= SAE 10W 88.1% + KEROSENE, DENSITY= 0.861 GM/CM^3
PARTICLE SIZE D_V= 0.0391 CM, D_t = 5.08 CM, D_V/D_t = 0.0077
SIEVE OPENINGS 0.295/0.351 MM, NO ELUTRIATION

EPS	U*NU(AVE) $0.01CM^3/SEC^2$	LG(EPS)	LG(U*NU)	STD.DEV.	NO.OF TESTS
0.95	7.27	-0.0223	0.861	0.13	4 **
0.92	6.61	-0.0362	0.820	0.12	3
0.90	5.90	-0.0458	0.771	0.08	3
0.88	5.19	-0.0555	0.715	0.04	4
0.85	4.40	-0.0706	0.643	0.10	3
0.83	3.81	-0.0809	0.581	0.05	3
0.80	3.10	-0.0969	0.491	0.02	3
0.77	2.50	-0.1135	0.397	0.03	3
0.74	2.02	-0.1308	0.305	0.05	4
0.71	1.60	-0.1487	0.205	0.01	4
0.68	1.27	-0.1675	0.104	0.02	3
0.65	0.99	-0.1871	-0.005	0.00	2

RE(O) 0.023- 0.028

LEAST SQUARES ESTIMATES
LOG(U*NU)= 1.0225 + 5.49*LOG(EPS)
U*NU = 10.533*EPS** 5.49
CONFIDENCE INTERVAL
N= 5.49 ± 0.05
LOG(U*NU)O 1.0225 ± 0.0054
(U*NU)EXT 10.402- 10.665

DIA. OF SPHERE CORRESPONDING TO
(U*NU)EXT= 10.533 0.0358 CM
CORRECTED FOR WALL 0.0361 CM
(U*NU)EXT OF 10.402- 10.665, 0.0355- 0.0360CM
CORRECTED FOR WALL 0.0358- 0.0363CM

RUN 5-3
PARTICLES= SLAT CRYSTALS DENSITY= 2.161 GM/CM^3
LIQUID= SAE 10W 88.1% + KEROSENE, DENSITY= 0.861 GM/CM^3
PARTICLE SIZE D_V= 0.0282 CM, D_t = 5.08 CM, D_V/D_t = 0.0056
SIEVE OPENINGS 0.208/0.250 MM, NO ELUTRIATION

EPS	U*NU(AVE) $0.01CM^3/SEC^2$	LG(EPS)	LG(U*NU)	STD.DEV.	NO.OF TESTS
0.950	3.691	-0.0223	0.567	0.018	3 **
0.920	3.314	-0.0362	0.520	0.012	2
0.905	3.061	-0.0434	0.486	0.056	3
0.890	2.795	-0.0506	0.446	0.027	2
0.870	2.464	-0.0605	0.392	0.011	2
0.850	2.221	-0.0706	0.346	0.023	2
0.830	1.962	-0.0809	0.293	0.028	2
0.800	1.565	-0.0969	0.195	0.015	2
0.770	1.288	-0.1135	0.110	0.026	2
0.740	1.033	-0.1308	0.014	0.009	2
0.710	0.821	-0.1487	-0.086		1
0.680	0.654	-0.1675	-0.184	0.008	2
0.650	0.497	-0.1871	-0.304	0.009	2

RE(O) 0.008- 0.010

LEAST SQUARES ESTIMATES
LOG(U*NU)= 0.7242 + 5.45*LOG(EPS)
U*NU = 5.300*EPS** 5.45
CONFIDENCE INTERVAL
N= 5.45 ± 0.08
LOG(U*NU)O 0.7242 ± 0.0083
(U*NU)EXT 5.200- 5.401

DIA. OF SPHERE CORRESPONDING TO
(U*NU)EXT= 5.300 0.0254 CM
CORRECTED FOR WALL 0.0255 CM
(U*NU)EXT OF 5.200- 5.401, 0.0252- 0.0256CM
CORRECTED FOR WALL 0.0253- 0.0258CM

RUN 6-4
PARTICLES= ABS CUBIC PELLETS DENSITY= 1.061 GM/CM^3
LIQUID= SAE 30 66% + KEROSENE DENSITY= 0.876 GM/CM^3
PARTICLE SIZE D_V= 0.2800 CM, D_t = 7.71 CM, D_V/D_t = 0.0374
NOMINAL LENGTH 1/10 INCH, NO SIEVING

EPS	U*NU(AVE) $0.01CM^3/SEC^2$	LG(EPS)	LG(U*NU)	STD.DEV.	NO.OF TESTS
0.95	40.87	-0.0223	1.689	0.81	2 **
0.92	42.23	-0.0362	1.626	0.30	3 **
0.90	39.49	-0.0458	1.597		1
0.88	34.76	-0.0555	1.541	0.76	2
0.85	28.92	-0.0706	1.461	0.45	3
0.83	25.91	-0.0809	1.414	0.65	4
0.80	20.46	-0.0969	1.311		1
0.77	17.05	-0.1135	1.232	0.02	2
0.74	13.60	-0.1308	1.133	0.19	2
0.71	10.86	-0.1487	1.036	0.21	2
0.68	9.75	-0.1675	0.989	0.16	2 **

RE(O) 0.036- 0.044

LEAST SQUARES ESTIMATES
LOG(U*NU)= 1.8461 + 5.44*LOG(EPS)
U*NU = 70.162*EPS** 5.44
CONFIDENCE INTERVAL
N= 5.44 ± 0.13
LOG(U*NU)O 1.8461 ± 0.0127
(U*NU)EXT 68.140- 72.243

DIA. OF SPHERE CORRESPONDING TO
(U*NU)EXT= 70.162 0.2470 CM
CORRECTED FOR WALL 0.2565 CM
(U*NU)EXT OF 68.140- 72.243, 0.2434- 0.2507CM
CORRECTED FOR WALL 0.2525- 0.2603CM

RUN 6-5
PARTICLES= ABS CUBIC PELLETS DENSITY= 1.061 GM/CM^3
LIQUID= SAE 30 66% + KEROSENE DENSITY= 0.876 GM/CM^3
PARTICLE SIZE D_V= 0.2880 CM, D_t = 10.12 CM, D_V/D_t = 0.0285
NOMINAL LENGTH 1/10 INCH, NO SIEVING

EPS	U*NU(AVE) $0.01CM^3/SEC^2$	LG(EPS)	LG(U*NU)	STD.DEV.	NO.OF TESTS
0.95	48.93	-0.0223	1.690	2.72	3 **
0.92	47.95	-0.0362	1.681		1 **
0.90	42.39	-0.0458	1.627	3.79	4
0.88	38.67	-0.0555	1.587	0.55	2
0.85	32.62	-0.0706	1.514	0.46	3
0.83	27.71	-0.0809	1.443	0.84	3
0.80	22.57	-0.0969	1.354	0.49	3
0.77	17.70	-0.1135	1.248		1
0.74	14.47	-0.1308	1.160	0.26	3
0.71	11.86	-0.1487	1.074	0.24	3
0.68	9.63	-0.1675	0.983	0.49	2

RE(O) 0.046- 0.070

LEAST SQUARES ESTIMATES
LOG(U*NU)= 1.8835 + 5.45*LOG(EPS)
U*NU = 76.479*EPS** 5.45
CONFIDENCE INTERVAL
N= 5.45 ± 0.22
LOG(U*NU)O 1.8835 ± 0.0241
(U*NU)EXT 72.355- 80.838

DIA. OF SPHERE CORRESPONDING TO
(U*NU)EXT= 76.479 0.2579 CM
CORRECTED FOR WALL 0.2655 CM
(U*NU)EXT OF 72.355- 80.838, 0.2509- 0.2652CM
CORRECTED FOR WALL 0.2583- 0.2730CM

RUN 9-2
PARTICLES= MINERAL CRYSTALS DENSITY= 2.632 GM/CM^3
LIQUID= SAE 10W 95% + KEROSENE, DENSITY= 0.862 GM/CM^3
PARTICLE SIZE D_V= 0.0508 CM, D_t = 3.78 CM, D_V/D_t = 0.0134
SIEVE OPENINGS 0.417/0.495 MM, SIEVING + ELUTRIATION

EPS	U*NU(AVE) $0.01CM^3/SEC^2$	LG(EPS)	LG(U*NU)	STD.DEV.	NO.OF TESTS
0.95	15.22	-0.0223	1.182	0.48	4 **
0.92	13.83	-0.0362	1.141	0.22	5 **
0.90	13.05	-0.0458	1.116	0.29	4
0.88	11.69	-0.0555	1.068	0.23	4
0.85	9.62	-0.0706	0.983	0.16	3
0.83	8.47	-0.0809	0.928	0.01	2
0.80	6.89	-0.0969	0.838	0.04	3
0.77	5.42	-0.1135	0.734	0.07	2
0.74	4.34	-0.1308	0.638	0.10	3
0.71	3.41	-0.1487	0.533	0.06	3
0.68	2.67	-0.1675	0.427	0.02	3
0.65	2.10	-0.1871	0.322		1

RE(O) 0.038- 0.057

LEAST SQUARES ESTIMATES
LOG(U*NU)= 1.3831 + 5.69*LOG(EPS)
U*NU = 24.160*EPS** 5.69
CONFIDENCE INTERVAL
N= 5.69 ± 0.07
LOG(U*NU)O 1.3831 ± 0.0085
(U*NU)EXT 23.691- 24.638

DIA. OF SPHERE CORRESPONDING TO
(U*NU)EXT= 24.160 0.0465 CM
CORRECTED FOR WALL 0.0471 CM
(U*NU)EXT OF 23.691- 24.638, 0.0460- 0.0469CM
CORRECTED FOR WALL 0.0467- 0.0476CM

RUN 9-3
PARTICLES= MINERAL CRYSTALS DENSITY= 2.632 GM/CM^3
LIQUID= SAE 10W 95% + KEROSENE, DENSITY= 0.862 GM/CM^3
PARTICLE SIZE D_V= 0.0508 CM, D_t = 5.08 CM, D_V/D_t = 0.0100
SIEVE OPENINGS 0.417/0.495 MM, SIEVING + ELUTRIATION

EPS	U*NU(AVE) $0.01CM^3/SEC^2$	LG(EPS)	LG(U*NU)	STD.DEV.	NO.OF TESTS
0.95	15.34	-0.0223	1.186	0.27	4 **
0.92	13.99	-0.0362	1.146	0.26	4 **
0.90	12.90	-0.0458	1.111	0.16	4
0.88	11.77	-0.0555	1.071	0.32	4
0.85	9.62	-0.0706	0.983	0.07	3
0.83	8.50	-0.0809	0.930	0.06	3
0.80	6.87	-0.0969	0.837	0.04	3
0.77	5.51	-0.1135	0.741	0.05	3
0.74	4.38	-0.1308	0.642	0.07	3
0.71	3.45	-0.1487	0.537	0.04	3
0.68	2.71	-0.1675	0.434	0.04	3
0.65	2.06	-0.1871	0.313		1

RE(O) 0.037- 0.057

LEAST SQUARES ESTIMATES
LOG(U*NU)= 1.3838 + 5.69*LOG(EPS)
U*NU = 24.201*EPS** 5.69
CONFIDENCE INTERVAL
N= 5.69 ± 0.10
LOG(U*NU)O 1.3838 ± 0.0113
(U*NU)EXT 23.578- 24.841

DIA. OF SPHERE CORRESPONDING TO
(U*NU)EXT= 24.201 0.0465 CM
CORRECTED FOR WALL 0.0470 CM
(U*NU)EXT OF 23.578- 24.841, 0.0459- 0.0471CM
CORRECTED FOR WALL 0.0464- 0.0476CM

RUN 10-2
PARTICLES= MINERAL CRYSTALS DENSITY= 2.632 GM/CM^3
LIQUID= SAE 10W 88.1% + KEROSENE, DENSITY= 0.858 GM/CM^3
PARTICLE SIZE D_v= 0.0426 CM, D_t = 3.78 CM, D_v/D_t = 0.0113
SIEVE OPENINGS 0.351/0.417 MM, SIEVING + ELUTRIATION

EPS	U*NU(AVE) 0.01CM^3/SEC^2	LG(EPS)	LG(U*NU)	STD.DEV.	NO.OF TESTS
0.95	13.42	-0.0223	1.128	0.60	2 **
0.92	10.99	-0.0362	1.041	0.32	4 **
0.90	10.49	-0.0458	1.021	0.26	3
0.88	9.12	-0.0555	0.960	0.29	2
0.85	7.01	-0.0706	0.846	0.09	2
0.82	5.94	-0.0862	0.766	0.17	3
0.80	5.28	-0.0969	0.723	0.18	3
0.77	4.15	-0.1135	0.618	0.06	3
0.74	3.30	-0.1308	0.519	0.04	2
0.71	2.49	-0.1487	0.396	0.03	3
0.68	1.93	-0.1675	0.286	0.02	2
0.65	1.55	-0.1871	0.191	0.02	2

RE(O) 0.054- 0.068

LEAST SQUARES ESTIMATES
LOG(U*NU)= 1.2815 + 5.89*LOG(EPS)
U*NU = 19.122*EPS** 5.89
CONFIDENCE INTERVAL
N= 5.89 ± 0.19
LOG(U*NU)O 1.2815 ± 0.0225
(U*NU)EXT 18.156- 20.139

DIA. OF SPHERE CORRESPONDING TO
(U*NU)EXT= 19.122 0.0412 CM
CORRECTED FOR WALL 0.0417 CM
(U*NU)EXT OF 18.156- 20.139, 0.0402- 0.0423CM
CORRECTED FOR WALL 0.0406- 0.0428CM

RUN 10-3
PARTICLES= MINERAL CRYSTALS DENSITY= 2.632 GM/CM^3
LIQUID= SAE 10W 88.1% + KEROSENE, DENSITY= 0.858 GM/CM^3
PARTICLE SIZE D_v= 0.0426 CM, D_t = 5.08 CM, D_v/D_t = 0.0084
SIEVE OPENINGS 0.351/0.417 MM, SIEVING + ELUTRIATION

EPS	U*NU(AVE) 0.01CM^3/SEC^2	LG(EPS)	LG(U*NU)	STD.DEV.	NO.OF TESTS
0.95	12.38	-0.0223	1.093	0.20	2 **
0.92	10.58	-0.0362	1.024	0.04	3 **
0.90	10.10	-0.0458	1.004	0.36	3
0.88	8.82	-0.0555	0.946	0.47	2
0.85	7.20	-0.0706	0.857	0.21	4
0.82	5.93	-0.0862	0.773	0.10	3
0.80	5.12	-0.0969	0.709	0.00	2
0.77	4.04	-0.1135	0.607	0.03	3
0.74	3.33	-0.1308	0.522	0.03	2
0.71	2.56	-0.1487	0.408	0.04	3
0.68	1.97	-0.1675	0.294	0.01	2
0.65	1.56	-0.1871	0.193	0.03	3

RE(O) 0.051- 0.065

LEAST SQUARES ESTIMATES
LOG(U*NU)= 1.2666 + 5.76*LOG(EPS)
U*NU = 18.476*EPS** 5.76
CONFIDENCE INTERVAL
N= 5.76 ± 0.08
LOG(U*NU)O 1.2666 ± 0.0099
(U*NU)EXT 18.060- 18.902

DIA. OF SPHERE CORRESPONDING TO
(U*NU)EXT= 18.476 0.0405 CM
CORRECTED FOR WALL 0.0409 CM
(U*NU)EXT OF 18.060- 18.902, 0.0401- 0.0410CM
CORRECTED FOR WALL 0.0404- 0.0413CM

RUN 11-2
PARTICLES= SUGAR CRYSTALS DENSITY= 1.590 GM/CM^3
LIQUID= SAE 30 66% + SAE 10W, DENSITY= 0.876 GM/CM^3
PARTICLE SIZE D_v= 0.1346 CM, D_t = 3.78 CM, D_v/D_t = 0.0356
SIEVE OPENINGS 0.991/1.168 MM, SIEVING + ELUTRIATION

EPS	U*NU(AVE) 0.01CM^3/SEC^2	LG(EPS)	LG(U*NU)	STD.DEV.	NO.OF TESTS
0.95	42.79	-0.0223	1.631	0.98	3 **
0.92	37.96	-0.0362	1.579	0.65	3 **
0.90	35.22	-0.0458	1.547	0.37	2 **
0.88	32.72	-0.0555	1.515	0.63	3
0.85	28.35	-0.0706	1.453	0.65	4
0.82	22.98	-0.0862	1.361	0.73	3
0.80	20.86	-0.0969	1.319	0.48	3
0.77	16.25	-0.1135	1.211	0.65	3
0.74	12.99	-0.1308	1.114	1.04	2
0.71	10.16	-0.1487	1.007	0.31	2
0.68	7.62	-0.1675	0.882		1

RE(O) 0.024- 0.029

LEAST SQUARES ESTIMATES
LOG(U*NU)= 1.8510 + 5.69*LOG(EPS)
U*NU = 70.960*EPS** 5.69
CONFIDENCE INTERVAL
N= 5.69± 0.33
LOG(U*NU)O 1.8510 ± 0.0377
(U*NU)EXT 65.054- 77.402

DIA. OF SPHERE CORRESPONDING TO
(U*NU)EXT= 70.960 0.1265 CM
CORRECTED FOR WALL 0.1311 CM
(U*NU)EXT OF 65.054- 77.402, 0.1211- 0.1321CM
CORRECTED FOR WALL 0.1255- 0.1369CM

RUN 11-3
PARTICLES= SUGAR CRYSTALS DENSITY= 1.590 GM/CM^3
LIQUID= SAE 30 66% + SAE 10W, DENSITY= 0.876 GM/CM^3
PARTICLE SIZE D_v= 0.1346 CM, D_t = 5.08 CM, D_v/D_t = 0.0265
SIEVE OPENINGS 0.991/1.168 MM, SIEVING + ELUTRIATION

EPS	U*NU(AVE) 0.01CM^3/SEC^2	LG(EPS)	LG(U*NU)	STD.DEV.	NO.OF TESTS
0.95	42.03	-0.0223	1.624	-0.00	2 **
0.92	38.13	-0.0362	1.581	0.66	3 **
0.90	35.60	-0.0458	1.554	0.48	3 **
0.88	32.31	-0.0555	1.509	0.21	3
0.85	28.88	-0.0706	1.461	0.03	2
0.82	22.91	-0.0862	1.360	0.03	2
0.80	21.21	-0.0969	1.326	0.29	3
0.77	16.46	-0.1135	1.217	0.08	3
0.74	13.41	-0.1308	1.127	0.23	4
0.71	9.94	-0.1487	0.997	0.09	2
0.68	7.74	-0.1675	0.889	0.00	2

RE(O) 0.024- 0.030

LEAST SQUARES ESTIMATES
LOG(U*NU)= 1.8511 + 5.66*LOG(EPS)
U*NU = 70.973*EPS** 5.66
CONFIDENCE INTERVAL
N= 5.66 ± 0.45
LOG(U*NU)O 1.8511 ± 0.0514
(U*NU)EXT 63.056- 79.885

DIA. OF SPHERE CORRESPONDING TO
(U*NU)EXT= 70.973 0.1265 CM
CORRECTED FOR WALL 0.1299 CM
(U*NU)EXT OF 63.956- 79.385, 0.1192- 0.1342CM
CORRECTED FOR WALL 0.1225- 0.1379CM

RUN 12-3
PARTICLES= SUGAR CRYSTALS DENSITY= 1.590 GM/CM^3
LIQUID= SAE 30 24% + SAE 10W, DENSITY= 0.870 GM/CM^3
PARTICLE SIZE D_v= 0.1133 CM, D_t = 5.08 CM, D_v/D_t = 0.0223
SIEVE OPENINGS 0.883/0.991 MM, SIEVING + ELUTRIATION

EPS	U*NU(AVE) 0.01CM^3/SEC^2	LG(EPS)	LG(U*NU)	STD.DEV.	NO.OF TESTS
0.95	32.32	-0.0223	1.509	1.06	3 **
0.92	29.61	-0.0362	1.471	0.29	3 **
0.90	28.24	-0.0458	1.451	0.69	5 **
0.88	25.94	-0.0555	1.414	0.62	3
0.85	23.08	-0.0706	1.363	0.62	3
0.82	18.12	-0.0862	1.258	0.14	2
0.80	16.14	-0.0969	1.208		1
0.77	12.99	-0.1135	1.114	0.14	2
0.74	9.86	-0.1308	0.994		1
0.71	7.65	-0.1487	0.884		1
0.68	6.04	-0.1675	0.781		1

RE(O) 0.051- 0.075

LEAST SQUARES ESTIMATES
LOG(U*NU)= 1.7612 + 5.83*LOG(EPS)
U*NU = 57.700*EPS** 5.83
CONFIDENCE INTERVAL
N= 5.83 ± 0.34
LOG(U*NU)O 1.7612 ± 0.0391
(U*NU)EXT 52.729- 63.139

DIA. OF SPHERE CORRESPONDING TO
(U*NU)EXT= 57.700 0.1132 CM
CORRECTED FOR WALL 0.1158 CM
(U*NU)EXT OF 52.729- 63.139, 0.1082- 0.1184CM
CORRECTED FOR WALL 0.1107- 0.1211CM

RUN 8-P
PARTICLES= MINERAL CRYSTALS DENSITY= 2.623 GM/CM^3
LIQUID= SAE 10W 89.1% + KEROSENE, DENSITY= 0.861 GM/CM^3
PARTICLE SIZE D_v= 0.0384 CM, D_t = 3.50 CM, D_v/D_t = 0.0110
FROM SIEVING 35/42 MESH, SEGGREGATION TEST

EPS	U*NU(AVE) 0.01CM^3/SEC^2	LG(EPS)	LG(U*NU)	STD.DEV.	NO.OF TESTS
0.90	9.24	-0.0458	0.966	0.20	4 **
0.85	7.01	-0.0706	0.846	0.04	2
0.80	4.90	-0.0969	0.690	-0.00	2
0.75	3.25	-0.1249	0.511	0.11	7
0.70	2.18	-0.1549	0.339	0.14	4

RE(O) 0.054- 0.062

LEAST SQUARES ESTIMATES
LOG(U*NU)= 1.2731 + 6.05*LOG(EPS)

RUN 3-M
PARTICLES= MINERAL CRYSTALS DENSITY= 2.623 GM/CM^3
LIQUID= SAE 10W 88.1% + KEROSENE, DENSITY= 0.861 GM/CM^3
PARTICLE SIZE D_v= 0.0378 CM, D_t = 3.50 CM, D_v/D_t = 0.0108
MIXTURE 90% 35/42 MESH + 10% 42/48 MESH, SEGGREGATION TES

EPS	U*NU(AVE) 0.01CM^3/SEC^2	LG(EPS)	LG(U*NU)	STD.DEV.	NO.OF TESTS
0.90	7.92	-0.0458	0.899	0.26	4 **
0.85	6.20	-0.0706	0.798	-0.00	2
0.80	4.48	-0.0969	0.651	0.02	3
0.75	3.08	-0.1249	0.488	0.03	7
0.70	2.07	-0.1549	0.316	0.12	4

RE(O) 0.043- 0.048

LEAST SQUARES ESTIMATES
LOG(U*NU)= 1.2039 + 5.73*LOG(EPS)
U*NU = 15.991*EPS** 5.73

APPENDIX IX DATA AND RESULTS FOR FREE SETTLING

Original Data

Run No.	Particles	Column	Page
2-Single	0.114 cm Glass Beads	7.71 cm	IX-2
7-Single	0.0492 cm Glass Beads	5.08 cm	IX-4
3-Single	0.0341 cm Salt Crystals	5.08 cm	IX-6
4-Single	0.0391 cm Salt Crystals	5.08 cm	IX-8
5-Single	0.0282 cm Salt Crystals	5.08 cm	IX-10
6-Single	0.288 cm ABS Pellets	7.71 cm	IX-12

Calculated Results

Run No.	Page
2-Single	IX-13
1-Single	IX-13
7-Single	IX-14
3-Single	IX-15
4-Single	IX-16
5-Single	IX-17
6-Single	IX-18

VISCOSITY DATA IX-19

The first number in Run No. indicates the same combination of particles and liquid as used in the hindered settling tests.

Run 2- Single 0.114 cm Glass Beads in 7.71 cm Column

TEMP DEG. F	DIST CM	SETTLING TIME SEC	U CM/SEC	U*NU $0.01CM^3/SEC^2$
70.50	10.0	16.4	0.61	123.32
70.50	10.0	15.6	0.64	129.65
70.50	20.0	28.5	0.70	141.93
70.60	20.0	27.4	0.73	147.37
70.60	20.0	35.1	0.57	115.04
70.60	20.0	35.1	0.57	115.04
70.80	20.0	32.4	0.62	124.20
70.80	20.0	35.3	0.57	113.99
70.80	20.0	32.7	0.61	123.06
70.80	20.0	34.1	0.59	118.01
70.80	20.0	35.8	0.56	112.40
70.80	20.0	36.1	0.55	111.47
70.80	20.0	33.5	0.60	120.12
70.80	20.0	34.2	0.58	117.66
70.10	20.0	35.0	0.57	116.37
70.20	20.0	27.2	0.74	149.49
70.20	20.0	33.9	0.59	119.94
70.20	20.0	30.4	0.66	133.75
70.20	20.0	33.2	0.60	122.47
70.20	20.0	35.7	0.56	113.89
70.20	20.0	38.0	0.53	107.00
70.20	20.0	34.7	0.58	117.18
70.20	20.0	35.0	0.57	116.17
70.20	20.0	35.9	0.56	113.26
70.20	20.0	32.0	0.63	127.06
70.20	20.0	28.4	0.70	143.17
70.20	20.0	35.4	0.56	114.86
70.20	20.0	31.5	0.63	129.08
70.20	20.0	35.6	0.56	114.21
70.20	20.0	29.8	0.67	136.44
70.20	20.0	33.2	0.60	122.47
70.20	20.0	38.0	0.53	107.00
70.20	20.0	30.0	0.67	135.53
70.20	20.0	27.2	0.74	149.49
70.20	20.0	35.0	0.57	116.17
70.20	20.0	37.4	0.53	108.72
70.20	20.0	28.7	0.70	141.67
70.20	20.0	35.0	0.57	116.17
70.20	20.0	31.2	0.64	130.32
70.20	20.0	36.4	0.55	111.70
70.20	20.0	31.0	0.65	131.16
70.20	20.0	33.5	0.60	121.37
70.20	20.0	30.7	0.65	132.44
70.20	20.0	28.2	0.71	144.18
70.20	20.0	31.0	0.65	131.16
70.20	20.0	27.4	0.73	148.39
70.20	20.0	26.9	0.74	151.15

70.20	20.0	29.2	0.68	139.25
70.20	20.0	36.1	0.55	112.63
70.20	20.0	31.3	0.64	129.90
70.20	20.0	26.6	0.75	152.86
70.20	20.0	38.1	0.52	106.72
70.20	20.0	35.7	0.56	113.89
70.20	20.0	35.3	0.57	115.18
70.20	20.0	33.6	0.60	121.01
70.20	20.0	37.4	0.53	108.72
70.20	20.0	33.8	0.59	120.30
70.20	20.0	36.1	0.55	112.63
68.85	10.0	17.6	0.57	118.96
68.68	20.0	30.0	0.67	140.09
68.65	20.0	36.3	0.55	115.85
68.65	20.0	36.0	0.56	116.82
68.65	20.0	31.6	0.63	133.09
68.80	20.0	34.0	0.59	123.29
68.80	20.0	29.0	0.69	144.55
68.80	20.0	31.9	0.63	131.41
68.80	20.0	29.9	0.67	140.20
68.90	20.0	33.0	0.61	126.76
69.00	20.0	31.3	0.64	133.35
69.00	20.0	29.6	0.68	141.01
69.00	20.0	31.8	0.63	131.26
69.00	20.0	32.6	0.61	128.04
69.00	20.0	34.8	0.57	119.94
69.00	20.0	34.8	0.57	119.94
69.00	20.0	32.9	0.61	126.87
69.00	20.0	35.3	0.57	118.24
69.25	20.0	31.7	0.63	130.93
69.70	20.0	32.2	0.62	127.58
69.25	20.0	34.6	0.58	119.96
69.25	20.0	36.2	0.55	114.65
69.40	20.0	32.8	0.61	126.11
69.40	20.0	35.4	0.56	116.85
69.40	20.0	30.6	0.65	135.18
69.50	20.0	26.4	0.76	156.33
69.50	20.0	34.8	0.57	118.59
69.50	10.0	15.4	0.65	133.99
69.50	20.0	36.6	0.55	112.76
69.50	20.0	33.6	0.60	122.83
69.70	20.0	33.1	0.60	124.11
69.70	20.0	28.8	0.69	142.65
69.70	10.0	16.8	0.60	122.27
69.70	20.0	33.7	0.59	121.91
69.70	20.0	34.2	0.58	120.12
69.70	20.0	34.0	0.59	120.83
69.70	20.0	33.6	0.60	122.27
69.70	20.0	30.2	0.66	136.03
69.70	10.0	16.8	0.60	122.27
69.80	20.0	29.4	0.68	139.41
69.80	20.0	28.6	0.70	143.31
69.90	20.0	35.9	0.56	113.91

Run 7- Single 0.0497 cm Glass Beads In 5.08 cm Column

TEMP DEG. F	DIST CM	SETTLING TIME SEC	U CM/SEC	U*NU $0.01CM^3/SEC^2$
69.75	10.0	52.4	0.19	21.69
69.75	10.0	48.8	0.20	23.29
69.70	10.0	44.8	0.22	25.39
69.70	10.0	52.8	0.19	21.55
69.70	10.0	44.2	0.23	25.74
69.70	10.0	45.6	0.22	24.95
69.80	10.0	47.8	0.21	23.75
69.80	10.0	43.6	0.23	26.04
69.80	10.0	50.6	0.20	22.44
69.90	10.0	46.4	0.22	24.42
70.00	10.0	56.6	0.18	19.98
70.05	10.0	50.0	0.20	22.59
70.05	10.0	47.2	0.21	23.93
70.10	10.0	38.8	0.26	29.08
70.10	10.0	46.8	0.21	24.11
70.10	10.0	38.0	0.26	29.69
70.40	10.0	54.2	0.18	20.69
70.40	10.0	43.0	0.23	26.08
70.40	10.0	48.2	0.21	23.27
70.40	10.0	44.0	0.23	25.49
70.45	10.0	42.0	0.24	26.68
70.50	10.0	45.6	0.22	24.55
70.50	10.0	49.4	0.20	22.66
70.50	10.0	47.6	0.21	23.51
70.60	10.0	44.8	0.22	24.93
70.60	10.0	50.2	0.20	22.25
70.70	10.0	44.0	0.23	25.34
70.70	10.0	47.8	0.21	23.32
70.75	10.0	49.0	0.20	22.73
70.75	10.0	43.2	0.23	25.78
70.80	10.0	43.8	0.23	25.40
70.80	10.0	40.6	0.25	27.40
70.80	10.0	43.6	0.23	25.52
70.90	10.0	51.4	0.19	21.60
70.90	10.0	55.3	0.18	20.08
70.90	10.0	50.4	0.20	22.03
70.95	10.0	53.8	0.19	20.62
71.00	10.0	45.8	0.22	24.19
71.00	10.0	39.8	0.25	27.84
71.00	10.0	51.2	0.20	21.64
71.00	10.0	52.9	0.19	20.95
71.05	10.0	45.8	0.22	24.17
71.05	10.0	58.5	0.17	18.92
71.10	10.0	48.2	0.21	22.94
71.10	10.0	44.0	0.23	25.13
71.15	10.0	51.6	0.19	21.41
71.15	10.0	51.8	0.19	21.33

71.15	10.0	46.6	0.21	23.71
71.50	10.0	56.8	0.18	19.32
71.50	10.0	51.6	0.19	21.27
71.50	10.0	52.9	0.19	20.75
71.50	10.0	46.4	0.22	23.65
71.50	10.0	43.6	0.23	25.17
71.50	10.0	44.0	0.23	24.94
71.40	10.0	48.6	0.21	22.62
71.40	10.0	44.4	0.23	24.76
71.40	10.0	44.2	0.23	24.88
71.40	10.0	42.0	0.24	26.18
71.40	10.0	43.6	0.23	25.22
71.55	10.0	42.0	0.24	26.10
71.55	10.0	43.0	0.23	25.50
71.55	10.0	48.0	0.21	22.84
71.55	10.0	52.0	0.19	21.08
71.60	10.0	44.0	0.23	24.89
71.60	10.0	43.6	0.23	25.12
71.60	10.0	39.5	0.25	27.73
71.60	10.0	40.4	0.25	27.11
71.70	10.0	52.6	0.19	20.78
71.70	10.0	53.8	0.19	20.32
71.70	10.0	40.8	0.25	26.79
71.70	10.0	40.6	0.25	26.93
71.70	10.0	45.6	0.22	23.97
71.70	10.0	40.2	0.25	27.19
71.70	10.0	48.6	0.21	22.49
71.80	10.0	54.0	0.19	20.21
71.80	10.0	47.5	0.21	22.97
71.80	10.0	51.6	0.19	21.15
71.80	10.0	42.2	0.24	25.86
71.80	10.0	49.6	0.20	22.00

Run 3- Single 0.0341 cm Salt Crystals In 5.08 cm Column

TEMP DEG. F	DIST CM	SETTLING TIME SEC	U CM/SEC	U*NU $0.01CM^3/SEC^2$
74.50	10.0	38.6	0.26	7.72
74.45	10.0	31.0	0.32	9.62
74.45	20.0	58.0	0.34	10.28
74.50	20.0	60.1	0.33	9.91
74.52	20.0	57.0	0.35	10.45
74.50	20.0	60.2	0.33	9.89
74.50	20.0	63.3	0.32	9.41
74.60	20.0	56.8	0.35	10.46
74.60	20.0	55.6	0.36	10.69
74.65	20.0	66.1	0.30	8.98
74.65	20.0	54.2	0.37	10.95
74.65	20.0	57.1	0.35	10.39
74.65	20.0	71.0	0.28	8.36
74.80	10.0	31.0	0.32	9.54
74.80	20.0	65.4	0.31	9.04
74.80	20.0	64.8	0.31	9.13
75.20	20.0	62.5	0.32	9.37
75.20	20.0	69.4	0.29	8.44
75.20	20.0	64.5	0.31	9.08
75.20	20.0	62.6	0.32	9.36
75.20	30.0	105.0	0.29	8.37
75.20	20.0	72.8	0.27	8.04
75.20	20.0	69.2	0.29	8.46
75.20	20.0	54.4	0.37	10.77
75.20	20.0	66.6	0.30	8.79
75.20	20.0	54.2	0.37	10.81
75.20	20.0	66.0	0.30	8.87
75.20	20.0	63.1	0.32	9.28
75.20	20.0	70.9	0.28	8.26
75.20	20.0	75.0	0.27	7.81
75.20	20.0	55.0	0.36	10.65
74.55	20.0	78.0	0.26	7.63
74.55	20.0	99.2	0.20	6.00
74.55	20.0	78.0	0.26	7.63
74.55	20.0	65.4	0.31	9.10
74.55	20.0	68.0	0.29	8.75
74.55	20.0	69.7	0.29	8.54
74.80	20.0	80.0	0.25	7.39
74.80	40.0	150.4	0.27	7.86
74.80	30.0	95.8	0.31	9.26
74.80	20.0	66.3	0.30	8.92
74.80	20.0	69.0	0.29	8.57
74.80	20.0	64.9	0.31	9.11
74.80	20.0	64.9	0.31	9.11
74.80	20.0	71.7	0.28	8.25
74.80	20.0	65.8	0.30	8.99
74.80	20.0	74.6	0.27	7.93

74.80	20.0	74.2	0.27	7.97
74.80	20.0	65.5	0.31	9.03
74.80	20.0	85.0	0.24	6.96
74.80	20.0	73.2	0.27	8.08
74.60	10.0	37.8	0.26	7.86
74.60	10.0	36.8	0.27	8.07
74.60	10.0	32.2	0.31	9.23
74.60	10.0	34.0	0.29	8.74
74.60	10.0	31.2	0.32	9.52
74.60	20.0	76.2	0.26	7.80
74.60	10.0	35.6	0.28	8.35
74.60	10.0	46.8	0.21	6.35
74.60	20.0	71.8	0.28	8.28
74.60	20.0	63.3	0.32	9.39
74.60	10.0	37.2	0.27	7.99
74.60	10.0	36.1	0.28	8.23
74.60	10.0	39.2	0.26	7.58
74.60	10.0	40.0	0.25	7.43
74.60	10.0	38.0	0.26	7.82
74.60	10.0	37.8	0.26	7.86
74.60	10.0	35.2	0.28	8.44
74.60	30.0	78.2	0.38	11.40
74.60	20.0	67.8	0.29	8.76
74.60	10.0	34.5	0.29	8.61

Run 4-Single 0.0391 cm Salt Crystals In 5.08 cm Column

TEMP DEG. F	DIST CM	SETTLING TIME SEC	U CM/SEC	U*NU $0.01CM^3/SEC^2$
73.60	10.0	28.6	0.35	12.73
73.60	10.0	30.1	0.33	12.09
73.75	10.0	28.0	0.36	12.95
72.80	10.0	28.6	0.35	12.99
72.80	10.0	25.6	0.39	14.51
72.80	10.0	29.0	0.34	12.81
72.80	10.0	25.0	0.40	14.86
73.10	10.0	28.7	0.35	12.84
76.65	10.0	25.6	0.39	13.13
76.65	10.0	27.5	0.36	12.22
76.65	10.0	30.0	0.33	11.21
76.65	10.0	29.6	0.34	11.36
76.65	10.0	29.4	0.34	11.43
76.65	10.0	29.2	0.34	11.51
76.65	10.0	24.9	0.40	13.50
76.65	10.0	32.0	0.31	10.51
76.65	10.0	29.4	0.34	11.43
71.70	30.0	107.4	0.28	10.69
71.70	10.0	25.6	0.39	14.94
71.70	20.0	50.6	0.40	15.12
71.70	10.6	27.6	0.38	14.69
71.80	10.0	27.2	0.37	14.03
71.90	10.0	27.2	0.37	13.99
72.00	10.0	27.6	0.36	13.75
72.05	10.0	28.0	0.36	13.54
72.10	10.0	34.4	0.29	11.00
72.20	10.0	35.8	0.28	10.55
72.20	10.0	25.9	0.39	14.58
72.20	10.0	28.6	0.35	13.20
72.20	10.0	34.0	0.29	11.10
72.20	10.0	30.8	0.32	12.26
72.40	10.0	54.5	0.18	6.89
72.20	10.0	30.3	0.33	12.46
72.40	10.0	32.4	0.31	11.59
72.40	10.0	25.8	0.39	14.56
72.40	10.0	33.8	0.30	11.11
72.50	10.0	30.6	0.33	12.24
72.50	10.0	32.0	0.31	11.70
72.50	10.0	31.4	0.32	11.93
72.50	10.0	34.6	0.29	10.83
72.50	10.0	28.4	0.35	13.19
72.50	10.0	31.8	0.31	11.78
72.50	10.0	30.0	0.33	12.48
72.50	10.0	30.6	0.33	12.24
72.50	20.0	67.2	0.30	11.15
72.50	10.0	32.0	0.31	11.70
72.50	10.0	31.4	0.32	11.93

72.50	20.0	55.0	0.36	13.62
72.50	10.0	34.2	0.29	10.95
72.50	10.0	29.6	0.34	12.65
71.50	10.0	37.2	0.27	10.34
71.50	10.0	33.4	0.30	11.52
71.50	10.0	35.2	0.28	10.93
71.50	10.0	32.6	0.31	11.80
71.50	10.0	33.0	0.30	11.66
71.50	10.0	32.2	0.31	11.95
71.50	10.0	32.4	0.31	11.87
71.50	10.0	34.9	0.29	11.02
71.50	10.0	28.6	0.35	13.45
71.50	10.0	31.8	0.31	12.10
71.50	10.0	34.6	0.29	11.12
71.50	10.0	27.9	0.36	13.79
71.50	10.0	36.1	0.28	10.66
71.60	10.0	35.1	0.28	10.93
71.60	10.0	35.6	0.28	10.78
71.60	20.0	56.8	0.35	13.51
71.60	10.0	33.6	0.30	11.42
71.60	10.0	30.0	0.33	12.79
70.60	10.0	38.4	0.26	10.26
70.60	10.0	46.2	0.22	8.53
70.50	10.0	83.6	0.12	4.72
70.50	10.0	32.6	0.31	12.11
70.50	10.0	37.7	0.27	10.48
70.50	10.0	38.9	0.26	10.15
70.50	10.0	40.7	0.25	9.70
70.50	10.0	35.6	0.28	11.09
70.40	10.0	42.2	0.24	9.38
70.40	10.0	37.5	0.27	10.56
70.40	10.0	45.4	0.22	8.72
70.40	10.0	75.5	0.13	5.24
70.40	10.0	37.4	0.27	10.59
70.40	10.0	55.0	0.18	7.20
70.40	10.0	33.2	0.30	11.93
70.80	10.0	30.0	0.33	13.06
70.80	10.0	31.6	0.32	12.40
71.10	10.0	32.4	0.31	12.00
71.20	10.0	29.0	0.34	13.37
71.20	10.0	29.8	0.34	13.01
71.20	20.0	65.2	0.31	11.89

Run 5-Single 0.0282 cm Salt Crystals In 5.08 cm Column

TEMP DEG. F	DIST CM	SETTLING TIME SEC	U CM/SEC	U*NU 0.01CM^3/SEC^2
74.40	10.0	85.2	0.12	4.18
74.40	20.0	148.2	0.13	4.81
74.20	20.0	124.0	0.16	5.78
74.50	10.0	62.8	0.16	5.66
74.50	10.0	56.0	0.18	6.35
74.50	10.0	47.8	0.21	7.44
74.50	10.0	59.6	0.17	5.96
74.60	10.0	47.5	0.21	7.46
74.60	10.0	57.8	0.17	6.13
74.60	10.0	56.0	0.18	6.33
74.60	10.0	67.2	0.15	5.28
74.60	10.0	60.2	0.17	5.89
74.60	10.0	68.0	0.15	5.21
74.60	10.0	63.4	0.16	5.59
74.60	20.0	140.7	0.14	5.04
74.60	10.0	48.8	0.20	7.26
74.60	10.0	65.3	0.15	5.43
74.60	10.0	62.9	0.16	5.64
74.60	10.0	63.4	0.16	5.59
74.60	10.0	60.6	0.17	5.85
74.60	10.0	55.6	0.18	6.38
74.60	10.0	60.9	0.16	5.82
74.60	10.0	63.0	0.16	5.63
74.60	10.0	67.6	0.15	5.24
74.60	10.0	65.3	0.15	5.43
74.60	10.0	62.3	0.16	5.69
74.60	10.0	58.8	0.17	6.03
74.60	10.0	69.0	0.14	5.14
74.20	10.0	56.4	0.18	6.35
74.60	10.0	57.0	0.18	6.22
74.60	10.0	48.0	0.21	7.39
74.60	10.0	49.6	0.20	7.15
74.60	10.0	41.0	0.24	8.65
74.60	10.0	44.0	0.23	8.06
74.60	10.0	45.4	0.22	7.81
74.60	10.0	45.0	0.22	7.88
74.90	20.0	106.2	0.19	6.62
75.10	20.0	102.0	0.20	6.86
75.10	10.0	45.0	0.22	7.77
75.20	20.0	90.6	0.22	7.70
75.20	10.0	45.2	0.22	7.72
75.20	10.0	47.0	0.21	7.42
75.20	10.0	49.4	0.20	7.06
75.20	10.0	45.8	0.22	7.62
75.20	10.0	57.2	0.17	6.10
75.20	20.0	97.2	0.21	7.18
75.30	10.0	57.2	0.17	6.08

75.30	10.0	50.0	0.20	6.96
75.30	10.0	54.6	0.18	6.37
75.30	10.0	55.5	0.18	6.27
75.40	10.0	63.3	0.16	5.48
75.40	10.0	53.6	0.19	6.48
75.40	10.0	53.4	0.19	6.50
75.40	10.0	55.1	0.18	6.30
75.40	10.0	46.4	0.22	7.48
75.40	20.0	92.9	0.22	7.47
75.40	10.0	44.0	0.23	7.89
75.60	10.0	57.8	0.17	5.97
75.60	10.0	50.8	0.20	6.80
75.60	10.0	47.8	0.21	7.22
75.60	20.0	106.2	0.19	6.50
75.60	10.0	49.1	0.20	7.03
75.60	10.0	57.6	0.17	5.99
75.80	10.0	57.4	0.17	5.98
75.80	10.0	57.1	0.18	6.02
75.80	10.0	51.2	0.20	6.71
76.00	10.0	51.4	0.19	6.65
76.00	10.0	44.6	0.22	7.66
76.00	10.0	56.0	0.18	6.10
76.00	10.0	56.0	0.18	6.10
76.00	10.0	50.4	0.20	6.78
76.10	10.0	45.8	0.22	7.44
76.20	10.0	44.2	0.23	7.69
76.20	10.0	49.4	0.20	6.88
76.20	10.0	46.6	0.21	7.30
76.20	10.0	52.2	0.19	6.51
76.20	10.0	55.8	0.18	6.09
76.30	20.0	112.0	0.18	6.06
76.30	30.0	143.6	0.21	7.09
76.30	10.0	53.4	0.19	6.35
76.30	20.0	117.0	0.17	5.80
76.30	10.0	59.0	0.17	5.75
76.40	10.0	54.8	0.18	6.17
76.40	10.0	57.2	0.17	5.91
76.40	10.0	51.4	0.19	6.58
76.40	10.0	58.4	0.17	5.79
76.40	10.0	50.0	0.20	6.77
76.40	10.0	53.6	0.19	6.31
76.40	10.0	52.8	0.19	6.41
76.40	10.0	57.6	0.17	5.87
76.40	20.0	103.1	0.19	6.56
76.40	10.0	44.4	0.23	7.62
76.50	10.0	60.4	0.17	5.59
76.50	10.0	46.9	0.21	7.20
76.50	20.0	91.0	0.22	7.42
76.50	30.0	155.3	0.19	6.52
76.50	10.0	46.1	0.22	7.32
76.50	10.0	51.2	0.20	6.59
76.50	10.0	49.2	0.20	6.86

Run 6-Single 0.288 cm ABS Pellets In 7.71 cm Column

TEMP DEG. F	DIST CM	SETTLING TIME SEC	U CM/SEC	U*NU $0.01CM^3/SEC^2$
70.20	16.0	36.8	0.43	93.40
70.20	16.0	40.2	0.40	85.50
70.20	16.0	36.2	0.44	94.95
70.20	16.0	36.8	0.43	93.40
70.20	16.0	38.2	0.42	89.98
70.30	16.0	38.8	0.41	88.28
70.30	16.0	36.8	0.43	93.08
70.40	16.0	36.9	0.43	92.51
70.40	16.0	39.2	0.41	87.08
70.40	16.0	35.6	0.45	95.88
70.50	16.0	44.3	0.36	76.79
70.50	16.0	46.0	0.35	73.95
70.55	16.0	38.4	0.42	88.43
70.55	16.0	43.0	0.37	78.97
70.55	16.0	40.0	0.40	84.89
70.60	16.0	33.7	0.47	100.59
70.60	16.0	36.7	0.44	92.36
70.60	16.0	34.7	0.46	97.69
70.60	16.0	36.9	0.43	91.86
70.65	16.0	51.0	0.31	66.35
70.65	16.0	34.5	0.46	98.08
70.65	16.0	38.2	0.42	88.58
70.90	16.0	39.4	0.41	85.13
70.90	16.0	41.8	0.38	80.24
70.90	16.0	37.7	0.42	88.97
70.90	16.0	40.0	0.40	83.86
70.85	16.0	38.0	0.42	88.43
70.85	16.0	39.2	0.41	85.72
70.85	16.0	37.4	0.43	89.84
70.82	16.0	40.7	0.39	82.65
70.85	16.0	39.5	0.41	85.07
70.85	8.0	19.2	0.42	87.50
70.85	16.1	45.4	0.35	74.34
70.85	16.0	38.8	0.41	86.60
70.85	16.0	38.2	0.42	87.96

Run 2-Single Calculated Results

106.72	107.00	107.00	108.72	108.72	111.47
111.70	112.40	112.63	112.63	112.76	113.26
113.89	113.89	113.91	113.99	114.21	114.65
114.86	115.04	115.04	115.18	115.85	116.17
116.17	116.17	116.37	116.82	116.85	117.18
117.66	118.01	118.24	118.59	118.96	119.94
119.94	119.94	119.96	120.12	120.12	120.30
120.83	121.01	121.37	121.91	122.27	122.27
122.27	122.47	122.47	122.83	123.06	123.29
123.32	124.11	124.20	126.11	126.76	126.87
127.06	127.58	128.04	129.08	129.65	129.90
130.32	130.93	131.16	131.16	131.26	131.41
132.44	133.09	133.35	133.75	133.99	135.18
135.53	136.03	136.44	139.25	139.41	140.09
140.20	141.01	141.67	141.93	142.65	143.17
143.31	144.18	144.55	147.37	148.39	149.49
149.49	151.15	152.86	156.33		

AVERAGE U*NU = 125.74 (0.01CM^3/SEC^2)
CORRECTED FOR WALL = 129.64 (0.01CM^3/SEC^2)
STANDARD DEVIATION = 11.89 (0.01CM^3/SEC^2)
NO. OF MEASUREMENTS= 100

Run 1-Single

Results from Run 2-Single corrected for liquid density,

U*NU = 123.7 (0.01cm^3/sec^2)
CORRECTED FOR WALL 127.6 (0.01cm^3/sec^2)

Run 7-Single Calculated Results

18.92	19.32	19.98	20.08	20.21	20.32
20.62	20.69	20.75	20.78	20.95	21.08
21.15	21.27	21.33	21.41	21.55	21.60
21.64	21.69	22.00	22.03	22.25	22.44
22.49	22.59	22.62	22.66	22.73	22.84
22.94	22.97	23.27	23.29	23.32	23.51
23.65	23.71	23.75	23.93	23.97	24.11
24.17	24.19	24.42	24.55	24.76	24.88
24.89	24.93	24.94	24.95	25.12	25.13
25.17	25.22	25.34	25.39	25.40	25.49
25.50	25.52	25.74	25.78	25.86	26.04
26.08	26.10	26.18	26.68	26.79	26.93
27.11	27.19	27.40	27.73	27.84	29.08
29.69					

AVERAGE U*NU = 23.81 ($0.01 CM^3/SEC^2$)
CORRECTED FOR WALL = 24.29 ($0.01 CM^3/SEC^2$)
STANDARD DEVIATION = 2.37 ($0.01 CM^3/SEC^2$)
NO. OF MEASUREMENTS= 79

Run 3-Single Calculated Results

6.00	6.35	6.96	7.39	7.43	7.58
7.63	7.63	7.72	7.80	7.81	7.82
7.86	7.86	7.86	7.93	7.97	7.99
8.04	8.07	8.08	8.23	8.25	8.26
8.28	8.35	8.36	8.37	8.44	8.44
8.46	8.54	8.57	8.61	8.74	8.75
8.76	8.79	8.87	8.92	8.98	8.99
9.03	9.04	9.08	9.10	9.11	9.11
9.13	9.23	9.26	9.28	9.36	9.37
9.39	9.41	9.52	9.54	9.62	9.89
9.91	10.28	10.39	10.45	10.46	10.65
10.69	10.77	10.81	10.95	11.40	

AVERAGE U*NU = 8.79 (0.01CM^3/SEC^2)
CORRECTED FOR WALL = 8.91 (0.01CM^3/SEC^2)
STANDARD DEVIATION = 1.08 (0.01CM^3/SEC^2)
NO. OF MEASUREMENTS= 71

Run 4-Single Calculated Results

4.72	5.24	6.89	7.20	8.53	8.72
9.38	9.70	10.15	10.26	10.34	10.48
10.51	10.55	10.56	10.59	10.66	10.69
10.78	10.83	10.93	10.93	10.95	11.00
11.02	11.09	11.10	11.11	11.12	11.15
11.21	11.36	11.42	11.43	11.43	11.51
11.52	11.59	11.66	11.70	11.70	11.78
11.80	11.87	11.89	11.93	11.93	11.93
11.95	12.00	12.09	12.10	12.11	12.22
12.24	12.24	12.26	12.40	12.46	12.48
12.65	12.73	12.79	12.81	12.84	12.95
12.99	13.01	13.06	13.13	13.19	13.20
13.37	13.45	13.50	13.51	13.54	13.62
13.75	13.79	13.99	14.03	14.51	14.56
14.58	14.69	14.86	14.94	15.12	

AVERAGE U*NU = 11.78 (0.01CM^3/SEC^2)
CORRECTED FOR WALL = 11.97 (0.01CM^3/SEC^2)
STANDARD DEVIATION = 1.88 (0.01CM^3/SEC^2)
NO. OF MEASUREMENTS= 89

Run 5-Single Calculated Results

4.18	4.81	5.04	5.14	5.21	5.24
5.28	5.43	5.43	5.48	5.59	5.59
5.59	5.63	5.64	5.66	5.69	5.75
5.78	5.79	5.80	5.82	5.85	5.87
5.89	5.91	5.96	5.97	5.98	5.99
6.02	6.03	6.06	6.08	6.09	6.10
6.10	6.10	6.13	6.17	6.22	6.27
6.30	6.31	6.33	6.35	6.35	6.35
6.37	6.38	6.41	6.48	6.50	6.50
6.51	6.52	6.56	6.58	6.59	6.62
6.65	6.71	6.77	6.78	6.80	6.86
6.86	6.88	6.96	7.03	7.06	7.09
7.15	7.18	7.20	7.22	7.26	7.30
7.32	7.39	7.42	7.42	7.44	7.44
7.46	7.47	7.48	7.62	7.62	7.66
7.69	7.70	7.72	7.77	7.81	7.88
7.89	8.06	8.65			

AVERAGE U*NU = 6.50 (0.01CM^3/SEC^2)
CORRECTED FOR WALL = 6.57 (0.01CM^3/SEC^2)
STANDARD DEVIATION = 0.83 (0.01CM^3/SEC^2)
NO. OF MEASUREMENTS= 99

Run 6-Single Calculated Results

66.35	73.95	74.34	76.79	78.97	80.24
82.65	83.86	84.89	85.07	85.13	85.50
85.72	86.60	87.08	87.50	87.96	88.28
88.43	88.43	88.58	88.97	89.84	89.98
91.86	92.36	92.51	93.08	93.40	93.40
94.95	95.88	97.69	98.08	100.59	

AVERAGE U*NU = 87.40 ($0.01 CM^3/SEC^2$)
CORRECTED FOR WALL = 94.27 ($0.01 CM^3/SEC^2$)
STANDARD DEVIATION = 7.29 ($0.01 CM^3/SEC^2$)
NO. OF MEASUREMENTS= 35

VISCOSITY DATA

Run 2-Single

Temperature	°F	68.00	69.00	70.00	71.00
Viscosity	cs	213.20	208.70	204.00	200.50

Run 3-Single

Temperature	°F	69.02	70.00	71.00	72.00	73.00	74.00	75.02	76.00
Viscosity	cs	33.94	33.06	32.24	31.46	30.67	29.88	29.15	29.43

Run 4-Single

Temperature	°F	69.02	69.98	71.00	72.00	73.10	74.00	75.05	76.00	77.20
Viscosity	cs	41.03	40.03	38.98	37.95	36.86	36.03	35.02	34.17	33.15

Run 5-Single

Temperature	°F	69.02	69.98	71.00	72.00	73.10	74.00	75.05	76.00	77.20
Viscosity	cs	41.03	40.03	3898	37.95	36.86	36.03	35.02	34.17	33.15

Run 6-Single

Temperature	°F	69.20	70.00	71.10	72.00
Viscosity	cs	221.86	216.3	208.16	200.66

Run 7-Single

Temperature	°F	69.00	70.00	71.00	71.90
Viscosity	cs	115.42	113.06	110.80	108.90

APPENDIX X MICROSCOPIC MEASUREMENT OF PARTICLE SIZE

The results were calculated from the measurement of particle images of an order of an inch by Vernier calipers, and arranged in an increasing order. Two dimensions of the salt crystals were measured.

INDEX

Run 1,2 Microscopic Measurement of 0.114 cm Glass Beads

0.1017	0.1019	0.1024	0.1031	0.1039	0.1044
0.1045	0.1049	0.1050	0.1056	0.1056	0.1056
0.1056	0.1058	0.1058	0.1060	0.1060	0.1060
0.1060	0.1063	0.1065	0.1065	0.1065	0.1066
0.1066	0.1067	0.1067	0.1067	0.1070	0.1071
0.1080	0.1081	0.1082	0.1082	0.1089	0.1090
0.1092	0.1094	0.1099	0.1099	0.1099	0.1100
0.1100	0.1102	0.1102	0.1104	0.1106	0.1108
0.1108	0.1108	0.1109	0.1112	0.1112	0.1112
0.1113	0.1114	0.1117	0.1117	0.1119	0.1119
0.1119	0.1122	0.1124	0.1125	0.1125	0.1125
0.1128	0.1132	0.1138	0.1140	0.1141	0.1141
0.1142	0.1145	0.1147	0.1154	0.1154	0.1164
0.1168	0.1169	0.1171	0.1173	0.1173	0.1175
0.1179	0.1189	0.1195	0.1207	0.1207	0.1210
0.1210	0.1213	0.1217	0.1217	0.1218	0.1223
0.1228	0.1229	0.1233	0.1236	0.1243	0.1245
0.1263	0.1272	0.1285			

AVERAGE LENGTH = 0.1123 CM (diameter)
STANDARD DEVIATION = 0.0063 CM
NO. OF MEASUREMENTS = 105

Run 7 Microscope Measurement of 0.0492 cm Glass Beads

0.0448	0.0450	0.0450	0.0450	0.0452	0.0454
0.0454	0.0455	0.0456	0.0456	0.0457	0.0458
0.0458	0.0458	0.0459	0.0459	0.0460	0.0460
0.0460	0.0461	0.0461	0.0462	0.0462	0.0462
0.0463	0.0465	0.0465	0.0465	0.0465	0.0465
0.0467	0.0467	0.0468	0.0469	0.0470	0.0470
0.0470	0.0470	0.0471	0.0471	0.0472	0.0474
0.0474	0.0475	0.0475	0.0475	0.0475	0.0476
0.0476	0.0476	0.0478	0.0478	0.0478	0.0480
0.0480	0.0480	0.0481	0.0481	0.0481	0.0482
0.0482	0.0484	0.0484	0.0484	0.0485	0.0485
0.0485	0.0486	0.0486	0.0486	0.0487	0.0487
0.0488	0.0488	0.0490	0.0492	0.0493	0.0494
0.0494	0.0495	0.0496	0.0497	0.0497	0.0497
0.0498	0.0498	0.0499	0.0500	0.0500	0.0503
0.0503	0.0503	0.0505	0.0505	0.0509	0.0511
0.0514	0.0516	0.0517	0.0520	0.0536	

AVERAGE LENGTH = 0.0479 CM (diameter)
STANDARD DEVIATION = 0.0018 CM
NO. OF MEASUREMENTS = 101

Run 3 Microscope Measurement of 0.0341 cm Salt Crystals

0.0208, 0.0230	0.0217, 0.0281	0.0225, 0.0272
0.0226, 0.0269	0.0230, 0.0221	0.0237, 0.0387
0.0239, 0.0227	0.0240, 0.0253	0.0240, 0.0237
0.0240, 0.0272	0.0240, 0.0264	0.0240, 0.0249
0.0245, 0.0255	0.0245, 0.0277	0.0245, 0.0262
0.0246, 0.0253	0.0248, 0.0230	0.0250, 0.0260
0.0250, 0.0258	0.0252, 0.0261	0.0252, 0.0240
0.0252, 0.0274	0.0254, 0.0254	0.0255, 0.0274
0.0256, 0.0244	0.0256, 0.0246	0.0257, 0.0280
0.0257, 0.0280	0.0261, 0.0283	0.0261, 0.0265
0.0261, 0.0258	0.0262, 0.0293	0.0262, 0.0273
0.0265, 0.0293	0.0265, 0.0236	0.0266, 0.0250
0.0266, 0.0277	0.0266, 0.0274	0.0266, 0.0268
0.0267, 0.0248	0.0267, 0.0257	0.0269, 0.0269
0.0269, 0.0275	0.0270, 0.0242	0.0271, 0.0252
0.0271, 0.0283	0.0271, 0.0278	0.0272, 0.0272
0.0272, 0.0272	0.0274, 0.0291	0.0274, 0.0266
0.0274, 0.0264	0.0275, 0.0235	0.0275, 0.0313
0.0275, 0.0301	0.0276, 0.0275	0.0276, 0.0301
0.0278, 0.0278	0.0278, 0.0295	0.0278, 0.0284
0.0279, 0.0265	0.0280, 0.0274	0.0280, 0.0265
0.0281, 0.0258	0.0282, 0.0278	0.0283, 0.0260
0.0283, 0.0291	0.0284, 0.0266	0.0284, 0.0266
0.0285, 0.0260	0.0285, 0.0293	0.0285, 0.0289
0.0286, 0.0293	0.0286, 0.0314	0.0287, 0.0269
0.0287, 0.0302	0.0287, 0.0291	0.0288, 0.0265
0.0288, 0.0267	0.0288, 0.0286	0.0288, 0.0305
0.0289, 0.0297	0.0289, 0.0265	0.0289, 0.0246
0.0289, 0.0280	0.0290, 0.0281	0.0290, 0.0296
0.0291, 0.0300	0.0291, 0.0304	0.0292, 0.0312
0.0293, 0.0311	0.0294, 0.0297	0.0294, 0.0276
0.0295, 0.0297	0.0296, 0.0248	0.0297, 0.0261
0.0302, 0.0277	0.0303, 0.0271	0.0304, 0.0316
0.0304, 0.0308	0.0307, 0.0286	0.0308, 0.0279
0.0309, 0.0304	0.0310, 0.0318	0.0314, 0.0291
0.0314, 0.0276	0.0319, 0.0300	0.0326, 0.0269

AVERAGE LENGTH = 0.0273, 0.0275 CM
STANDARD DEVIATION = 0.0023, 0.0024 CM
NO. OF MEASUREMENTS = 108 PAIRS

Run 4 Microscopic Measurement of 0.0391 cm Salt Crystals

0.0233, 0.0233	0.0262, 0.0335	0.0269, 0.0291
0.0278, 0.0319	0.0280, 0.0295	0.0286, 0.0370
0.0288, 0.0335	0.0290, 0.0320	0.0290, 0.0297
0.0293, 0.0302	0.0294, 0.0312	0.0295, 0.0279
0.0298, 0.0338	0.0299, 0.0291	0.0300, 0.0286
0.0300, 0.0300	0.0300, 0.0307	0.0300, 0.0343
0.0301, 0.0312	0.0302, 0.0310	0.0303, 0.0332
0.0303, 0.0311	0.0303, 0.0314	0.0304, 0.0296
0.0304, 0.0296	0.0305, 0.0358	0.0306, 0.0306
0.0307, 0.0300	0.0307, 0.0344	0.0308, 0.0323
0.0309, 0.0326	0.0309, 0.0299	0.0309, 0.0306
0.0309, 0.0286	0.0309, 0.0305	0.0309, 0.0310
0.0309, 0.0311	0.0312, 0.0312	0.0312, 0.0356
0.0313, 0.0305	0.0313, 0.0343	0.0313, 0.0315
0.0315, 0.0302	0.0315, 0.0311	0.0315, 0.0297
0.0315, 0.0301	0.0316, 0.0341	0.0318, 0.0292
0.0318, 0.0318	0.0319, 0.0319	0.0319, 0.0336
0.0319, 0.0321	0.0320, 0.0335	0.0320, 0.0309
0.0321, 0.0349	0.0321, 0.0318	0.0322, 0.0307
0.0322, 0.0309	0.0323, 0.0259	0.0325, 0.0300
0.0325, 0.0316	0.0325, 0.0347	0.0326, 0.0296
0.0327, 0.0344	0.0327, 0.0323	0.0329, 0.0311
0.0330, 0.0289	0.0330, 0.0329	0.0330, 0.0337
0.0330, 0.0374	0.0331, 0.0324	0.0332, 0.0341
0.0334, 0.0316	0.0335, 0.0343	0.0336, 0.0331
0.0336, 0.0338	0.0336, 0.0334	0.0337, 0.0370
0.0337, 0.0359	0.0338, 0.0334	0.0342, 0.0355
0.0345, 0.0349	0.0347, 0.0360	0.0349, 0.0320
0.0352, 0.0283	0.0358, 0.0337	0.0383, 0.0354
0.0427, 0.0325		

AVERAGE LENGTH = 0.0316, 0.0319 CM
STANDARD DEVIATION = 0.0024, 0.0025 CM
NO. OF MEASUREMENTS = 88 PAIRS

Run 5 Microscopic Measurement of Particle Size

0.0197, 0.0181	0.0198, 0.0198	0.0201, 0.0212
0.0203, 0.0210	0.0205, 0.0227	0.0206, 0.0189
0.0207, 0.0218	0.0207, 0.0260	0.0208, 0.0278
0.0208, 0.0223	0.0209, 0.0216	0.0211, 0.0221
0.0211, 0.0250	0.0212, 0.0262	0.0213, 0.0234
0.0214, 0.0212	0.0215, 0.0255	0.0215, 0.0228
0.0215, 0.0232	0.0216, 0.0200	0.0216, 0.0237
0.0217, 0.0218	0.0217, 0.0242	0.0217, 0.0221
0.0218, 0.0221	0.0219, 0.0230	0.0220, 0.0275
0.0220, 0.0240	0.0221, 0.0224	0.0222, 0.0222
0.0222, 0.0244	0.0223, 0.0227	0.0223, 0.0217
0.0223, 0.0250	0.0224, 0.0228	0.0225, 0.0215
0.0225, 0.0239	0.0225, 0.0265	0.0227, 0.0213
0.0227, 0.0231	0.0227, 0.0229	0.0229, 0.0235
0.0230, 0.0264	0.0230, 0.0247	0.0230, 0.0220
0.0230, 0.0241	0.0230, 0.0213	0.0230, 0.0244
0.0231, 0.0215	0.0232, 0.0258	0.0234, 0.0223
0.0235, 0.0227	0.0235, 0.0239	0.0235, 0.0226
0.0237, 0.0224	0.0237, 0.0230	0.0237, 0.0223
0.0240, 0.0221	0.0241, 0.0222	0.0244, 0.0241
0.0246, 0.0220	0.0246, 0.0247	0.0246, 0.0264
0.0247, 0.0214	0.0247, 0.0243	0.0248, 0.0282
0.0250, 0.0237	0.0251, 0.0227	0.0252, 0.0234
0.0252, 0.0254	0.0253, 0.0226	0.0254, 0.0244
0.0254, 0.0231	0.0255, 0.0232	0.0258, 0.0232
0.0259, 0.0205	0.0269, 0.0285	0.0280, 0.0224

AVERAGE LENGTH = 0.0229, 0.0232 CM
STANDARD DEVIATION = 0.0017, 0.0020 CM
NO. OF MEASUREMENTS = 78 PAIRS

APPENDIX XI DATA ON SETTLED BED POROSITY

INDEX

RUN 1-1 0.114 CM GLASS BEADS

EPS	SETTLED BED HEIGHT CM	SETTLED BED POROSITY	APPROX. TIME	
0.90	11.10	0.439		
0.88	13.28	0.437		
0.85	16.55	0.436		
0.80	22.20	0.439	1	HR
0.77	25.60	0.440		
0.74	29.00	0.442		
0.74	28.90	0.440		
0.74	29.00	0.442		
0.74	29.00	0.442		
0.70	33.38	0.440		
0.70	33.22	0.438	10	HRS
0.67	36.40	0.435		
0.67	36.35	0.435	5	HRS
0.64	39.64	0.434	10	HRS

RUN 1-2 0.114 CM GLASS BEADS

EPS	SETTLED BED HEIGHT CM	SETTLED BED POROSITY	APPROX. TIME	
0.90	11.10	0.442		
0.88	13.25	0.439		
0.85	16.53	0.438		
0.85	16.55	0.438		
0.83	18.80	0.440		
0.80	22.15	0.440	1	HR
0.77	25.35	0.438		
0.77	25.40	0.439	5	HRS
0.74	28.60	0.437		
0.70	33.05	0.437		
0.70	33.13	0.439		
0.70	33.10	0.438		
0.67	36.05	0.433	2	HRS
0.67	36.12	0.434	2	HRS
0.64	39.35	0.433	4	HRS
0.64	39.40	0.434	3	HRS
0.64	39.35	0.433	5	HRS

RUN 1-3 0.114 CM GLASS BEADS

EPS	SETTLED BED HEIGHT CM	SETTLED BED POROSITY	APPROX. TIME	
0.90	11.10	0.444	25	MINS
0.88	13.20	0.439	1.5	HRS
0.85	16.50	0.439		
0.85	16.50	0.439	10	MINS
0.83	18.70	0.439	20	MINS
0.80	22.00	0.439	1.5	HRS
0.80	21.97	0.439	5	MINS
0.77	25.20	0.437	20	MINS
0.74	28.50	0.437	0.5	HR
0.74	28.50	0.437	2	MINS
0.74	28.48	0.437	40	MINS
0.70	32.90	0.438	10	MINS
0.70	32.85	0.437	1	HR
0.67	36.10	0.436	10	MINS
0.67	36.50	0.442	30	MINS
0.67	36.00	0.435	3.5	HRS
0.64	39.38	0.436		
0.64	39.23	0.434	1	MIN
0.64	39.15	0.433	6.5	HRS
0.64	39.15	0.433	1.75	HRS

RUN 2-1 0.114 CM GLASS BEADS

EPS	SETTLED BED HEIGHT CM	SETTLED BED POROSITY	APPROX. TIME	
0.90	11.10	0.442	2.5	HRS
0.88	13.15	0.434	16	HRS
0.85	16.45	0.435	0.5	HR
0.85	16.45	0.435	1	HR
0.83	18.60	0.434	2	HRS
0.80	21.80	0.431	14	HRS
0.80	21.85	0.433	20	MINS
0.77	24.80	0.425	36	HRS
0.77	25.15	0.433	0.5	HR
0.77	25.05	0.431	2.5	HRS
0.74	28.20	0.429	2	HRS
0.74	28.15	0.428	11	HRS
0.70	32.75	0.432	5.5	HRS
0.67	35.55	0.425	10	HRS

RUN 2-2 0.114 CM GLASS BEADS

EPS	SETTLED BED HEIGHT CM.	SETTLED BED POROSITY	APPROX. TIME	
.88	13.20	0.44	1.75	HRS
0.85	16.45	0.438	15	MINS
0.85	16.40	0.436	15	HRS
0.83	18.60	0.437	11.5	HRS
0.80	21.88	0.437	15	HRS
0.77	25.20	0.437	2	HRS
0.74	28.40	0.436	3.33	HRS
0.70	32.40	0.429	9	HRS
0.67	36.00	0.435	3	HRS
0.64	38.90	0.430	0.5	HR
0.64	38.70	0.427	10.5	HRS

RUN 2-3 0.114 CM GLASS BEADS

EPS	SETTLED BED HEIGHT CM	SETTLED BED POROSITY	APPROX. TIME	
0.90	11.05	0.442		
0.90	11.00	0.439	3	DAYS
0.88	13.25	0.441	1	HR
0.85	16.45	0.438		
0.85	16.45	0.438	10	MINS
0.83	18.65	0.438	1.5	HRS
0.80	21.85	0.435	50	MINS
0.80	21.85	0.435	20	MINS
0.77	25.20	0.437	10	MINS
0.74	28.55	0.438	14	MINS
0.74	28.50	0.437	18	MINS
0.70	32.40	0.429	11	HRS
0.64	39.40	0.436	16	MINS
0.64	39.20	0.434	17	MINS
0.64	39.40	0.436	11	MINS

RUN 7-3 0.0492 CM GLASS BEADS

EPS	SETTLED BED HEIGHT CM	SETTLED BED POROSITY	APPROX. TIME	
0.92	8.75	0.436	10.5	HRS
0.90	10.95	0.437	24	HRS
0.88	13.05	0.433	4	HRS
0.85	16.40	0.436	20	HRS
0.82	19.50	0.430	11	HRS
0.82	19.65	0.435	40	MINS
0.80	21.80	0.434	2.75	HRS
0.77	24.95	0.431	0.5	HR
0.74	28.20	0.431	4	HRS
0.71	31.40	0.430	9	HRS
0.68	34.65	0.430	50	MINS
0.68	34.70	0.431	4	HRS
0.68	34.50	0.428	10	HRS

RUN 3-1A 0.0341 CM SALT CRYSTALS

EPS	SETTLED BED HEIGHT CM	SETTLED BED POROSITY	APPROX. TIME	
.95	5.80	0.462	58	MINS
.92	9.30	0.465	1.75	HRS
.90	11.60	0.46	1	HR
0.88	13.92	0.464	24	HRS
0.85	19.60	0.524	9	HRS
0.83	17.36	0.391	3.5	HRS
0.80	23.03	0.460	2	HRS
0.77	26.46	0.459	2	HRS
0.74	29.93	0.459	1	HRS
0.71	33.33	0.459	10	HRS
0.68	36.72	0.458	1.5	HRS
0.65	40.05	0.456	12	HRS

RUN 3-2 0.0341 CM SALT CRYSTALS

EPS	SETTLED BED HEIGHT CM	SETTLED BED POROSITY	APPROX. TIME	
0.95	5.80	0.469	50	MINS
0.92	9.32	0.471	1.75	HRS
0.90	11.63	0.470	1	HR
0.88	13.92	0.469	24	HRS
0.85	17.36	0.467	3.5	HRS
0.83	19.60	0.465	9	HRS
0.80	23.03	0.465	2	HRS
0.77	26.45	0.464	2	HRS
0.74	29.86	0.463	1	HR
0.71	33.28	0.463	10	HRS
0.68	36.60	0.461	1.5	HRS
0.65	39.90	0.459	12	HRS

RUN 3-3 0.0341 CM SALT CRYSTALS

EPS	SETTLED BED HEIGHT CM	SETTLED BED POROSITY	APPROX. TIME	
0.95	5.70	0.459	10	MINS
0.95	5.70	0.459	10	HRS
0.92	9.17	0.462	21	MINS
0.90	11.40	0.459	3.5	HRS
0.88	13.63	0.457	2.5	HRS
0.85	17.00	0.456	23	HRS
0.83	19.20	0.454	12	HRS
0.80	22.55	0.453	2	HRS
0.77	25.90	0.452	1.5	HRS
0.74	29.20	0.451	33	HRS
0.71	32.60	0.451	6	MINS
0.68	35.90	0.450	17.5	MINS
0.65	39.28	0.450	15	HRS

RUN 3-4 0.0341 CM SALT CRYSTALS

EPS	SETTLED BED HEIGHT CM	SETTLED BED POROSITY	APPROX. TIME	
0.88	13.70	0.460	3	HRS
0.85	17.00	0.456	20	HRS
0.83	19.20	0.454	18	HRS
0.80	22.55	0.453	1	HRS
0.77	25.85	0.451	0.5	HR
0.74	28.90	0.445	16	HRS
0.71	32.40	0.448	3.5	HRS
0.68	35.70	0.447	11	HRS
0.65	39.00	0.446	2.5	HRS

RUN 4-2 0.0391 CM SALT CRYSTALS

EPS	SETTLED BED HEIGHT CM	SETTLED BED POROSITY	APPROX. TIME	
0.95	5.75	0.464	10	HRS
0.92	9.15	0.461	3	HRS
0.90	11.40	0.459	25	MINS
0.88	13.60	0.456	16	HRS
0.85	16.95	0.455	3	HRS
0.83	19.20	0.454	57	MINS
0.80	22.50	0.452	17	HRS
0.77	25.86	0.452	2.75	HRS
0.74	29.20	0.451	9.5	HRS
0.71	32.53	0.451	3	HRS
0.68	35.78	0.449	4	HRS
0.65	38.93	0.446	0.7	HR
0.65	39.20	0.450	0.7	HR

RUN 4-3 0.0391 CM SALT CRYSTALS

EPS	SETTLED BED HEIGHT CM	SETTLED BED POROSITY	APPROX. TIME	
0.95	5.80	0.468	10	HRS
0.92	9.20	0.464	3	HRS
0.90	11.40	0.459	25	MINS
0.88	13.65	0.458	16	HRS
0.85	17.05	0.457	3	HRS
0.83	19.30	0.457	57	MINS
0.80	22.60	0.454	17	HRS
0.77	25.96	0.453	2.75	HRS
0.74	29.30	0.453	9.5	HRS
0.71	32.65	0.452	3	HRS
0.68	35.95	0.451	4	HRS
0.65	39.28	0.450	0.7	HR

RUN 5-3 0.0282 CM SALT CRYSTALS

EPS	SETTLED BED HEIGHT CM	SETTLED BED POROSITY	APPROX. TIME	
0.92	9.30	0.469		
0.89	12.70	0.466	3	HRS
0.87	14.97	0.464	20	HRS
0.85	17.15	0.460	18	HRS
0.80	22.80	0.459	0.5	HR
0.77	26.10	0.456	16	HRS
0.74	29.60	0.458	3.5	HRS
0.71	32.97	0.457	11	HRS
0.68	36.33	0.457	2.5	HRS
0.65	39.65	0.455	3.5	HRS

RUN 6-4 0.288 CM ABS PELLETS

EPS	SETTLED BED HEIGHT CM	SETTLED BED POROSITY	APPROX. TIME	
0.95	6.00	0.486	0.5	HR
0.92	9.90	0.501		
0.90	12.10	0.490		
0.85	17.75	0.479	1.5	HR
0.83	20.10	0.478	2	HRS
0.80	23.30	0.470	1.0	HR
0.77	26.50	0.465	11	HRS
0.74	29.70	0.460	6.5	HRS
0.71	32.90	0.456	16	HRS
0.68	36.10	0.453	24	HRS

RUN 6-5 0.288 CM ABS PELLETS

EPS	SETTLED BED HEIGHT CM	SETTLED BED POROSITY	APPROX. TIME	
0.92	8.30	0.414	3	HRS
0.90	12.10	0.497		
0.83	19.60	0.472	9	HRS
0.80	23.00	0.471	3	HRS
0.74	29.60	0.466	3	HRS
0.71	33.00	0.465	0.5	HR
0.68	36.00	0.459	8	HRS

RUN 9-2 0.0508 CM MINERAL CRYSTALS

EPS	SETTLED BED HEIGHT CM	SETTLED BED POROSITY	APPROX. TIME	
0.95	6.10	0.495	1.5	HRS
0.92	9.70	0.492	0.5	HR
0.90	12.10	0.491	1.5	HRS
0.90	12.10	0.491	10	HRS
0.88	14.45	0.488	43	MINS
0.85	18.10	0.489	2	HRS
0.83	20.50	0.489	43	MINS
0.80	24.00	0.486	17	MINS
0.77	27.55	0.485	16	HRS
0.74	31.15	0.486	43	MINS
0.71	34.70	0.485	19	MINS
0.68	38.10	0.482	3	HRS
0.68	38.25	0.484	18	MINS
0.65	41.66	0.482	14	HRS

RUN 9-3 0.0508 CM MINERAL CRYSTALS

EPS	SETTLED BED HEIGHT CM	SETTLED BED POROSITY	APPROX. TIME	
0.95	6.10	0.494	1.5	HRS
0.92	9.75	0.494	1	HR
0.92	9.75	0.494	1	HR
0.90	12.10	0.490	1.5	HRS
0.88	14.50	0.489	43	MINS
0.85	18.15	0.490	2	HRS
0.83	20.55	0.490	43	MINS
0.80	24.05	0.487	17	MINS
0.77	27.60	0.486	16	HRS
0.74	31.20	0.486	43	MINS
0.71	34.70	0.484	19	MINS
0.68	38.20	0.483	3	HRS
0.68	38.20	0.483	18	MINS
0.65	41.70	0.482	14	HRS

RUN 10-2 0.0426 CM MINERAL CRYSTALS

EPS	SETTLED BED HEIGHT CM	SETTLED BED POROSITY	APPROX. TIME	
0.95	6.15	0.499		
0.92	9.75	0.494	1.5	HRS
0.90	12.15	0.493	15	MINS
0.88	14.30	0.483	20	MINS
0.85	17.95	0.485	25	MINS
0.85	18.00	0.486	3	HRS
0.82	21.45	0.483	1.2	HR
0.80	23.90	0.484	10	HRS
0.77	27.50	0.484	5	MINS
0.74	31.05	0.484	3.5	HRS
0.71	34.60	0.483	2.5	HRS
0.68	38.10	0.482	0.5	HR
0.65	41.43	0.479	9.5	HRS

RUN 10-3 0.0426 CM MINERAL CRYSTALS

EPS	SETTLED BED HEIGHT CM	SETTLED BED POROSITY	APPROX. TIME	
0.95	6.20	0.502		
0.92	9.75	0.494	1.5	HRS
0.90	12.15	0.492	15	MINS
0.88	14.40	0.486	20	MINS
0.85	18.05	0.487	25	MINS
0.85	18.15	0.490	3	HRS
0.82	21.65	0.487	1.2	HRS
0.80	23.95	0.485	10	HRS
0.77	27.63	0.486	20	MINS
0.77	27.70	0.488	5	MINS
0.74	31.40	0.489	3.5	HRS
0.71	34.85	0.487	2.5	HRS
0.68	38.45	0.487	0.5	HR
0.65	41.80	0.483	9.5	HRS

RUN 11-2 0.135 CM SUGAR CRYSTALS

EPS	SETTLED BED HEIGHT CM	SETTLED BED POROSITY	APPROX. TIME	
0.95	6.20	0.503	15	MINS
0.92	9.70	0.492	1	HR
0.90	12.10	0.491	1	HR
0.88	14.50	0.490	0.5	HR
0.85	18.00	0.486	0.5	HR
0.82	21.65	0.488	0.5	HR
0.80	24.00	0.486	10	HRS
0.80	23.90	0.484	0.5	HR
0.77	27.45	0.484	3.5	HRS
0.74	31.05	0.484	40	MINS
0.71	34.45	0.481	9	HRS
0.68	37.95	0.480	2	HRS

RUN 11-3 0.135 CM SUGAR CRYSTALS

EPS	SETTLED BED HEIGHT CM	SETTLED BED POROSITY	APPROX. TIME	
0.95	6.25	0.506	15	MINS
0.92	9.80	0.496	1	HR
0.90	12.20	0.494	1	HR
0.88	14.55	0.491	0.5	HR
0.85	18.05	0.487	0.5	HR
0.82	21.70	0.488	0.5	HR
0.80	24.00	0.486	10	HRS
0.80	24.00	0.486	0.5	HR
0.77	27.55	0.485	3.5	HRS
0.74	31.00	0.483	40	MINS
0.74	31.00	0.483	9	HRS
0.71	34.45	0.481	35	MINS
0.68	38.10	0.482	4	HRS

RUN 12-3 0.113 CM SUGAR CRYSTALS

EPS	SETTLED BED HEIGHT CM	SETTLED BED POROSITY	APPROX. TIME	
0.95	6.25	0.506	9	HRS
0.92	9.90	0.501	1.0	HR
0.90	12.20	0.494	3	HRS
0.88	14.55	0.491	1.5	HR
0.85	18.05	0.487	9	HRS
0.82	21.60	0.486	20	MINS
0.80	24.00	0.486	2.5	HRS
0.77	27.50	0.484	12	MINS
0.74	31.00	0.483	10	MINS
0.71	34.35	0.479	22	MINS
0.68	37.70	0.476	8	HRS

APPENDIX XII SAMPLE PLOT OF EXPERIMENTAL BED HEIGHT vs. SETTLING TIME

Run 3-2 $\epsilon = 0.88$ Jan 22. 68

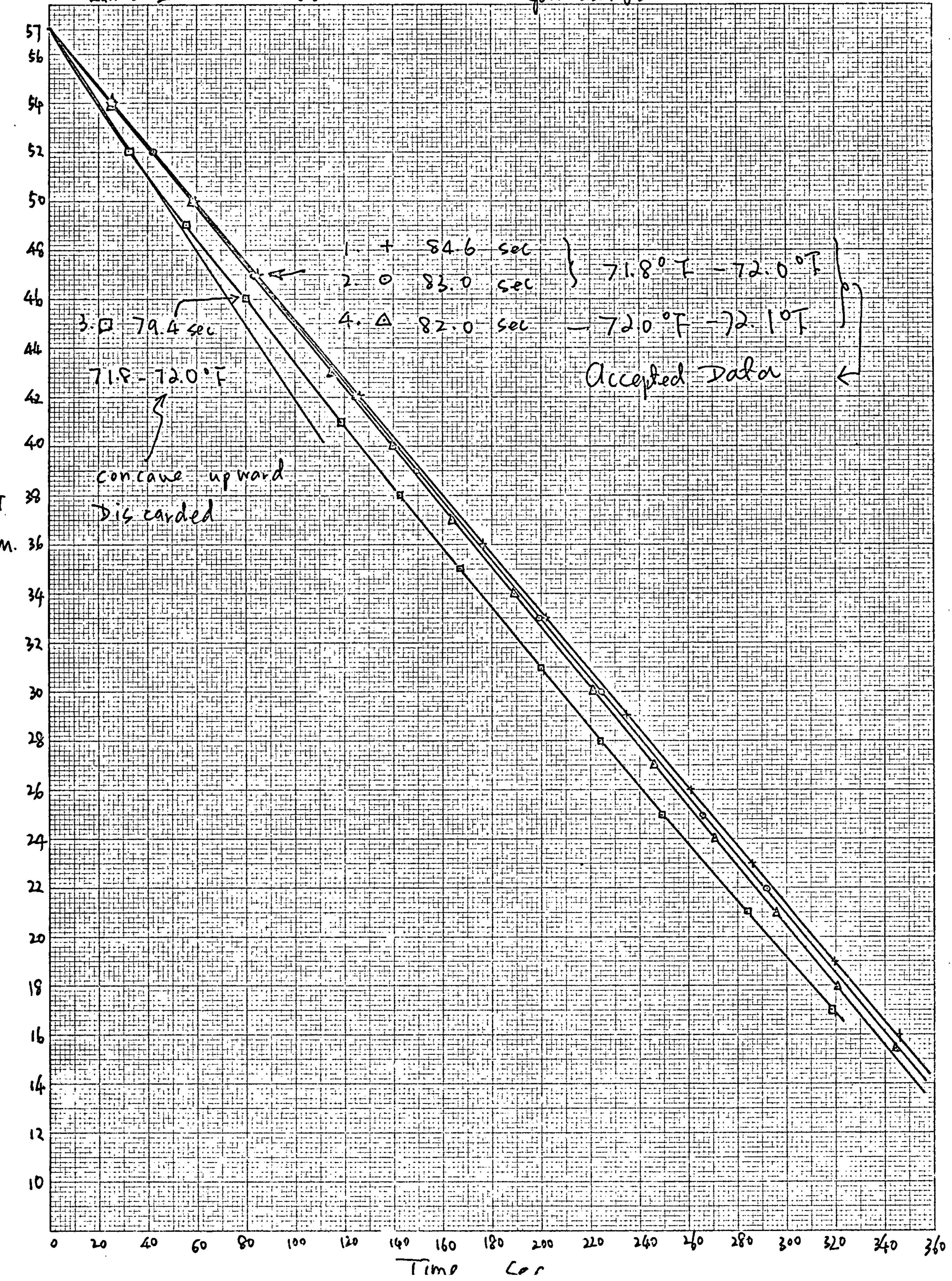

APPENDIX XIII SAMPLE CALCULATIONS AND ERRORS

Sample calculations are given below; random cases for error analysis are included.

1. (Settling rate)x(Liquid viscosity)

$$u = \text{DIST}/\text{TIME}$$

By linear interpolation between short temperature interval,

$$\nu = \nu_1 + \frac{(\text{TEMP}-\text{TEMP}_1)}{(\text{TEMP}_2-\text{TEMP}_1)} \times (\nu_2 - \nu_1)$$

a. Run 3-1A at $\epsilon = 0.92$

DIST = 10.0 ± 0.2 cm

TIME = 65.4 ± 0.2 sec

u = 10.0/65.4 = 0.153 cm/sec

Maximum relative error in u

$$= \pm \left(\frac{0.2}{10.0} + \frac{0.2}{65.4}\right) = \pm 2.4\%$$

TEMP = 71.8 ± 0.15 deg. F

where ± 0.15 deg. F is the uncertainty in the estimated liquid temperature.

TEMP_1 = 70.1 ± 0.03 deg. F

TEMP_2 = 72.01 ± 0.03 deg. F

ν_1 = 32.24 (± 0.2%) cs

ν_2 = 31.39 (± 0.2%) cs

By linear interpolation

$\nu = 31.57$ cs

Maximum relative error in estimated ν

$$\pm\left[0.002\times\frac{32.24}{31.57}+\left(\frac{0.15+0.03}{0.79}+\frac{0.03+0.03}{1.0}+\frac{0.002+0.002}{0.85}\right)\times\frac{0.67}{31.57}\right]$$
$= \pm 0.8\%$

Thus maximum relative error in $u\nu$,

$$= \pm\ (2.4 + 0.8) = \pm\ 3.2\%$$

b. Run 3-2 at $\epsilon = 0.74$ with the largest temperature variation

DIST = 10.0 $\pm$ 0.2 cm

TIME = 205.0 $\pm$ 0.2 sec

u = 10.0/205.0 = 0.0488 cm/sec

Maximum relative error in u

$$= \pm\left(\frac{0.2}{10.0}+\frac{0.2}{205.0}\right) = \pm\ 2.0\%$$

TEMP = 74.3 $\pm$ 0.5 deg. F

TEMP_1 = 73.0 $\pm$ 0.03 deg. F

TEMP_2 = 75.02 $\pm$ 0.03 deg. F

ν_1 = 30.63 ($\pm$ 0.2%) cs

ν_2 = 29.15 ($\pm$ 0.2%) cs

By interpolation

$\nu = 29.68$ cs

Maximum relative error of estimated ν

$$= \pm\left[0.002\times\frac{30.63}{29.68}+\left(\frac{0.5+0.03}{1.3}+\frac{0.03+0.03}{2.02}+\frac{0.002+0.002}{1.48}\right)\times\frac{0.95}{29.68}\right]$$
$= \pm\ 1.6\%$

Maximum relative error in $u\nu$

$$= \pm\ (2.0+1.6)\% = \pm\ 3.6\%$$

Error in the linear interpolation of viscosity over a small temperature interval should be comparatively negligible.

2. Porosity

Porosities were selected to calculate the required amount of particles to be weighed

$$WT = V\ (1-\epsilon)\rho_s$$
$$WT = \sum\ (\text{incremental weight for porosity change of} \Delta\epsilon)$$
$$= V \sum \Delta\epsilon\, \rho_s$$
$$\epsilon = 1 - WT/V\rho_s$$

a. Run 3-1A at $\epsilon = 0.65$

$$V = 313.0 \pm 1.0\ \text{cm}^3$$
$$\rho_s = 2.169 \pm 0.005\ \text{g/cm}^3$$
$$WT = 313 \times 2.169 \times (0.05+0.03\text{x}8+0.02\text{x}3) = 237.4\ \text{g.}$$

accuracy

$$WT = 237.4 \pm 0.3\ \text{g}$$

Maximum relative error in ϵ

$$\doteq \pm\ \left(\frac{0.36}{237.4} + \frac{1.0}{313.0} + \frac{0.005}{2.169}\right) \times \frac{0.35}{0.65}$$
$$= \pm\ 0.37\%$$

b. Run 3-3 at $\epsilon = 0.65$

$$V = 1250 \pm 1.0 \text{ cm}^3$$

$$WT = 1250 \times 2.169 \times (0.05 + 0.03 \times 8 + 0.02 \times 3)$$

$$= 949.2 \pm 0.4 \text{ g}$$

Maximum relative error in ϵ

$$= \pm \left(\frac{0.4}{949.2} + \frac{1}{1250} + \frac{0.005}{2.169}\right) \times \frac{0.35}{0.65}$$

$$= \pm 0.19\%$$

3. Fixed bed porosity

$$\epsilon_b = 1 - \frac{WT/\rho_s}{HTB x D_t^2 x 0.7854}$$

Run 3-3 at $\epsilon = 0.65$

$$WT = 1250x2.169x(0.05\pm0.03x8+0.02x3)$$

$$= 949.2+0.4 \text{ g}$$

$$\rho_s = 2.169\pm0.005 \text{ g/cm}^3$$

$$HTB = 39.28\pm0.05 \text{ cm}$$

$$D_t = 5.08\pm0.01 \text{ cm}$$

$$\epsilon_b = 1 - \frac{949.2/2.169}{39.28x5.08^2x0.7854}$$

$$= 0.450$$

Maximum relative error in ϵ_b

$$= \pm \left(\frac{0.4}{949.2} + \frac{0.005}{2.169} + \frac{0.05}{39.28} + \frac{0.01x2}{5.08}\right) \times \frac{0.55}{0.45}$$

$$= \pm 0.96\%$$

4. Effect of Uncertainty of ϵ on $u\nu$

Consider equation 1a, taking n = 5. A 0.4% uncertainty in ϵ could cause an uncertainty of 2% in $u\nu$. Therefore any variation in $u\nu$ which was larger than its own maximum error plus that caused by ϵ, should be considered to arise from the minor nonuniformities in the suspension dicussed in the text.

5. Computation

The data on hindered settling were processed by the computer program A on page XIII-6 which does the viscosity interpolation, averaging of $u\nu$ and preliminary least squares calculation. Program B was used to do the least squares estimates of the processed data from program A.

Program A

Variables of the programs

RUN	run number	
PTC	particle name	
LIQ	description of liquid	
SCREEN	sieve opening	
T(A)	t_A, 0.05 value	
TIME	settling time, sec	
DIST	settling distance, cm	
EPS	porosity	
U	settling rate, cm/sec	
NU	kinematic viscosity, cs	
UNU	$u\nu$, (0.01 cm^3sec^{-2})	
UNUA	average $u\nu$, (0.01 cm^3sec^{-2})	
TEMP	temperature ^oF or ^oC	
TEMPS	read-in temperature of viscosity data, unit same as TEMP	
NUS	read-in viscosity data in cs at TEMPS	
NUMIN, NUMAX,	minimum and maximum value of NU in a run	
DENP	particle density	g/cm^3
DENLIQ	liquid density	g/cm^3
DV	diameter of sphere of same volume as the particle	cm
DT	column diameter	cm
DRATIO	DV/DT	
NTEST	number of tests	
STNDD	standard deviation of average $u\nu$, (0.01 cm^3sec^{-2})	
LGUNUA	log. of average $u\nu$	
LGEPS	log. of ϵ	

SLUNU	sum of log $(u\nu)$
SLGE	sum of $\log\epsilon$
SLUNU2	sum of $[\log(u\nu)]^2$
SLUNE	sum of $\log(u\nu) \times \log\epsilon$
SLGE2	sum of $(\log\epsilon)^2$
N	least squares estimated Richardson-Zaki index n
LGUNUO	extrapolated log $(u\nu)$ to $\epsilon = 1$
UNUO	$(u\nu)_{ext}$ calculated from extrapolated log $(u\nu)$ $(0.01\ cm^3/sec^2)$
CFDN	95% confidence interval of n
CFDLUN	95% confidence interval of extrapolated log $(u\nu)$
UNUO1-UNUO2	95% confidence limits of extrapolated $(u\nu)_{ext}$, $(0.01\ cm^3/sec^2)$
DPEXT	sphere diameter calculated from $(u\nu)_{ext}$, cm
DPEXT1-DPEXT2	sphere diameter calculated from 95% confidence limits of $(u\nu)_{ext}$, cm
DPEXCO	sphere diameter calculated from $(u\nu)_{ext}$ corrected by wall, cm
REOMIN, REOMAX	maximum and minimum Re_o based on DPEXT

JOB NUMBER 16116 CATEGORY F USER'S NAME- YU-SEN CHONG USER

JOB START 10HRS 34MIN 05.53EC V9M011 OFF-

OB 16116 CHONG YU-SEN

AGE 80

IME 3

ORTRAN **PROGRAM A**

```
      REAL NU,N,NUS,LGUNUA,LGEPS  ,LGUNUO,NUMIN,NUMAX
      COMMON TEMP,I,NU,TEMPS,NUS,UNUA,NUMIN ,NUMAX
      DIMENSION TIME(10),DIST(10),EPS(15),U(10),UNU(15),
     1TEMP(20),NU(20),TEMPS(20),NUS(20),UNUA(20),LGUNUA(15),LGEPS(15)
      DIMENSION PTC(3),LIQ(4),SCREEN(12),RUN(2)
      DIMENSION T(14)
      DATA T(2),T(3),T(4),T(5),T(6),T(7),T(8),T(9),T(10),T(11),T(12),T(1
     13),T(14)/4.303,3.182,2.776,2.571,2.447,2.365,2.306,2.262,2.228,2.2
     201,2.179,2.160,2.145/
      DIMENSION FMT(16),FMOUT1(16),FMOUT2(16),FMOUT3(16)
      DIMENSION  STNDD(15),NTEST(15)
10000 READ 114,RUN,PTC,DENP,LIQ,DENLIQ,DV,DT,SCREEN
114   FORMAT ( 2A6,3A6,F6.3,4A6,F10.4/2F10.4/12A6 )
      WRITE (7,114) RUN,PTC,DENP,LIQ,DENLIQ,DV,DT,SCREEN
      READ 111, (TEMPS(M),NUS(M),M=1,12)
111   FORMAT (8F10.0)
      READ 1,FMT,FMOUT1, FMOUT2, FMOUT3
1     FORMAT (16A5 )
      WRITE(7,11) FMOUT2,FMOUT3
11    FORMAT (16A5/)
      NUMIN=2000.0
      NUMAX=0.0
      DRATIO=DV/DT
      PRINT 2,RUN,PTC,DENP,LIQ,DENLIQ,DV,DT,DRATIO,SCREEN
2     FORMAT (1H1,//////,22X,2A6/23X,11HPARTICLES= ,3A6,8X,8HDENSITY= ,
     1F6.3,7H GM/CM /23X,11HLIQUID=       ,4A6,2X,8HDENSITY= ,F6.3,7H GM/C
     2M /23X,17HPARTICLE SIZE D = ,F7.4,9H CM, D  =,F6.2,12H CM, D /D  =
     3,F7.4/23X ,12A6  /)
      PRINT 21
21    FORMAT (26X,4HTEMP,5X,4HDIST,4X,8HSETTLING,5X,1HU,8X,4HU*NU,6X,3HE
     1PS/36X,2HCM,5X,8HTIME SEC ,2X,6HCM/SEC,2X,11H0.01CM /SEC / )
      DO 1000II=1,15
      DO 100 I=1,10
      READ (5,FMT) TEMP(I),DIST(I),TIME(I),EPS(II), IDCTR
      IF (IDCTR.NE.0) GO TO 10
      IF (TEMP(I).EQ.0.) GO TO 2000
100   CONTINUE
10    CALL NUCAL
      NTEST(II)=I
      SUM=0
      SUMSQA=0.
      DO 200 K=1,I
      U(K)=DIST(K)/TIME(K)
      UNU(K)=U(K)*NU(K)
      WRITE (6,FMOUT1) TEMP(K),DIST(K),TIME(K),U(K),UNU(K),EPS(II)
      SUMSQA=SUMSQA+UNU(K)**2
```

```
  200 SUM=SUM+UNU(K)
      UNUA(II)=SUM/FLOAT(I)
      IF (I.EQ.1) GO TO 201
      STNDD(II)=SQRT((SUMSQA-SUM**2/FLOAT(I))/FLOAT(I-1))
  201 LGUNUA(II)=ALOG10(UNUA(II))
      LGEPS(II)=ALOG10(EPS(II))
 1000 CONTINUE
 2000 II=II-1
      SLUNU=0.
      SLGE=0.0
      SLUNU2=0.0
      SLUNLE=0.0
      SLGE2=0.0
      DO 30    I=1,II
      SLUNU=SLUNU+LGUNUA(I)
      SLGE=SLGE+LGEPS(I)
      SLUNU2=SLUNU2+LGUNUA(I)**2
      SLUNLE=SLUNLE+LGUNUA(I)*LGEPS(I)
      SLGE2=SLGE2+LGEPS(I)**2
   30 CONTINUE
      N=(FLOAT(II)*SLUNLE-SLGE*SLUNU)/(FLOAT(II)*SLGE2-SLGE**2)
      LGUNU0=(SLUNU-N*SLGE)/FLOAT(II)
      UNU0=10.0**LGUNU0
      REAL LGEAVE
      LGEAVE=SLGE/FLOAT(II)
      SDLUN2=(SLUNU2-LGUNU0*SLUNU-N*SLUNLE)/(FLOAT(II)-2.0)
      SDLUN=SQRT(SDLUN2)
      SLELE2=SLGE2-SLGE**2/FLOAT(II)
      CFDN=T(II-2)*SDLUN/SQRT(SLELE2)
      CFDLUN=T(II-2)*SDLUN*SQRT(1.0/FLOAT(II)+LGEAVE**2/SLELE2)
      VARN=SDLUN2/SLELE2
      SDN=SQRT(VARN)
      UNU0=10.0**LGUNU0
      UNU01=10.0**(LGUNU0-CFDLUN)
      UNU02=10.0**(LGUNU0+CFDLUN)
      PHYPRO=0.18*DENLIQ/((DENP-DENLIQ)*980.)
      DPSQ=UNU0*PHYPRO
      DPE1SQ=UNU01*PHYPRO
      DPE2SQ=UNU02*PHYPRO
      DPEXT=SQRT(DPSQ)
      DPEXT1=SQRT(DPE1SQ)
      DPEXT2=SQRT(DPE2SQ)
      CURFAC=1.0+2.104*DRATIO
      CORF=SQRT(CORFAC)
      DPEXCO=DPEXT*CORF
      REOMIN=DPEXT*UNU0/NUMAX**2*100.0
      REOMAX=DPEXT*UNU0/NUMIN**2*100.0
      PRINT 2,RUN,PTC,DENP,LIQ,DENLIQ,DV,DT,DRATIO,SCREEN
      PRINT 22,REOMIN,REOMAX
   22 FORMAT (23X,5HRE(0),4X,F6.3,1H-,F6.3//28X,3HEPS,2X,9HU*NU(AVE) ,
     12X,7HLG(EPS),2X,8HLG(U*NU),2X,8HSTD.DEV.,1X,5HNO OF/32X,12H0.01CM
     2/SEC ,19X,13H          TEST    /)
      WRITE(7,221) NUMIN,NUMAX
  221 FORMAT (2F10.3)
      DO 3000 K=1,II
      IF (NTEST(K).EQ.1 ) GO TO 110
      WRITE (6,FMOUT2)EPS(K),UNUA(K),LGEPS(K),LGUNUA(K), STNDD(K),NTEST(
     1K)
      WRITE (7,FMOUT2)EPS(K),UNUA(K),LGEPS(K),LGUNUA(K), STNDD(K),NTEST(
```

```
     1K)
      GO TO 3000
110   WRITE(6,FMOUT3) EPS(K),UNUA(K),LGEPS(K),LGUNUA(K),NTEST(K)
      WRITE(7,FMOUT3) EPS(K),UNUA(K),LGEPS(K),LGUNUA(K),NTEST(K)
3000  CONTINUE
       PRINT 8,LGUNUO,M,UNUO,M,N,CFDN,LGUNUO,CFDLUN,UNUO1,UNUO2
8     FORMAT (/23X,24HLEAST SQUARES ESTIMATES  /27X,10HLOG(U*NU)=,F7.4,2
     1H +,F6.2,9H*LOG(EPS) /27X, 6HU*NU =,F8.3,6H*EPS**,F5.2 /27X,19HCON
     2FIDENCE INTERVAL /28X,2HN=,8X,F5.2,3X,F5.2 /28X,10HLOG(U*NU)O,F7.4
     3,1X,F7.4 /28X,9H(U*NU)EXT ,F8.3,1H-,F8.3 )
      PRINT 9,UNUO,DPEXT,DPEXCO,UNUO1,UNUO2,DPEXT1,DPEXT2
9     FORMAT (/23X,31HDIA. OF SPHERE CORRESPONDING TO  /27X,10H(U*NU)EXT
     1=,F8.3,14X,F7.4,3H CM/27X,18HCORRECTED FOR WALL,14X,F7.4,3H CM/ 27
     2X,12H(U*NU)EXT OF,F8.3,1H-,F8.3,1H,,2X,F7.4,1H-,F7.4,2HCM  )
      GO TO 10000
      END
C.
```

```
      SUBROUTINE NUCAL
      REAL NU,NUS,NUMIN,NUMAX
      COMMON TEMP,I,NU,TEMPS,NUS,UNUA,NUMIN,NUMAX
      DIMENSION TEMP(20),NU(20),TEMPS(20),NUS(20),UNUA(20)
      DO 22 K=1,I
      DO 11 M=1,12
      IF (TEMP(K).GT.TEMPS(M).AND.TEMP(K).LE.TEMPS(M+1)) GO TO 12
   11 CONTINUE
   12 RATIO =(NUS(M+1)-NUS(M))/(TEMPS(M+1)-TEMPS(M))
      NU(K)=NUS(M)+(TEMP(K)-TEMPS(M))*RATIO
      IF (NU(K).LT.NUMIN) NUMIN=NU(K)
      IF(NU(K).GT.NUMAX) NUMAX=NU(K)
   22 CONTINUE
      RETURN
      END
$ENTRY
```

EASE RETURN TO THE CHEMICAL ENGINEERING BUILDING

JOB NUMBER 16116 CATEGORY F USER'S NAME- YU-SEN CHONG USER

JOB START 01HRS 50MIN 06.4SEC V9M011 OFF-

OB 16116 CHONG YU-SEN

AGE 35

IME 3

ORTRAN **PROGRAM B**

```
          REAL NU,N,NUS,LGUNUA,LGEPS  ,LGUNUO,NUMIN,NUMAX
          INTEGER DISCAR
          DIMENSION TIME(10),DIST(10),EPS(15),U(10),UNU(15),
         1TEMP(20),NU(20),TEMPS(20),NUS(20),UNUA(20),LGUNUA(15),LGEPS(15)
          DIMENSION PTC(3),LIQ(4),SCREEN(12),RUN(2)
          DIMENSION T(14)
          DATA T(2),T(3),T(4),T(5),T(6),T(7),T(8),T(9),T(10),T(11),T(12),T(1
         13),T(14)/4.303,3.182,2.776,2.570,2.447,2.365,2.306,2.262,2.228,2.2
         201,2.179,2.160,2.145/
          DIMENSION FMT(16),FMOUT1(16),FMOUT2(16),FMOUT3(16),FMOUT4(16),FMOU
         1T5(16)
          DIMENSION  STNDD(15),NTEST(15)
    10000 READ 114,RUN,PTC,DENP,LIQ,DENLIQ,DV,DT,SCREEN,NUMIN,NUMAX
    114   FORMAT ( 2A6,3A6,F6.0,4A6,F10.0/2F10.0/12A6 /2F10.0 )
          READ 1,     FMOUT2,FMOUT3,FMOUT4,FMOUT5
    1     FORMAT(16A5 )
          DRATIO=DV/DT
          PRINT 2,RUN,PTC,DENP,LIQ,DENLIQ,DV,DT,DRATIO,SCREEN
    2     FORMAT (1H1,22X,2A6/23X,11HPARTICLES= ,3A6,8X,8HDENSITY= ,F6.3,7H
         1GM/CM /23X,11HLIQUID=     ,4A6,2X,8HDENSITY= ,F6.3,7H GM/CM /23X,1
         2HPARTICLE SIZE D = ,F7.4,9H CM, D  =,F6.2,12H CM, D /D  =,F7.4/23
         3,12A6 /)
          PRINT 21
    21    FORMAT ( 28X,3HEPS,2X,9HU*NU(AVE),2X,7HLG(EPS),2X,8HLG(U*NU),2X,8H
         1STD.DEV.,1X,5HNO.OF  /32X,12H0.01CM /SEC  ,19X,14H         TESTS/
          SLUNU=0.
          SLGE=0.0
          SLUNU2=C.0
          SLUNLE=0.0
          SLGE2=0.0
          I=0
          DO 30 J=1,14
          I=I+1
          READ (5,31) EPS(I),UNUA(I),LGEPS(I),LGUNUA(I), STNDD(I),NTEST(I),
         1ISCAR
    31    FORMAT (26X,F9.0,F9.0,F10.0,F9.0,F11.0,I1,4X,I1)
          IF (EPS(I).LT.0.C001) GO TO 40
          IF (DISCAR.NE.0) GO TO 32
          IF (NTEST(I).EQ.1) GO TO 110
          WRITE (6,FMOUT2)EPS(I),UNUA(I),LGEPS(I),LGUNUA(I), STNDD(I),NTEST
         1I)
          GO TO 35
    110   WRITE(6,FMOUT3) EPS(I),UNUA(I),LGEPS(I),LGUNUA(I),NTEST(I)
    35    SLUNU=SLUNU+LGUNUA(I)
          SLGE=SLGE+LGEPS(I)
          SLUNU2=SLUNU2+LGUNUA(I)**2
```

```
      SLUNLE=SLUNLE+LGUNUA(I)*LGEPS(I)
      SLGE2=SLGE2+LGEPS(I)**2
      GO TO 30
 32   IF(NTEST(I).EQ.1) GO TO 33
      WRITE (6,FMOUT4)EPS(I),UNUA(I),LGEPS(I),LGUNUA(I), STNDD(I),NTEST(
     1I)
      I=I-1
      GO TO 30
 33   WRITE(6,FMOUT5) EPS(I),UNUA(I),LGEPS(I),LGUNUA(I),NTEST(I)
      I=I-1
 30   CONTINUE
 40   II=I-1
      N=(FLOAT(II)*SLUNLE-SLGE*SLUNU)/(FLOAT(II)*SLGE2-SLGE**2)
      LGUNUO=(SLUNU-N*SLGE)/FLOAT(II)
      UNUO=10.0**LGUNUO
      REAL LGEAVE
      LGEAVE=SLGE/FLOAT(II)
      SDLUN2=(SLUNU2-LGUNUO*SLUNU-N*SLUNLE)/(FLOAT(II)-2.0)
      SDLUN=SQRT(SDLUN2)
      SLELE2=SLGE2-SLGE**2/FLOAT(II)
      CFDN=T(II-2)*SDLUN/SQRT(SLELE2)
      CFDLUN=T(II-2)*SDLUN*SQRT(1.0/FLOAT(II)+LGEAVE**2/SLELE2)
      VARN=SDLUN2/SLELE2
      SDN=SQRT(VARN)
      UNUO=10.0**LGUNUO
      UNUO1=10.0**(LGUNUO-CFDLUN)
      UNUO2=10.0**(LGUNUO+CFDLUN)
      PHYPRO=0.18*DENLIQ/((DENP-DENLIQ)*980.)
      DPSQ=UNUO*PHYPRO
      DPE1SQ=UNUO1*PHYPRO
      DPE2SQ=UNUO2*PHYPRO
      DPEXT=SQRT(DPSQ)
      DPEXT1=SQRT(DPE1SQ)
      DPEXT2=SQRT(DPE2SQ)
      CORFAC=1.0+2.104*DRATIO
      CORF=SQRT(CORFAC)
      DPEXCO=DPEXT*CORF
      DPE1CO=DPEXT1*CORF
      DPE2CO=DPEXT2*CORF
      REOMIN=DPEXT*UNUO/NUMAX**2*100.0
      REOMAX=DPEXT*UNUO/NUMIN**2*100.0
      PRINT 22,REOMIN,REOMAX
 22   FORMAT(/23X,5HRE(O),7X,F6.3,1H-,F6.3)
       PRINT 8,LGUNUO,N,UNUO,N,N,CFDN,LGUNUO,CFDLUN,UNUO1,UNUO2
 8    FORMAT (/23X,24HLEAST SQUARES ESTIMATES  /27X,10HLOG(U*NU)=,F7.4,
     1H +,F6.2,9H*LOG(EPS) /27X, 6HU*NU =,F8.3,6H*EPS**,F5.2 /27X,19HCO
     2FIDENCE INTERVAL /28X,2HN=,3X,F5.2,3X,F5.2 /28X,10HLOG(U*NU)O,F7.
     3,1X,F7.4 /28X,9H(U*NU)EXT ,F8.3,1H-,F8.3 )
      PRINT 9,UNUO,DPEXT,DPEXCO,UNUO1,UNUO2,DPEXT1,DPEXT2,DPE1CO,DPE2CO
 9    FORMAT (/23X,31HDIA. OF SPHERE CORRESPONDING TO  /27X,10H(U*NU)EX
     1=,F8.3,14X,F7.4,3H CM/27X,18HCORRECTED FOR WALL,14X,F7.4,3H CM/ 2
     2X,12H(U*NU)EXT OF,F8.3,1H-,F8.3,1H,,2X,F7.4,1H-,F7.4,2HCM/27X,18H
     3ORRECTED FOR WALL  ,14X,F7.4,1H-,F7.4,2HCM )
      GO TO 10000
      END
$ENTRY
```